

Engineering bacteria for the enhanced production of high-value chemicals

John Andrew Linney

Doctor of Philosophy

Aston University

May 2021

© John Linney 2021

John Linney asserts his moral right to be identified as the author of this thesis

This copy of the thesis has been supplied on condition that anyone who consults it is understood to recognise that its copyright belongs to its author and that no quotation from the thesis and no information derived from it may be published without appropriate permission or acknowledgement.

Thesis Summary

Engineering bacteria for the enhanced production of high-value chemicals

John Linney

Doctor of Philosophy

2021

There is a growing interest in the use of microbial cell factories to produce butanol, an industrial solvent and platform chemical. Biobutanol can also be used as a biofuel and represents a cleaner and more sustainable alternative to the use of conventional fossil fuels. Solventogenic *Clostridia* are the most popular microorganisms used due to the native expression of butanol synthesis pathways. A major drawback to the wide scale implementation and development of these technologies is the product toxicity of butanol. This study aims to develop a deeper understanding of butanol toxicity at the membrane. Using liposome membrane models and *in vitro* assays to investigate characteristics such as permeability, fluidity, and diameter, it was found that altering the composition of membranes can convey tolerance to butanol. The effect of butanol on membrane proteins was also investigated, with it causing unfolding of bacteriorhodopsin. The changes to the lipidome of *Clostridium saccharoperbutylacetonicum* N 1-4 in different butanol environments were investigated with thin layer chromatography and mass spectrometry. In higher butanol concentrations, levels of phosphatidylglycerol and oleic acid had increased significantly. Several metabolic targets were selected for the genetic engineering of *Clostridium saccharoperbutylacetonicum* N 1-4 (HMT) in an attempt to improve tolerance in butanol. The three targets investigated consisted of two membrane proteins and one enzyme. The first membrane protein, GlpF, a putative butanol channel which appeared to grant a butanol-independent advantage to growth when overexpressed. The second membrane protein, TtgB, is a transporter and overexpression increased cellular growth rate during fermentation. The final protein PssA is involved in lipid synthesis and showed no effect when overexpressed and knockouts appeared to inhibit growth in fermentation. Ultimately, this work highlights the detrimental impact of butanol-membrane interactions, how the cell responds and presents some novel strains, some of which have produced promising results.

Key words: Butanol toxicity, Membrane Engineering, *Clostridia*, Industrial biotechnology, Lipids

Acknowledgements

Firstly, I would like to thank my supervisor, Dr. Alan Goddard. He has provided me with unending support, advice, and knowledge throughout my entire PhD. He has always made me feel like a priority despite him being one of the busiest people I know - I could not ask for a better supervisor.

My thanks also go to those who have lent me their expertise over the years. Professor Corinne Spickett and Professor Andy Pitt for their general support and help with mass spectrometry, Dr John Simms for his advice and teachings of computational biology, and Mandy, Anna, and Liz from Biocleave for their knowledge and support during the strain engineering. All of these people have enabled me to experience new bits of science and have helped to make this thesis what it is. Thanks also to Tony Larson for his lipidomics analysis.

Everybody in the Goddard group and AMPL deserve thanks. I appreciate all of your friendship, technical help and support with experiments and methods, as well as the feedback on presentations / talks you have all provided. You have made my understanding of science much better and have helped me to improve my own scientific contributions. A special thanks goes to both Sarah and Monse from my lab. Sarah, thank you for all of your help in the lab over the years - mass spec would have been impossible without you! Monse, thank you for your help with construct design and for finishing off our fermentations (also thank you for all of the Mexican food). Thank you to my friends in 331, 347 and neuroscience for putting up with my complaining about failed experiments and for always lifting my spirits during the not-so-nice parts of this PhD.

Finally, I am grateful for my friends and family and for their love and support during my PhD - this would not have been possible without you all.

Table of contents

Thesis Summary.....	2
Acknowledgements.....	3
Table of contents	4
List of abbreviations.....	7
List of Figures.....	10
List of Tables	13
1. Introduction	14
1.1 Butanol	14
1.2 <i>Clostridia</i> : the native producers of butanol	16
1.3 Fermentation as a route to butanol	19
1.3 Cell envelope properties and architecture	20
1.4 Butanol toxicity	36
1.4.1 Mechanisms of butanol toxicity	36
1.4.2 Measuring butanol toxicity at the membrane	39
1.5 Cellular response to butanol.....	41
1.5.1 Changes to lipidome	41
1.5.2 Changes in gene expression and protein synthesis.....	43
1.6 Strategies to increase productivity and reduce toxicity	45
1.6.1 Non-engineering strategies.....	45
1.6.2 Non-targeted engineering.....	46
1.6.3 Towards more targeted engineering.....	46
1.6.4 Targeted engineering of lipid species.....	48
1.6.5 Efflux systems.....	49
1.6.6 Engineering targets in this work.....	51
1.7 Aims and Objectives	53
2. Materials and Methods	56
2.1 Materials	56
2.2 Molecular Biology	56
2.3 <i>In vitro</i> liposome assays.....	56
2.4 Total lipid extraction and quantification	58
2.5 <i>in silico</i> molecular dynamics	59
2.6 Thin layer chromatography.....	59
2.7 Lipidomics: HPLC-ESIMSMS	60

2.8 Unfolding assay	60
2.9 Glycerol uptake facilitator protein (GlpF) expression and purification	62
2.10 CLEAVE™: Genome editing of <i>Clostridium saccharoperbutylacetonicum</i> N1-4 (HMT)	63
2.11 Atomic Force Microscopy	66
3. <i>In vitro</i> characterisation of the interactions between butanol and membranes	67
3.1 Introduction	67
3.2 Results	69
3.2.1 <i>In vitro</i> assay optimisation	69
3.2.2 Altering headgroup composition.....	71
3.2.3 Acyl chain modifications	75
3.2.4 Exogenous compound addition to the membrane.....	79
3.2.5 Dynamic light scattering	86
3.2.6 <i>In silico</i> modelling.....	89
3.2.7 Atomic force microscopy	91
3.2.8 Membrane protein unfolding assay	93
4. Characterisation of <i>C. saccharoperbutylacetonicum</i> N 1-4 (HMT) lipidome.....	98
4.1 Introduction	98
4.2 <i>C. saccharoperbutylacetonicum</i> lipidome analysis in response to butanol.....	100
4.2.1 <i>C. saccharoperbutylacetonicum</i> N1-4 fermentation	100
4.2.2 Thin layer chromatography of <i>C. saccharoperbutylacetonicum</i> N1-4 extracts.....	101
4.2.3 Lipidomic analysis of <i>C. saccharoperbutylacetonicum</i> N1-4 extracts using mass spectrometry to support	108
5. Rational metabolic engineering of <i>C. saccharoperbutylacetonicum</i> N 1-4 (HMT) and <i>E. coli</i> to increase butanol tolerance and production	125
5.1 Introduction	125
5.2 Generation of CLEAVE™ constructs and testing their effect on growth in <i>Clostridium saccharoperbutylacetonicum</i> N1-4 (HMT)	128
5.2.1 PssA Knock out (Δ PssA) construct design	128
5.2.2 CLEAVE™ construct diagnostics and subcloning	131
5.2.3 TtgB construct cloning	132
5.2.4 Strain characterisation.....	135
5.2.5 GlpF cloning and expression	137
6. <i>Clostridium saccharoperbutylacetonicum</i> N1-4 (HMT) TtgB homology model	141
6.1 Introduction	141
6.2 TtgB homology model	142
6.3 Discussion	Error! Bookmark not defined.

7. General Discussion	149
7.1 How does butanol impact membrane properties and functions?	151
7.1.1 The importance of phospholipid head group.....	151
7.1.2 Phospholipid tail and hydrophobic core	156
7.2 Butanol has a detergent-like mechanism	161
7.3 How do the cells respond	163
7.3.1 Limitations of these data sets	168
7.4 How does butanol transverse the membrane?	169
7.5 Alternative strategies	175
8. Future work and conclusions.....	178
8.1 Future work.....	178
8.2 Conclusions	181
References.....	185

List of abbreviations

ABE - Acetone-butanol-ethanol

ACP - Acyl carrier protein

ADP - Adenosine diphosphate

AFM - Atomic force microscopy

ATP - Adenosine triphosphate

bp - Base pair

C. – *Clostridium*.

CDP - Cytidine diphosphate

CerP - Ceramide

CF - 5(6)-Carboxyfluorescein

CFA - Cyclopropane fatty acid

CHAPSO - 3-{Dimethyl[3-(3 α ,7 α ,12 α -trihydroxy-5 β -cholan-24-amido)propyl]azaniumyl}propane-1-sulfonate

CL - Cardiolipin

CoA - Coenzyme A

CRISPR - Clustered regularly interspaced short palindromic repeats

CTI - *Cis-trans* isomerase

DAG - Diacylglycerol

DGDG - Digalactosyldiacylglycerol

DLS - Dynamic light scattering

DMPC - 1,2-dimyristoyl-sn-glycero-3-phosphatidylcholine

DSPC - 1,2-distearoyl-sn-glycero-3-phosphatidylcholine

E. coli - *Escherichia coli*

ECL - Enhanced chemiluminescence

EDTA - Ethylenediaminetetraacetic acid

ESI - Electrospray ionisation

x g – Centrifugal force

g - gram

G3P - Glycerol-3-phosphate

GC - Gas chromatography

GP - General polarisation

HPLC - high performance liquid chromatography

hr - hour

HRP - Horseradish peroxidase

IPTG - Isopropyl β - d-1-thiogalactopyranoside

kbp / kb – Kilobase pair

L - Litre

LB - Lysogeny broth

M - Molar

m/z - Mass to charge ratio

m - Milli

Mg/ ml - milligrams per millilitre

MGDG - Monogalactosyldiacylglycerol

MJ - Megajoule

M - Molar

MMgal - One million gallons

MS - Mass spectrometry

mSa - Monovalent streptavidin

NAD - Nicotinamide adenine dinucleotide

n - Nano

nt – nucleotide

OD_x - optical density at x wavelength in nm

OM - Outer membrane

P. - *Pseudomonas*

PA - Phosphatidic acid

PAGE - Polyacrylamide gel electrophoresis

PE - Phosphatidylethanolamine

PG - Phosphatidylglycerol

POPC - 1-palmitoyl-2-oleoyl-sn-glycero-3-phosphatidylcholine

PS - Phosphatidylserine

RND - Resistance-nodulation-cell division

ROS - Reactive oxygen species

Rpm - Revolutions per minute

S - second

SD - standard deviation

SDS - Sodium Dodecyl Sulfate

SEM - standard error of the mean

SSA - Supramolecular self-associating amphiphiles

TAG - Triacylglycerol (triglyceride)

TEMED - Tetramethylethylenediamine

TLC – Thin layer chromatography

T_m - Melting temperature

UV - Ultraviolet

V - Volts

v/v - Volume per volume

WT - wild type

μl – Micro

List of Figures

Figure 1.1 Simplified acetone-butanol-ethanol (ABE) fermentation pathway.....	17
Figure 1.2 Simplified biological membrane.....	22
Figure 1.3 Phospholipids and phospholipid headgroup.....	24
Figure 1.4 Type II fatty acid synthesis.....	27
Figure 1.5 Phospholipid headgroup synthesis in bacteria.....	30
Figure 1.6 Phospholipid membrane phase behaviour.....	32
Figure 1.7 The structures sterols of the hopanoid bacteriohopanetetrol and cholesterol.....	33
Figure 1.8 The structures butanol and palmitoyl-oleoyl-phosphatidylethanolamine.....	36
Figure 1.9 Structure of glycerol like facilitator protein (GlpF),	53
Figure 1.10 Processes to improve butanol yield from ABE fermentation.....	56
Figure 2.1 CLEAVE™ technology for <i>C. saccharoperbutylacetonicum</i> N1-4 (HMT) genome editing.....	65
Figure 3.1. Objectives and experimental workflow for Chapter 3.....	68
Figure 3.2 Optimisation of liposome based biophysical assays	70
Figure 3.3. Carboxyfluorescein (CF) fluorescence dye release and of membrane models with different lipid headgroup compositions following butanol exposure.....	72
Figure 3.4. Laurdan probe general polarisation (GP) of membrane models with different lipid headgroup compositions following butanol exposure.....	74
Figure 3.5 Carboxyfluorescein (CF) fluorescence dye release and of membrane models with different acyl chain compositions following butanol exposure.....	77
Figure 3.6. Laurdan probe general polarisation (GP) of membrane models with different acyl chain compositions following butanol exposure.....	78
Figure 3.7. (A) Carboxyfluorescein (CF) fluorescence dye release and (B) laurdan probe general polarisation (GP) of membrane models with the addition of 20% cholesterol as a surrogate membrane modulator following butanol exposure.....	80

Figure 3.8 The structures of a series of self-associating amphiphilic membrane active compounds.....	81
Figure 3.9 Laurdan probe general polarisation (GP) of POPC liposomes with the addition of several serially diluted compounds.....	82
Figure 3.10 Laurdan probe general polarisation (GP) of POPC liposomes with the addition of compounds at different concentrations following butanol exposure.....	84
Figure 3.11 Laurdan probe general polarisation (GP) of POPC liposomes with the addition of compounds at different concentrations following butanol exposure (16-24 hincubation).....	85
Figure 3.12. The diameter of liposome models and polystyrene standards in response to butanol.....	88
Figure 3.13 Corse-grained molecular dynamics of butanol and a 3 POPE: 1 POPG membrane.....	90
Figure 3.14 AFM force measurements and images of POPC bilayers interacting with butanol.....	92
Figure 3.15 Monovalent streptavidin purification, western blots, and steric trapping assay.....	94-95
Figure 4.1 Objectives and experimental workflow for Chapter 4.....	99
Figure 4.2 <i>Clostridium saccharoperbutylacetonicum</i> N1-4 (HMT) fermentation characterisation.....	101
Figure 4.3 Copper sulphate developed thin layer chromatography of <i>Clostridium saccharoperbutylacetonicum</i> N 1-4 biomass from time points throughout fermentation.....	103
Figure 4.4 Molybdenum Blue developed thin layer chromatography of <i>Clostridium saccharoperbutylacetonicum</i> N 1-4 biomass from time points throughout fermentation.....	105
Figure 4.5 Ninhydrin thin layer developed chromatography of <i>Clostridium saccharoperbutylacetonicum</i> N 1-4 biomass from time points throughout fermentation.....	106
Figure 4.6. Lipid class coverage for several <i>Clostridial</i> species and <i>E. coli</i> annotated using LipidBlast....	109
Figure 4.7. Lipid class coverage for several <i>C. saccharoperbutylacetonicum</i> grown in environments with different butanol concentrations.....	111
Figure 4.8. Abundance of individual lipids ordered by area in positive mode.....	112-113
Figure 4.9. Abundance of individual lipids ordered by area in negative mode.....	114-115

Figure 4.10. Fatty acid prevalence scores of all fatty acids in (A) positive and (B) negative mode found in the LipidBlast database.....	117-118
Figure 4.11 Abundance of lipid classes throughout fermentation. (A) negative ionisation mode (B) positive ionisation mode.....	121
Figure 4.12 Total chain length abundance as a percentage of all annotated acyl chains. (A) negative ionisation mode (B) positive ionisation mode.....	122
Figure 4.13. The proportion of unsaturated fatty acids over the course of fermentation.....	123
Figure 5.1. Objectives and experimental workflow for Chapter 4.....	126
Figure 5.2 Generation of the PssA knockout (Δ PssA) construct for genome integration.....	129
Figure 5.3 Generation of the PssA knockout spacer sequences for CLEAVE™.....	130
Figure 5.4 Restriction digest of the PssA spacer and the targeting vector S3V9.....	131
Figure 5.5 Colony PCR of <i>E. coli</i> colonies transformed with the targeting vector S3V9 containing the PssA spacer.....	132
Figure 5.6 TtgB sequence Protein BLAST output.....	133
Figure 5.7 Colony PCR of <i>Clostridium saccharoperbutylacetonicum</i> N1-4 colonies transformed with the expression vector pMTL82151.....	134
Figure 5.8 Optical density and pH of engineered <i>Clostridium saccharoperbutylacetonicum</i> N1-4 (HMT) strains during the small bottle screen.....	136
Figure 5.9. (A) <i>GlpF</i> KOD PCR.....	138
Figure 5.10. Effect of <i>GlpF</i> overexpression in the presence of (A) 5 mg/ml exogenous butanol and (B) Ethanol and NaCl.....	139

Figure 6.1 Structural alignments of the two TtgB homology model monomers, from <i>P. putida</i> and <i>C. saccharoperbutylacetonicum</i> generated using SWISSPlot.....	157
Figure 6.2 <i>C. saccharoperbutylacetonicum</i> TtgB homology model and QMEANBrane analysis.....	147-148
Figure 7.1 Overall model of the interactions between butanol and <i>Clostridia</i>	153
Figure 7.2 Diagram of possible substrate paths through TtgB.....	174

List of Tables

Table 2.1 The 5' to 3' sequences of oligonucleotide primers used to amplify GlpF.....	62
Table 2.2 CLEAVE™ Targets.....	64
Table 2.3 HPLC run parameters for analysis of fermentation analytes.....	66
Table 4.1 Summary of total lipid species changes seen in <i>Clostridium saccharoperbutylacetonicum</i> N 1-4 biomass taken from time points throughout fermentation.....	107

1. Introduction

1.1 Butanol

n-butanol, herein referred to as butanol, is an important high-value alcohol with a wide range of applications in industry. It is used as a platform chemical in the synthesis of derivative molecules including: polymers, plasticisers and solvents (Mascal, 2012). The second main application of butanol is within the fuel market where it can be used as a “drop-in” substitute for petroleum. Butanol has been historically produced through two main methods. Firstly, chemical production with a two-step process involving initial hydroformylation of propylene, and hydrogenation of the subsequently produced butyraldehyde to form *n*-butanol (Mascal, 2012). Secondly, via ABE fermentation whereby mainly solventogenic *Clostridia* utilise an array of carbon sources to produce acetone, butanol and ethanol in a 3:6:1 molar ratio, respectively (Rabari and Banerjee, 2013). The exact ratio may vary depending on strain, but butanol is the consistent major product.

In recent years there has been an international resurgence in interest in the bioproduction through fermentation and commercialisation of butanol, with many international enterprises investing in related infrastructure and technologies. This primarily stems from unstable petroleum prices, concerns of energy security, and the detrimental impact of fossil fuels on the environment (Zheng *et al.*, 2009). Thus, there is a desire to move to a more sustainable, green economy which relies less on the use of fossil fuels. The utilisation of cell factories to produce butanol from ample waste biomass presents an important growing technology to achieve such aims. Several microorganisms have been used to ferment butanol with solventogenic *Clostridia* (mainly, *Clostridium acetobutylicum*, *C. saccharoperbutylacetonicum*, *C. beijerinckii*), native producers, being the most popular commercially (Chen 2012).

An ideal replacement biofuel would have fuel properties that are comparable to gasoline enabling an efficient conversion to a biofuel-based economy. The compatibility of the biofuel with conventional

engines, storage and transport infrastructure is of paramount importance. In 2016, 15,413 MMgal of bioethanol were produced in USA, compared with 1,568 MMgal of biodiesel and other renewable fuels (U.S. Energy Administration Information, 2018). However, ethanol is unsuitable for current storage and transport facilities primarily due to its corrosive and hygroscopic properties (Lee, Chou, *et al.*, 2008; Peralta-Yahya and Keasling, 2010). Therefore, the widespread use of ethanol will require extensive investments in infrastructure, which is predicted to amount to hundreds of billions of dollars (Fischer *et al.*, 2008).

Currently it is predicted that in excess of 1.2 billion gallons of butanol are consumed every year (Mordor Intelligence, 2018). The market size of butanol is estimated to be growing a rate of 3.0-5.1% per year and is expected to be approximately ~\$18 billion by 2022 (Grand View Research, 2020). This growth is likely to continue in accordance with the Energy Independence Act (2007), which required 30 billion gallons of renewable fuels be sold in the USA by 2020. Many international companies have shown an interest in the fermentative production of butanol including: Green Biologics (UK), Cathay Industrial Biotech (China), Tetravita Bioscience (USA) and Butamax (BP and DuPont) (Ndaba *et al.*, 2015; Nanda *et al.*, 2017). Unlike bioethanol, butanol is considered a “drop-in” fuel which can be used in current infrastructure without the need for modification. Along with beneficial physical properties, butanol is thought to have better fuel properties (Choi *et al.*, 2014). The energy content of butanol is 29.2 MJ/L, only 10% lower than gasoline’s (32.5 MJ/L) and 30% higher than ethanol’s (21.2 MJ/L) (Nanda *et al.*, 2017). Additional advantageous characteristics of butanol over bioethanol include: (i) Reduced corrosiveness (ii) Higher blending capabilities (any concentration of butanol and gasoline can be used, whereas ethanol is limited to <85%) (iii) Lower pressures of butanol vapour, making it safer to work with (iv) A more comparable air-fuel ratio of 14.6, 11.2 and 3.0 for gasoline, butanol and ethanol respectively (Dürre, 2007; Berezina *et al.*, 2009). More extensive comparisons between the fuel capabilities of butanol and ethanol as fuels can be found in previous studies (Dürre, 2007; Szulczyk, 2010; Surisetty *et al.*, 2011; Nanda *et al.*, 2017).

1.2 *Clostridia*: the native producers of butanol

Clostridia spp. are a vast collection of metabolically diverse, anaerobic, spore-forming bacteria. Many of bacteria within this group can utilise a range of substrates to produce important products through metabolic processes (Sun et al., 2018). One such process is the Acetone-butanol-ethanol (ABE) fermentation in which solventogenic *Clostridia* anaerobically ferment carbohydrate polymers using an array of glycosyl hydrolases to produce several acids, solvents and hydrogen (Li et al., 2020). With a focus on the butanol production in ABE, *Clostridium acetobutylicum*, *C. beijerinckii*, *C. saccharoacetobutylicum* and *C. saccharoperbutylacetonicum* are the most common microorganisms used in the process (Cho et al., 2012). *C. acetobutylicum* is a typical species used for ABE fermentation. *C. beijerinckii* is considered to be a good candidate for the utilisation of waste biomass / lignocellulose (which normally requires pre-treatment before it is suitable for fermentation) (Liu et al., 2010). Finally, *C. saccharoperbutylacetonicum* N 1-4 (HMT) has been shown to be a high butanol producing strain and has been used in CRISPR-Cas9 based engineering efforts (Tashiro et al., 2004; Wang et al., 2017). *C. saccharoperbutylacetonicum* N 1-4 (HMT) is often used in industrial fermentation, and because of this was chosen to be used in Chapter 5 for strain engineering. Fermentations using *C. saccharoperbutylacetonicum* N 1-4 (HMT) are typically between 48-72 h and produce solvent concentrations of ~15-17 g/L, with a final pH of 5.5-8 (Keis et. al, 2001).

During batch fermentation, *Clostridium spp.* undergoes two initial distinct phases of growth, namely the acidogenic and solventogenic (Gheshlaghi et al., 2009) (Figure 1.1). During exponential growth, the cells produce acetate and butyrate in the acidogenic phase and generate a surplus of ATP. Following the efflux of these acids, the extracellular pH decreases resulting in a cessation of acid production and growth (Huang et al., 1985). It is thought that acetate and butyrate act to induce expression of solventogenic enzymes and the switch to solventogenesis phase (Ballongue et al., 1985). The acids are

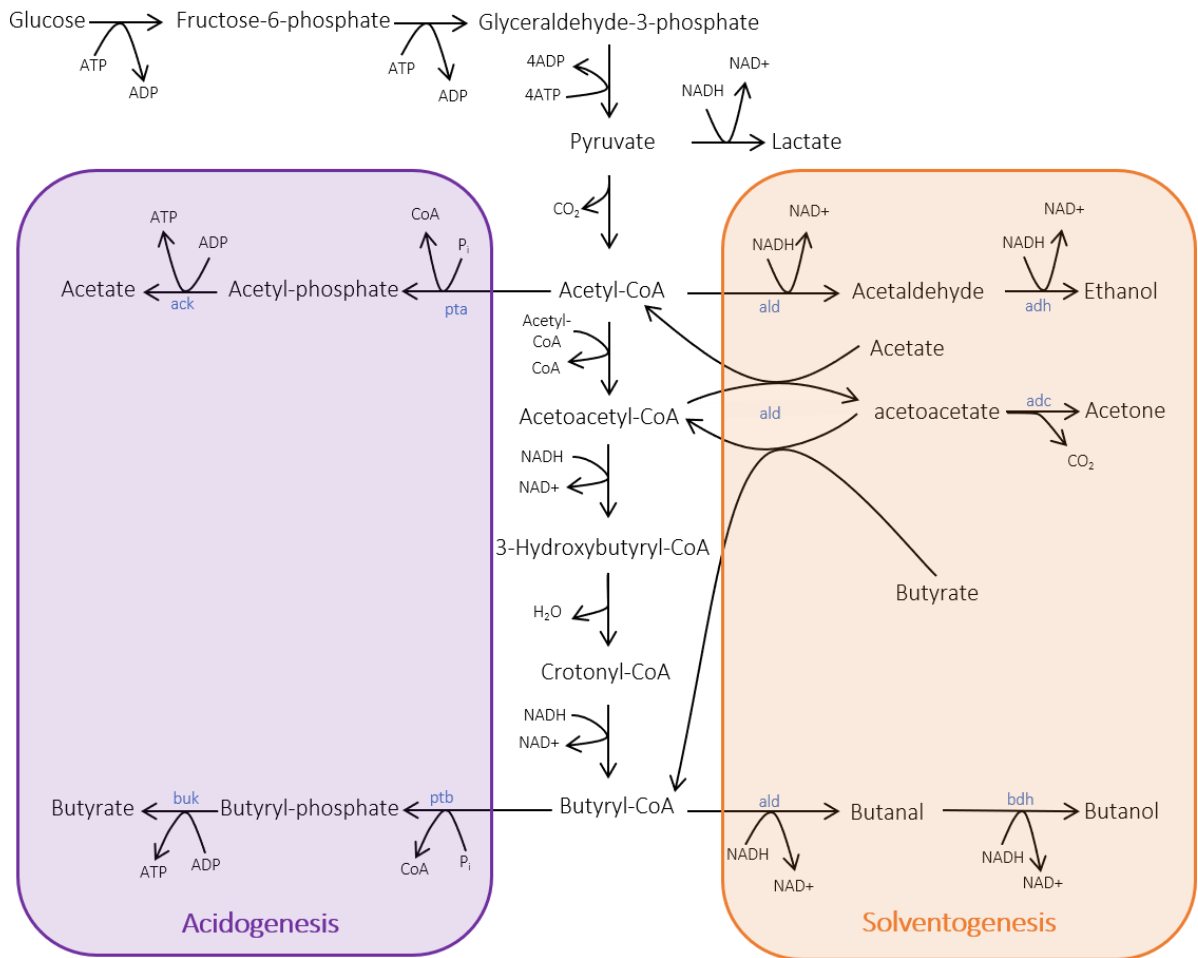


Figure 1.1 Simplified acetone-butanol-ethanol (ABE) fermentation pathway. Cells initially produce acetate and butyrate in acidogenesis during exponential growth. During stationary phase growth, *Clostridia* switch to solvent production as a survival mechanism in response to decreasing extracellular pH. Generally, acidogenesis and solventogenesis are two distinct phases of growth, however, in some strains overlap can occur. The left panel represents the acidogenic phase and the right panel represents the solventogenic phase. Selected enzymes are shown in blue: Acetate kinase (ack); aldehyde dehydrogenase (ald); Alcohol dehydrogenase (adh); acetoacetate decarboxylase (adc); butanol dehydrogenase (bdh); butyrate kinase (buk); phosphotransacetylase (pta); phosphate acetyltransferase (ptb).

then re-assimilated and act as co-substrates for solvent production in the solventogenic phase as coenzyme A derivatives (Agu *et al.*, 2018; Li *et al.*, 2020). This re-assimilation in turn increases the external pH, protecting the cells from the toxic low pH. Effective pH control of the fermentation medium is important. Rapid intracellular accumulation of excess non-dissociated acids (>57 mmol/L (Maddox *et al.*, 2000) can lead to an acid crash. Acid crashes prevent the switch to solventogenesis and result in cell death due to disruptions to the proton gradient (Wang *et al.*, 2011; Xue *et al.*, 2013). Acid crashes are caused by a very high metabolic / growth rate of *C. acetobutylicum* (Maddox *et al.*, 2000). During

stationary phase growth solvent production is inhibited following the transition into sporulation. This is another drawback of *Clostridia* and is an important consideration for engineering. However, sporulation encompasses a meticulously controlled series of events involving many enzymes, transcription factors and sigma factors. The molecular details of *Clostridial* sporulation, in particular how it influences solvent production, remain elusive increasing the difficulty of rationally designed engineering targeting sporulation. For example, the exact role of sporulation-specific sigma factors in solventogenesis is unknown (Jones *et al.*, 2011). It is thought that the switch between growth phases is controlled by the master regulator, Spo0A which could represent a possible opportunity to improve butanol production (Ravagnani *et al.*, 2000; Paredes *et al.*, 2005). In addition to solventogenesis, Spo0A regulates sporulation and knocking out Spo0A has been shown to increase butanol productivity and growth rates (Sandoval *et al.*, 2015). Alternatively, overexpression of Spo0A may initially increase levels of solvent production, cells will also undergo accelerated phase differentiation and enhanced sporulation which prevents solventogenesis (Xu *et al.*, 2014). Non-sporulating strains are considered to be a useful base organism for further engineering and refinement (Lütke-Eversloh and Bahl, 2011) as solvents are only produced during a short period of the sporulation cycle (Jones and Woods, 1986). This highlights the lack of knowledge surrounding fermentation and its regulation in *Clostridia*.

Engineering of other non-native microbes to produce butanol has also been pursued. This is owing to slow growth rates and a lack of understanding relating to genetic regulation and manipulation of the above *Clostridia* species. Whilst not having native butanogenic pathways, *Escherichia coli* and *Saccharomyces cerevisiae* are traditionally more genetically malleable than *Clostridia*, allowing for easier engineering of solvent production and tolerance. Early attempts at transferring butanol production pathways were successful but yielded low titre, for example *E. coli* (<1 g/L) (Shen *et al.*, 2011) and *S. cerevisiae* (2.5 mg/L) (Steen *et al.*, 2008). This suggests the solventogenic process is more complex than first anticipated, or resistance to pathway integration exists. The engineering of non-native produces offer a potentially fruitful path for developing excellent strain, with some showing superior yields to

Clostridia (Dong *et al.*, 2017). Non-native producers are still plagued with the same major hinderance present in convention ABE fermentation - butanol toxicity. *Clostridia* cannot survive in butanol concentrations >2 % (v/v), thus continuous gas stripping is required to remove butanol *in situ* (Chin *et al.*, 2017). *Clostridia* are obligate anaerobes and have complex metabolic regulations making them harder to work with than *E. coli* (Choi *et al.*, 2014; Eckert and Trinh, 2016). Additionally, there has historically been a lack of necessary molecular tools to enable *Clostridial* engineering (Cho and Lee, 2017; Agu *et al.*, 2018). However, with the advent of novel gene editing technologies like the CRISPR-Cas9 system (Li, Chen, *et al.*, 2016; Wang *et al.*, 2017) and advances in bioinformatics such as RNA-Seq (Wang *et al.*, 2009), developing deeper understanding and capabilities regarding metabolomic manipulation is possible.

1.3 Fermentation as a route to butanol

Humans have been utilising fermentative microorganisms as cell factories for several thousand years to produce food and beverages and more recently other products of high-value. As mentioned above there has been a trend towards synthesising butanol through a more sustainable process to reduce the dependence on fossil fuels. Acetone-butanol-ethanol (ABE) fermentation (Figure 1.1) was one of the first fermentation processes to be discovered, being reported by Louis Pasteur in 1861. Large scale ABE fermentation began in 1916 following the large demand for acetone during the First World War. Throughout the interwar period, butanol was used in the growing automobile industry; however, the ABE focus shifted back to acetone production during the Second World War (Sauer, 2016). Following the Second World War, interest in the ABE process declined due to competition from the cheaper petrochemical production of butanol (Jones and Woods, 1986). Recently, there has been renewed interest in the use of the native producers *Clostridium spp.* to obtain butanol as a high-value chemical and an alternative biofuel; with several international enterprises taking interest (see above) (Berezina *et al.*, 2009). This is in line with the global community becoming more conscious about the negative ramification of convention fossil fuel usage - with butanol production exemplifying the international

effort to build a greener chemical industry. Despite a huge amount of progress being made in the past century, there still remain several fundamental drawbacks which hamper the ability for ABE fermentation to economically rival petrochemical production. There are issues present throughout the entire process of butanol production by ABE fermentation, all of which will need to be addressed and mitigated if fermentation is to become economically competitive. The sourcing of suitable feedstock at a low price which will not influence the food industry, product inhibition and toxicity, strain engineering, fermentation optimisation and downstream product recovery are all areas for improvement to improve butanol yields and reduce associated costs (Li *et al.*, 2020). This thesis investigates the problem of product toxicity and the effects of butanol on the cell membranes of the solventogenic *Clostridia*. Butanol is known to interact with the cell membrane of *Clostridia* based on previous research, however there is a lack of understanding surrounding the precise effects on the cell membrane and the how the composition of the membrane can play a role in mitigating butanol perturbation. The membrane of solventogenic *Clostridia* represents a major focal point for research and engineering.

1.3 Cell envelope properties and architecture

1.3.1 Cell wall

The cell envelope it is comprised of cell wall and membrane(s). Gram-positive bacteria have a single, cytoplasmic membrane and a thick peptidoglycan cell wall. Gram-negative bacteria differ by having a thinner layer of peptidoglycan and a second, external membrane, termed the outer membrane (OM) which has a different composition to the cytoplasmic membrane (discussed later, 1.3.2 Cell membranes). The cell wall consists of crosslinked peptidoglycan polymers, which in turn are made up of alternating monosaccharide residues β -1,4-linked N-acetylglucosamine (GlcNAc) and N-acetylmuramic acid (MurNAc). The strength of the cell wall comes from the multidimensional covalent bonds which peptidoglycan can form, creating a strong, cross-linked, mesh-like structure. The cell wall is integral in withstanding intracellular pressure and maintaining the shape of the bacterium and is hence vital for cellular longevity (Scheffers and Pinho, 2005).

Despite it being an important component of the cell envelope, there has been little study into the effects of butanol on peptidoglycan. Fletcher and colleagues (2016) have shown 2-5 % (v/v) butanol resulted in cell wall bleb formations in *E. coli*, a characteristic of cell wall damage. The exact mechanism of this damage is unclear – it may be due to denaturation of peptidoglycan biosynthesis enzymes (these enzymes have been seen to be upregulated in solvent stress (Atsumi *et al.*, 2010). At these concentrations cells could not sustain growth, suggesting there is another, more potent effect of butanol which occurred at a lower concentration (<2 % (v/v)) before any major cell wall damage. Using enzymatic and fluorescence assays and microscopy, cells were seen to be elongated and both the cytoplasmic membrane and the OM were perturbed at lower butanol concentrations (1 % (v/v)). This may support an alternative mechanism – one where damage to the membranes results in subsequent damage to the cell wall at higher butanol concentrations.

Based on bond length calculations, the length of one molecule of butanol is ~ 0.8 nm. The pore size of the smallest peptidoglycan pore is ~7 nm (Meroueh *et al.*, 2006), much larger than butanol. This means that butanol can likely diffuse through the pores of crosslinked peptidoglycan unencumbered, and damage to the cell wall would only occur in a minimal way. It is probable that another element of the cell would give way before the cell wall, and that peptidoglycan damage at biologically relevant concentrations (< 30 mg/ml butanol) would occur indirectly. Further research into this area may prove useful, especially with the creation of more tolerant stains, in which peptidoglycan damage might become a limiting factor. However currently, the lipid membranes and entities within are still the predominant location in which butanol damages the cell envelope, and where cells are most susceptible. Because of this membrane engineering should take precedence over the rest of the cell envelope.

1.3.2 Cell membranes

The cellular membranes present in both Gram-positive bacteria (e.g. *Clostridia*) and Gram-negative bacteria (e.g. *E. coli*), are integral components of life and are responsible for compartmentalising the cytoplasm from the extracellular space. This maintains ion gradients and prevents the loss of resources needed from metabolism, it also acts to protect the cell from environmental stressors. Due to the importance of the cytoplasmic membrane, cells are extremely susceptible to chemicals which target and perturb its equilibrium, one such chemical being butanol.

The cytoplasmic membrane of bacteria is comprised of lipids and proteins in similar proportions by mass (Strahl and Errington, 2017) (See Figure 1.2). Membrane proteins have diverse structures and roles in a cell from regulating movement of substances over the membrane to biosynthesis and cell signalling. Integral proteins are permanently associated with the membrane and include transmembrane proteins such as transporters. Alternatively, some integral proteins do not span the full length of the membrane

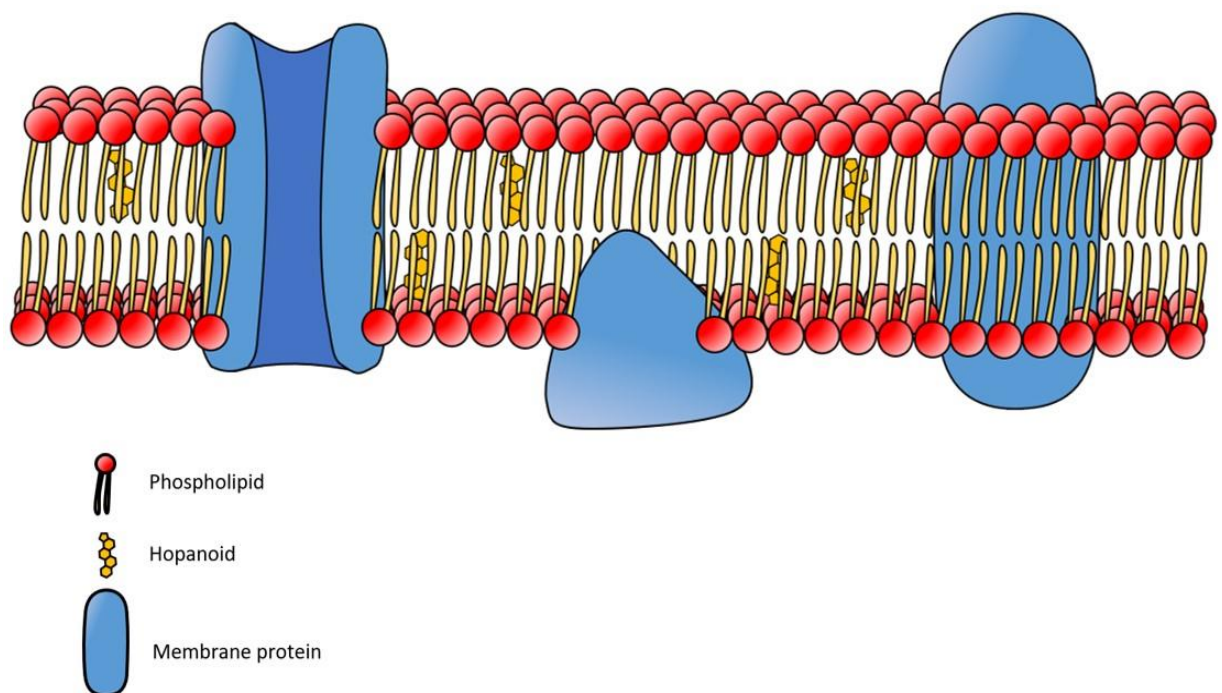


Figure 1.2 Simplified biological membrane. Membranes contain several different lipid and protein species and are roughly equal parts by mass protein to lipid. The function of a membrane is to compartmentalise the internal regions of the cell from the extracellular space and is vital for life. Due to this importance, cells are especially susceptible to xenocompounds which disrupt its structure.

and only associated with one leaflet such as *cis-trans* isomerase (CTI) (Holtwick *et al.*, 1997). Peripheral proteins transiently interact with the membrane via electrostatic or hydrophobic mechanism and have a diverse role. An example would be glycosyltransferases responsible for cell wall synthesis. In Gram-negative bacteria some membrane proteins can span the entire length of the periplasm, bridging the cytoplasm to the extracellular space. These mainly include nutrient transporter and efflux systems. Despite the crucial role of membrane proteins, the effect of butanol on their structure and function is not well documented. Membrane proteins may represent a useful target for engineering strains - through increasing the robustness of the proteins or through overexpression of proteins designed to mitigate solvent stress, such as butanol transporters. The other major component of the cytoplasmic membrane is the lipid portion which gives the cell the ability to compartmentalise, important for maintaining ion gradients and preventing the loss of compounds crucial for life. Due to its hydrophobic core, ions and most hydrophilic molecules are unable to diffuse across the membrane, allowing for the regulation of important conditions such as pH and salt concentration. Bacteria have incredibly diverse membrane compositions depending on their environment. Variations exist between species and even down to individual cells within a population of the same species. Generally, bacteria possess a large array of amphipathic lipid including phospholipids, the most common of which being phosphatidylethanolamine (PE), phosphatidylglycerol (PG) and cardiolipin (CL) and the less common phosphatidylcholine (PC), phosphatidylinositol (PI) (Figure 1.3). Other lipid components in the membrane include glycolipids, sphingolipids and hopanoids. The composition of the membrane is subject to internal and external factors and is one of the most adaptable features of bacteria in response to less than ideal conditions (Sohlenkamp and Geiger, 2016). Phospholipids are generally the most frequent form of lipid found within a bacterial membrane (Figure 1.3). They are comprised of two acyl chains which are linked with an ester linkage to a glycerol moiety (other linkages are possible, for example plasmalogens have a vinyl ether linkage on one of their acyl chains). The glycerol moiety connects to a phosphate group linked to a variable head group. Variation can occur within the acyl chains such as chain length, saturation, and branching; and also, within the specific head group. These

variations will alter the physiochemical properties of the individual lipid and will influence the characteristics of the overall membranes.

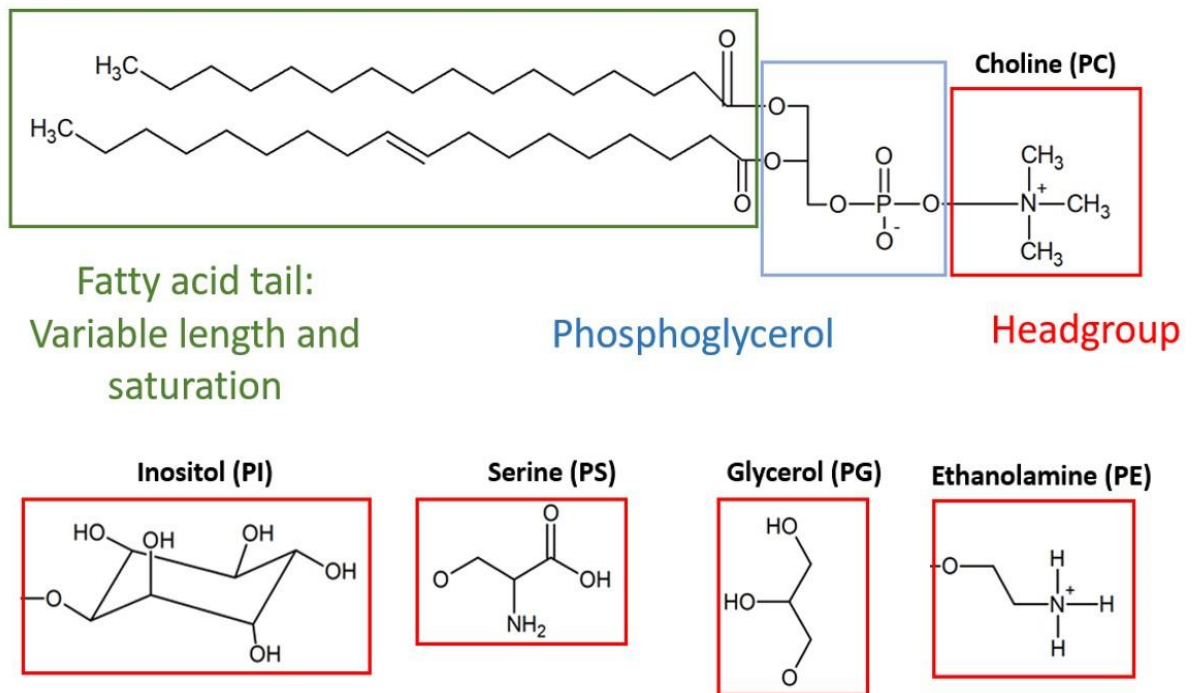


Figure 1.3 Phospholipids and phospholipid headgroup structure. The phospholipid shown is 1-palmitoyl-2-oleoyl-sn-glycero-3-phosphatidylcholine (POPC). The red boxes denote a selection of the different headgroups possible. Each headgroup will alter the shape and characteristics of the phospholipid. This will in turn influence the properties of the membrane.

The headgroup region of a phospholipid determines bilayer surface chemistry and has a lesser (albeit still important) impact on phase behaviour. This region is polar and can be neutral or charged depending on the pH. At a pH of 7.0 PE and PC are neutral, and PG, CL and phosphatidylserine (PS) are negatively charged. The headgroup can also influence the shape and area of a lipid molecule, and therefore what aggregated structure it will form in an aqueous environment. A typical polar head group composition of a *Clostridial* cytoplasmic membrane is 50-75 % PE, 25-40 % PG and CL, with other minor species in lower amounts (Durre, 2005). However as stated earlier, this is subject to the environment and the specific bacterial species in question. Generally a 75 % PE and 25 % PG is considered to be a good mimic of a bacterial cytoplasmic membrane (Murzyn *et al.*, 2005).

1.3.2.1 Bacterial membrane lipid synthesis

Early work investigating the biosynthesis of phospholipids and fatty acids was carried out in *E. coli* as a model organism for bacteria. Despite many parallels, it has become apparent that these pathways are not common to all bacteria and that there is a great deal of diversity among different species (Parsons and Rock, 2013). For recent reviews on bacterial lipid synthesis see (Parsons and Rock, 2013; Yao and Rock, 2017; Tang *et al.*, 2018; Geiger *et al.*, 2019). Bacteria make the fatty acid elements of their phospholipids through a process known as type II fatty acid synthesis (FASII). The first step is the carboxylation of acetyl-CoA by acetyl-coA carboxylase (ACC) to form malonyl-CoA, which is then converted to malonyl-ACP. FabH catalyses the condensation of malonyl-ACP with acyl-CoA to form acetoacyl-ACP, which in turn goes into the elongation cycle where the chain length is increased by 2 carbons per cycle (Figure 1.4). The acyl-ACP can then be transferred to G3P to make phospholipid precursors (Parsons and Rock, 2011). Unsaturated bonds can be added to the growing acyl chains through an anaerobic mechanism before they are attached to G3P (Geiger *et al.*, 2019). FabA, FabB and FabM are responsible for the anaerobic synthesis of unsaturated bonds in bacteria, however these enzymes are absent in *Clostridia*. It was proposed that *Clostridial* FabZ may have been able to shuffle acyl chains between the saturated and unsaturated pathways, however FabZ was found to be unable to synthesise unsaturated intermediates, and unsaturation occurs via an unknown mechanism (Zhu *et al.*, 2009; Parsons and Rock, 2013). A FabF homologue was able to replace FabB and FabF in *E. coli*. (Zhu *et al.*, 2009) and has also been suggested to be involved in unsaturation (Patakova *et al.*, 2019). Some bacteria are able to introduce an unsaturated bond into a phospholipid which has already been synthesised. *B. subtilis* can introduce a *cis* double bond using DesA (Δ -5-desaturase) a process which is oxygen dependent (Geiger *et al.*, 2019). *P. aeruginosa* have an analogous enzyme, DesA (Δ -9-desaturase). Further modifications to these unsaturated bonds are possible. Cyclopropane fatty acid synthase can methylate an unsaturated bond leading to cyclopropane group (Zhao *et al.*, 2003). A less prevalent post-synthesis modification would be the conversion of the geometric isomerism from *cis* to *trans* catalysed by CTI. It is unknown whether *Clostridia* are capable of this conversion. It is thought that

plasmalogen synthesis in bacteria is a result of direct modification of the 1-acyl chain of a phospholipid. Firstly, this would be a reduction of the ester linkage forming an intermediate. The vinyl ether linkage is then formed by the elimination of a water molecule. Recently CarF has been discovered which is responsible for plasmalyethanolamine synthesis in bacteria (Gallego-García *et al.*, 2019).

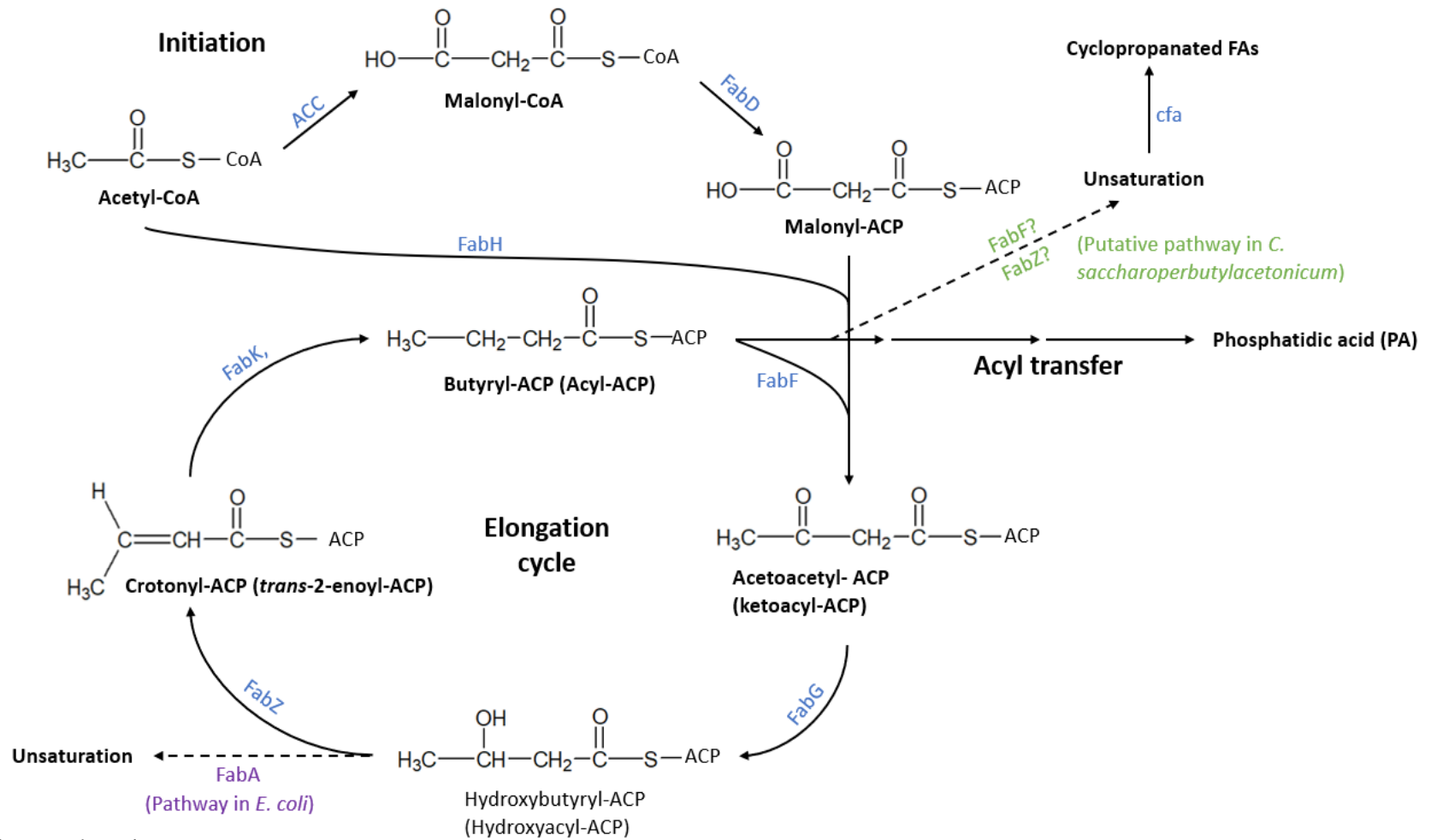


Figure 1.4 Type II fatty acid synthesis.

The first steps in the process involve the generation of malonyl-ACP via the carboxylation of acetyl-CoA by ACC, and subsequent transfer of the malonyl group to ACP. Fatty acids are synthesised by the repetition of the elongation cycle. This cycle begins with the condensation of malonyl-ACP with acetyl-CoA. Enzymes are in blue. Enzymes present in *E. coli* responsible for unsaturation are in purple. Putative pathways or enzymes in *Clostridia* in green.

The two major acyltransferase systems in bacteria are the PlsB pathway and the PlsX/PlsY pathway. These are responsible for the transferal of acyl groups from carrier intermediates to G3P, initiating phospholipid synthesis (Yao and Rock, 2017). The PlsB pathway utilises acyl-acyl carrier protein (acyl-ACP) or acyl-coenzyme A (acyl-CoA) to acylate G3P and is found in *E. coli* and eukaryotes (Tang *et al.*, 2018). The PlsX/PlsY is the alternative, and more widespread pathway found in other bacteria in which PlsX transfers acyl groups from acyl-ACP to acyl-PO₄, followed by PlsY transferring the fatty acid to G3P (Parsons and Rock, 2011). The second acyl chain is added by PlsC (Geiger *et al.*, 2019). Phosphatic acid (PA) is the universal precursor of phospholipids. The acylation of glycerol-3-phosphate (G3P) forms lysophosphatidic acid (lysoPA) which then after a second acetylation results in PA (Tang *et al.*, 2018). PA is a minor component of bacterial membranes and the vast majority is used in the production of other phospholipid species. PA reacts with cytidine triphosphate (CTP) to form cytidine diphosphate-diacylglycerol (CDP-DAG). Various molecules, such as serine, choline and G3P can then attack CDP-DAG to form the respective lipid classes. Some of the resulting lipids generated are then subject to further modifications through decarboxylation and dephosphorylations. The reactions are summarised in Figure 1.5. Phosphatidylserine synthase (PssA) represents an attractive locus for manipulation of phospholipid synthesis – upregulation should lead to more PS, PE, and PC whereas a PssA KO should lead to more PG, CL, and inositol derivatives.

The acyl chains are the main determinant of membrane fluidity and phase behaviour due to the interactions between adjacent acyl chains. Individual interlipid forces are not strong, however the sheer number of them accounts for their ability to form a stable bilayer. The most common length of chain is 14-20 carbons but can be as low as 12 carbons and high as 24 carbons (Denich *et al.*, 2003). Acyl chains are commonly even numbered due the addition of two carbons during synthesis by an elongase enzyme, however odd chain lengths are also present (Denich *et al.*, 2003). In general, one of the two acyl chains will be saturated and the other will have at least one unsaturated bond. Multiple unsaturations in one chain are possible but rare. Additionally, the geometric isomerism of an individual double bond (*cis* or

trans) is subject to change. Other modifications to the chains exist - methyl group branching occurs in <5 % *Clostridia* (Durre, 2005) but can be much more prevalent in other species (Denich *et al.*, 2003). Cyclopropane fatty acids derived from monounsaturated acyl chains are also found in some *Clostridia*. This breadth in components of membrane lipids enables bacteria to adapt to adverse conditions that perturb the membrane. This is achieved through alterations to the above functional groups (through *de novo* synthesis or enzymatic catalysis) which in turn will lead to a change in the properties of the lipids and thus, the membrane.

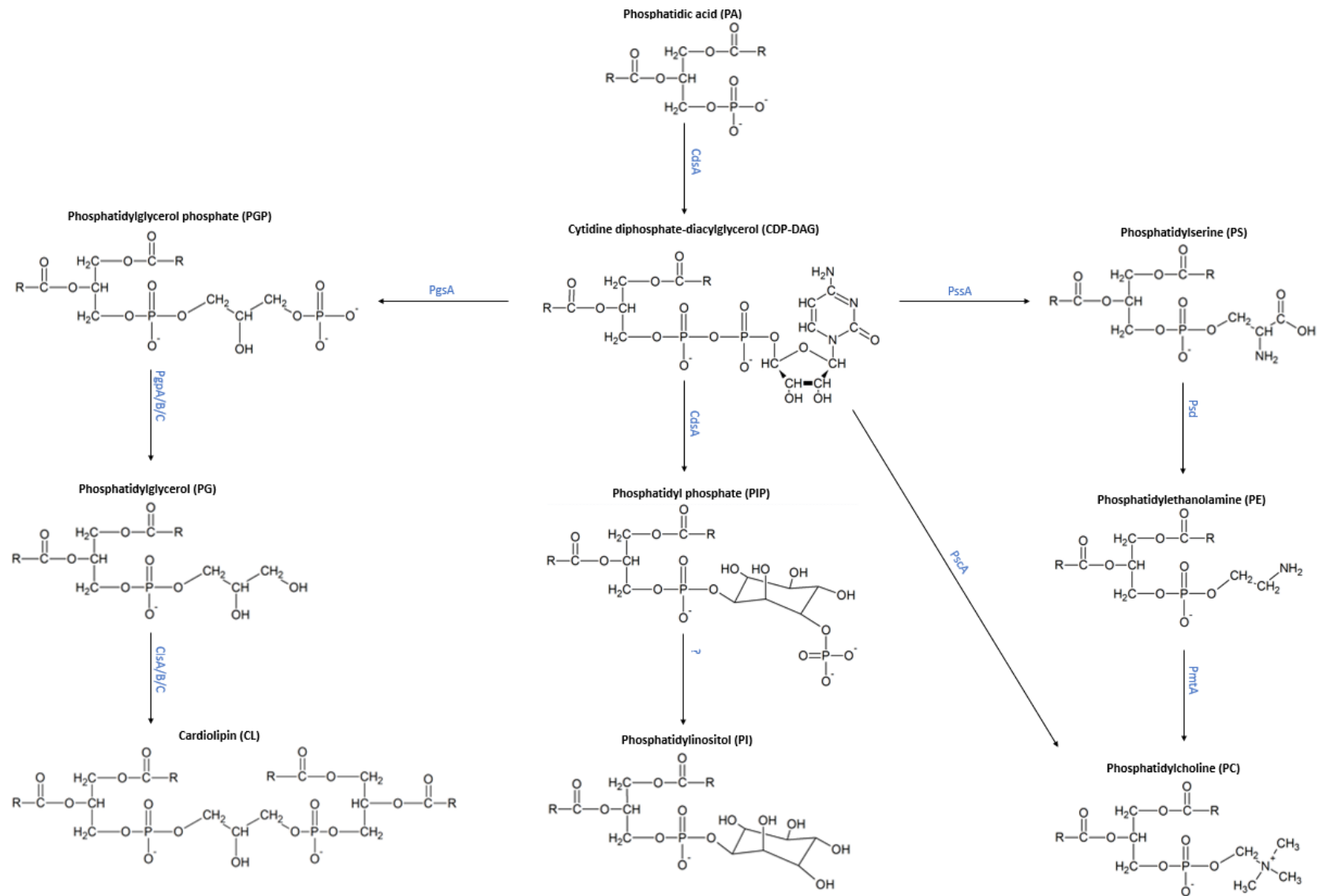


Figure 1.5 Phospholipid headgroup synthesis in bacteria. Different headgroups will impact the properties of the phospholipid and therefore the overall membrane. Manipulating the expression of these enzymes relative levels of will therefore change the characteristics of the membrane. Because of this they represent a possible route for strain engineering. Enzymes are in blue. Not all enzymes are present in *Clostridia*

1.3.2.2 Membrane properties

Membrane fluidity is a measure of viscosity and can affect the lateral diffusion and rotation of lipids and proteins within the bilayer. It can also be defined as the relative motility of an individual entity in the bilayer. Homeoviscous adaptation is the process through which bacteria modulate the membrane to maintain a balance between being too fluid and too rigid. Fluidity is determined by how well the lipids pack together, which in turn is determined by the shape of the lipid molecule and is thus a result of the head group and acyl chains. Increasing the length of the acyl chains and the degree of saturation will increase the number of interlipid Van de Waals forces. This will increase the amount of energy required to break these bonds and cause a phase transition. The degree and isomerism of unsaturation also has a bearing. The presence on a *cis* unsaturated bond will result in a 30° kink in the acyl chain (similarly with branched chains). This disrupts the ordered packing of the lipids, introducing spaces inbetween them and allowing for more flexible movement, ultimately resulting in reduced the lateral interactions. *Trans* isomers do not cause a kink and are thought to behave more like a saturated chain. Additionally, different headgroups can have more minor impact on lipid packing and phase behaviour.

The packing of lipids also impacts various mechanical properties such as bending, stretching, compressibility, bilayer thickness and resistance to sheer stress (Denich *et al.*, 2003). There is an optimal range of fluidity within which lipids and proteins are free enough to move, without compromising the integrity and permeability of the membrane. Fluidity is constantly changing due to myriad environmental factors and bacteria aim to maintain the homeoviscosity of their membranes. This can be done through altering the lipid composition to be more rigid or fluid with for example, acyl chain length or saturation. The phase behaviour of a lipid system is related to the overall fluidity of the membrane and the liquid crystalline phase is considered to be the biologically active and desired phase state of the membrane (Figure 1.6). In a solid, or gel state, acyl chains are fully extended and more constrained, and diffusion and rotation occurs less frequently. This reduces the ability of cells to localise proteins and repair holes formed in the membrane. The transition between phases will occur at a specific temperature, based on lipid composition and environmental influences. The most biologically

relevant transition is the of the solid-liquid crystalline transition. This transition is accompanied by increased chain disordering, increase headgroup hydration and an increase in area per lipid (Koynova and Tenchov, 2013). A large amount of energy is required to overcome the many Van de Waals interaction between adjacent lipids, a process which can be measured using differential scanning calorimetry where transitions manifest as sharp peaks.

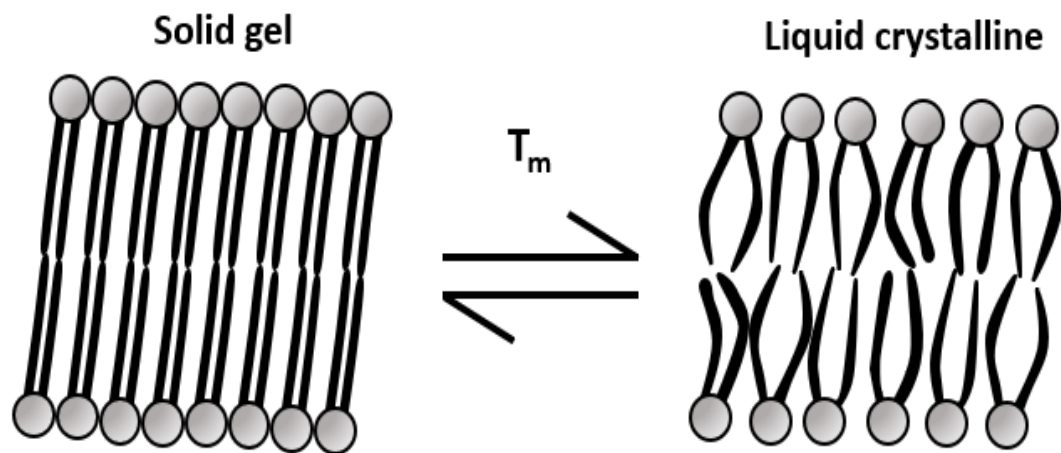


Figure 1.6 Phospholipid membrane phase behaviour. In the solid state phospholipids have a greater degree of adjacent interaction and are thus more constrained, and diffusion and rotation occurs less frequently. This phase occurs at lower temperatures. The liquid crystalline phase is characterised by more freely moving chains and lateral diffusion within the membrane. This phase occurs at higher temperatures and is more fluid. Cells will have an ideal level of membrane fluidity which they modulate through homeoviscous adaptation. T_m denotes the temperature at which the phase transition occurs. Compounds, such as butanol, which interfere with the macro-behaviour of phospholipids will also change the point of phase transition. Additionally, this will impact the broader properties of the membrane leading to altered membrane functionality.

Different lipids may localise together in a membrane resulting in discrete domains, such as CL localised domains at the polar regions of *E. coli* (Mileykovskaya and Dowhan, 2000). It has been suggested that the localisation of CL is due to a lack of miscibility with PE and that this domain formation is important for maintaining overall cell shape in *E. coli* (Malanovic and Lohner, 2016). These domains have different properties and can be functionally specific. They are can be determined by different headgroups, local fluidities and curvature (Epanand and Epanand, 2009; Strahl and Errington, 2017). It has been hypothesised that certain antimicrobials can interact with the membrane and disrupt the organisation of domains, potentially leading to a reduced barrier function (Epanand and Epanand, 2009).

Hopanoids are pentacyclic sterol-like molecules and are an example of a non-phosphate containing neutral lipids comprising 1-90 % of lipid in bacterial membranes depending on species and growth conditions (Belin et al., 2018) (See Figure 1.7).

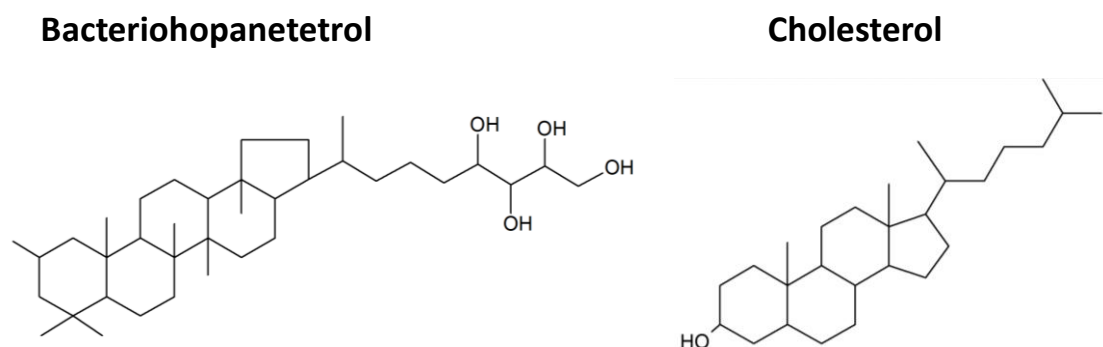


Figure 1.7. The structures sterols of the hopanoid bacteriohopanetetrol (left), and cholesterol (right). Both are sterol-based membrane entities which play a role in regulating membrane fluidity and can influence other membrane properties. Due to difficulties sourcing a bacterial hopanoid, cholesterol was used as a surrogate in these experiments.

Akin to sterols in eukaryotic cells, hopanoids regulate the fluidity of the membrane (Denich *et al.*, 2003). Despite their similarities, the membrane-related effects of hopanoids and sterols are not identical. Hopanoids were found to only partially compensate for a lack of cholesterol in *Mycoplasma mycoides*, with cells having a reduced growth rate when using hopanoids a sterol replacement (Kannenberg and Poralla, 1982). Hopanoids can reduce the area per lipid and decrease permeability whilst maintaining

fluidity and compressibility (Mangiarotti *et al.*, 2019), and thus may be involved somewhat in butanol tolerance. Diversity of hopanoid structure can influence how they pack into a membrane and interact with lipids, potentially also their distribution in the membrane (Belin *et al.*, 2018). This can alter the hopanoids effect on membrane characteristics and give them more nuanced functions. For example, simulations of an extended hopanoid, bacteriohopanetetrol, was shown to orient vertically in bacterial membrane causing lipids to condense (Poger and Mark, 2013). Diploptene on the other hand was found inbetween the two leaflets and may reduce permeability (Poger and Mark, 2013; Belin *et al.*, 2018). Hopanoids are involved in stress tolerance in bacteria. The content of extended hopanoids was found to correlate with increasing temperature in thermophilic *Bacillus acidocaldarius*, probably due to its ability to rigidify the membrane, combating the higher temperatures. In *Zymomonas mobilis* mutants with disrupted hopanoid biosynthesis genes had significantly lower survival rates in 20% ethanol compared to wild types. Additionally, in liposome models it was found that hopanoids protected against lipid interdigitation and bilayer dissolution caused by ethanol (Brenac *et al.*, 2019). It has also been suggested that hopanoid function is not limited to membrane properties but may also effect membrane protein function - hopanoid deletion was found to impair energy dependent efflux (Sáenz *et al.*, 2015). Due to their role in membrane fluidity, there has been speculation about a potential application of hopanoid in strain engineering in response to adverse environments (Guo *et al.*, 2019). Tuning expression may allow for control over fluidity with the view to mitigate the detrimental effects of membrane active high-value chemicals.

1.3.2.3 Bilayer asymmetry

Phospholipids are amphipathic in their structure, having an apolar region (acyl chains) and a polar region (head group). When exposed to an aqueous environment, phospholipids will spontaneously self-assemble into a two-leaflet structure with the headgroups of the phospholipids in contact with the aqueous solvent. This shields the apolar region of the phospholipid from the aqueous environment and creates a hydrophobic barrier separating internal and external regions of the cell. This formation is

driven by hydrophobic interactions and the overall structure of the membrane is maintained by non-covalent interaction. Because of this the membrane's integrity is susceptible to compounds which can interfere with the interactions between the lipids within the membrane. The two leaflets of phospholipid bilayer can be asymmetrical, having a varied lipid composition. The exact reason for asymmetry is unclear, although it likely arises from exposure to different environments and may act as a mechanism for the cell to control membrane-linked functions through changing lipid compositions (Fadeel and Xue, 2009). Having different lipids in each leaflet may impact various membrane properties including: surface charge and membrane potential, shape and permeability (Marquardt *et al.*, 2015). The propensity of specific lipid species to interact with certain proteins and other entities exposed to the leaflet in question is also a factor. Another reason for asymmetry is the very high energy barrier which must be overcome if a phospholipid from one leaflet is to spontaneously move into the other. Following *de novo* synthesis most lipids are inserted into the cytoplasmic leaflet; flippases and floppases are a group of ABC transporters which move lipids between the leaflets enabling the generation and maintenance of asymmetry (van Meer, 2011; Marquardt *et al.*, 2015). Asymmetry exists in bacteria, a particular example being the outer membrane of Gram-negative bacteria. A phospholipid leaflet is exposed to the intracellular region whilst the opposite leaflet contains lipopolysaccharide residues. Asymmetry is maintained through the targeted degradation or conversion of unwanted lipid species and active transport (May and Silhavy, 2017).

1.3.2.4 Outer membrane

The composition of the OM in Gram-negative bacteria is different to the cytoplasmic membrane. The inner leaflet of the OM contains phospholipids whilst the outer leaflet is made up of lipopolysaccharide (LPS) monomers, containing glycosylated lipid A molecules (Koebnik *et al.*, 2000). LPS monomers laterally associate with each other and use divalent cations as coordinator ions to stabilise LPS (Clifton *et al.*, 2015). Gram-negative cells can increase their hydrophobicity to promote biofilm formation following environmental stressors (Baumgarten *et al.*, 2012). This is achieved through bulging of the OM

regions containing hydrophilic LPS residues and their eventual secretion in vesicles leaving a more hydrophobic OM (Eberlein *et al.*, 2018). LPS has also been shown relate to butanol tolerance - lower charge densities of LPS enables a greater degree of butanol insertion into the OM and results in reduced growth in *E. coli* in butanol compared to WT LPS (Guo *et al.*, 2020). Additionally, longer LPS cores appeared to be more effective barriers to butanol entry in the OM.

1.4 Butanol toxicity

1.4.1 Mechanisms of butanol toxicity

A major route of solvent toxicity is through the phospholipid membrane and associated functions. Of the solvents produced in the solventogenic phase, butanol is most toxic, leading to more membrane destabilisation compared to other short-chain alcohols (Ly and Longo, 2004). This is because there is a general trend of increased toxicity with greater hydrophobicity (longer chain lengths) (Rutherford *et al.*, 2010). Butanol is an amphipathic solvent - the polar hydroxyl (–OH) group can associate with polar head groups of phospholipids. Additionally, the aliphatic tail of butanol can insert into the phospholipid tails of the membrane, disrupting their ordering and inter-lipid Van der Waals forces, resulting in increased membrane fluidity (Kurniawan *et al.*, 2013) (See Figure 1.8).

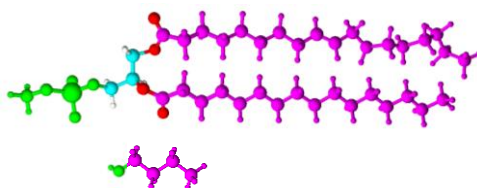


Figure 1.8 The structures butanol (below) and palmitoyl-oleoyl-phosphatidylethanolamine (POPE) (above). Regions of the same colour interact with each other. Green regions represent the polar headgroup of the POPE and the hydroxyl group of butanol. Magenta regions represent the apolar hydrocarbon chain

Butanol is thought to partition into the membrane and disrupt phospholipid packing leading to destabilisation, thinning and an increase in lateral diffusion and fluidity within the membrane (Vollherbst-Schneck *et al.*, 1984). A recent study from Guo and others (2019) showed butanol to interact

preferentially with the phospholipid headgroup, causing thinning of the membrane and acyl chain splaying. Exposing *Clostridium acetobutylicum* to sub-inhibitory concentrations of butanol (<1.5 % (v/v)) resulted in an increase in membrane fluidity of between 20-30% (Vollherbst Schneck *et al.*, 1984). Dysregulation of membrane fluidity can lead to leakage of intracellular components and the disruption of the maintenance of ion gradients over the cell membrane (Sandoval and Papoutsakis, 2016). Butanol can also negatively impact membrane linked-functions and energy metabolism at concentrations below those which would cause disruptions to ion gradients (Wang *et al.*, 2005). Based on the chaotropic effects (disrupts hydrogen bonding) on the membrane, butanol indirectly inhibits glycolysis by interfering with sugar uptake via the PEP group translocation system. This is supported by Bowles and Ellefson (1985) who found that butanol exerts a pH-independent reduction in ATP production coupled with reduced glucose uptake. In *E. coli*, respiration may also be inhibited through the inhibition of quinone, the electron-carrier membrane protein (Brynildsen and Liao, 2009). Membrane proteins are also susceptible to damage from butanol. Despite making up a significant portion of the cell membrane, there has been a lack of research surrounding their interactions with butanol. The correct folding of a protein is vital to its structure and as an extension, its function. Membrane protein folding is influenced by the lipid portion of the membrane, which are able to laterally diffuse within a leaflet (Maurya *et al.*, 2013). Factors such as membrane fluidity and lateral pressure and bilayer microdomains can all impact the folding of a membrane protein (Simons and Ikonen, 1997; Phillips *et al.*, 2009; Lucena *et al.*, 2018) . It is unknown whether disruptions to membrane proteins are a result of direct interactions with said proteins, or an indirect secondary phenomenon stemming from the disordered lipids.

Oxidative stress may be another mechanism of toxicity. Through using fluorescent dye assays (Carboxy-H2DCFDA), Rutherford and others (2010) saw an increase in reactive oxygen species (ROS) in *E. coli* following 0.8 % (v/v) butanol exposure. This was accompanied by an upregulation of oxidative stress related genes, for example superoxide dismutase. ROS can directly attack cellular macromolecules, leading to chain reactions and further damage to DNA, protein and lipid (Sigler *et al.*, 1999). During lipid

peroxidation (oxidative degradation of lipids), a single initiation event can propagate and damage between 200 and 400 lipid molecules before the reaction terminates (Jones, 2008). Chin and others (2017) were able to improve butanol production in *E. coli* almost 3-fold by expressing tilapia metallothionein (TMT), a ROS scavenger. This would suggest that butanol production may result in an accumulation of ROS and that scavenging these can promote growth and tolerance. In anaerobic bacteria, the oxidative stress may come from ABE intermediates, such as aldehydes (see Figure 1.1).

A large amount of current knowledge regarding butanol-membrane toxicity has utilised homogenous membrane models, which may not entirely be reflective of the more complex, heterogeneous *in vivo* membranes (Kurniawan *et al.*, 2013). Different combinations of lipid species may have beneficial or detrimental effects in response to butanol exposure. For example, Kurniawan and others (2013) found that more butanol partitioned into DPPC:DOPC membranes and caused tilting and greater expansion with increasing DOPC content. This is likely due to the kinked tail in unsaturated lipids which occupies more space and alters the packing, making room for additional solvent molecules (Kurniawan *et al.*, 2012). Similarly, Bothun and colleagues (2016) show that the presence of exogenous unsaturated fatty acids increases butanol partitioning more than exogenous saturated fatty acids. This highlights the importance of investigating mixed lipid membranes and their effects on butanol tolerance.

Greater understanding of butanol toxicity will enable the generation of more tolerant strains, ultimately allowing for more butanol to be more competitive with conventional fossil fuels. The advantageous properties and similarities with gasoline make butanol an attractive alternative to ethanol and gasoline. However, widespread butanol production is hindered by the lack of a high-producing and highly-tolerant strain (Fischer *et al.*, 2008). Research into the production of more tolerant and higher producing strains will enable butanol's development as a biofuel. Some strains have been engineered to be extremely tolerant to butanol, but produce lower yields limiting their industrial application (Zhao *et al.*, 2003), suggesting there may be little association between tolerance and production (Liu *et al.*, 2013). Interestingly, there are several studies that have obtained high producing strains when screening for

tolerance. (Xue et al., 2013; Li et al., 2016). The maximum titres achieved by wild-type *Clostridia* are approximately 13 g/L (García et al., 2011) and solvent concentrations of ~15 g/L or above begin to inhibit cellular metabolism (Lee et al., 2008). Attempts to improve tolerance through mutagenesis have been successful, with several strains being able to produce titres of 17-21 g/L (Patakova et al., 2017). A deeper understanding of butanol toxicity and tolerance is necessary to produce new and modify current high producing and high tolerant strains (Patakova et al., 2017). A multi-disciplinary approach to this is encouraged, encompassing areas including the effect of butanol on the lipidome and membrane composition, and the identification of novel butanol transporters. The high level of toxicity often results in low yields which, in turn, increases the cost of down-stream processing and purification per unit of butanol. Hence, understanding the various mechanisms of butanol toxicity and the ways in which cells react to butanol is an important step in engineering tolerance. These effects can be investigated in cellular models, such as liposomes allowing for rational strain design. Promoting tolerance in solventogenic microorganisms will enhance the bio-production of butanol as an alternative to conventional fossil fuel routes.

1.4.2 Measuring butanol toxicity at the membrane

There exists an array of *in vitro* models which if applied appropriately can shed light the relationship between butanol and the cell membrane and its constituents. Liposomes represent a useful model of microbial membranes which can range from simple, single lipid mixes to more complex multi-lipid compositions which more accurately reflect an *in vivo* membrane (Routledge et al. 2019). Biophysical properties such as membrane fluidity, membrane permeability, and liposome diameter were investigated in Chapter 3. These data were used to inform strategies for engineering bacterial membranes *in vivo* to mitigate the detrimental impact of butanol on the lipid portion of the membrane. Carboxyfluorescein (CF) dye release assays were used to investigate membrane integrity and permeability. More than 97 % of fluorescence is quenched at 200 mM (Raymond et al., 1988). CF is loaded into liposomes at these high concentrations following rehydration of lipid films with an aqueous

CF solution. Unincorporated CF on the outside of the liposomes can be removed by a series of centrifugation and wash cycles - resulting in CF-containing liposomes in buffer. Butanol can then be applied to investigate any impact on the permeability of the model system, as once CF dye leaks from the liposomes it becomes diluted and fluoresces. Thus, an increase in fluorescence is indicative of an increase in permeability. Laurdan is another fluorescent molecule which was used in Chapter 3 to investigate the fluidity of the membrane. The probe has both a hydrophilic region and a hydrophobic region causing there to be a dipole present and allowing it to integrate into the membrane whilst remaining in proximity to the solvent. Upon excitation of Laurdan, the dipoles of surrounding solvent molecules are reoriented, a process which requires energy and results in emission at a higher wavelength (fluorescence). The ratio of the intensities of excitation and emission wavelengths (general polarisation, (GP)) can show how exposed the probe is to the solvent, which is a proxy measurement of membrane fluidity. Dynamic light scattering is an optical technique allowing for the sizing of liposomes in solution and how butanol impacts this. Monochromatic light is fired at the sample causing the light to undergo Rayleigh scattering. The intensities of the scattering are recorded, and the fluctuations of these intensities is related to the Brownian motion of the liposomes in the sample (Hupfeld, 2006). Smaller particles will move more quickly resulting in greater fluctuations of scattering intensities compared with large particles which are slower. Using the Stokes-Einstein relationship and the Brownian motion, the size of the particle can be calculated (Bhattacharjee, 2016).

Bicelles are another model system which are formed when mixing long-chain lipid with detergents (Figure 3.1) and are useful in the study of membrane proteins. They form a “disc” of lipids surrounded by a border of detergent molecules. Bicelles have been used historically for the investigation of membrane protein structure; they are a good representative of a membrane whilst having advantageous properties for biophysical studies (Dürr *et al.*, 2013). In order to study the effects of butanol on membrane protein folding in Chapter 3, bacteriorhodopsin (bR) was reconstituted in DMPC / CHAPSO bicelles - the method was adapted from Chang and Bowie (2014). Two cysteine residues,

which are subsequently biotinylated, were added to bR at spatially close positions when the protein is folded. Upon addition of monovalent streptavidin (mSa) only one binding event between mSa and the biotin tags can occur. Binding of mSa to the second tag is prevented due to steric hinderance, however becomes available if bR unfolds, this also traps the protein in an unfolded state. When unfolded, there is also a reversible loss in retinal absorbance (an intrinsic chromophore in bR). Using the wavelengths stated in section 2.7.2 (particularly 560 nm for retinal) additional insight into the folded state of bR in the presence of butanol was able to be obtained (Schlebach *et al.*, 2012).

1.5 Cellular response to butanol

1.5.1 Changes to lipidome

As the membrane is a major site of butanol toxicity, the cell's stress response includes measures to stabilise and reduce fluidity mediated by butanol. Membrane fluidity generally refers to the ease of movement and encompasses factors such as: lateral diffusion, acyl chain flexibility and rotation (García *et al.*, 2005). A balance of fluidity is required to enable lateral diffusion and correct distribution of membrane bound entities, whilst being rigid enough to function as a barrier and maintain ion gradients (Venkataramanan *et al.*, 2014). To maintain optimal membrane fluidity in volatile environments, bacteria can adapt aspects of their lipidome through homeoviscous adaptation a process of homeostatic adjustment of their membranes in the face of non-ideal environmental conditions (Zhang and Rock, 2008).

Perhaps the most well know homeoviscous response is an alteration to the ratio of saturated to unsaturated lipids (sat:unsat). Several studies have noted an increase in sat:unsat in *Clostridia*, following exogenous butanol addition or during butanol production (Baer *et al.*, 1987; Lepage *et al.*, 1987; Isar and Rangaswamy, 2012). This trend has also been reported in *S. cerevisiae* under ethanol using gas chromatography-mass spectrometry, suggesting a common mechanism of protection against short-chain alcohols exists (Li *et al.*, 2012). In an extreme example, *C. beijerinckii* can completely sequester unsaturated lipid production (Huffer *et al.*, 2011). For organisms which cannot produce unsaturated

lipids, a decrease in the branched:unbranched lipids has been seen (Huffer et al., 2011). Membranes with a greater proportion of saturated fatty acids will be more ordered and rigid, with individual lipid molecules packing together better (as there are fewer unsaturated, kinked acyl chains). This enables stronger intermolecular Van der Waals forces and hydrogen bonding, reducing fluidity and countering the effects of butanol. This increase in sat:unsat is far more pronounced following exogenous butanol exposure, when compared to when butanol is produced by the cell (Kolek et al., 2015). Perhaps there is some form of prophylactic mechanism in place when cells are producing butanol to attempt to adequately protect the cell during solventogenesis. The ability to convert the geometric isomerism of double bonds between *cis* and *trans* is absent in *Clostridia* due to the lack of a CTI. The major classes of *Clostridial* lipids are: phosphatidylglycerol (PG), phosphatidylethanolamine (PE) and cardiolipin (CL) (Durre, 2005; Kolek et al., 2015). Lipidomics data from Kolek and others (2015) suggest that plasmalogens (vinyl-ether bond, *sn*-1 position (Braverman and Moser, 2012) are involved in the response of *C. pasteurianum* to butanol stress during fermentation, possibly acting to stabilise unsaturated membranes. The highest concentration of plasmalogens coincided with the highest production of butanol (mid-exponential). Cardiolipin (and its plasmalogens) have also been seen to be increased during ABE fermentation (Reyes et al., 2013; Tian et al., 2013) suggesting a role in the response to butanol (Reyes et al., 2013). Additionally, Tian et al., (2013) report in *C. acetobutylicum* that levels of mono-/digalactosyldiacylglycerol modified with ethanolamine-phosphate (Etn-P-glycolipids) were increased following exogenous octanol stress, possibly mediating increase membrane stability. It remains unclear from this study whether the increase in Etn-P-glycolipids manifested in improved solvent tolerance and growth rates comparably to cultures with no exogenous octanol. Furthermore, the effects on butanol on Etn-P-glycolipids were not investigated, however, this is likely because the resulting changes would be similar. Octanol was found to produce comparable changes to butanol regarding the sat:unsat in fermenting *C. acetobutylicum*, suggesting a common mechanism of toxicity between the two solvents as well as a common cellular response (Tian et al., 2013). It is likely that other head-group modifications play an important role in the solvent stress response in *Clostridium spp.* Kolek

et al., (2015) also noted a difference in the ratios of saturated: unsaturated lipids depending on whether butanol was exogenous or endogenous. This discrepancy seen in response between exogenous and endogenous to butanol exposure is discussed later (see discussion). The ratio of saturated: unsaturated was higher for exogenous than endogenous butanol - It appears that the response to exogenous butanol is more rapid than endogenous butanol. The exact changes to the lipidome remain unknown, furthermore, there is a lack of data regarding the changes throughout the entirety of ABE fermentation (Wang *et al.*, 2016).

1.5.2 Changes in gene expression and protein synthesis

Through microarray analysis of *C. acetobutylicum* transcription in response to butanol and butyric acid stress (Wang *et al.*, 2013) found that several genes and metabolic pathways had altering expression. For example, during butanol stress, genes for fatty acid metabolism, polysaccharide catabolism and several chaperones were all upregulated. Interestingly, using the same strain 824 (pGROE1) and under similar conditions, Tomas *et al.*, (2004) reported a reduction in expression of the major fatty acid synthesis operon, despite the importance of fatty acid and membrane alterations in the solvent stress response (Xu *et al.*, 2017). However, there was a correlation between lower levels of operon expression and higher levels of growth inhibition, reaffirming the importance of the homeoviscous response. Luo and colleagues (2009) found an increase in *E. coli* growth rate upon exposure to exogenous ethanol in strains overexpressing *fabA*.

In *E. coli*, genes related to stress response, membrane functions and sugar and amino acid transporters were upregulated after n-butanol challenge (Reyes *et al.*, 2011). Additionally when biotin synthesis genes were upregulated, there was an increase in butanol tolerance of up to 50 % (Reyes *et al.*, 2011). Biotin is an important coenzyme, involved in fatty acid synthesis and gluconeogenesis. It has been suggested that insufficient biotin synthesis can limit the productivity of solventogenic *Clostridia*. Yang and colleagues (2016) were able to overexpress plasmid-based biotin synthesis and transport genes in *C. acetobutylicum* which resulted in better growth in addition to a high butanol titre of 21.9 g/L. Directly

manipulating chromosomal expression may yield even better results as it would circumvent the metabolic burden placed on cells by the plasmid (Glick, 1995). Acetyl-CoA carboxylase (a crucial enzyme in the committed initiation of fatty acid synthesis) possesses a biotin carboxylase domain which is involved in the formation of malonyl-CoA (Evans et al., 2017). Therefore, fatty acid synthesis may be influenced levels of biotin. This could explain the increased tolerance seen to butanol with more biotin as modulating the lipidome is an important response to maintain optimal bilayer properties.

The transcriptional response of *C. acetobutylicum* to butanol (0.25-0.75 % v/v) appears to be broad with the upregulation of stress protein families; *dnaKJ*, *HSP18* and *HSP90* and chaperones such as *groES/EL* (Tomas et al., 2004). Interestingly, genes involved in solventogenesis were also upregulated. Strain 824 (pGROE1) overexpresses *groES/EL* which was found to increase butanol tolerance and seemingly mitigate the inhibitory effects of butanol on glucose metabolism. Similarly, Abdelaal and colleagues (2015) found that expressing *Clostridial groES/SL* in *E. coli* resulted in butanol tolerance. This suggests that heat shock proteins (HSPs) and the general stress response system may play an important role in butanol tolerance (Tomas et al., 2004; Zingaro and Papoutsakis, 2012). Rutherford and others (2010) also noted the commonalities between butanol stress and other stress responses including, oxidative and heat shock. HSP chaperone systems, such as *dnaKJ* and *groES/EL*, have a crucial role in the folding of nascent proteins or those which are misfolded or damaged, possibly due to solvent stress (Zingaro and Papoutsakis, 2012; Jia et al., 2014). Butanol titres and tolerance were significantly improved (23.0 - 49.4 % titre increases) upon overexpression of *DnaK* and *groES/EL* from the extremophile, *Deinococcus wulumuqiensis* (Liao et al., 2017). HSPs are upregulated in *E. coli* following butanol stress (Reyes et al., 2011) and, in line with Tomas et. al., 2004, have been shown to improve tolerance to n-butanol, when upregulated (Zingaro and Terry Papoutsakis, 2013). Optimising the expression of multiple HSP systems has the potential to drastically improve solvent tolerance. Expression of *ClpB*, *GrpE* and *GroES/EL* together resulted in an increase in viable *E. coli* cells of almost 400 % in response to 1 % n-butanol (Zingaro and Papoutsakis, 2012). HSP expression was found to mirror acidogenesis and solventogenesis

in *C. beijerinckii* NRRL B-598 (Patakova *et al.*, 2019). General stress responses represent a promising route to improving butanol tolerance in solventogenic *Clostridia*.

1.6 Strategies to increase productivity and reduce toxicity

As previously alluded to, the process of generating butanol through ABE fermentation is fraught with several issues hindering its efficiently and widespread implementation. Among these is the product toxicity of butanol for the fermenting cell factories. A tolerant, high-producing strain would go a long way in making ABE fermentation a more economically competitive process. With the development of novel genetic manipulation techniques in recent years there are greater possibilities to produce robust strains.

1.6.1 Non-engineering strategies

Carbon utilisation is an important aspect of ABE fermentation and could potentially lead to more economically efficient butanol production if optimised. Having a low-cost feedstock for fermentation becomes increasingly more important with larger scale operations. The use of starch-based feedstock has led to the development of the Food vs. Fuel debate, where the production of a biofuel is in direct competition with the production of food crops (Zhang *et al.*, 2010). This may be directly through the use of food crops in fermentation, for example first-generation bioethanol requires food crops, including sugar cane, wheat and corn, or alternatively through redistribution of farmland to favour biofuel feedstock crops. Hence, there is a movement toward second-generation biofuels which are inherently more sustainable as it utilises the non-edible part of the plant (Ndaba *et al.*, 2015). Butanol is a second-generation biofuel which can be fermented from an array of feedstocks including lignocellulose-based waste biomasses (Antizar-Ladislao and Turrion-Gomez, 2008). The fact that waste biomasses can be utilised as a substrate for butanol fermentation means that the growth of biofuel production will not be in a position to threaten food supply. In addition to this, there is already ample supply of lignocellulosic matter which is produced at relatively low costs making it a good butanol feedstock (Ndaba *et al.*, 2015). Unfortunately *Clostridia* are incapable of metabolising lignocellulose directly and require it to undergo energetically-costly pretreatment (Jiang *et al.*, 2015; Li *et al.*, 2020).

Co-culturing with microorganism capable of breaking down lignocellulose or identifying novel strains which are also capable of solventogenesis is an attractive route which will enable single step fermentation from lignocellulose. Recently, Jiang and others (2018), were able to generate a co-culture system with *Thermoanaerobacterium sp.* M5 and *C. acetobutylicum* NJ4 which produced 8.34 g/L butanol from xylan. *Thermoanaerobacterium sp.* M5 was able to release xylose from the xylan which was then converted more efficiently into butanol by *C. acetobutylicum* NJ4. A number of studies have been carried out harnessing various second generation feedstocks: rice straw (Gottumukkala et al., 2013), corncobs (Marchal et al., 1992), spoiled date palm fruit (Abd-Alla and Elsadek El-Enany, 2012) and cellulosic material from beech wood (Tippkötter et al., 2014).

1.6.2 Non-targeted engineering

Early engineering strategies comprised of random mutagenesis through chemical and physical means, for example with *N*-methyl-*N*-nitro-*N*-nitrosoguanidine (NTG), which works by alkylating thymine bases. Through this method several strains capable of producing more butanol were yielded, for example; *C. beijerinckii* BA101, with an increase in butanol yield from 9 g/l to 19 g/L (Formanek et al., 1997) and *C. acetobutylicum* BKM19 with a butanol titre of 18 g /L (Jang et al., 2013). Similarly for *C. acetobutylicum* GX01, mutagenesis and genome shuffling successfully improved butanol production from 16 g/L to 20 g/L (Li et al., 2016). Whilst random mutagenesis has yielded some of the highest producing strains it is difficult to improve them further due to the lack of knowledge surrounding the mutated genes.

1.6.3 Towards more targeted engineering

With the advent of targeted genome engineering techniques such as CRISPR-Cas in recent decades, rational metabolic engineering strategies have become easier. CRISPR/ Cas9 technology is based on a bacterial immune mechanism against bacteriophage genetic elements and allows for the manipulation of genomic DNA (Charpentier, 2015). The system is constituted of a Cas9 nuclease and guide RNA which enables cleavage at specific sites followed by DNA repair culminating in the desired genomic alteration

(Zhang *et al.*, 2014). This enables specific genomic changes and has already been applied to solventogenic *Clostridia* in several studies (Wang *et al.*, 2015, 2017a; Atmadjaja *et al.*, 2019).

Rational design has generally targeted specific aspects of *Clostridial* physiology in order to obtain high-producing strains. Manipulating genes related to solventogenesis may provide beneficial effects to productivity. Butanol production can occur independently of acetone formation (another product of ABE fermentation); hence it is desirable to reduce acetone production to free up carbon resources and maximise butanol productivity (Jones and Woods, 1986). One approach to this is to knock-out the *adc* gene for acetoacetate decarboxylase, important for acetone production. Jiang *et al.*, (2009) disrupted the *adc* gene with TargeTron Knockout System, leading to reduced acetone production (0.21 g/L) and a 13.8% increase in butanol yield. However, by knocking out *adc* cells may be at a higher risk of acid stress due to an accumulation of precursors, acetate and butyrate and a subsequent drop in intracellular pH. Furthermore, lower butanol titres are often seen in acetone-uncoupled mutants (Croux *et al.*, 2016). The use of antisense RNA to prevent acetone formation has also been attempted, with limited success (Tummala *et al.*, 2003). Several studies have disrupted genes associated with the formation of acetone and butyrate, namely *buk*, *pta* and *ptb*. Whilst this has shown some promise, with increased yields of butanol, acetone often remains a major fermentation product (Lütke-Eversloh and Bahl, 2011; Lee *et al.*, 2012). Alternatively, it has been found that disrupting acetone production resulted in reduced solvent production suggesting a complex relationship between the pathways (Lehmann *et al.*, 2012). These somewhat conflicting results suggest that directly engineering genes and pathways associated with solventogenesis (particularly reducing acetone formation) may have limited reliable effectiveness. Overexpression of aldehyde/alcohol dehydrogenase (*adhE*) in *C. acetobutylicum* was found to increase butanol productivity when combined with a *pta/buk* KO mutant (Lee, Jang, Lee, Lee, Park, Im, Eom, Lee, Lee, Song, Cho, and Seung, 2012). Recently the active site and binding chamber of *adhE* was engineered to have a higher selectivity for butanol production, resulting in an increase in the butanol: ethanol product ratio of more than 5 times (Cho *et al.*, 2019). Butanol only pathways are desirable however

remain hard to achieve without obtaining other undesirable phenotypes, such as acid assimilation. This is primarily due to the lack of understanding about regulation and relationships between the various pathways (Li et al., 2020).

1.6.4 Targeted engineering of lipid species

Besada-Lombana et al., (2017) found that increasing the proportion of oleic acid (18:1) in *S. cerevisiae* through the expression of a mutant acetyl-CoA carboxylase (S1157A) resulted in 3.2-fold higher optical densities than the wild type strain following exposure to 1.3% n-butanol. Additionally, there was an 11-fold reduction in intracellular ion leakage, suggesting higher levels oleic acid (including exogenously supplemented media) mediate increased membrane stability (Liu et al., 2013). The introduction of rat elongase 2 (*rELO2*) (C 16:0 → C 18:0) to *S. cerevisiae* increased C 18:1 content (but not total proportion of unsaturated fatty acids) and tolerance to several short-chain alcohols, including butanol. The introduction of *rELO2* produced vaccenic acid (C 18:1), which has the same structure as oleic acid with a different position for the carbon-carbon double bond, yielded no increased solvent tolerance. This suggests that the position of the unsaturated bond, or other small inter-lipid species differences may have a more important bearing on solvent resistance (Yazawa et al., 2011).

Tan et al., (2016) show that the expression of CTI from *Pseudomonas putida* allowed for incorporation of trans-unsaturated fatty acids (TUFA) into the membrane of *E. coli*. The incorporation of TUFAs resulted in increased membrane rigidity and tolerance of several alcohols and unfavourable industrial conditions e.g. high temperature and acidity. The optimal level of TUFA depends on the compound's class and hydrophobicity (Tan et al., 2016). Due to the lack of knowledge surrounding the *Clostridial* lipidome, it is unclear whether *C. acetobutylicum* naturally produced TUFAs. *Trans* double bonds have a more similar effect on membrane fluidity to saturated acyl chains than they do to *cis* double bonds (Roach et al., 2004).

The effects of altered head groups of phospholipids on butanol sensitivity remain a potentially important, relatively unexplored area (Sandoval and Papoutsakis, 2016). Recently, Tan and other (2017) overexpressed phosphatidylserine synthase (*PssA*) in *E. coli* (see Figure 1.5). The resulting strain was more tolerant to several solvents including acetate, ethanol and octanoic acid which have similar detrimental effects as butanol. Whilst the beneficial effects are attributed to an increased proportion of phosphatidylethanolamine (PE) head-groups; there was a concurrent increase in chain length which may have influenced tolerance (Tan et al., 2017). Molecular dynamic simulations showed the membranes with higher PE content were thicker and more resistant to ethanol insertion. It is important to investigate the effects of different head group and acyl chain compositions and how they act in combination with one another. Manipulating levels of *PssA* presents a good way to change the lipid composition of the bacteria's membrane and thus alter the related properties.

1.6.5 Efflux systems

It is vital to identify protective membrane properties as these will likely represent strong candidates for engineering. Of equal importance developing a more robust cell factory is the identification and promotion of transporters or other mechanisms to prevent intracellular build-up of butanol exceeding tolerable levels (Jarboe et al., 2018). Efflux is a common method of dealing with intracellular toxins. For example, in *E. coli* and *Pseudomonas* efflux is an important mechanism of toluene and hexane resistance (Ramos et al., 2002). Historically, small uncharged alcohols, including butanol, were thought to leave the cell via diffusion. Recent studies have shown that the need for transporters is inherent across several small, uncharged molecules which were previously thought to flux by diffusion (Kell et al., 2015). In light of this, a greater emphasis should be put on efflux and transporters as it is likely that *Clostridia* possesses a native butanol efflux mechanism not reliant on diffusion over the membrane. Recently, several *Clostridia* strains were found to possess sequences for the AcrB inner membrane domain, which may play a role in butanol excretion (Dehoux et al., 2016; Patakova et al., 2017). The AcrAB-TolC system

results in tolerance against several long chain solvents, hence it is possible that it yields tolerance to butanol (Reyes et al., 2013).

Currently, there have been no native butanol transporters identified in *Clostridia* (Dunlop et al., 2011). Fisher et al., (2014) engineered AcrB, an efflux pump in *E. coli*, to excrete butanol which is a non-native substrate with the aim of enhancing tolerance. Whole-gene error-prone PCR was utilised to create a library of AcrB mutants, upon exposure to 0.7 % butanol mutated AcrB variants, Var1 and Var2, grew to 25-30 % higher cell densities than wild-type AcrB. Also, mutated AcrB variants had a lower intracellular butanol concentration than wild type, confirming the action of butanol efflux. Foo and Leong (2013), yielded similar results, improving tolerance of *E. coli* to n-octane through directed evolution. More recently, a native butanol transporter was identified in *P. putida* (Basler et al., 2018). Expression of the TtgABC efflux system in *P. putida* increased cell survival in butanol and was shown to actively efflux butanol. TtgB, the inner membrane pump, has 65 % amino acid homology with AcrB (Basler et al., 2018) and represents a potential native butanol transporter in *Clostridia*. These works highlight the importance of membrane transporters and efflux in the development of tolerance to n-butanol and other solvents.

The numerous toxic mechanisms of butanol and the complex stress response solventogenic *Clostridia* present several fronts which can be targeted for engineered tolerance. The development of a robust strain capable of withstanding high levels of butanol is a paramount precursor to a high-producing strain. Understanding more about how butanol negatively impacts the membrane and its constituent components will enlighten possibly beneficial membrane properties which could mitigate perturbation and lead to more tolerance. Additionally, developing a deeper understanding of how the lipidome changes throughout fermentation following increasing butanol concentration will give a more biologically relevant explanation of how the cell attempts to reduce toxicity. These data can then be utilised in designing rational engineering strategies, which once implemented will hopefully provide a robust phenotype with high productivity (see Figure 1.7). Butanol is an important chemical with growing

interest as a biofuel within wider industrial applications. Ultimately improving the tolerance and production to butanol will lead to higher yields, and in turn lower down-stream processing and purification costs. This will place butanol, produced via the ABE fermentation route, in a more economically competitive position when compared with the conventional, fossil-fuel based approach.

1.6.6 Engineering targets in this work

Three protein targets were chosen to be either overexpressed or knocked out based on results from Chapters 3 and 4 and are shown in Table 2.2. Two of the targets utilised CLEAVE™ technology (see Methods 2.10 CLEAVE™), a CRISPR based technology, whilst the third target used plasmid-based technology. CRISPR/ Cas9 technology is based on a bacterial immune mechanism against bacteriophage genetic elements and allows for the manipulation of genomic DNA (Charpentier, 2015). The system is constituted of a Cas9 nuclease and guide RNA which enables cleavage at specific sites followed by DNA repair culminating in the desired genomic alteration (Zhang *et al.*, 2014). CELAVE™ is a CRISPR-Cas technology and has been applied to *C. saccharoperbutylacetonicum* N1-4 (HMT) generating a *Spo0A* deletion (Atmadjaja *et al.*, 2019).

The first target was TtgB, the inner membrane section from ttgABC, a resistance-nodulation-cell division (RND) efflux system (a structure is shown in Figure 6.1). Recent findings by Basler and colleagues (2018) showed that expression of the TtgABC efflux system in *P. putida* enabled active butanol flux. TtgB, has 65% amino acid homology (Basler *et al.*, 2018) with AcrB and genome mining in *Clostridia* reveals an AcrB-like protein. This work in combination with that of Fisher *et al.* (2014) who engineered AcrB to efflux butanol, indicated that the AcrB/TtgB-like protein in *Clostridia* may be involved in butanol efflux. TtgABC is the first native system found to be capable of exporting butanol and thus represents a very attractive target for over expression. As *Clostridia* are Gram-positive and thus do not have both a cytoplasmic and an outer membrane, the formation of ttgABC would not be possible. TtgC is the outer membrane channel and TtgB is the cytoplasmic section and ttgA links the two together. Because of this, only TtgB homologues were searched for in the *C. saccharoperbutylacetonicum* N1-4 (HMT) genome.

The other target for CLEAVE™ genome modification was phosphatidylserine synthase (PssA), a biosynthetic enzyme responsible for the formation of phosphatidylserine (PS) lipids (See Figure 1.5). In turn, PS lipids are converted into phosphatidylethanolamine lipids (PE) which means that regulating the expression of PssA can crudely regulate the amount of PE in the membrane. If overexpressed, there will be a greater portion of PE lipids, and if knocked out there should be a lower amount (as the cell can no longer utilise this pathway). The PssA knockout bacteria would then be forced to shunt lipid synthesis down other pathways which may lead to increase levels of PG lipids (see Figure 1.5 for pathway). PssA was chosen due to its place in the biosynthetic pathway of *Clostridial* lipids and due to some previous studies showing its effective as an engineering target. Past work by Tan and colleagues (2017) in *E. coli* showed that increasing the expression of PssA lead to increases in tolerance to toluene, ethanol and other industrially relevant inhibitors, as well as octanol (used as a membrane damaging model compound). Interestingly, this increase in specific growth rate in toxic compounds of the modified strains did not extend to butanol. Hence it is interesting to explore both an overexpression and a knockout of PssA to gain a more all-inclusive understanding of how manipulating these enzymes can alter tolerance levels to butanol.

The final target which was overexpressed in *E. coli* (BL21) using the expression plasmid *pET17-b* was a putative butanol channel, glycerol uptake facilitator protein (GlpF) (See Figure 1.9). In *Clostridium acetobutylicum*, GlpF is upregulated during butanol stress (Alsaker *et al.*, 2010) and it has been suggested that GlpF can improve tolerance to polar and nonpolar solvents (Mukhopadhyay, 2015). This upregulation occurs during the acidogenic phase, meaning that it may be a prophylactic measure to ensure that the cell is protected before it starts producing butanol in the solventogenic phase (Mao *et al.*, 2010; Dong *et al.*, 2016). It is speculated that structural similarities between glycerol and butanol and previous reports of overexpression in fermentation, may indicate a possible role in butanol translocation across the membrane.

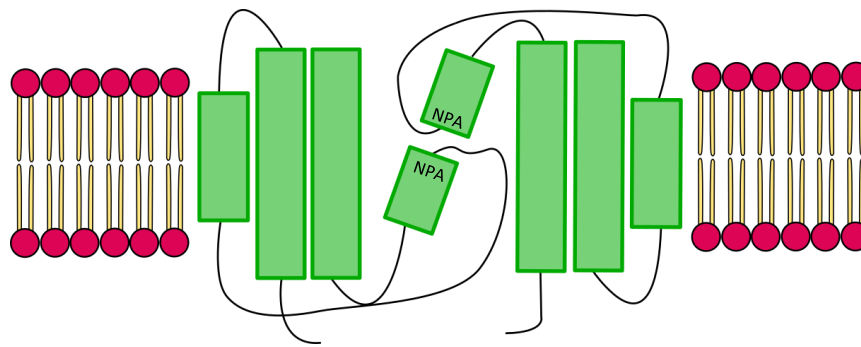


Figure 1.9 Structure of glycerol like facilitator protein (GlpF), a putative butanol channel. Each channel is formed of two inverted subdomains, each subdomain is comprised of three full-membrane spanning α helices and two half-membrane spanning α -helices. The two half-spanning helices meet in the centre of the channel and are orientated so their N-terminals are facing one another. The conserved asparagine-proline-alanine (NPA) motifs responsible for substrate selectivity exist on each helix at this interface.

1.7 Aims and Objectives

The overarching aim of this project was to understand more about the interaction of butanol and cellular membranes with a view to developing more tolerant phenotypes to ultimately reduce costs associated with ABE processing. The aims and chapters of this thesis are summarised in Figure 1.7. The first section of the study (Chapter 3) has used *in vitro* liposomes to model membranes and enable characterisation of their interaction with butanol. The compositions of these models were altered in order to assay any potentially protective effect of certain specific lipid components and membrane fluidity regulators. Additionally, Chapter 3, *in vitro* characterisation of the interactions between butanol and membranes, aimed to further describe the mechanism of butanol damage in terms of perturbation to essential membrane properties and also attempts to begin to shed light on the interactions between butanol and membrane proteins. The fourth chapter, Characterisation of *C. saccharoperbutylacetonicum* N 1-4 (HMT) lipidome in a butanol environment, involved looking at the effects of butanol on the lipidome of industrially relevant fermentative strains. Lipids extracted from solventogenic *Clostridial* biomass were examined using thin layer chromatography to show the relative changes in lipid species across fermentation. These data were then be coupled with TOF-MSMS techniques to provide a more specific description of any lipidome changes. Chapter 5, Rational metabolic engineering of *C.*

saccharoperbutylacetonicum N 1-4 (HMT) and *E. coli* to increase butanol tolerance and production, encompassed data from previous chapters to develop a more tolerant phenotype. Rational design of these strains was based on the changes in the lipidome, and any protective effects seen in the *in vitro* studies. Strains were created using genome editing technology CLEAVE™ (Biocleave) once targets were selected. These targets were informed by the previous chapters and included enzymes involved in the lipid biosynthesis pathways and in the active movement of butanol across the membrane. Downstream processing of ABE to purify butanol is a major contributor to the poor economic feasibility of ABE fermentation. Having a strain more tolerant to butanol will likely result in higher yields of butanol in the ABE process which will reduce the costs associated with purification. Ultimately this will make ABE fermentation more attractive economically, reducing overheads, allowing for greater profit margins and being more appealing as an investment. This will increase the competitiveness of the technology with conventional non-renewable energy sources and may enable large corporations already established in the energy sector to view ABE fermentation as a valid successor to their current, unsustainable petrochemical-based business model.

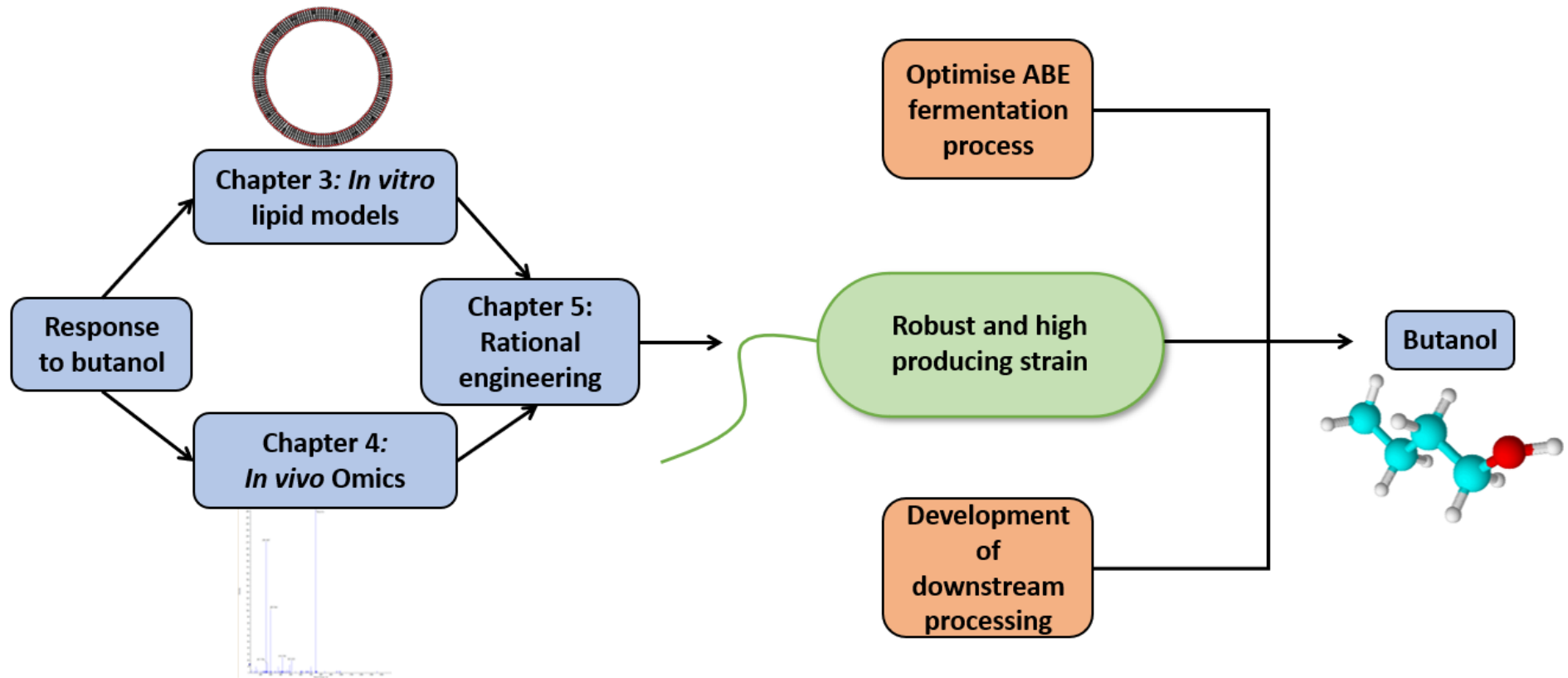


Figure 1.10 Processes to improve butanol yield from ABE fermentation. Data from *in vitro* models combined with *in vivo* fermentation data can be used to inform strain engineering and produce a robust and highly productive phenotype. ABE economic feasibility can be further improved through optimising the fermentation process and downstream processing.

2. Materials and Methods

2.1 Materials

Extrusion equipment and lipids were purchased from Avanti Polar Lipids. All media were made in accordance with the manufacturer's instructions. All solvents were purchased from Fisher Scientific unless stated otherwise. All biochemicals were purchased from Melford unless otherwise stated. Primers were sourced from Eurofins Genomics or Thermo Fisher Scientific. *Clostridia saccharoperbutylacetonicum* N1-4 samples were a kind gift from Green Biologics Ltd. (Now Biocleave Ltd.), Oxfordshire, UK.

2.2 Molecular Biology

2.3 *In vitro* liposome assays

Liposomes were prepared using commercially purchased lipids (Avanti Polar) or extracted lipids. All preparation was carried out at temperatures above the phase transition temperatures of the component lipids. Lipids in chloroform were dried down in a round-bottom flask under a stream of nitrogen until completely dry. Resulting lipid films were stored at -20 °C under nitrogen to prevent oxidation. Lipid films were rehydrated in liposome buffer (50 mM Tris, 50 mM NaCl, pH 7.4), or in 100 mM 5(6)-Carboxyfluorescein pH 7.4 (CF) (Sigma-Aldrich) made up in liposome buffer. This was done through vortexing, resulting in large, multilamellar vesicles (LMV). Following this, resuspended lipid solutions were incubated for 1 hour at 120 rpm shaking at a temperature above the phase transition temperature of the lipid components. LMVs were extruded to produce smaller unilamellar liposomes at a size of 400 or 100 nm depending on the application. For CF liposome solutions, excess unincorporated dye molecules were removed through 3 wash cycles: Liposomes were centrifuged at 100,000 x g for 30 minutes, pellets were resuspended in liposome buffer. This was repeated twice more. For Laurdan assays, extruded liposomes were incubated with 2.5 µM Laurdan (in DMSO) for at least 1 h above the phase transition temperature.

2.3.1 Carboxyfluorescein and laurdan fluorescence assays

CF was used at 100 mM dissolved in liposome buffer. The gradual addition of sodium hydroxide pellets was required in order to dissolve all CF powder when making the 100 mM stock. CF becomes increasingly more soluble as the pH increased, being totally dissolved at pH 7.4. CF release assays were carried out in black 96-well plates (Greiner). CF liposomes were used at working concentrations of 0.25 mg/ml and a 5% SDS solution was added to some wells as a positive control. Following butanol addition to wells, plates were incubated at room temperature with occasional agitation for 10 minutes in the dark after which fluorescence was recorded. Fluorescence was read at the following wavelengths for CF: 485 nm and emission and 535 nm. Butanol data was normalised to wells containing no butanol.

Laurdan assays were also carried out in black 96-well plates (Greiner) liposomes were used at working concentrations of 2.0 mg/ml. The general polarisation (GP) of Laurdan was calculated from the ratio of emission intensities via the following equation:

$$GP = \frac{I_{485} - I_{535}}{I_{485} + I_{535}}$$

Where I_{485} and I_{535} refer to emission intensities at 485 nm and 535 nm, respectively. For live cell Laurdan assays overnight cultures were set up in Luria Broth (LB) (Melford). These were then diluted 1:100 in fresh LB the next morning. Cells were grown to an OD_{600} of 0.4 after which 5 μ M Laurdan was added and cells were incubated in the dark for 1 h. Following this, cells were harvested by centrifugation (~16,000 x g, 60 seconds) and resuspended in liposome buffer containing butanol which was subsequently incubated at room temperature for 10 minutes before the fluorescence was read.

2.3.2 DLS

The average liposome diameter in a solution was determined using dynamic light scattering on a NanoBrook 90Plus Zeta in accordance with the manufacturer's instructions. Prior to measurement, sample solutions were filtered with a 0.2 μ m syringe filter to remove any dust or large particles. Each

sample was read in triplicate. Liposome samples were diluted to <0.125 mg/ml, or to an ideal counts per second of ~400kcps.

2.3.3 Differential scanning calorimetry (DSC)

Liposome sample were prepared as described above after which they were underwent a cycle of heating and cooling in a thermal cycler followed by incubation at 4°C under nitrogen gas to equilibrate the sample's thermal history. The effect of butanol on the suspension of liposomes was investigated using a Q200 Differential Scanning Calorimeter (TA). Between 3-5 mg of 30 mg/ml liposome solution was weighed into a Tzero Low-Mass Pan (TA instruments) and the corresponding lid was placed on top and sealed. The Heat Flow (mW) was recorded across the range of 5 - 50°C at a gradient of 1°C / minute. This temperature range allowed for the main phase transition of samples, between gel and liquid crystalline (see introduction), to be recorded.

2.4 Total lipid extraction and quantification

Total bacterial lipids were extracted using a modified Bligh and Dyer method (Bligh and Dyer, 1959). To 50 mg pelleted cells, 500 µl of methanol at 50 °C was added. Following incubation in a sonicating water bath for 15 minutes, 500 µl of chloroform was added and the incubation was repeated. After the second 15 minute incubation, 500 µl of 0.88 % KCl was added and the mixture was vortexed. The organic and aqueous phases were separated by centrifugation at 1000 x g for 2 minutes. The total lipids present in the organic phase was then quantified using the Stewart Assay (Stewart, 1980) and a standard curve of 0-50 µg of 1 POPE: 1 POPG: POPC. This assay enables quantification based on the complex formed between phospholipids and ammonium ferrothiocyanate. Briefly, lipids in chloroform on an unknown concentration were diluted and mixed with with ferrothiocyanate assay reagent (0.1 M FeCl₃.6H₂O, 0.4 M ammonium thiocyanate) to a 2:1 ratio of lipid to assay reagent. Following centrifugation at 14,500 x g for 5 minutes, the chloroform layer (now coloured) was collected and the absorbance read at 488 nm.

2.5 *in silico* molecular dynamics

In silico techniques were used to visualise the interaction between butanol and 3 POPE: 1 POPG membrane. Initial molecular dynamic simulations utilised a coarse-grained model in which some atoms are grouped together. These were carried out in GROMACS 5.1.2 using the MARTINI 2 forcefield. Coarse-graining drastically decreases the computational demand for running longer simulations however, there is a concurrent loss of atomistic resolution. These were initially carried out to provide a low-resolution idea of whether butanol interacts with the membrane. The 3 POPE: 1 POPG membrane of 336 lipid molecules was made using the insane.py script (Wassenaar *et al.*, 2015) (8533 atoms in total. 90 NA, 6 CL, 4,400 SOL and 5 butanol, 126 POPE and 42 POPG molecules). The membrane generated using insane.py underwent a short md run of 20 ns to enable relaxation and more realistic packing of the lipid beads after initial energy minimisations. Following this, 5 solvent beads were substituted for 5 butanol beads before the system's energy was minimised once again. After this, the simulation was run for 200 ns and was visualised using Visual Molecular Dynamics (VMD) (University of Illinois). The simulation was run at 293 k using a Berendsen thermostat. The Verlet cutoff-scheme was used with a Van der Waals radius of 1.1 nm. The constrain algorithm used was Lincs.

2.6 Thin layer chromatography

Lipid species present in *Clostridium saccharoperbutylacetonicum* N 1-4 extracts were investigated using thin layer chromatography following extraction and total lipid quantification. Along with standards, 20 µg of sample was dotted onto silica coated aluminium TLC plates (Merck) and was allowed to dry. Following this, plates were placed into a TLC tank with a small amount of mobile phase (70 Hexane: 30 diethyl ether: 1 acetic acid; 25 chloroform: 15 methanol: 4 acetic acid: 2 H₂O) in which they were left until the solvent front was near the top of the plates. Plates were allowed to dry before visualisation. For neutral lipids, plates were dipped into a copper sulphate solution (10% CuSO₄.5H₂O; 8 % H₃PO₄) and then baked at 150 °C for 10 minutes in an oven. Ninhydrin and molybdenum blue spray reagents (Sigma-

Aldrich) were used to visualise PE, and PS, PC and PG, respectively. Densitometry analysis was carried out using ImageJ.

2.7 Lipidomics: HPLC-ESIMSMS

Lipid extracts were initially passed through a reversed phase Accucore™ C18 column on an UltiMate 3000 HPLC system (Thermo Fisher Scientific/Fisher). Running solvent A was 50 H₂O: 50 acetonitrile, 50 mM ammonium formate, 0.1% formic acid and solvent B was 85 isopropanol: 10 acetonitrile: 5 H₂O. The gradient of solvents began with 90:10 A:B and ended with 5:95 after 21 minutes and was isocratic for the remaining 14 minutes at 90:10. The flow rate was 150 µl/ minute. And the column temperature was maintained at 50°C. For subsequent ESI-MS analysis, all samples were analysed in positive and negative ion mode on a TripleTOF® 5600 (Sciex). The ESI temperature was set to 300 °C, the mass range was 200-1600 m/z and the ion spray voltage of 5500 V and -4500 V for positive and negative ion modes, respectively. An Information Dependent Acquisition (IDA) was run for MS-MS analysis – with a maximum of 5 candidate ions per cycle chosen. The instrument was calibrated using APCI Negative Calibration Solution (Sciex). Data was analysed using PeakView 2.2 (Sciex) and were additionally searched against public lipidomic libraries such as LipidMaps using Progenesis QI v2.1 (Nonlinear Dynamics).

2.8 Unfolding assay

2.8.1 Monovalent streptavidin expression and purification

Mutated bacteriorhodopsin (bR) and monovalent streptavidin (mSa) plasmids were a kind gift from Yu-Chu Chang, Taipei Medical University. Both mSA variants (an active form with a his-tag (wt-mSa), and an inactive form without a polyhistidine-tag (d-mSa)) were expressed in BL21 (DE3) and purified as previously described (Hong *et al.* 2010). Overnight cultures of 5 ml were used to inoculate large cultures of ~500 ml of either d-mSa or wt-mSa. Expression was induced at an OD₆₀₀ of 0.7 using 1 mM IPTG, after which cells were incubated overnight. After harvesting (4,000 x g, 4°C, 20 minutes), cells were resuspended in ~ 20 ml lysis buffer (50 mM Tris, 0.75 M sucrose, 1 mg/ml lysozyme, pH 8.0) per mSa variant, and subjected to 3 cycles of lysis with the French Press (1,500 PSI). To reduce viscosity, 0.3

mg/ml DNase was added and the suspension was incubated for 1 hour at 4°C. The pellet was harvested by centrifugation (20,500 RPM in Ti-70, 4 °C, 20 minutes) and was washed in 50 mM Tris, 1.5 M NaCl, 0.5% TritonX100, pH 8.0, using a tissue homogeniser to break up the pellet. The washing step was repeated twice more with TritonX100 and followed by once without TritonX100. The resulting inclusion body was solubilised in denaturing buffer (6 M GdnHCl, pH 2.0), again with use of a homogeniser and was centrifuged at 45,000 RPM for 45 minutes in a TLA-120.2 rotor. The OD₂₈₀ was then read for each variant and they were mixed to be in a 3 d-mSa : 1 wt-mSa ratio, based on the OD₂₈₀ reading multiplied by the volume per variant. The mixture was refolded by adding it drop by drop to prechilled and stirred sodium phosphate buffer (20 mM sodium phosphate, 200 mM NaCl, pH 7.5) to a final dilution of 1:50. The resulting solution was centrifuged (6,100 x g in a JA-14 rotor, 4°C, 1 h) to pellet any precipitated protein. The supernatant containing refolded mSa tetramers in a 3:1 ratio of d-mSa: wt-mSa was then mixed with equilibrated Ni-NTA resin and incubated overnight at 4°C. Protein was eluted as described above – mSa eluted at 60 mM and 70 mM imidazole. Higher levels of imidazole yielded undesirable mSa tetramers with different ratios, those being 2:2 or 1:3 d-mSa: wt-mSa. Depending on the visible sample purity on an SDS-PAGE, a second purification involving rebinding and elution was carried out. The resulting protein was then dialysed overnight using SnakeSkin Dialysis Tubing (Thermo Fisher Scientific) at 4°C and was dialysed against sodium phosphate buffer. Following this, dialysed protein was concentrated using a 15 ml Amicon® Ultra Centrifugal Filters 30 kDa cut off (Sigma Aldrich) to 1-2 ml for use in the assay.

2.8.2 Bacteriorhodopsin labelling and unfolding assay

Biotinylation of bR and the membrane protein stability experimental procedures were carried out as previously described (Chang and Bowie, 2014). Mutated bR containing two cysteine residues was a kind gift from Yu-Chu Chang. It was biotinylated in a reaction following the mixture of two solutions. The first was 750 µl of 40 µM bR, 40 mM phosphate buffer (pH 8.0) and 2 mM of TCEP (Pierce) and this was mixed with the second solution of 250 µL of 4–6 mM of N-(biotinoyl)-N'-(iodoacetyl)ethylenediamine

(Biotium) and 1 mM of free biotin (Sigma-Aldrich). Following this the reaction was incubated overnight at 25°C in the dark. Excess reagents were removed through centrifugal washing in 20 mM phosphate buffer (pH 7.0). Labelling was confirmed with SDS-PAGE and western blot analysis. For the steric trapping experiment, 5 µM mutated bR was reconstituted in 15 mM DMPC: 15 mM CHAPSO bicelles in 20 mM phosphate buffer (pH 7.0), 15 µM mSa was then added to the bR and was incubated at room temperature for 1 hour in the dark. Butanol was added to the steric trapping experiment at a concentration of 0-20 mg/ml just before absorbances were recorded on a plate reader in an attempt to quantify unfolding induced by butanol. Several wavelengths were read: 390 nm (free retinal), 440 nm (unfolded protein retaining retinal), 560 nm (folded bR retaining retinal) and 700 nm (control). Unfolding was analysed with a two-phase exponential decay in GraphPad Prism 7 (GraphPad Software, Inc).

2.9 Glycerol uptake facilitator protein (GlpF) expression and purification

GlpF was amplified from a lab stock plasmid, *pAG5-GlpF* using the primers in Table 2.1 and subcloned into pTZ19R in DH5- α *E. coli* cells (where lowercase letters denote non-complementary bases to the original amplicon):

	Sequence
Forward Primer	gggggatcccatATGACAATTTTTTTAGCAGAATTAGTAGG
Reverse Primer	ccccagcttTTAatgatgatgatgatgatgCATAATCATTGTATAACATACTGCACC

Table 2.1. The 5' to 3' sequences of oligonucleotide primers used to amplify GlpF. Lower case letters indicate additional bases which are not complementary of the original sequence of the amplicon. The coloured lower case bases represent restriction sites: red, BamHI; blue, NdeI; green, HindIII.

Following this, GlpF was cloned into the expression vector pET17b and was expressed in BL21 (DE3) *E. coli*. GlpF expression was carried out as previously described above for monovalent streptavidin. Membrane protein extraction made use of the styrene maleic acid co-polymers. Following cell lysis, the lysate underwent a 650 x g spin for 10 minutes to pellet unbroken cells and debris. After this the supernatant was centrifuged in a Beckman Coulter Optima L-100k – 70Ti rotor for 20 minutes at 100,000

x g yielding a membrane pellet. The supernatant was discarded and the wet pellet weight was calculated. Membrane pellets were resuspended to a concentration of 60mg/ml in SMA buffer. This was then combined with a 5 % SMA2000 (Cray Valley) solution to yield a 30 mg/ml membrane: 2.5 % SMA2000 solution which was incubated for 1 hour at room temperature on a rocker at 60 RPM to allow for the SMA polymer to integrate into the membrane. Insoluble material was pelleted by centrifugation at 100,000 x g for 20 minutes. The supernatant was mixed in a 20:1 ratio with Nickel NTA agarose resin (ABT). Nickel resin was stored in 20 % ethanol and was prepared through a series of consecutive washes in excess SMA buffer at 500 x g for 3 minutes. The SMALP:Ni resin mixture was incubated overnight at 4 °C on a rocker at 60 RPM. Following this, the SMALP:Ni resin was poured into a 20 ml disposable column and was washed with 5 x 10 column volumes of wash buffer (20 mM imidazole in SMA buffer). His-tagged proteins were eluted with 5 x 1 column volumes of elution buffer (200 mM imidazole in SMA buffer).

2.9.3 Tolerance assay

Initially, 30ml universal tubes containing LB + ampicillin were inoculated with a single colony and grown overnight at 37 °C and 180 RPM. 100 µl of this was then added to fresh LB + ampicillin media and was induced with 0.5-1.0 mM IPTG and allowed to grow for between 5-16 hours. Cultures were then diluted to an optical density at 600nm (OD₆₀₀) of 0.1 before use in growth assays. Growth assays were carried out either in a clear 96-well plate (Thermo Fisher Scientific) or in a 30 ml universal and the OD₆₀₀ was measured every 2 hours for 8 hours.

2.10 CLEAVE™: Genome editing of *Clostridium saccharoperbutylacetonicum* N1-4 (HMT)

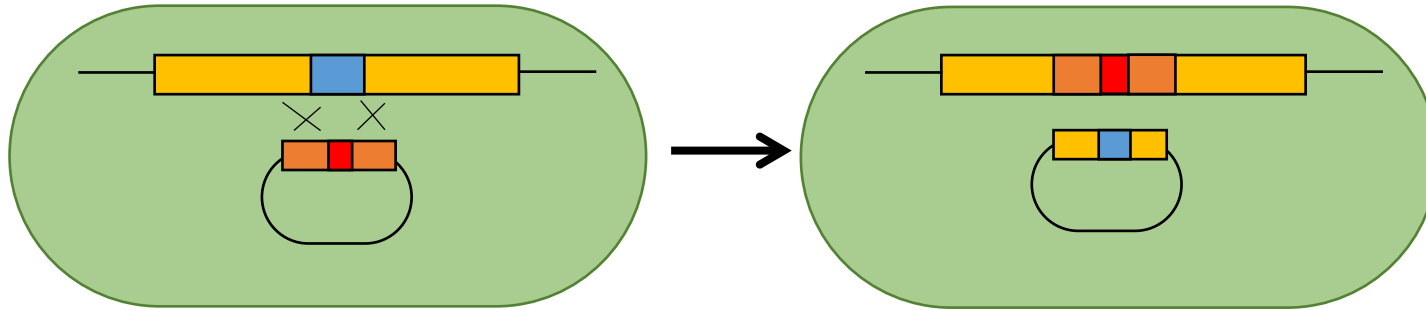
Genome editing of *C. saccharoperbutylacetonicum* N1-4 (HMT) was done using CLEAVE™ technology, a proprietary method for introducing exogenous DNA into wild type *Clostridia* (See Figure 2.1). Homologous gene of interest sequences in N1-4 were gathered using BLAST (NCBI) (summarised in table 2.2). The genes were then synthesised by GeneArt (Thermo Fisher Scientific) and were cloned into several vectors according to the CLEAVE™ standard operating procedure and was carried out at the

Gene Name	Function of encoded protein	Modification type
<i>ttgB</i>	Inner membrane portion of organic solvent efflux system	+
<i>pssA</i>	Phospholipid biosynthetic enzyme (see Figure 1.5)	+ / Δ
<i>glpF</i>	Aquaglyceroporin an putative butanol channel in solventogenic Clostridia	Δ

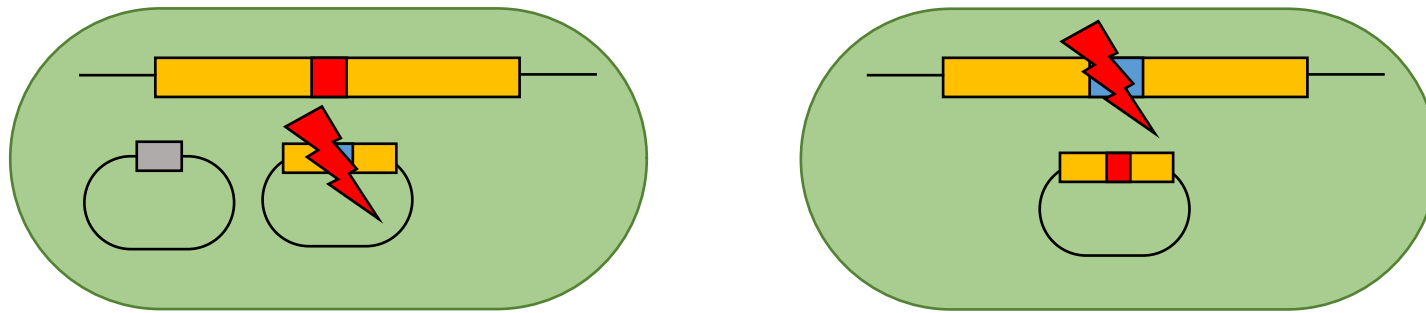
Table 2.2 CLEAVE™ Targets. These genes were identified using NCBI BLAST and CLEAVE™ constructs were synthesised by GeneArt (Thermo Fisher Scientific). Using proprietary CRISPR-Cas9-based technology, CLEAVE™, recombinant solventogenic Clostridia were produced and the affects of these genes on fermentation characteristics were investigated. + , overexpression; Δ, knockout.

Biocleave laboratories in Milton Park, Oxford. Glycerol stocks in competent *E. coli* (DH5-α or BL21 (DE3)) were made by mixing equal parts recombinant overnight cultures with sterile 50 % glycerol. All molecular biology procedures in CLEAVE™ were carried out as described above in 2.2 Molecular Biology or in recent work by Atmadjaja and colleague, (2019). In short CLEAVE™ is comprised of two steps (Figure 2.1). The first step involved homologous recombination of the desired deletion (*PssA* in this case) into the genome of N1-4. The sequence used for this contains only the last 14 amino acid residues of the original gene (in addition to the Met and stop codons), this flanked either end with 1,000 bp upstream and downstream of the original gene (homology regions / homology arms). Homologous recombination will thus result in a truncated gene. The second step involved the introduction of targeting vector (S3V9) for the native CRISPR-Cas system. Contained within this plasmid is the spacer sequence (guide sequence) of approximately 36 NT which corresponds to a sequence in the middle of the original gene sequence (i.e. not overlapping with the recombinant truncated sequence). Any bacterium which contain the wild type gene sequence will therefore be targeted by the targeting vector and these sequences will be cleaved (the efficiency of the designed targeting vector sequence was determined using wild type N-14 and plating the cultures following electroporation). Because the N1-4 used are unable to repair double-stranded breaks they cannot survive this process. This leaves bacterium which underwent homologous recombination in the first stage of CLEAVE™ alive as they do not contain the spacer sequence within their genome. Thus, a population of knockouts at the genome level can be produced.

STEP 1: Introduce plasmid with homology arms and modification for homologous recombination



STEP 2: Introduce targeting vector (with spacer) that directs the native CRISPR/Cas system to destroy WT cells



Recombinant cells survive

WT cells are destroyed

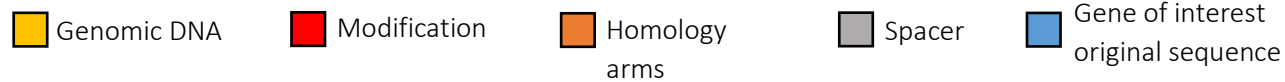


Figure 2.1 CLEAVE™ technology for *C. saccharoperbutylacetonicum* N1-4 (HMT) genome editing. In this case a deletion was introduced in a two step process. In the first step a plasmid containing the deletion sequences is transformed into the for *C. saccharoperbutylacetonicum* N1-4 (HMT) cells where it undergoes homologous recombination into the genome using two homology arms (see Figure 5.1). In the second step, the targeting vector (S3V9) is transformed into the cells. This vector contains a spacer sequence in it (~36 NT in length, see Figure 5.2), which guides the native CRISPR-Cas system to a site for cleavage based on the spacer's sequence. Therefore, the sequence of the spacer should correspond to a locus in the original sequence in the gene of interest. Crucially the spacer should not be found in the sequence of the deletion. WT sequences containing the spacer will be targeted by the CRISPR-Cas system and cleaved. Recombinant cells will not be targeted as they do not contain these sequences due to the truncated deletions.

The now engineered strains were inoculated overnight in 30 ml reinforced *Clostridial* media (RCM) in an anaerobic environment at 30°C. Following this, 6 ml was taken in triplicate from the overnights and used to inoculated 54 ml of TYIR for the characterisation assay. Approximately 4 ml fermentation samples were taken at 0 h, 4 h, 24 h and 48 h, with the OD₆₀₀ and pH being measures and the cell viability being assessed using a microscope. The following analytes were also measured at each of the time points: glucose, acetic acid, butyric acid, lactic acid, acetone, butanol, ethanol. Samples were run on an Agilent 1260 HPLC using a refractive index (RI) detector and an Aminex HPX-87H (300 x 7.8 mm) column (Bio-Rad). The following standards were used glucose 50g/L, acetic acid 0.2g/L, butyric acid 0.2g/L, lactic acid 0.2g/L, acetone 5g/L, butanol 15g/L, ethanol 3g/L. The parameters for running samples are summarised in Table 2.3.

Condition	Setting
Flow rate	0.9 ml/min
Elution mode	Isocratic
Method length	45 min
Column	Aminex HPX-87H
Oven temperature	85 °C
Injection volume	10 µl
Detector	Refractive index at 35 °C
Mobile phase	5 mM H ₂ SO ₄

Table 2.3 HPLC run parameters for analysis of fermentation analytes. Fermentation broth time points were taken at 0 h, 6 h, 24 and 48 h. The supernatant of these samples was filtered prior to analysis.

2.11 Atomic Force Microscopy

POPC liposomes extruded to 100 nm were used to make the bilayers. Approximately 100 µl of 1 mg/ml liposome solution was pipetted onto the sample freshly cleaved mica (aluminium silicate) discs, this was then incubated at room temperature for 1 hour. An additional 10 mM Mg²⁺ solution was used to help liposome rupture and bilayer formation. This was subsequently washed with dH₂O. Sample were run using a Dimension FastScan Bio™ (Bruker) using a FastScan-A probe. Butanol solutions were added to the supported bilayers during scanning to enable the effects to be recorded instantly.

3. *In vitro* characterisation of the interactions between butanol and membranes

3.1 Introduction

In order to improve the tolerance to butanol and productivity of solventogenic *Clostridia*, a deeper understanding of butanol's mechanism of toxicity is required. This will enable the creation of targeted strategies to mitigate the effects of it on the cell. In order to obtain such information, it is essential to understand the fundamental relationships between butanol and the membrane. In particular, it is necessary to understand how important membrane properties (those outlined in section 1.3.2) are perturbed by their interaction with butanol and what impact this will have on the overarching behaviour of the membrane. Due to the complex and holistic response to butanol *in vivo*, identification and understanding of these important interactions between butanol and the membrane have remained somewhat elusive. The use of *in vitro* methods can allow for a greater specificity when it comes to investigating certain properties that can be cross correlated with *in vivo* data. This is due to the ability to generate bespoke models with desired compositions, which can be subject to direct and minute changes in order to investigate a potential relationship between said component and butanol. Thus, *in vitro* models are an important first step to help better understand this relationship and to inform rational strain design for later *in vivo* experiments.

The experimental plan of this Chapter pertains to the interaction between butanol and liposomal model membranes and is summarised in Figure 3.1. The first set of experiments used CF leakage and laurdan GP to investigate the permeability and fluidity of the liposomes, respectively. The compositions of these liposomes began with POPC, a simple, single-lipid system. This was compared to 3 POPE: 1 POPG which is more akin to the membrane composition of a bacterium (Murzyn *et al.*, 2005). Later experiments used 3 POPE: 1 POPG as a base composition, to which other lipids were added to investigate their specific effect. These additional lipids were chosen to alter properties of the membrane, such as thickness, saturation: unsaturation ratio and, the geometric isomerism of unsaturated bonds. The effects of these

changes on fluidity and permeability were then examined. A range of exogenous compounds were also tested to assay whether their presence could mitigate the effect of butanol on the membrane. This included cholesterol, a sterol known to regulate membrane fluidity; and a series of self-associating amphiphilic membrane active compounds, synthesised at the University of Kent. These first experiments provided information about potential protective lipids and which properties of the membrane are important to consider for butanol toxicity. The next experiments were undertaken to understand the mechanism of the interaction of butanol and the membrane. This included DLS to investigate liposome diameter, which was supported by *in silico* coarse-grain molecular dynamic simulations to give an indication of the spatial position of butanol when in the membrane. Additionally, AFM was carried out to show the effects of butanol on mechanical properties of the membrane, supporting the initial fluorescence experiments, as well as to show a topological view of the membrane to complement the DLS. Finally, the effect of butanol on the structure of membrane proteins (their degree of folding) was investigated to provide more information about the holistic nature of butanol toxicity.

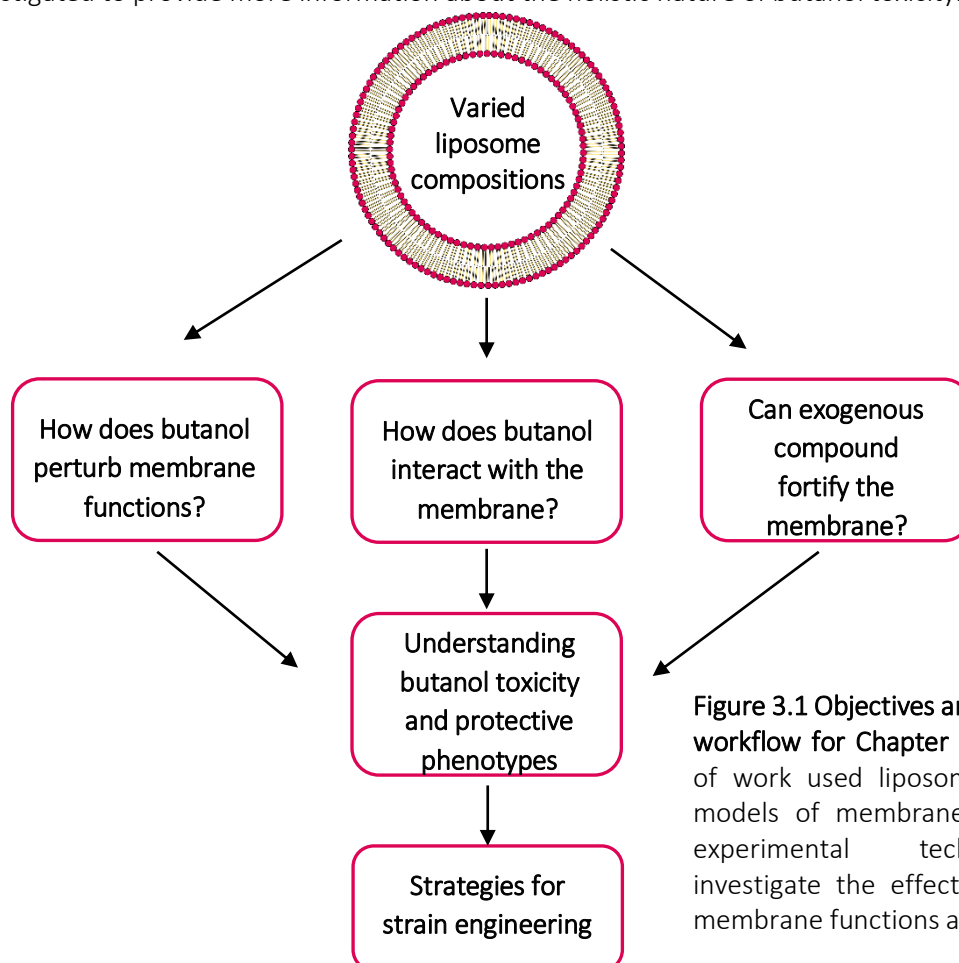


Figure 3.1 Objectives and experimental workflow for Chapter 3. This Chapter of work used liposomes as *in vitro* models of membranes, and several experimental techniques to investigate the effect of butanol of membrane functions and properties.

3.2 Results

3.2.1 *In vitro* assay optimisation

Initial carboxyfluorescein release assays experiments included the optimisation of carboxyfluorescein concentrations as well as both liposome concentration and incubation time (Figure 3.2). A two-fold serial dilution from 1 mg/ml of CF-containing POPC liposomes were exposed to 1 % SDS to obtain the optimal concentration to use in later experiments (Figure 3.2B). The optimum working liposome concentration was found to be 0.25 mg/ml, above which fluorescence begins to plateau. To investigate the mechanism of butanol mediated membrane permeabilisation, a time course was initially carried out (Figure 3.2C). Fluorescence for all difference concentrations of butanol (0, 7.5, 15 and 25 mg/ml) was found to be highest between 10-20 minutes following exposure to exogenous butanol. In subsequent experiments, fluorescence was read 10-20 minutes after addition of butanol to enable a maximum reading. Additionally, the fluorescence was recorded over several days following storage at 4 °C between readings. A 5 % SDS solution was used to fully rupture liposomes leading to maximum CF release. CF-liposomes in buffer were normalised to the SDS wells to investigate the effect of storage on the viability of the membrane. The fluorescence of stored liposomes relative to fully ruptured SDS liposomes appeared to increase with longer storage times. Liposomes were therefore made fresh for each assay and used within one day of making them, in order to minimise the effects of passive loss of liposome integrity on butanol assays. The \log_{10} fluorescence of CF can be seen in Figure 3.2B. across a range of 1:1 serial dilutions with liposome buffer. The self-quenching effect of high concentrations can be seen at the higher concentrations. As the CF was diluted further fluorescence exceeded the maximum limit of the fluorescence reader and plateaus. Following sufficient dilution, fluorescence decreased accordingly. The desired fluorescence of CF within the liposomes should be high enough to ensure self-quenching, which will enable a quantitative indicator of a loss of membrane integrity when exposed to butanol. It was decided that liposomes would be loaded with 100 mM CF as this showed a high degree of self-quenching which increased in fluorescence once diluted in buffer.

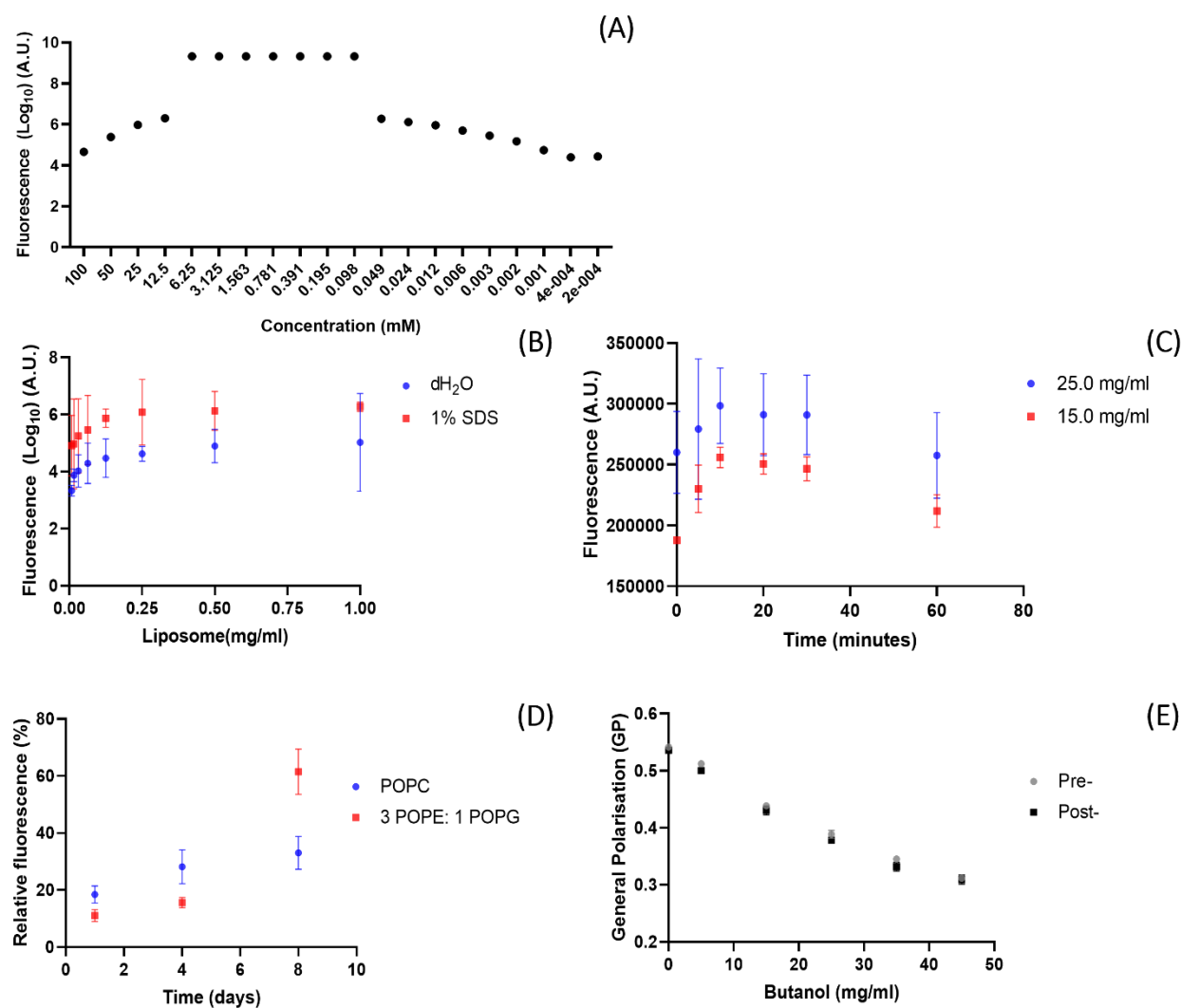


Figure 3.2 Optimisation of liposome based biophysical assays – laurdan probe and carboxyfluorescein CF dye leakage. Aspects relating to the experimental design of the two assays along with various control experiments initially carried out. These included the optimal CF and liposome concentrations and the optimal incubation time with butanol. (A) A two-fold serial dilution of carboxyfluorescein starting from 100 mM showing quenched fluorescence at high concentrations. \log_{10} (B) Dilution series of POPC liposomes containing carboxyfluorescein. (C) Time course of CF fluorescence from 3 POPE: 1 POPG liposomes to optimise incubation time. (D) Time course of CF fluorescence from 3 POPE: 1 POPG and pure POPC liposomes to investigate storage. Fluorescence is relative to freshly made liposomes. (E) Comparing the general polarisation (GP) of Laurdan from two methods. Pre-, where laurdan powder was added to chloroform containing lipid before lipids were dried down; and Post-, where Laurdan dissolved in DMSO was added to freshly extruded liposomes and then incubated for 1hr at ~ 10 °C above the phase transition temperature. Different scales are used. $N=3$, ± 1 SEM.

Laurdan is required to integrate into the membrane in order to act as a fluidity proxy probe and provide information about the state of the membrane. The probe can be added to the liposomes at two different points. Dry laurdan or laurdan dissolved in chloroform can be added to the lipid solution before evaporation of the organic solvent. Alternatively, a concentrated stock of laurdan dissolved in DMSO

can be added to an aqueous liposome solution following rehydration of the lipid film. It is important to determine the method which provided the greatest degree of integration into the membrane. Two populations of POPC liposomes were prepared as above and were run through a routine butanol fluidity assay. It can be seen in Figure 3.2E that there was no difference in general polarisation found between the two methods, both showing the same trend of increasing GP (i.e. increased fluidity) with increasing butanol concentrations. Whilst it should be noted that raw fluorescence values were slightly higher for the laurdan added to the organic acid method, the second method (addition to the aqueous liposomes) was taken forward. This is due to the second method enabling a greater degree of freedom when generating samples. A large batch of liposomes can be made with the second method, which can be subsequently divided up before the addition of the laurdan probe. A portion can be used in laurdan assay and another in other membrane property assays.

3.2.2 Altering headgroup composition

Initial experiments involved the use of liposomes as model cell membranes to investigate the effect of altering lipid composition on butanol tolerance. This involved mixing together different phospholipids of interest to create desired compositions, which were then used to generate liposomes. These liposomes were tested using a variety of *in vitro* assays (see 2.3 *In vitro* liposome assays) to investigate fluidity, permeability, and diameter in order to gain more understanding regarding butanol-phospholipid interactions. Changes were made to the headgroups species and several aspects of the tails (see Figure 1.3 Phospholipids and phospholipid headgroup structure, for phospholipid structures), including POPE: POPG is considered a more accurate model of a bacterial membrane than pure POPC bilayers - Both PE and PG headgroups constitute major components of the lipid membrane in *Clostridia* (Řezanka *et al.*, 2012). Because of this, comparisons between POPC and 3 POPE: 1 POPG liposomes were made and can be seen in Figure 3.3A-B. CF leakage assays provide quantitative information about the state of the membrane.

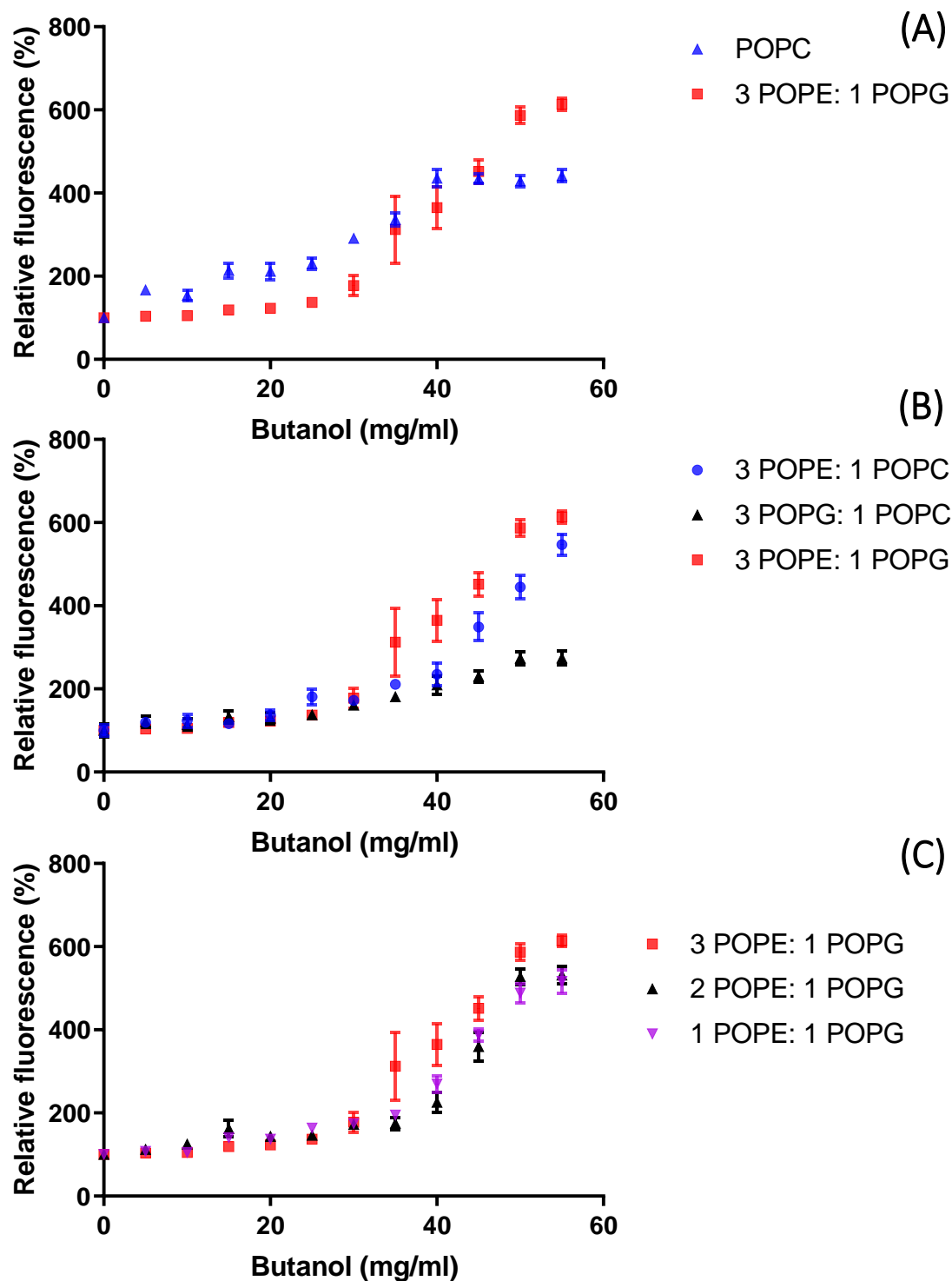


Figure 3.3. Carboxyfluorescein (CF) fluorescence dye release and of membrane models with different lipid headgroup compositions following butanol exposure. (A) Comparing 3 POPE: 1 POPG and pure POPC liposomes. (B) Comparing liposomes with varied headgroup ratios. (C) Comparing liposome with varying amounts of POPG. CF fluorescent dye was loaded inside liposomes with different lipid compositions. These were then exposed to a range of butanol concentrations and the fluorescence was recorded. A higher relative fluorescence denotes lower membrane permeability. Fluorescence was measured on a Mithras LB940 with the following wavelengths for CF; Excitation: 485 nm Emission: 535 nm. N=3, ± 1 SEM

The amount of CF released following butanol exposure implies and indicates the relative permeability of the membrane. If butanol impacts the permeability of the membrane, an alteration in fluorescence will subsequently occur. The mixed composition of 3 POPE: 1 POPG was found to have lower fluorescence than POPC at biologically relevant concentrations ($< \sim 25$ mg/ml) ($P > 0.05$). The rise in fluorescence of POPC began much earlier, reaching 200 % relative fluorescence by 10-15 mg /ml. Meanwhile, 3 POPE: 1 POPG fluorescence only begins to rise at higher butanol concentrations and had exceeded 200 % relative fluorescence until 30-35 mg/ml. Relative fluorescence appears to plateau at concentrations above 40 mg/ml, whereas 3 POPE: 1 POPG continues to rise. Laurdan reveals information about membrane fluidity, and it can be seen that for both POPC and 3 POPE: 1 POPG membranes become increasing fluid upon increasing butanol exposure, with POPC being significantly more fluid than 3 POPE: 1 POPG at the across all butanol concentrations (Figure 3.4A).

Following these initial investigations, a mix of POPE: POPG was considered to be a good base lipid composition for further experiments. This is based on it previously being used as a mimic of an internal membrane and also due to the lower fluorescence shown in Figure 3.3A indicating a more protective effect. Further experiments were carried out to determine the optimal ratio of POPE to POPG and whether spiking in more POPG would prove beneficial (Figure 3.3C). In the biologically relevant range of < 30 mg/ml butanol, there appears to be little difference in fluorescence following the addition of more PG in the forms of 1 POPE: 1 POPG and 1 POPE: 3 POPG. Above this range however, both models with additional PG appear to have lower fluorescence than 3 POPE: 1 POPG which continues to climb with higher butanol concentrations, whereas 1 POPE: 1 POPG and 1 POPE: 3 POPG plateau at 40 mg/ml. Despite this apparent trend there was found to be no significant difference from 3 POPE: 1 POPG liposomes. The 3 POPE: 1 POPG compositions was still used as a base in later experiments due to the comparable fluorescence seen in the relevant butanol ranges. Interestingly, 2 POPE: 1 POPG appeared to be less susceptible to fluidity changes induced by butanol as 3 POPE: 1 POPG (Figure 3.4). However,

upon addition of more PG, in the 1 POPE: 1POPG model, there was found to be the same trend in fluidity as was seen in 3 POPE: 1 POPG.

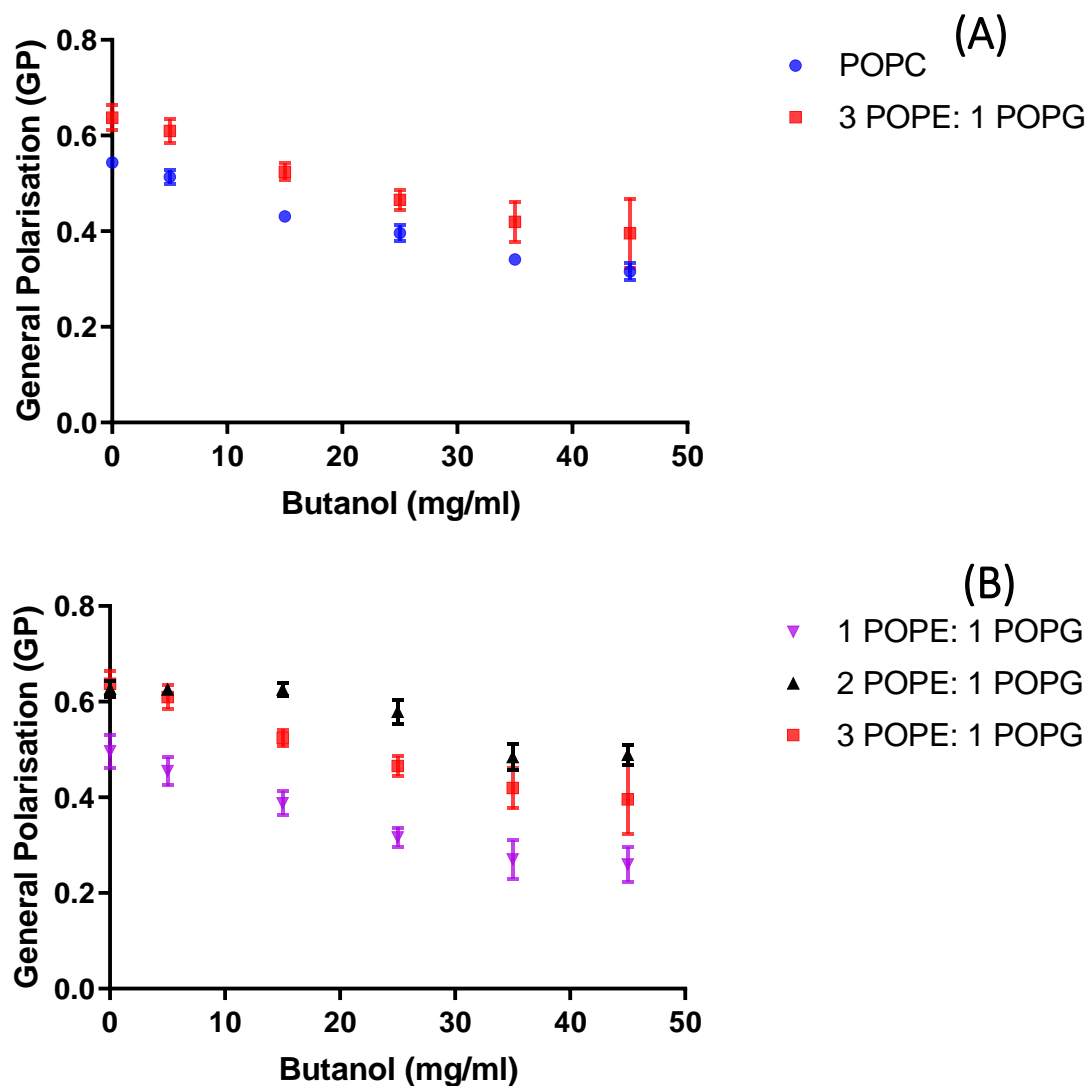


Figure 3.4. Laurdan probe general polarisation (GP) of membrane models with different lipid headgroup compositions following butanol exposure. (A) Comparing 3 POPE: 1 POPG and pure POPC liposomes. (B) Comparing liposome with varying amounts of POPG. A lower GP indicates higher membrane fluidity. Fluorescence was measured on a Mithras LB940 with the following emission wavelengths, 460 nm and 535 nm. The laurdan fluorescent probe was added to aqueous liposome solutions after lipid film rehydration. After a 1 h incubation period, the liposomes were exposed to a range of butanol concentration and the fluorescence was recorded. The GP value was then calculated using the equation described in 2.3.1 Carboxyfluorescein and laurdan fluorescence assays. N=3, ± 1 SEM.

The composition of 3 POPG: 1 POPC showed a comparable CF response to 3 POPE: 1 POPG up until 25 mg/ml. Above this concentration, there is a comparatively lesser effect of butanol on 3 POPG: 1 POPC

than 3 POPE: 1 POPG. This is similar to using pure POPC liposomes (CF fluorescence flattened at higher concentrations) and so there might be some protective effect of POPC at high butanol concentrations. Alternatively, it may be that these compositions have a higher base line of CF leakage and therefore would show a flatter relative change in fluorescence. Comparisons with a 5 % SDS control can be drawn to investigate this further. At 0 mg/ml 3 POPG: 1 POPG showed a 31.27 % CF fluorescence of the 5 % SDS control. For 3 POPE: 1 POPG this value was 7.23 %, thus this disparity may impact the direct comparison of the relative fluorescence. Both POPC and POPG are bilayer-forming lipids based on the shape of each individual lipid molecules. The flatter fluorescence release may be due to bilayer being made entirely of bilayer-forming lipids or alternatively it may be because of some protective effect of having 75 % POPG in the bilayer. 3 POPE: 1 POPG and 3 POPE: 1 POPC were found to have very similar CF releases, with the latter being significantly less leaky at 50 mg/ml butanol only. Altering the headgroup can impact the permeability and fluidity of the membrane following butanol exposure. Alterations to the tail portion of the phospholipids were then carried out as a means of investigating the impacts of this part of phospholipids on butanol toxicity.

3.2.3 Acyl chain modifications

These changes to acyl chain composition have been implemented to mainly target fluidity as this is likely an integral factor in butanol related membrane toxicity. The consequences of butanol exposure were measured using a combination of CF release, laurdan GP and DLS. It is hypothesised that there is a relationship between liposome compositions which have a lower base-line fluidity (denoted by higher GP values), and susceptibility to butanol-mediated permeabilisation (determined by relative CF release). The lipid species under investigation was added in an equal ratio to the base liposome composition of 3 POPE: 1 POPG. This was done to show how these alterations would impact the interaction with butanol within a model resembling the normal compositions of a bacterial membrane. Firstly, the length of the acyl chains was investigated whereby either DMPC (14 carbons) or DSPC (18 carbons) was added to the base composition. These chain lengths were chosen due to their existence in *Clostridial* membranes,

and due to the fact that they will impart different influences on the membrane as a whole in terms of fluidity, thickness and interlipid interactions. Secondly, the degree of saturation and geometrical isomerism of any unsaturated bonds was investigated using variants of DOPC ($\Delta 9$ -*Trans* or $\Delta 9$ -*Cis*). Altering *Cis-Trans* isomer ratios is a response to alcohol stress which has been seen in other organisms such as *Pseudomonas putida* (Tan *et al.* (2016)). Finally, changing the proportion of phosphoglycerol backbone lipids with the addition of plasmalogen species which contain a vinyl ether linkage instead of an ester linkage on the sn-1 position. Plasmalogens have also been suggested to play a role in butanol stress response in solventogenic *Clostridia* (see 1.4 Butanol toxicity, (Kolek *et al.* (2015)). CF leakage was found to be significantly higher ($p < 0.001$) in 3 POPE: 1 POPG: 4 DMPC than in 3 POPE: 1 POPG: 4 DSPC liposomes following butanol exposure > 25 mg/ml (Figure 3.5A-B). Similarly, liposomes with the *cis* geometric isomer were found to release significantly more ($p < 0.02$) CF in response to butanol (>30 mg/ml) than the *trans* isomer (Figure 3.5B). Liposomes with the additional longer-chained lipids (DSPC) were also significantly less fluid at all butanol concentrations compared to DMPC-containing liposomes (Figure 3.5A). Geometrical isomerism appeared to have less impact on membrane fluidity in response to increasing butanol concentrations (Figure 3.6B). The disparities in membrane fluidity between the *cis* and *trans* isomers was significantly different at 0 and 5 mg/ml butanol, above which there was no significant difference (Figure 3.6B). The substitution of 12.5 % (mass) POPE for POPE which contained a plasmalogen also appeared to have a small effect on CF leakage. Liposomes containing the plasmalogen species had lower fluorescence at high butanol concentrations (> 30 mg/ml). However, there appeared to be no difference in CF leakage in the biologically relevant ranges of butanol (15-30 mg/ml) (Figure 3.5C). Additionally, the fluidity of plasmalogen containing species was significantly lower than 3 POPE: 1 POPG at all butanol concentrations. Altering the fatty acid portions of phospholipids appears to mitigate the effects of butanol on the membrane, possibly with more rigid membranes being more protective. The ability of non-phospholipid elements to stabilise the membrane was investigated as a potential means to augment and the effect of changing lipid composition.

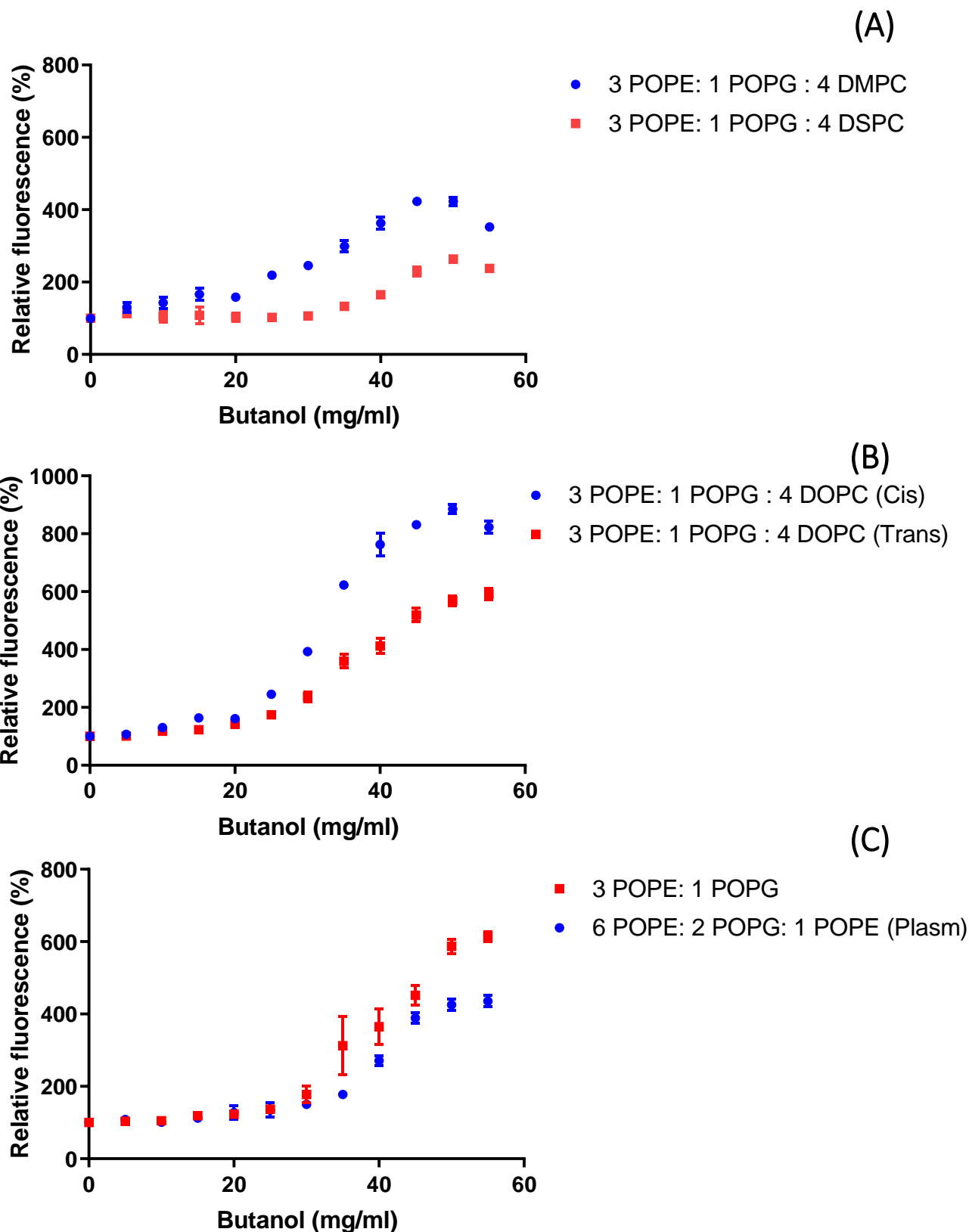


Figure 3.5 Carboxyfluorescein (CF) fluorescence dye release and of membrane models with different acyl chain compositions following butanol exposure. (A) Comparing chain length using DMPC (14 carbons) and DSPC (18 carbons) was added when in an equal ratio. (B) Comparing geometrical isomerism using DOPC (*Cis*) and DOPC (*Trans*). (C) Investigating the effect of adding plasmalogen containing species. CF fluorescent dye was loaded inside liposomes with different lipid compositions. These were then exposed to a range of butanol concentrations and the fluorescence was recorded. 3 POPE: 1 POPG was used as a base composition. Prior to liposome generation, other lipid species were added to 3 POPE: 1 POPG in an equal amount (mg/mg), generating a range of compositions. Fluorescence was measured on a Mithras LB940 with the following wavelengths for CF; Excitation: 485 nm Emission: 535 nm. Difference Y-axis scales are used. N=3, ± 1 SEM.

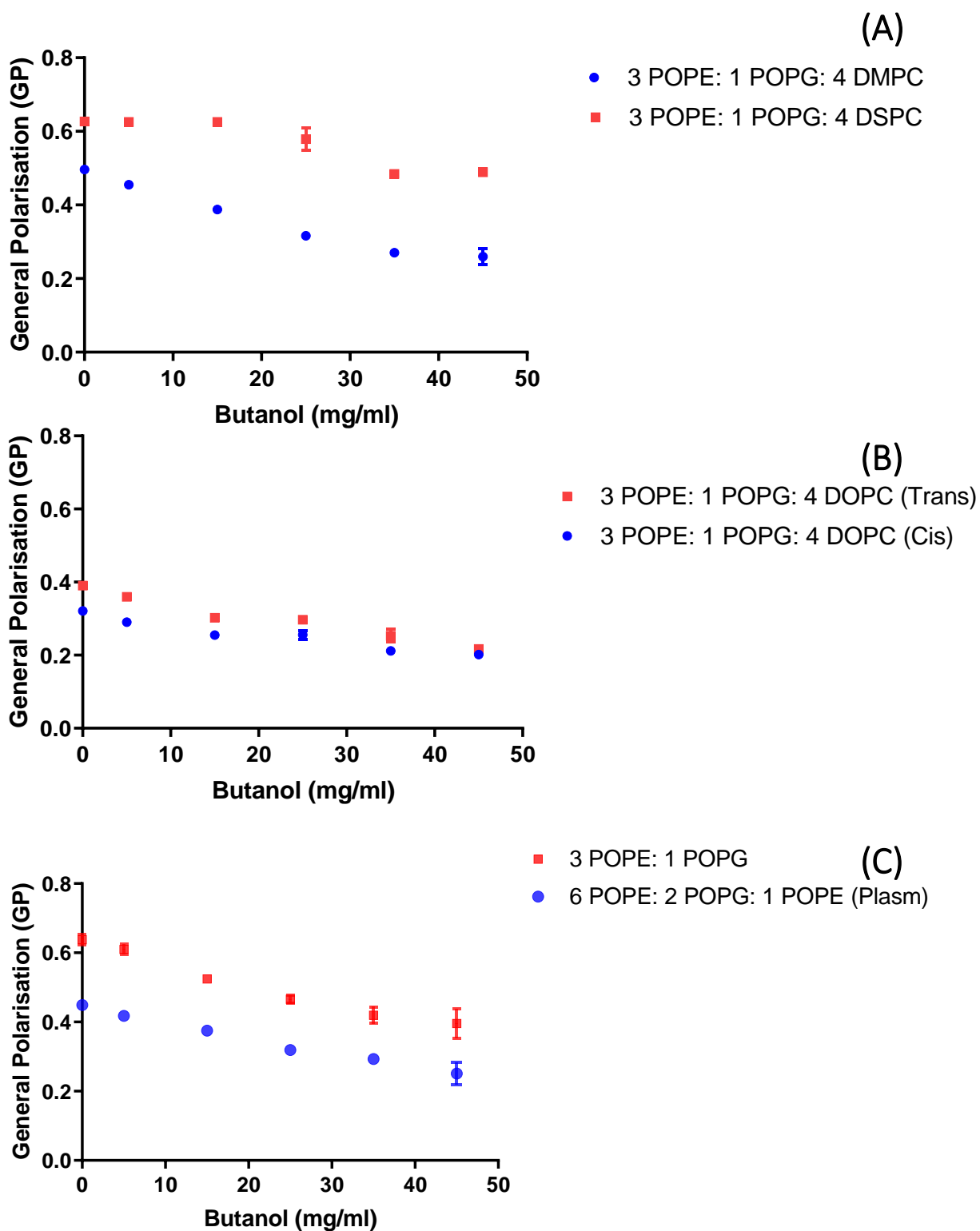


Figure 3.6. Laurdan probe general polarisation (GP) of membrane models with different acyl chain compositions following butanol exposure. (A) Comparing chain length using DMPC (14 carbons) and DSPC (18 carbons) was added when in an equal ratio. (B) Comparing geometrical isomerism using DOPC (*Cis*) and DOPC (*Trans*). (C) Investigating the effect of adding plasmalogen containing species. 3 POPE: 1 POPG was used as a base composition. Prior to liposome generation, other lipid species were added to 3 POPE: 1 POPG in an equal amount (mg/mg), generating a range of compositions. The laurdan fluorescent probe was added to aqueous liposome solutions after lipid film rehydration. After a 1 h incubation period, the liposomes were exposed to a range of butanol concentration and the fluorescence was recorded. The GP value was then calculated using the equation described in 2.3.1 Carboxyfluorescein and laurdan fluorescence assays.

3.2.4 Exogenous compound addition to the membrane

Addition of membrane active molecules such as cholesterol was also investigated. As discussed in the introduction, there may be subtle and nuanced differences in the mechanisms of membrane regulation between different classes of these compounds. Whilst this is the case, cholesterol has been used as a replacement due to difficulties sourcing a bacterial hopanoid. Due to the simplicity of the membrane models used, the effects on the membrane should be broadly similar between cholesterol and bacterial hopanoids. At lower biologically relevant butanol concentrations (< 15 mg/ml) liposome populations with 20 % cholesterol show a slightly lower amount of leakage, however this was found to be not significantly lower than 3 POPE: 1 POPG (Figure 3.7A-B). However, at 20 mg/ml and above, the addition of 20 % cholesterol had no observable effect on the leakage of CF from 3 POPE: 1 POPG showing a similar trend to liposomes containing no cholesterol. Increasing butanol concentrations resulted in a larger degree of CF leakage. At higher concentrations of butanol (> 40 mg/ml), liposomes with 20 % cholesterol had significantly lower CF leakage than the 3 POPE: 1 POPG population. This may suggest a protective effect only when there is a certain degree of membrane fluidisation by butanol. No significant difference in fluidity was observed for 20 % cholesterol however, with 10 % cholesterol a significant increase in fluidity was seen at all butanol concentrations. Cholesterol appeared to be able to fortify the membrane against perturbation at high concentrations of butanol, however this effect was limited in the lower concentration range. A range of synthetic membrane active compounds were then tested, to investigate the possible use as fermentation additives.

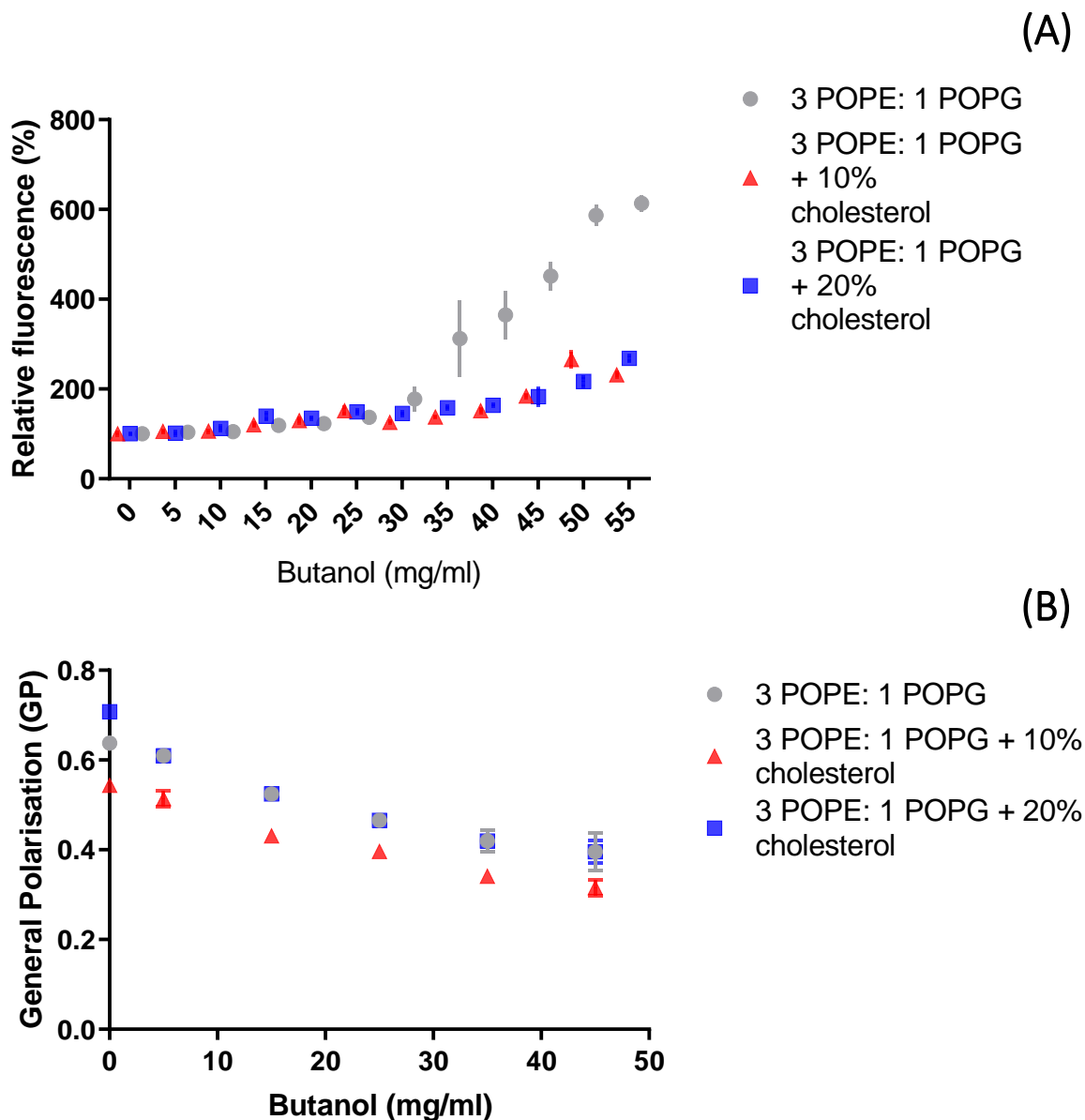


Figure 3.7. (A) Carboxyfluorescein (CF) fluorescence dye release (B) laurdan probe general polarisation (GP) of membrane models with the addition of 20% cholesterol as a surrogate membrane modulator following butanol exposure. CF fluorescent dye was loaded inside liposomes with different lipid compositions. These were then exposed to a range of butanol concentrations and the fluorescence was recorded. The laurdan fluorescent probe was added to aqueous liposome solutions after lipid film rehydration. After a 1 h incubation period, the liposomes were exposed to a range of butanol concentration and the fluorescence was recorded. The GP value was then calculated using the equation described in 2.3.1 Carboxyfluorescein and laurdan fluorescence assays A lower GP indicates higher membrane fluidity. Fluorescence was measured on a Mithras LB940. N=3, ± 1 SEM.

Fermentation additives may provide a fairly simple means to improve yield of butanol. Additives may include exogenous compounds which can integrate into the membranes of fermenting bacteria and stabilise them. Jessica Boles and Dr Jennifer Hiscock at the University of Kent have kindly synthesised and provided self-associating amphiphilic salts (C1, C3, C8, C30, C38, C39, C40, and C43). The structures of the compounds can be seen in Figure 3.8. The structures of a series of self-associating amphiphilic membrane active compounds, and C1 and C3 can be seen in work by White and colleagues (2017). They are 8 potentially membrane active compounds and some may provide stability to the membrane in response to butanol toxicity. Investigations on the effect of the compounds on the fluidity of the 3 POPE: 1 POPG membrane were carried out using the laurdan probe.

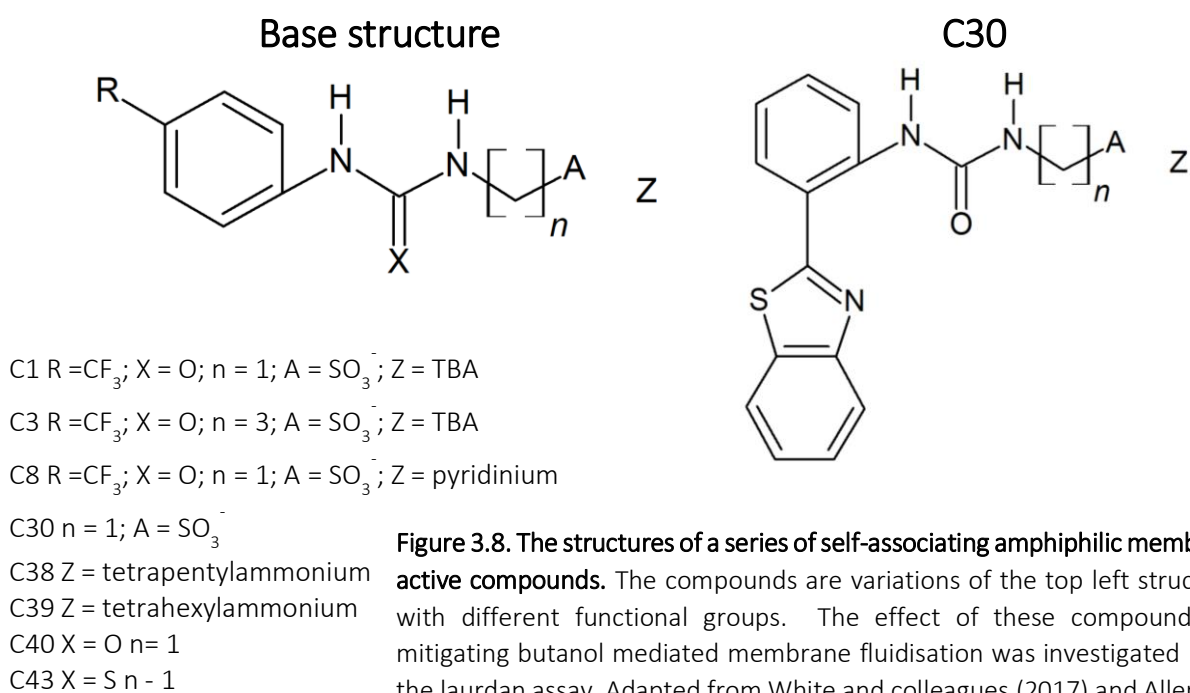


Figure 3.8. The structures of a series of self-associating amphiphilic membrane active compounds. The compounds are variations of the top left structure, with different functional groups. The effect of these compounds on mitigating butanol mediated membrane fluidisation was investigated using the laurdan assay. Adapted from White and colleagues (2017) and Allen and colleagues (2020). Structures drawn in ChemSketch.

Initial experiments were conducted using POPC liposomes as a model membrane, and the effects of the compounds on the fluidity of the liposomes was measured in absence of butanol (Figure 3.9). This was done to investigate effects on the liposomes that are independent of butanol ingress into the membrane. The compounds were serially diluted (1:1) in buffer starting at 2 mg/ml compound to a final ~ 2 µg/ml. For C1, C3, C8 and C30 there was found to be no change in GP across all concentrations. There was a lower GP found for C38 at higher concentrations suggesting a reduction in membrane

fluidity. However, due to the nature of the trend and the very large reduction in GP value it may be an artefact of molecule's structural elements. It may be that the decrease in GP seen for C38 is due to an intrinsic fluorescence emission at one of the wavelengths measured as this would also result in the same trend. An interesting trend was seen for C39 which displayed a skewed bell-shaped GP response across the serial dilution range. Beginning at 0.461, the GP of C39 increased and peaked at 0.876, at a concentration of 0.0625 mg/ml. This would not be due to a change in the fluorescence emanating from the laurdan fluorophore as this has remained at a constant concentration. Beyond this the GP gradually decreased to 0.732, at 2 mg/ml. C40 and C41 both showed a generally flat GP across all dilutions until 1 mg/ml and 2 mg/ml, where it increased.

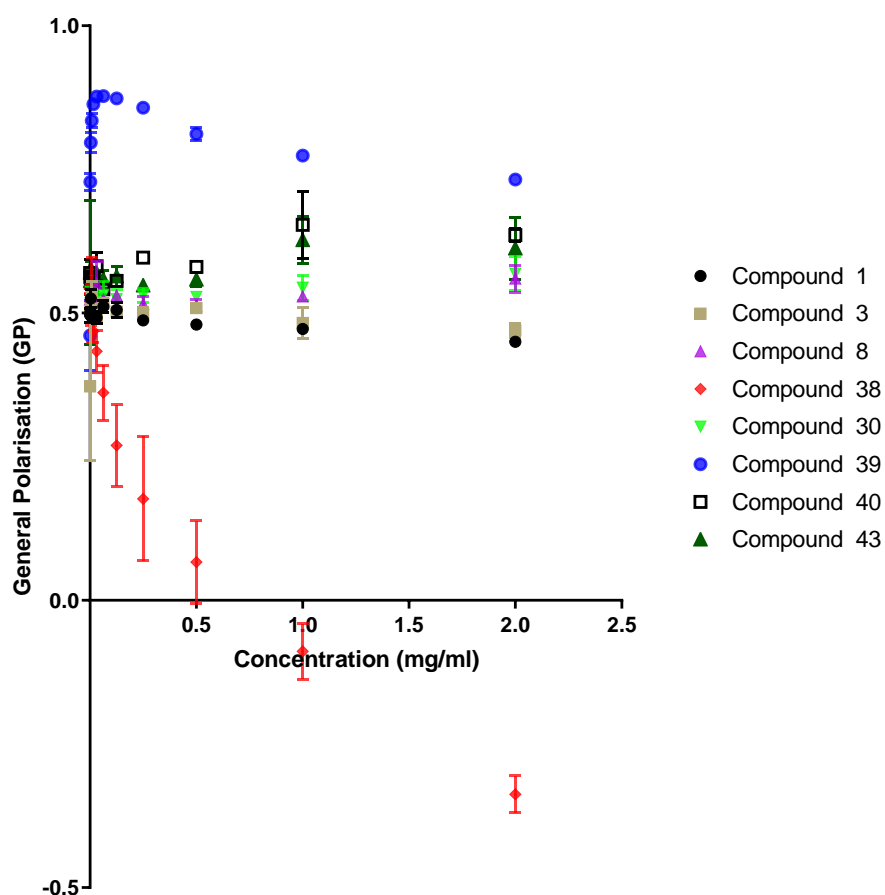


Figure 3.9 Laurdan probe general polarisation (GP) of POPC liposomes with the addition of several serially diluted compounds. The compounds were diluted two-fold A lower GP indicates higher membrane fluidity. Fluorescence was measured on a Mithras LB940. The laurdan fluorescent probe was added to aqueous liposome solutions after lipid film rehydration. After a 1 h incubation period, the liposomes were exposed to a range of butanol concentration and the fluorescence was recorded. The GP value was then calculated using the equation described in 2.3.1 Carboxyfluorescein and laurdan fluorescence assays. N=3, ± 1 SEM.

The ability for these compounds to alter the fluidity of membranes, a potential means to protect against butanol perturbation, was investigated using POPC liposomes containing the laurdan probe. Liposomes solutions were mixed with 0.25, 0.5, 1.0 or 2.0 mg/ml of each compound, to which 0, 5, 15, 25, 35, or 45 mg/ml butanol was then subsequently added (Figure 3.10). All conditions showed a decreasing in laurdan GP upon exposure to increasing concentrations of butanol, suggesting a reduction in membrane fluidity. There appeared to be no difference in GP value when any of the compounds were added at all of the concentrations. Additionally, there was found to be no significant difference in laurdan GP for any of the compounds and POPC alone. All trends are similar with overlapping GP values for individual compound at different concentrations. Different GP trends were seen for C38 and C39 (Figure 3.9E-F), with the former showing decreasing GP values with increasing compound concentrations, and the latter showing much higher GP values. These results are likely due to the intrinsic fluorescence of the two compounds and not due to their interaction with the cell membrane or butanol. Based on previous work published by the group at Kent (see discussion) a further set of experiments was carried out where the liposomes were incubated with the compounds overnight (Figure 3.11). In theory this should have allowed time for the compounds to integrate within the membrane if this was a limiting factor in their potentially protective effects. It was found however, that there was still seemingly no benefit of exposing the liposomes to the compounds for an extended period, prior to exposure to butanol. The fluidities of the liposomes were the same at all butanol concentrations despite the compound concentrations. Overall, these experiments may require further optimisation to allow for any effect of the compounds to be realised. This would include using a different composition of lipids (3 POPE: 1 POPG instead of pure POPC) as this will likely interact better with the compounds (discussed further in discussion). If these compounds are shown to be protective it may be due to them being able to prevent butanol intercalation into the membrane. The following experiments using dynamic light scattering aimed to provide some mechanistic insight on the intercalation of butanol and phospholipids, and whether intercalation resulted in changes to the structure of liposomes. Understanding intercalation of butanol into the membrane could help design additives to which prevent this from occurring.

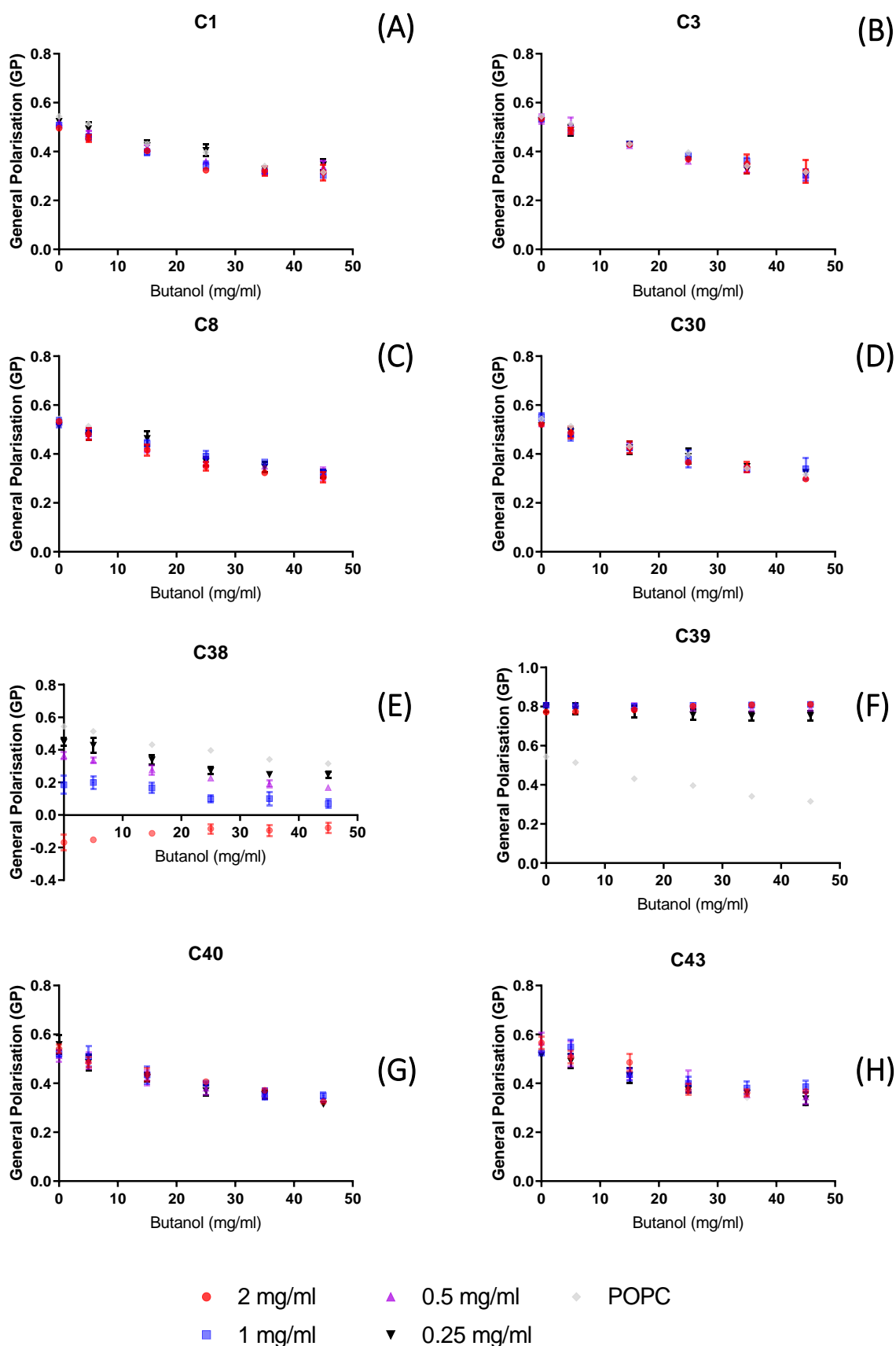


Figure 3.10 Laurdan probe general polarisation (GP) of POPC liposomes with the addition of several compounds at different concentrations following butanol exposure. A lower GP indicates higher membrane fluidity. Fluorescence was measured on a Mithras LB940. The laurdan fluorescent probe was added to aqueous liposome solutions after lipid film rehydration. After a 1 h incubation period, the liposomes were exposed to a range of butanol concentration and the fluorescence was recorded. The GP value was then calculated using the equation described in 2.3.1 Carboxyfluorescein and laurdan fluorescence assays. N=3, ± 1 SEM.

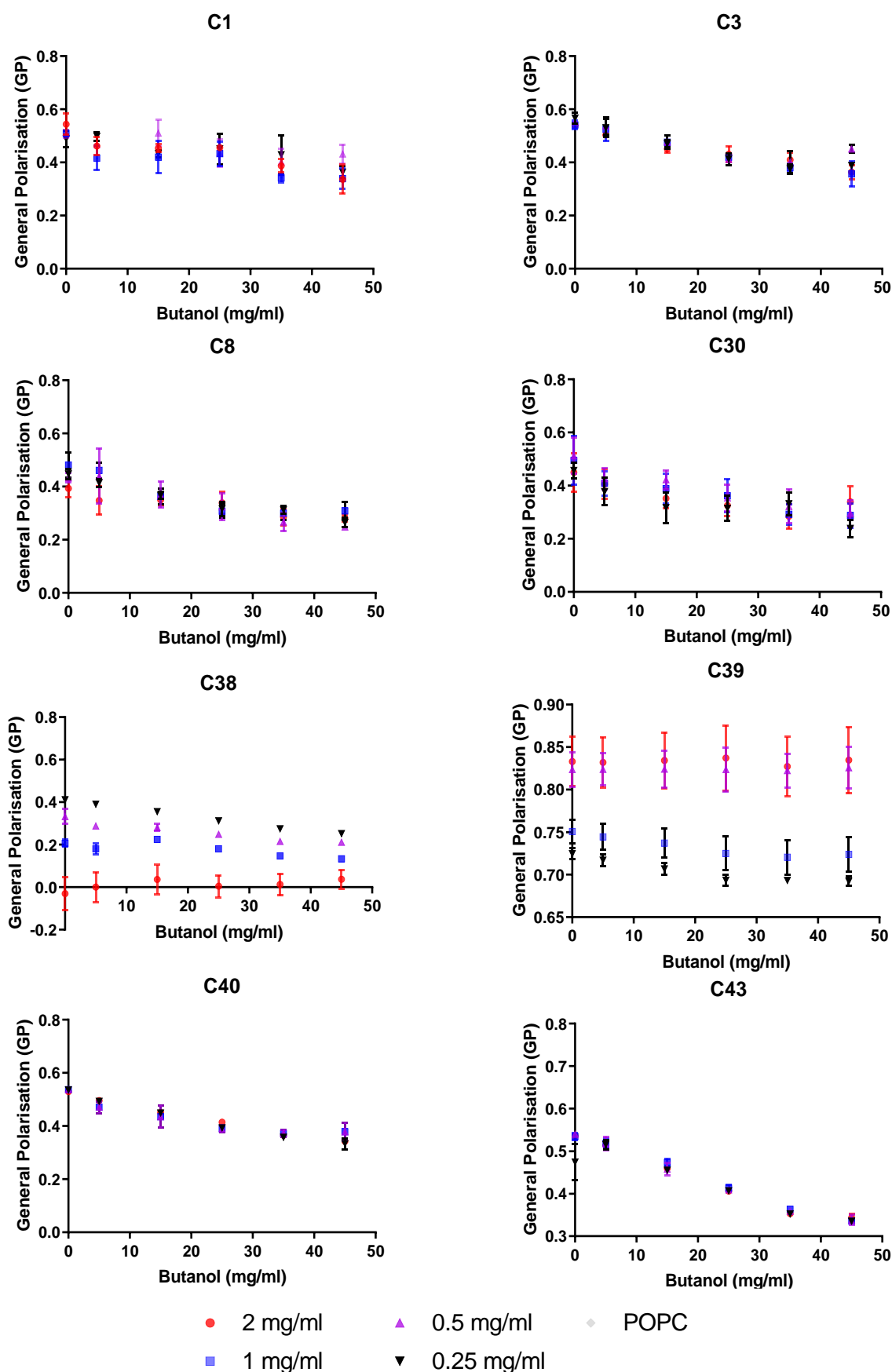


Figure 3.11 Laurdan probe general polarisation (GP) of POPC liposomes with the addition of several membrane active compounds at different concentrations following butanol exposure. Liposomes were incubated with the compounds for 16-24 h before butanol addition to allow for integration into the membrane. The laurdan fluorescent probe was added to aqueous liposome solutions after lipid film rehydration. After a 1 h incubation period, the liposomes were exposed to a range of butanol concentration and the fluorescence was recorded. The GP value was then calculated using the equation described in 2.3.1 Carboxyfluorescein and laurdan fluorescence assays. N=3, ± 1 SEM.

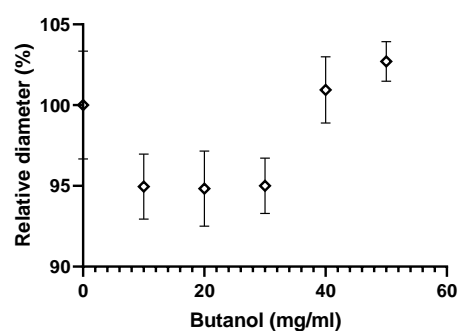
3.2.5 Dynamic light scattering

Dynamic light scattering (DLS) was used to investigate whether butanol ingress into the phospholipid portion of the membrane would result in any changes to the diameter of the liposomes models. It was predicted that the partitioning of butanol into the membrane would result in liposome swelling due the disruptive effect of butanol in regard to interlipid bonding. Understanding more about this mechanism may help to provide information for developing strategies to prevent butanol insertion. A similar array of membrane compositions to previous assays were also compared to see if there were any differing responses to butanol in terms of model diameter.

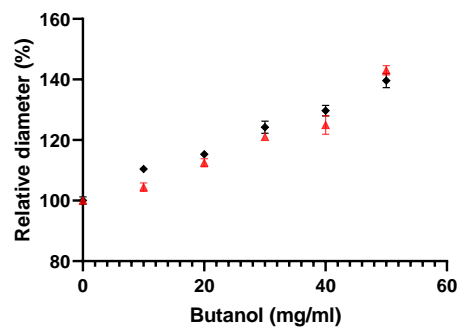
As DLS work on the Brownian motion of a particle in solution, it is possible that, based on butanol being more viscous than water, increasing the butanol concentration could result in artificial data. Therefore, initial experiments on 100 nm polystyrene beads (non-butanol reactive) were carried out. There was found to be some variation in size however this was within the manufacturing error ($\pm 3\%$) and thus it can be concluded that DLS remains a viable method for assaying the diameters of membrane models exposed to butanol (Figure 3.12A). A concentration dependent increase in liposome diameter was seen in response to butanol for all liposomal compositions (Figure 3.12B-F). This would suggest that butanol ingress results in liposomal swelling stemming from butanol's ability to intercalate within the lipids. Additionally, this swelling effect of butanol occurred immediately upon addition of butanol. Because of this rapid onset of action, it may have been possible that the increase in diameter seen was an artefact of the measuring principles of dynamic light scattering. Since the speed of particles being measured is an essential element needed to calculate the diameter of said particles, the viscosity of the solution can thus directly impact the calculated diameter. Particles in a more viscous solution (e.g. butanol) will have less Brownian motion and will therefore be moving at a slower speed. This will reduce the frequency of fluctuations in light scattering. Ultimately, this may result in the false reporting of an increase in particle diameter as the concentration of the more viscous solvent is increased. As butanol is more viscous than water, increasing the proportion of butanol in these DLS experiments may have resulted in this

phenomenon occurring. In order to determine a real effect of butanol on liposome diameter, a negative control was utilised (Figure 3.12A). This consisted of 100 nm inert polystyrene standards which are not subject to direct butanol-mediated swelling but will be impacted by the viscosity of the solution. It was found that up to 50 mg/ml butanol had no significant impact on the measured sizes of these polystyrene standards. The use of DLS to investigate the effect of butanol on liposome diameter is therefore not influenced by the increasing viscosity of the sample solution at higher butanol levels.

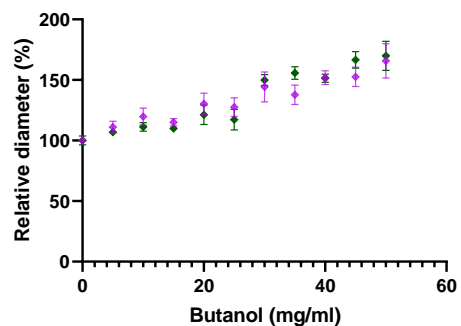
Altering the headgroup composition on the liposomes was found to generally have no effect on the swelling caused by butanol, however, showed a significantly different greater increase in size at 25 mg/ml and 45 mg/ml butanol for 3 POPE: 1 POPG liposomes compared to POPC (Figure 3.12B). The addition of a plasmalogen containing species to the 3 POPE: 1 POPG model yielded similar result with, on the whole, there being no significant differences between the population except for at 10 mg/ml where 6 POPE: 2POPG: 1PE(plasm) liposomes were significantly larger (Figure 3.12C). No significant difference was found between DMPC and DSPC containing liposomes at any butanol concentrations, with both compositions showing a similar trend of increasing diameter in response to increasing butanol concentrations (Figure 3.12E). Altering the geometric isomerism of the double bond in DOPC had some effects on the diameter following exposure to 20 mg/ml < butanol. DOPC (*Cis*) containing liposomes were significantly smaller than DOPC (*Trans*) liposomes at 25, 35, 40, 45 and 55 mg/ml butanol (Figure 3.11D). Finally, 3 POPE: 1 POPG liposomes with 20% cholesterol (as a replacement for hopanoid species) were significantly smaller than 3 POPE: 1 POPG alone at ≥ 20 mg/ml butanol (Figure 3.12F). Ultimately, for the majority of alterations made to the liposome models there were few discernible trends found relating to a composition that could protect against butanol-mediated swelling. Butanol causes a concentration dependent increase in liposome diameter, which could possibly have been an artefact of butanol accumulation on the surface of the liposomes. To investigate this further, molecular dynamic simulations were carried out to see where butanol interacts within the membrane.



(A)



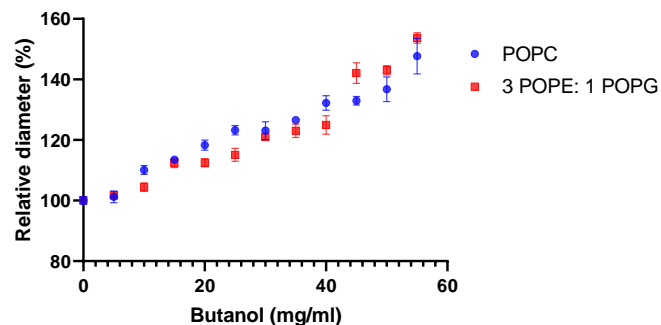
(B)



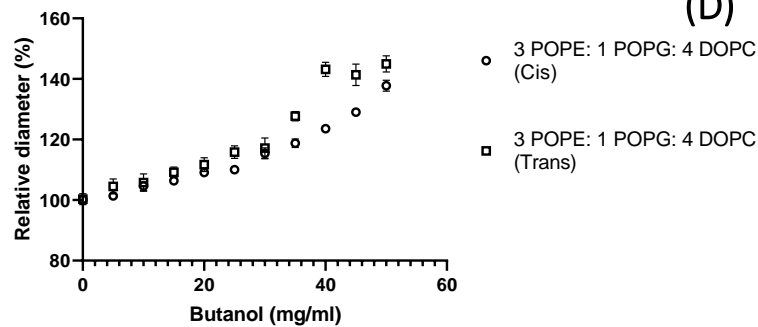
(C)



(D)



(E)



(F)

Figure 3.12. The normalised diameter of liposome models and polystyrene standards in response to butanol. (A) 100 nm polystyrene standards. (B) Comparison of POPC and 3 POPE: 1 POPG liposomes diameter. (C) Comparison of 3 POPE: 1 POPG and 6 POPE: 2 POPG: 1 POPE (Plasmalogen) liposomes diameter. (D) Comparison of 3 POPE: 1 POPG: 4 DOPC (*Cis*) and 3 POPE: 1 POPG: 4 DOPC (*Trans*) liposomes diameter. (E) Comparison of 3 POPE: 1 POPG: 4 DMPC and 3 POPE: 1 POPG: 4 DPSC liposomes diameter. (F) Comparison of 3 POPE: 1 POPG and 3 POPE: 1 POPG + 20% cholesterol. Liposome size was read using dynamic light scattering following butanol exposure. Samples were diluted to an ideal counter per second as determined by the software used. Diameters were normalised to 0 mg/ml. Different Y-axis scales have been used. $N=3 \pm 1SEM$.

3.2.6 *In silico* modelling

Coarse-grained modelling using the MARTINI 2 force field was employed to predict the spatial location of butanol-phospholipid interaction, and to confirm swelling seen with DLS due to butanol insertion and not butanol accumulation on the liposome surface. In coarse-grain simulations atoms are grouped together to form beads. This reduces the computing power required and enables longer simulations at the cost of atomistic resolution. For initial experiments pertaining to obtaining a general understanding of the interaction, this lower resolution attempt should suffice. Figure 3.13 shows the progression of the simulation from a starting point at 0 ns to the end of the simulation at 200 ns. Butanol was represented as a single bead (enlarged red bead) and can be seen in the starting panel (0 ns) to be occupying several locations ranging in distance from the phospholipids on both sides of the bilayer. Butanol molecules were diffusing freely around the bulk solvent, however once in close proximity to the membrane they moved into the headspace region and existed around the phosphate group (orange beads). There appeared to be a range of butanol localisations once an interaction had been established, from the upper acyl chains to the head group regions of the phospholipids (green beads represent POPS and blue beads represent POPE. The headgroup region pertains to the green and blue bead on the outer side of the phosphate groups, closer to the bulk solvent). At 1 ns there are 3 butanol beads occupying this area and as the simulation progresses to 10 ns and 20 ns it can be seen that an additional 2 butanol beads enter into this zone too (one at 10 ns and one at 20 ns). At 100 ns, the mid-point, in the simulation a butanol bead is seen to have returned to the bulk solvent, however by the end of the simulation all butanol molecules were at the interface between the phospholipids and the bulk solvent. During the simulation the interaction appeared to be transient with butanol beads moving in and out of this headgroup zone several times throughout the whole simulation. It should be noted that butanol bead would remain in the head group for several ns or tens of ns at a time, suggesting the presence of a real interaction and not an artefact. Butanol is seen to penetrate to the headgroup region, and not simply interact at the interface region. Furthermore, butanol was unable to diffuse through the membrane.

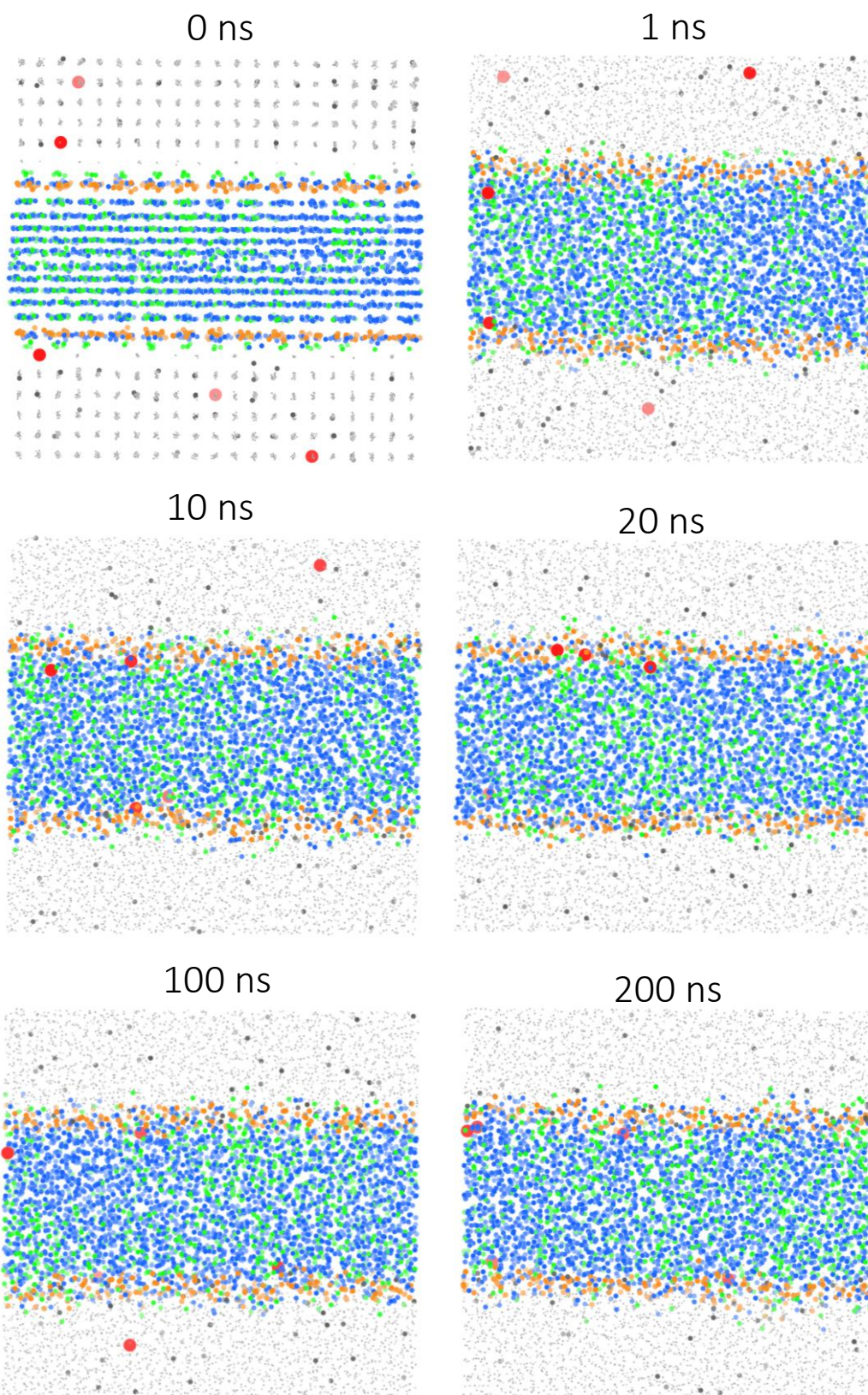


Figure 3.13 Coarse-grained molecular dynamic simulation of butanol interacting with a 3 POPE: 1 POG membrane. The coloured beads represent groups of atoms (colour, atom group): red, butanol; water, light grey; ions, Dark grey; POPE, Blue; POG, Lime green; PO₄²⁻ group, Orange. The 0 ns panel shows the starting positions. By 20 ns all butanol molecules were within the headgroup region, however later in the simulation butanol molecules were found within the bulk solvent, suggesting a non-permanent interaction with the membrane. Simulations were carried out in GROMACS 5.1.2 with the MARTINI 2 forcefield. The system was run for 200 ns and visualised using Visual Molecular Dynamics (VMD) (University of Illinois).

3.2.7 Atomic force microscopy

Atomic force microscopy was employed to give a visual representation of butanol's interaction with the lipid monolayers an extended period. Lipid monolayers are deposited onto a solid support. A cantilever then scans across the surface of the membrane providing topological and mechanical information. This was carried out to provide more information about the effect of butanol on mechanistic properties i.e. strength of the membrane, and also structural information – whether butanol interactions forms membrane pores. Butanol at concentrations of 1%, 3% and 6% were used, and due to time constraints POPC was the only composition investigated. A fluid POPC monolayer was formed successfully which can be seen in Figure 3.14. Upon addition of 1% butanol there was a decrease in bilayer integrity and force resistance and subsequent interdigitation denoted by the force curve seen in Figure 3.13. Additionally, topological changes in response to butanol are seen after 20 minutes of exposure (Figure 3.14). There appears to be an increase expansion resulting in swelling which is accompanied by blebbing of nanoscale vesicles on the surface of the monolayer. This can be seen in the microscopy images with an increase in the amount of white areas of the monolayer, showing an increase in vertical topology i.e. the formation of surface vesicles. For later experiments, 3% butanol caused an increase diameter of nanoscale pores in the POPC monolayers over time. It is unclear whether pore formation is a mechanism through which butanol damage occurs, or whether in this case, butanol has simple exacerbated pores already present due to imperfect monolayer deposition onto the support. A higher concentration of 6% butanol resulted in a large amount of detachment of the monolayer from the support. Panels 004 and 005 show the initial force measurements and just after the addition of 1% butanol, respectively. It can be seen that there is an intact monolayer has formed. Following 3 minutes of incubation (Panel 017), the integrity of the monolayer has decreased due to the ingress of butanol. This is denoted by the loss of the shoulder of the blue line, which shows a loss of resistance against the force of the cantilever. AFM shows butanol to alter mechanical properties as well as possibly cause membrane pore formation. The following experiments pertained to examining butanol's interaction with membrane proteins to complement the large amount of data gathered on the impact on the lipid portion of the membrane.

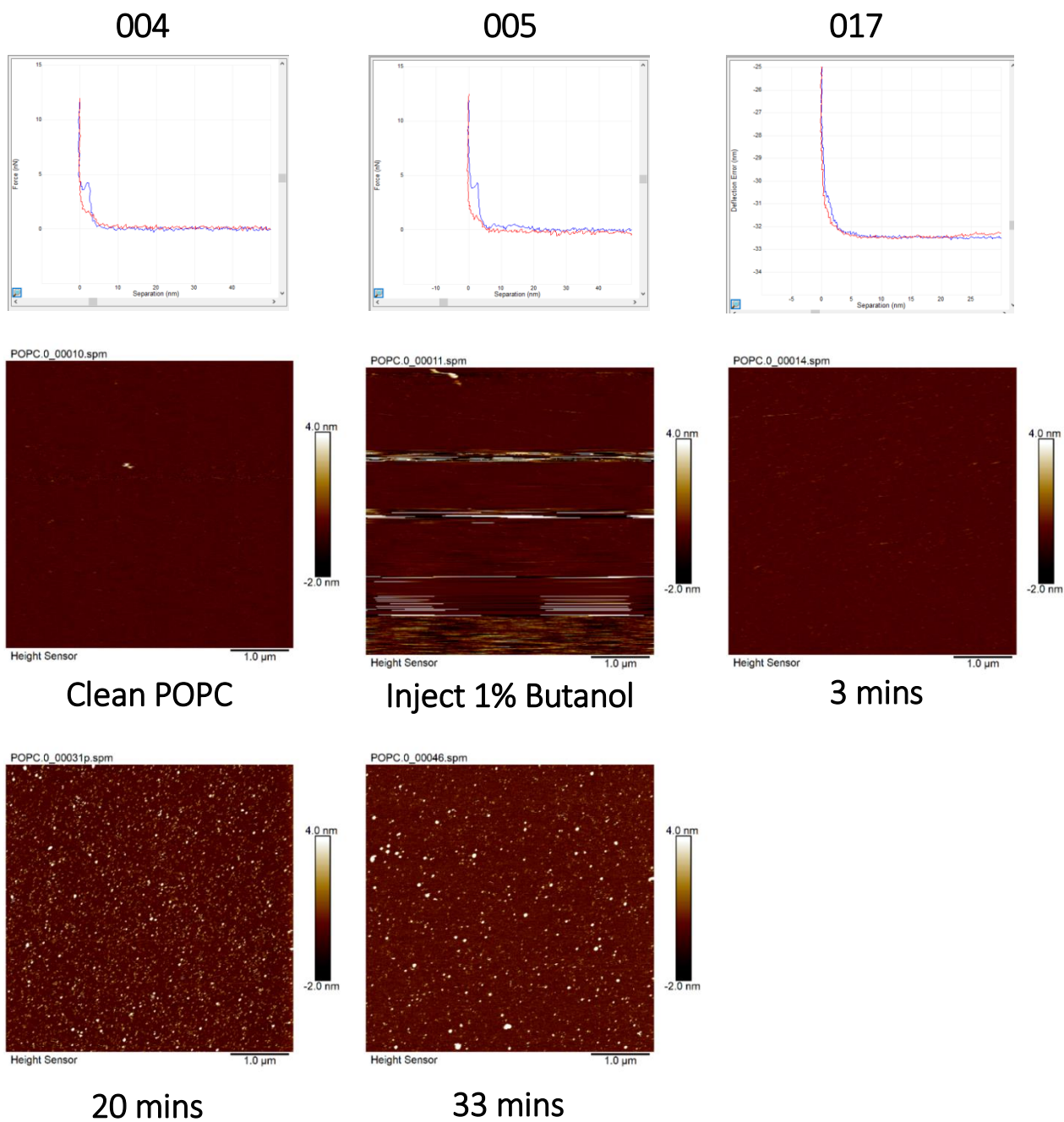


Figure 3.14 Atomic force microscopy force measurements and images of POPC bilayers interacting with butanol. POPC liposomes were deposited on to solid supports forming monolayers. Varying amounts of butanol were added and the topological and mechanical properties of the membrane were then recorded. The numbers above the force measurements correspond to the AFM iterations which can also be seen at the top of the topology images.

3.2.8 Membrane protein unfolding assay

Membrane proteins are vital and make up a significant portion of the cell membrane and are thus, at least indirectly effected by solvent stress. Despite this, there has been minimal research surrounding their interactions with butanol. Firstly, individual mSa variants were expressed in BL21 (DE3) inclusion bodies and were denaturation in Gdn-HCl. Following this, both the wt-mSa and d-mSa variants were mixed in refolding buffer in a 1 wt-mSa: 3 d-mSa ratio and purified with His-tag nickel chromatography of the tetrameric form of mSa. Due to the possibility of the formation of mSa tetramers with different variant compositions (i.e. 2 wt-mSa: 2 d-mSa) several different imidazole concentrations were used to elute mSa tetramers. Species which contained no wt-mSa variants (and therefore, no His-tag) were unable to bind to the column and species with more than one wt-mSa variants (therefore possessing multiple His-tags) bound more strongly to the column and thus required more imidazole to elute them. Therefore, it was possible to selectively elute the desired 1 wt-mSa: 3 d-mSa tetramer (Figure 3.15A). The biotinylation of bR can also be seen in Figure 3.15C, where the presence of bR bound to biotin prevents access of the anti-biotin antibody. The effect of butanol on membrane protein structure was investigated with a membrane protein stability experiment utilising biotinylated bR reconstituted in a 1:1 CHAPSO: DMPC bicelle. The absorbance of retinal (bR cofactor) disappears when the bR is unfolded, and the addition of mSA to unfolded, doubly biotinylated-bR in the steric trapping method prevents refolding. This enables insights into the structural stability of bR in response to butanol exposure. In Figure 3.15E, a decrease in absorbance at 560 nm (retinol, folded bR) can be seen over the 16-hour incubation period following butanol addition. Furthermore, higher concentrations of butanol result in lower absorbances, meaning a greater degree of bR exists in an unfolded state. A similar drop in absorbance is seen when butanol is replaced with SDS (Figure 3.14D), perhaps suggesting a commonality between the two mechanisms of membrane protein unfolding. It should be noted that some unfolding likely occurred before measurement could begin, due to limitations with the methodology. This explains the different y-axis intercepts seen in Figure 3.15E for the different butanol concentrations.

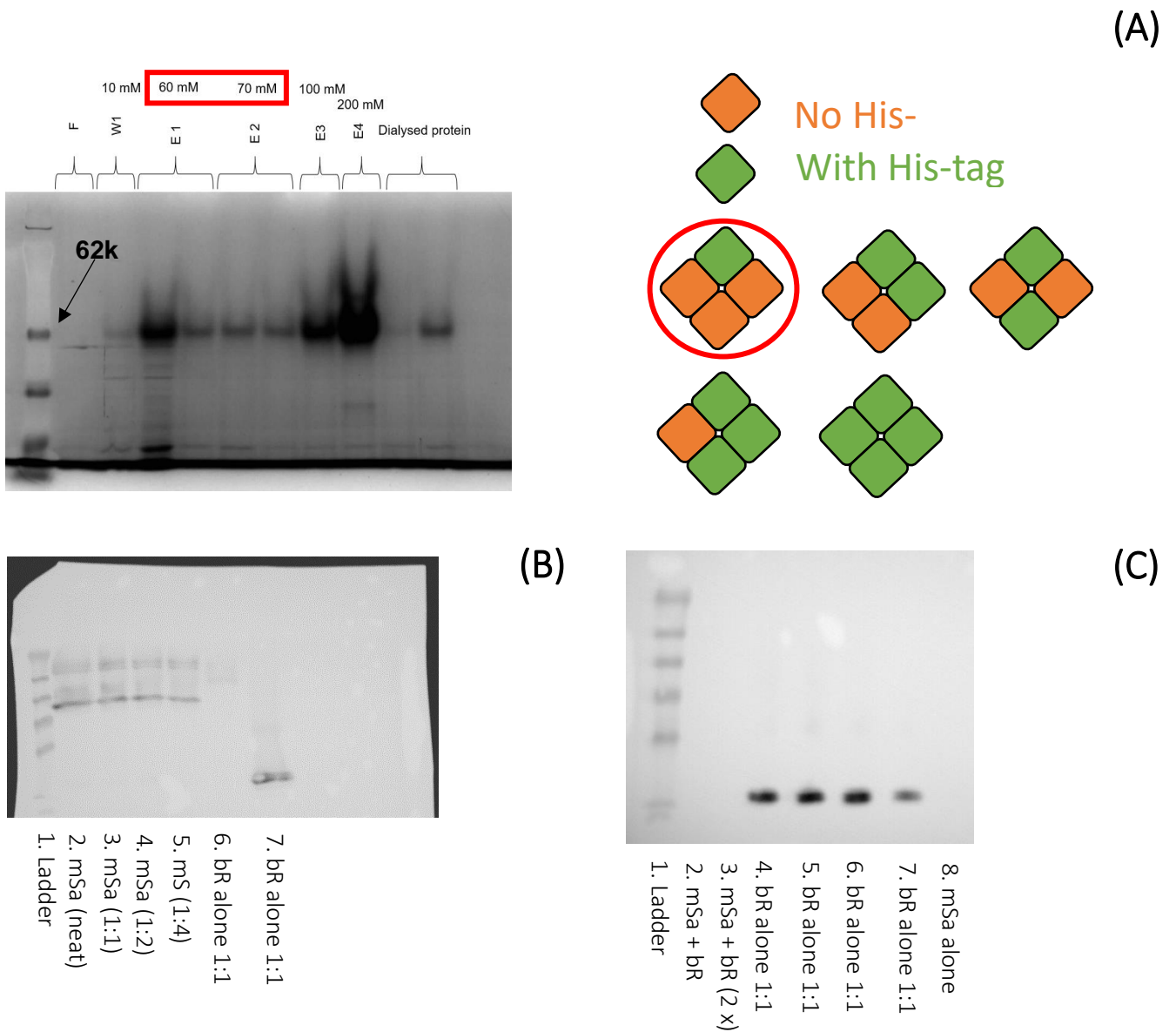


Figure 3.15. (A) Monovalent streptavidin (mSa) purification gel and Western blot. Several different imidazole concentrations were used to elute mSa tetramers. Species which contained no wt-mSa variants (and therefore, no His-tag) were unable to bind to the column and species with more than one wt-mSa variants (therefore possessing multiple His-tags) bound more strongly to the column and thus required more imidazole to elute them. Therefore, it was possible to selectively elute the desired 1 wt-mSa: 3 d-mSa tetramer. **(B) Anti-His western blot showing labelled mSa labelled with bR at a higher MW species.** **(C) Anti-biotin western blot of bR dilutions and bR-mSa mixtures, post overnight incubation together.** The lack of a band in lanes 2 and 3 might signify a lack of antibody accessibility to biotin residues on the bR following mSa incubation.

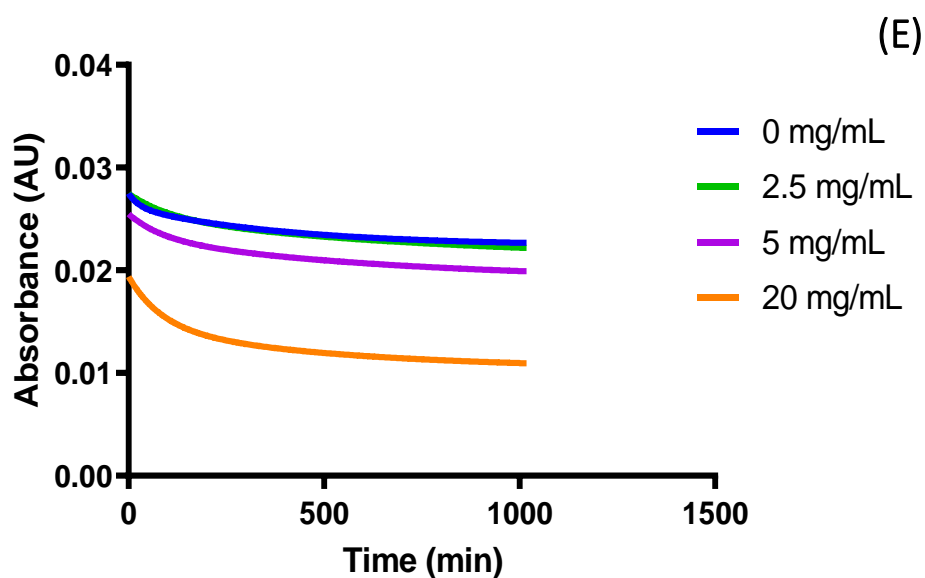
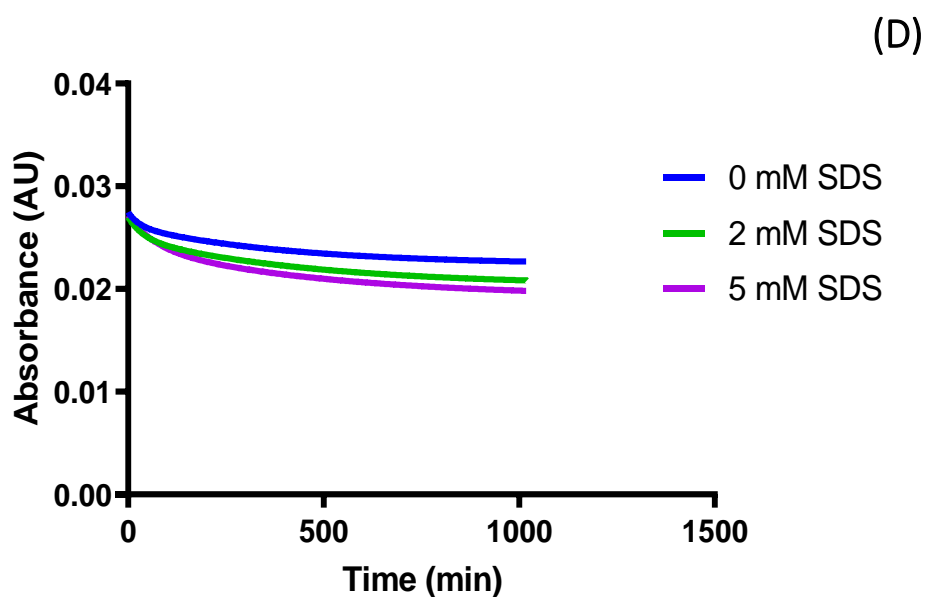


Figure 3.15. (D) The effect of SDS exposure on bacteriorhodopsin (bR) folding by the steric trapping method. (E) The effect of butanol exposure on bacteriorhodopsin (bR) folding by the steric trapping method. Steric trapping leads to a loss of retinal absorbance, acting as an intrinsic signal of protein conformation. Exposure to either butanol or SDS resulted in concentration-dependent unfolding in bR. N1 shown

The work carried out in this chapter aims to showcase the important relationship between membrane composition and butanol toxicity. Butanol was shown to have a detrimental impact on various properties of the membrane integral to its proper functionality. These included an increase in fluidity and diameter and an increase in membrane permeability. Further, AFM experiments revealed more changes to the membrane including, thinning, a reduction in bilayer integrity, and vesicle formation on the surface. These line up with previous reports of toxicity of butanol and other similar solvents. The amphipathic nature of butanol enables it to insert into the membrane and disrupt the packing of the phospholipids resulting in the above response, supported by *in silico* coarse-grained modelling. Additionally, the modulation of liposome compositions in the *in vitro* experiments has shown that increasing the presence of certain lipid species can lead to a more tolerant phenotype. These often pertain to membrane fluidity, and increasing the rigidity of the membrane can act as a prophylactic measure to reduce butanol's fluidising effect. Several compositional characteristics of the lipid membrane, such as, head group, chain length and unsaturation have been shown to influence resistance to butanol in membrane models. Butanol was found to interfere with the folding of membrane proteins; however it remains unclear whether this is due to direct interactions with the protein or indirectly through the surrounding lipids. Moreover, a comparison has been drawn between the mechanisms of butanol and that of detergents was made, acting in a similar way to disrupt membrane and membrane protein models. It is currently unknown as to whether butanol forms ordered supramolecular structures (i.e. pores) at the membrane or whether toxicity is based on molecules of butanol acting individually. This could further be studied with modified leakage assays. Utilising fluorescent molecules with different molecular weight tags would give greater understanding about the extent of butanol's ability to cause intracellular leakage. Using a range of leakage reporters will shed light on the size of the pores formed and which types of molecules would be lost from the intracellular environment following butanol exposure.

Understanding how the lipidome in *C. saccharoperbutylacetonicum* N 1-4 (HMT) changes throughout fermentation following increasing butanol exposure was investigated in the following chapter. This was done by collecting biomass from specific times during fermentation denoting key points in *Clostridial* fermentation life cycle. The lipids were then extracted from the fermentation biomass using a modified Bligh-Dyer extraction (see Methods 2.4), and the concentration of the resulting organic phase was determined using an ammonium ferrothiocyanate assay. The lipids present were then either run on a thin layer chromatography (TLC) system or was analysed through electron spray ionisation tandem mass spectrometry (ESI-MSMS). The relative amounts of specific lipid species could be roughly determined across the various time points. These could subsequently be cross-referenced with the *in vitro* data gathered in this chapter. If a specific lipid species is shown to be protective in the *in vitro* liposome assays and is also seen to be upregulated in stages of fermentation with higher concentrations of butanol, then it is likely that that particular lipid is of importance in mitigating butanol damage. This could then provide good evidence to upregulate the expression of these lipids to see if they have an impact on fermentation characteristics and cell survival.

4. Characterisation of *C. saccharoperbutylacetonicum* N 1-4 (HMT) lipidome

4.1 Introduction

Based on the previous chapter, it is clear that the lipid composition of the membrane is an important factor when considering butanol toxicity. It is thus important to investigate how butanol causes changes to the lipidome during *in vivo* fermentation. Assaying the lipids present in *C. saccharoperbutylacetonicum* N 1-4 (HMT) during fermentation would therefore further help to determine potentially protective phenotypes and could be cross-referenced with findings from the previous chapter. This would help to provide greater evidence and rationale for desired compositions which could then be genetically engineered in the fermentative strains.

In order to investigate the lipids present in the lipidome two techniques were employed, namely thin layer chromatography (TLC) and mass spectrometry. The relatively recent advances in chromatography and mass spectrometry mean that it is now possible to answer fundamental questions regarding lipids and their cellular roles, extending also to related lipid compositions (Ivanova *et al.*, 2009). One disadvantage is that the current lipids databases used to determine the lipids in a sample are mainly geared towards mammalian compositions and may be missing staple lipids present in bacteria (Appala *et al.*, 2020). Thus, it can sometimes prove difficult to accurately establish the species found in bacterial samples. This highlights the importance of using secondary techniques such as TLC. Thin layer chromatography is a fast and relatively inexpensive way to determine the lipids present in a sample (Fuchs *et al.*, 2011) through comparison with known lipid standards. TLC will be used to provide a semi-quantitative method to investigate specific lipids of interest and to inform the mass spectrometry data analysis. Two sets of lipidomic analysis experiments were run. The first was carried out by Dr. Tony Larson (University of York) and contained two *C. saccharoperbutylacetonicum* samples from a high and a low butanol environment. This enables a direct comparison between lipids present in two environments of different butanol concentrations. The second set of experiments involved using *C.*

saccharoperbutylacetonicum biomass (provided by Green Biologics, now Biocleave) from several different points during fermentation to give a more in-depth view of the lipidome at different stages throughout the lifecycle of *Clostridia*. Understanding which lipids are present in both high and low butanol environment shows the natural changes that occur *in vivo* when exposed to butanol. Together, and in conjunction with the TLC data an understanding of the changing lipidome was generated which aided in the selection of good targets for engineering. The experimental workflow is summarised in Figure 4.1

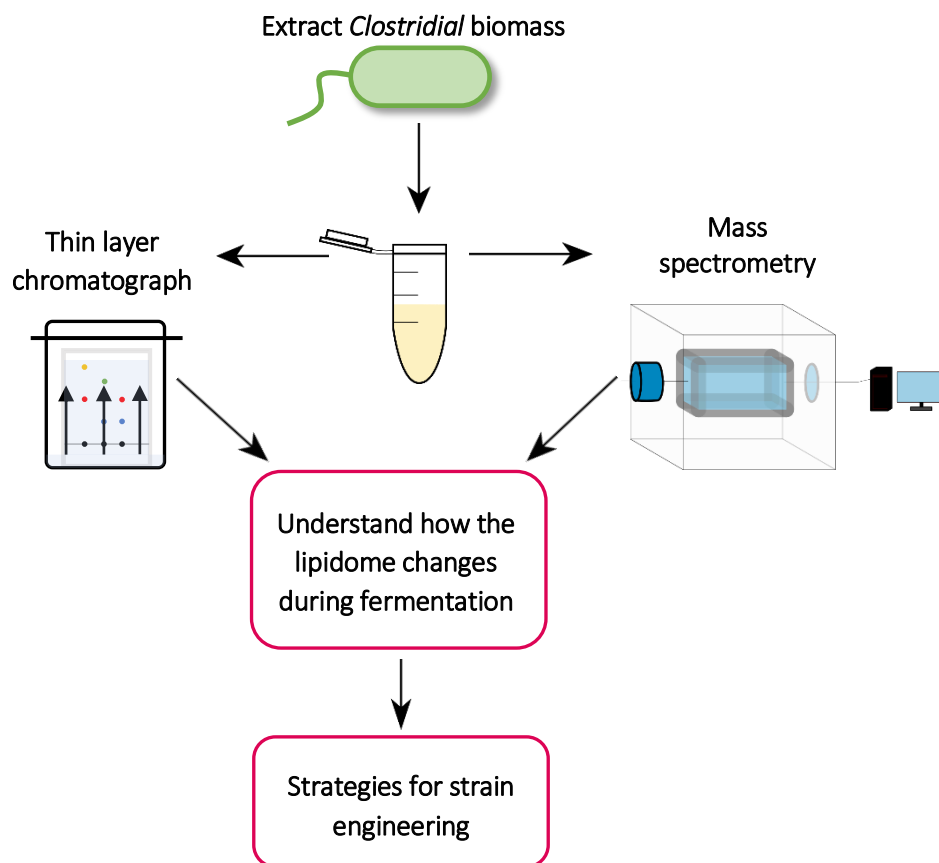


Figure 4.1. Objectives and experimental workflow for Chapter 4. This Chapter of work investigated the lipidome of *C. saccharoperbutylacetonicum* and how this changes over the course of a fermentation and in different butanol environments. This was done by extracting the lipids which were subsequently analysed with thin layer chromatography and mass spectrometry

4.2 *C. saccharoperbutylacetonicum* lipidome analysis in response to butanol

4.2.1 *C. saccharoperbutylacetonicum* N1-4 fermentation

Fermentations of *C. saccharoperbutylacetonicum* N1-4 were carried out by Green Biologic (now Biocleave) and several time points selected for harvesting biomass. The total lipids from these time points were then extracted using the Bligh-Dyer method, and identified using a combination of TLC and mass spectrometry. The time points selected are shown in Figure 4.2, along with associated fermentation data. The black arrows along the OD₆₀₀ denote the timepoints, each of which roughly corresponds to different part of the cells' lifecycle: 5 h, end of lag and start of log; 10 h, mid log; 15 h, midpoint of fermentation; 23 h beginning of stationary phase growth; 35 h, before death phase. The consumption of glucose can be seen with a concurrent increase in OD₆₀₀ and production of solvents. There is a steady increase in butanol concentration throughout the fermentation, which aligns with the increase in OD₆₀₀, and plateaus when the growth of the cells stops. It should be noted that there is no distinct acidogenic or solventogenic phase (which can be seen with solvent synthesis occurring concurrently with acid synthesis in Figure 4.2) in this particular strain. The increase in butanol seen throughout fermentation should also have an impact on the lipids present. This is based on the importance of the lipid membrane a site of butanol toxicity, and previous reports of alterations to the membrane composition following butanol exposure (see 1.5.1 Changes to lipidome). Following extraction, lipids were analysed to further shed light on the response of *C. saccharoperbutylacetonicum* N1-4 to rising endogenous butanol levels in fermentation.

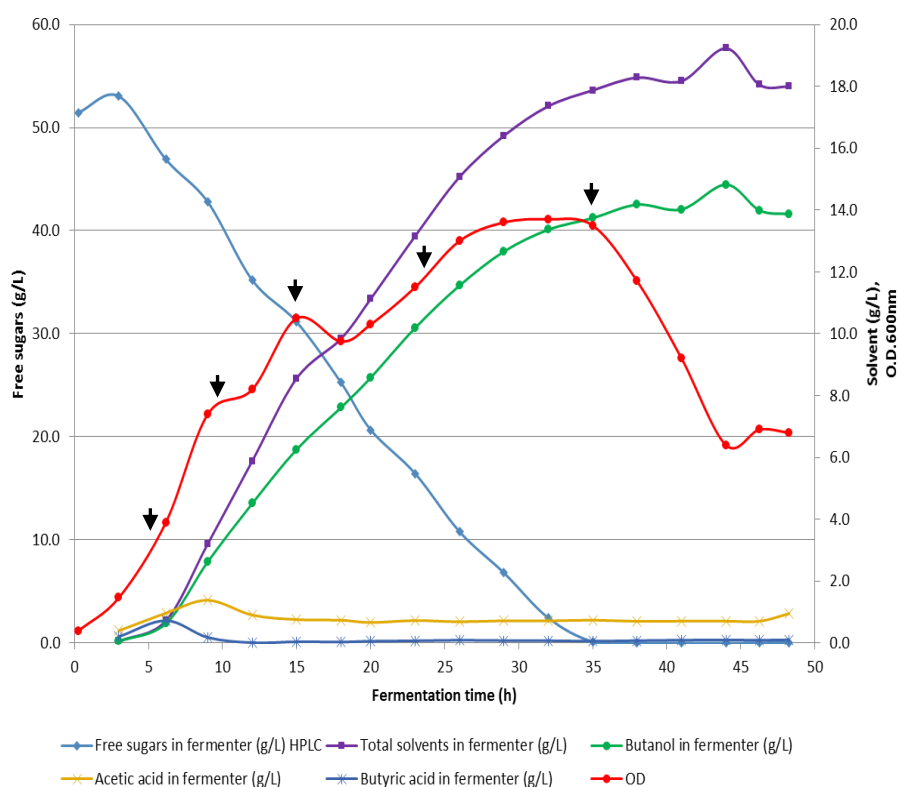


Figure 4.2 *Clostridium saccharoperbutylacetonicum* N1-4 (HMT) fermentation characterisation. The black arrows denote the timepoints where biomass was harvested for lipidomic analysis. They were chosen to reflect different points in the life cycle of the cells. Timepoints: 5 h, end of lag and start of log; 10 h, mid log; 15 h, midpoint of fermentation; 23 h beginning of stationary phase growth; 35 h, before death phase.

4.2.2 Thin layer chromatography of *C. saccharoperbutylacetonicum* N1-4 extracts

Initial experiments to assay the total lipids present in the *C. saccharoperbutylacetonicum* N1-4 biomass taken from the ABE fermentation timepoints (Figure 4.2) were carried out using thin layer chromatography. The first TLC system used a mobile system of 70 Hexane: 30 diethyl ether: 1 acetic acid and used a 10% copper sulphate solution (10% $\text{CuSO}_4 \cdot 5\text{H}_2\text{O}$; 8% H_3PO_4) as the visualisation method to reveal neutral lipids. Two standards containing 20 μg (an equal mass to the sample loaded) of oleic acid and triacylglycerol (TAG) were run to allow for identification of these lipids in *Clostridial* samples. It can be seen in Figure 4.3, that lipid species were detected in the *Clostridial* samples which migrated

to a similar extent to the TAG and oleic acid standards. It is assumed therefore that the bands detected in the samples are the same lipids as the standards which have migrated the same (in this case TAG and oleic acid). The levels of TAG detected in all samples was much lower than the standard, and there was found to be no significant difference or change at any of the timepoints. ImageJ densitometry was used to quantitatively compare lipid band intensities. Therefore, the faintness of these bands meant that any small differences across the sample could have been missed. This highlights an issue with relying solely on TLC for quantitative lipidomic analysis. The levels of oleic acid were much more intense and thus, quantitative comparison between time points was easier. Oleic acid levels appeared to increase throughout the fermentation and were significantly higher at the 35 h timepoint than when compared to the 0 h time point. There were several other bands seen on the plate following visualisation, the majority of which are consistently present across the timepoints, however it is unclear what these species are. Additionally, a large amount of material was still present at the bottom of the plate where the first sample was initially spotted. This likely means that the species present were unable to dissolve in the mobile phase and thus remained. Because of this the use of alternative solvent systems was explored. The two bands just below the solvent front in the same lanes as the 10 h and 15 h samples remain unidentified.

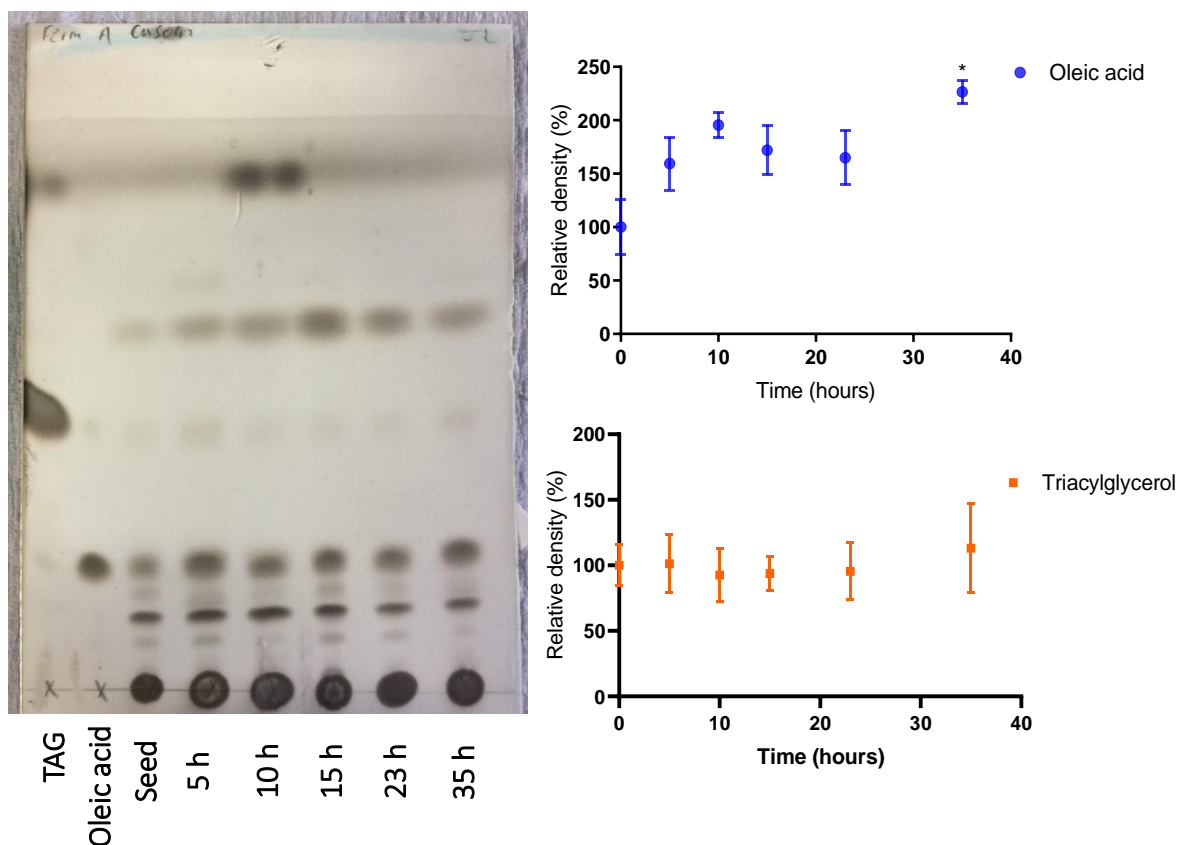


Figure 4.3. Copper sulphate developed thin layer chromatography of *Clostridium saccharoperbutylacetonicum* N 1-4 biomass from time points throughout fermentation. Total bacterial lipids were extracted using a modified Bligh and Dyer method and quantified using the Steward Assay. Equal concentration of lipids were run in 70 Hexane: 30 diethyl ether: 1 acetic acid and were dipped into a copper sulphate solution (10% $\text{CuSO}_4 \cdot 5\text{H}_2\text{O}$; 8% H_3PO_4). They were then baked at 150°C for 10 minutes in an oven. Densitometry analysis was carried out using ImageJ. 3 technical repeats of 2 biological repeats were carried out * = $p < 0.05$. Different Y-axis scales have been used.

Following this, the same samples were run using an alternative solvent system and visualisation method to quantify different lipid species. For assaying POPC, POPG and POPS, 25 chloroform: 15 methanol: 4 acetic acid: 2 H₂O was used as the mobile phase and molybdenum blue was used to visualise the lipids (Figure 4.4). The levels of POPC were too low to be determined through densitometry as no clear band could be seen at the same migration level as the standard. This is in line with previous works which did not detect phosphatidylcholine lipids in a range of *Clostridia* (Durre, 2005). Both POPS and POPG were detected in all sample and the levels of POPG appear to increase steadily through the course of the fermentation. This increase is roughly correlated with the increase in butanol concentrations seen in Figure 4.2. The levels of POPG were highest in the later portion of the fermentation and were significantly higher at 15 h and 35 h than compared to the start of the fermentation. Levels of POPS appear to somewhat mirror growth in the cells, i.e. POPS is at its highest when there would be the highest amount of proliferation in the culture. However, there was found to be no significant difference at any of the timepoints. Finally, POPE was investigated using the same solvent system as the molybdenum blue samples but with ninhydrin being used to visualise the lipids. There was found to be no significance differences across the fermentation (Figure 4.5). The changes for the various species measured are summarised in Table 4.1. TLC provided a semi quantitative look at how the lipids were of the *C. saccharoperbutylacetonicum* were changing through fermentation. The next experiments were used mass spectrometry to corroborate the findings with TLC.

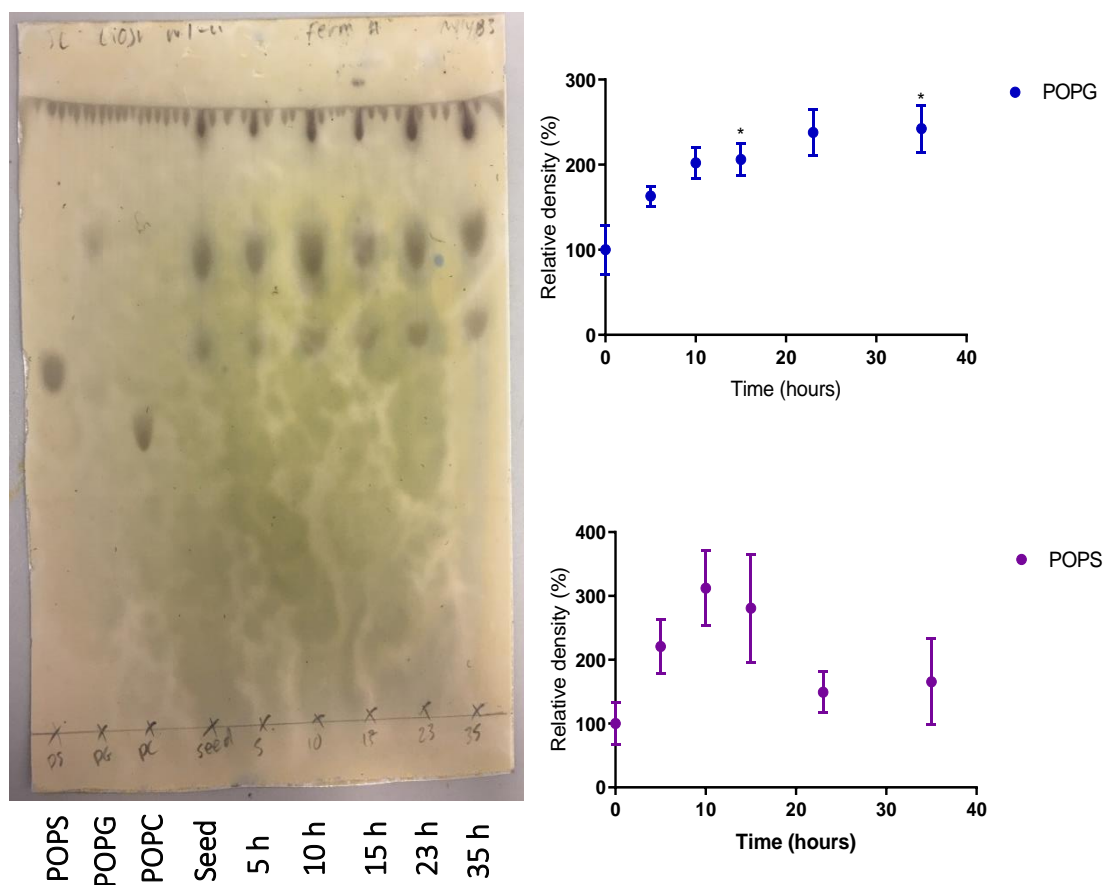


Figure 4.4. Molybdenum Blue developed thin layer chromatography of *Clostridium saccharoperbutylacetonicum* N 1-4 biomass from time points throughout fermentation. Total bacterial lipids were extracted using a modified Bligh and Dyer method and quantified using the Steward Assay. Equal concentration of lipids were run in 25 chloroform: 15 methanol: 4 acetic acid: 2 H₂O and were sprayed with and molybdenum blue spray reagent. The concentrations were determined by densitometry analysis was using ImageJ. 3 technical repeats of 2 biological repeats were carried out * = p < 0.05. Different Y-axis scales have been used.

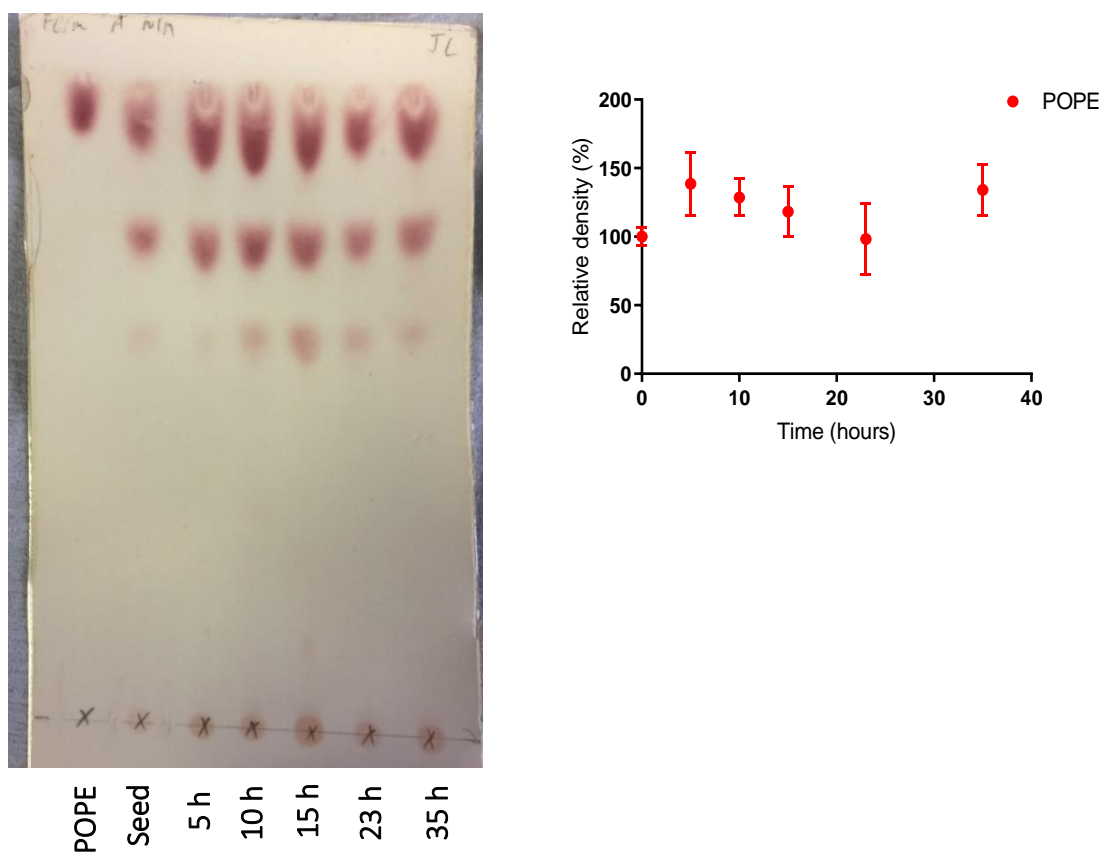


Figure 4.5 Ninhydrin thin layer developed chromatography of *Clostridium saccharoperbutylaceticum* N 1-4 biomass from time points throughout fermentation. Total bacterial lipids were extracted using a modified Bligh and Dyer method and quantified using the Steward Assay. Equal concentration of lipids were run in 25 chloroform: 15 methanol: 4 acetic acid: 2 H₂O and were sprayed with ninhydrin spray reagent. They were then baked at 150°C for 10 minutes in an oven. Densitometry analysis was carried out using ImageJ. 3 technical repeats of 2 biological repeats were carried out * = p < 0.05. Different Y-axis scales have been used

Lipid species	Change in relative spot intensity to 0 hat time point (hr)				
	5	10	15	23	35
Oleic acid	-	-	-	-	↑
TAG	-	-	-	-	-
POPE	-	-	-	-	-
POPG	-	-	↑	-	↑
POPS	-	-	-	-	-

Table 4.1 Summary of total lipid species changes seen in *Clostridium saccharoperbutylacetonicum* N 1-4 biomass taken from time points throughout fermentation. Band intensity was recorded using ImageJ. ↑ denotes species which have significantly higher band intensities at when compared the Seed (0 h time point). – denotes no significant differences from the 0 h time point were seen. No species were found to significantly decrease.

4.2.3 Lipidomic analysis of *C. saccharoperbutylacetonicum* N1-4 extracts using mass spectrometry to support

Because of the various drawbacks and relative simplicity of TLC, mass spectrometry was also carried out on *Clostridial* samples to corroborate and allow for cross-reference. Initial *Clostridial* lipidomics were carried out at the University of York. *C. saccharobutylicum* (DSM 13864) and *C. saccharoperbutylacetonicum* (DSM 2152) samples were extracted with hot isopropanol / hexane extraction protocol (HIPA). *C. beijerinckii* (NRRL B-591) and *C. acetobutylicum* (DSM 1732) - sample were extracted with standard the Bligh-Dyer method (see Methods 2.4). For optimisation of the extraction method *E. coli* BW251133 was extracted with both extraction methods described above. All extraction protocols were tested with fresh and lyophilised starting material. There was found to be little difference between the extraction methods used (data not shown). In total in positive ionisation mode more than 500 features were detected within the samples (defined as those within reasonable limits expected for lipids), of which ~27% could be annotated with LipidBlast. In negative ionisation mode, there were ~200 features detected of which ~30% could be annotated with LipidBlast. A summary of the lipid classes found in both positive and negative ion modes can be seen in Figure 4.5.

The major lipid class in both *E. coli* (*E. coli* data was included as a control) and *Clostridia* appears to be PE containing lipids in positive mode (Figure 4.6). There was found to be a much greater proportion of plasmalogen containing PE lipids in the *Clostridial* sample than compared to the *E. coli* samples. The negative mode showed a small amount of PG in *Clostridia* and a larger amount in *E. coli* and also mirrored the positive mode with regards to PE lipids. Interestingly the vast majority of lipids in negative mode and the majority in positive mode were unknown in *Clostridial*, meaning they were not present in the LipidBlast database. This could be due to these databases focusing more on mammalian compositions. Additionally, this may also suggest that *Clostridial* have vastly different lipid profiles to that of *E. coli* and that there is potentially some novel or unusual lipid species present. This could be a possibility when considering that *Clostridia* are Gram-positive.

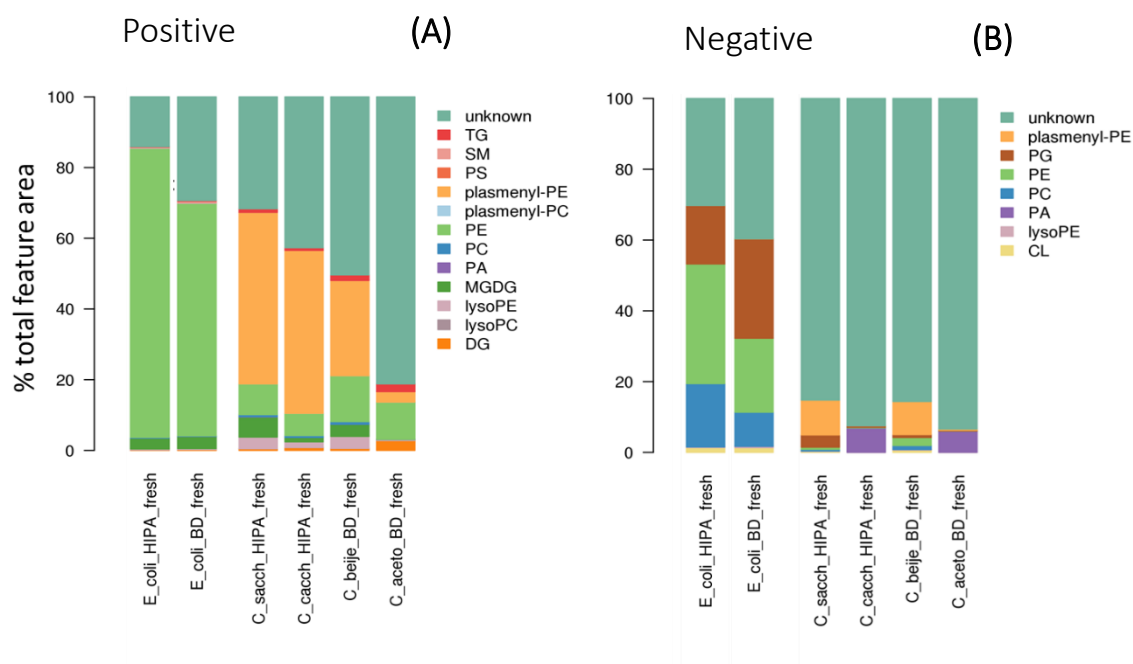


Figure 4.6. Lipid class coverage for several *Clostridial* species and *E. coli* annotated using LipidBlast. A C30 column was used for positive HESI mode (A) and the same samples were run on a C8 column in negative HESI mode (B). *Clostridial* lipids showed a large amount of unknown lipids. The full species names of the sample are :*C. saccharobutylicum* (DSM 13864); *C. saccharoperbutylacetonium* (DSM 2152); *C. beijerinckii* (NRRL B-591); *C. acetobutylicum* (DSM 1732). The lipid classes are as follows: TG, triacylglycerides; SM, sphingomyelins; PS, phosphatidylserines; PE, phosphatidylethanolamine; PG, phosphatidylglycerol; PC, phosphatidylcholine; PA, phosphatidic acid; MGDG, Monogalactosyldiacylglycerol; DG, diacylglycerides; CL, cardiolipin. ‘Plasmeyl-’ denotes the presence of plasmalogen containing acyl.

The following set of lipidomics experiments was carried out on *C. saccharoperbutylacetonicum* samples from a high butanol and a low butanol environment. These environments were generated through the use of different carbon sources during fermentation with mannitol for high butanol and galacturonic acid for low butanol. When comparing the two different butanol environments, Figure 4.7 shows a large reduction in the levels of plasmalogen-containing PE and an increase in the amount of triglycerides and the fraction of unknown lipids. In negative mode there is an increase in amount of PG lipids and cardiolipin. This data is also represented in Figures 4.8 and 4.9 as is ordered by the most prevalent individual lipids and colour coded according to the lipid class. In low butanol the most prevalent lipids are plasmalogen containing PE species and PG for positive mode and negative modes, respectively. In high butanol the abundance of one specific PG species is much higher which could possibly be in response to the increase butanol. Furthermore, there is a cardiolipin species which is also more prevalent in high butanol conditions. In positive mode for high butanol concentrations, it can be seen that plasmalogen species appear to decrease in proportion to triacylglycerol species. It might be perhaps that the levels of triacylglycerols are increased due to their use as an acyl chain storage and butanol stress may incur a higher acyl chain turnover in the membrane to ensure homeoviscosity of the membrane. An additional point to note is the large number of unknown lipid species which were not found in the LipidBlast database.

C. saccharoperbutylacetonicum

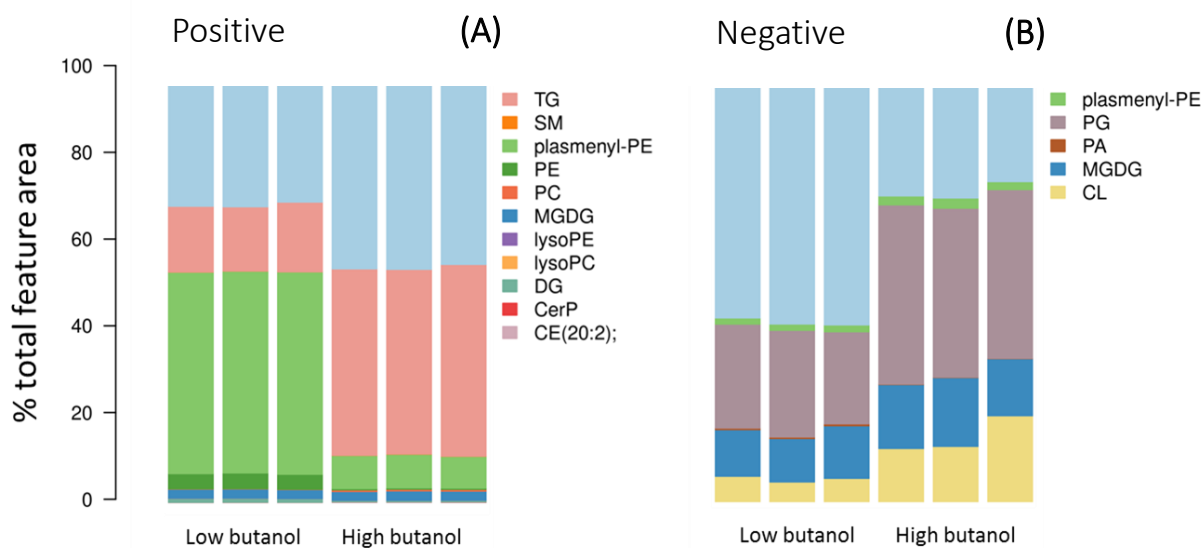


Figure 4.7. Lipid class coverage for several *C. saccharoperbutylacetonicum* grown in environments with different butanol concentrations. Three technical repeats are shown for both high and low butanol. A C30 column was used for both positive mode (A), and negative mode (B). The lipid classes are as follows: TG, triacylglycerides; SM, sphingomyelins; PS, phosphatidylserines; PE, phosphatidylethanolamine; PG, phosphatidylglycerol; PC, phosphatidylcholine; PA, phosphatidic acid; MGDG, Monogalactosyldiacylglycerol; DG, diacylglycerides; CL, cardiolipin; CerP, ceramides; CE, sterol. 'Plasmeyl-'denotes the presence of plasmalogen containing acyl. Lyso lipids contain only one acyl chain. Light blue represents unknown lipids species.

(A)

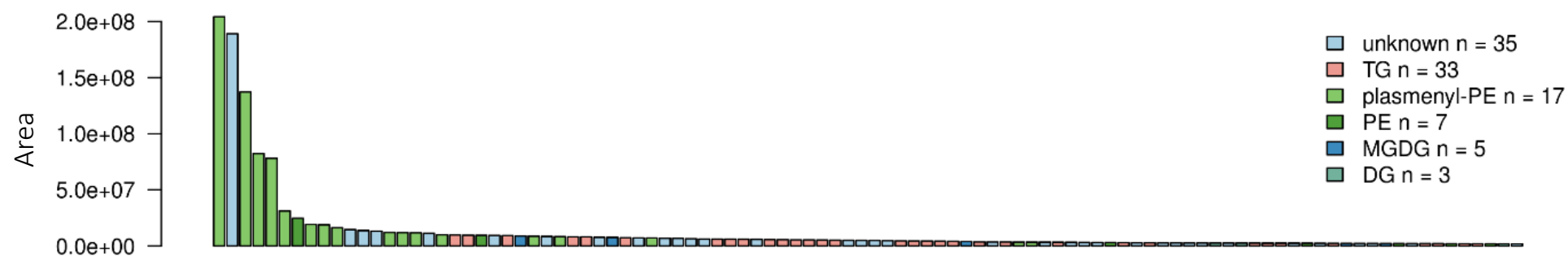
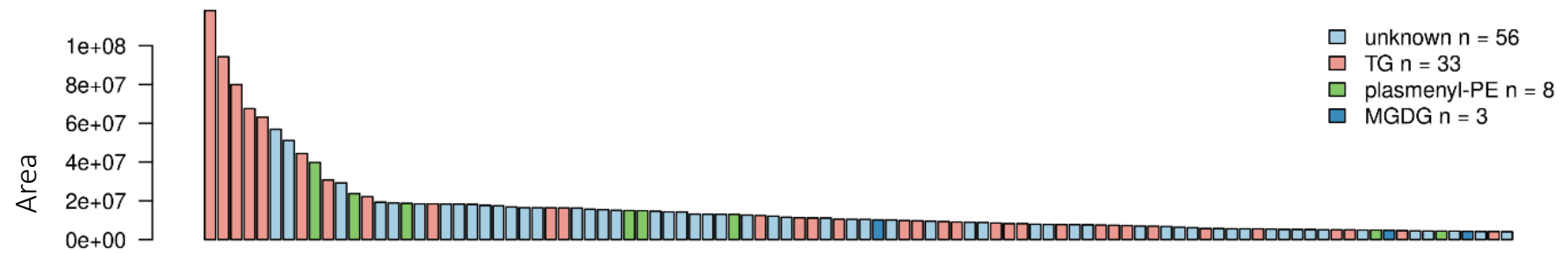


Figure 4.8. Top 100 most abundant individual lipids ordered by area in positive mode. Different colours denote the class of the lipid in low (A) and high (B) butanol conditions. Legend numbers give the number of individual species detected in the top 100. TG, triacylglycerides; DG, diacylglycerides; MGDG, Monogalactosyldiacylglycerol; PE, phosphatidylethanolamine; PA, phosphatidic acid; PG, phosphatidylglycerol

'Plasmeyl-'denotes the presence of plasmalogen containing acyl.

(B)



(A)

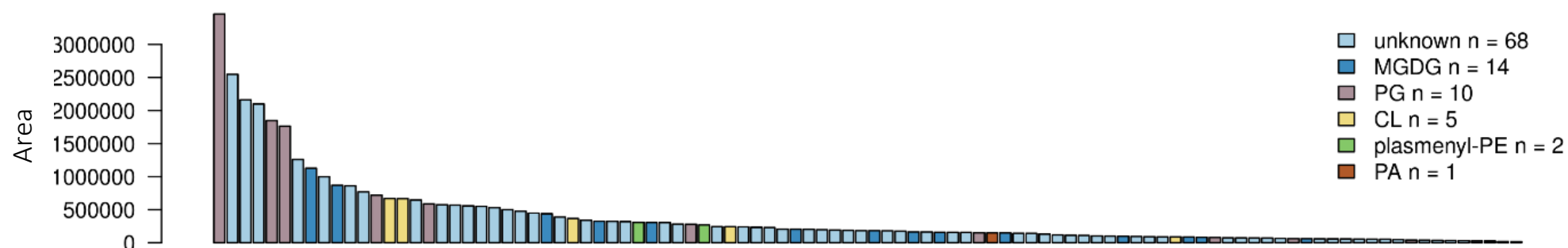


Figure 4.9. Top 100 most abundant individual lipids ordered by area in negative mode. Different colours denote the class of the lipid in low (A) and high (B) butanol conditions. Legend numbers give the number of individual species detected in the top 100. CL, cardiolipin; MGDG, Monogalactosyldiacylglycerol; PE, phosphatidylethanolamine; PA, phosphatidic acid; PG, phosphatidylglycerol. 'Plasmeyl-'denotes the presence of plasmalogen containing acyl. Different Y-axis scales have been used

(B)



Some data regarding the fatty acid chains of the lipids can be mined based on database hits and a relative abundance was calculated using the following formula:

$$\frac{\text{fatty acid}}{\text{all lipid features}} * \text{area for each lipid}$$

The data need to be treated carefully as fatty acids were not looked for directly and the calculation above give a crude measurement for comparability. These data is presented in Figure 4.9 and show colour-coded bars comparing high and low butanol concentrations. The positive mode data (Figure 4.9B) show decreases in *cis*-17:1, P-16:0 and P-18:0 in high butanol, whereas there were increases in 18:1 and 18:2. The may be a slight preference towards longer chained or *trans* (E) containing isomers in negative mode but mostly changes were not as apparent as in positive mode, suggesting that most fatty acid changes occurred in the TG and phospholipid classes, which are more amenable to positive mode ionization.

(A)

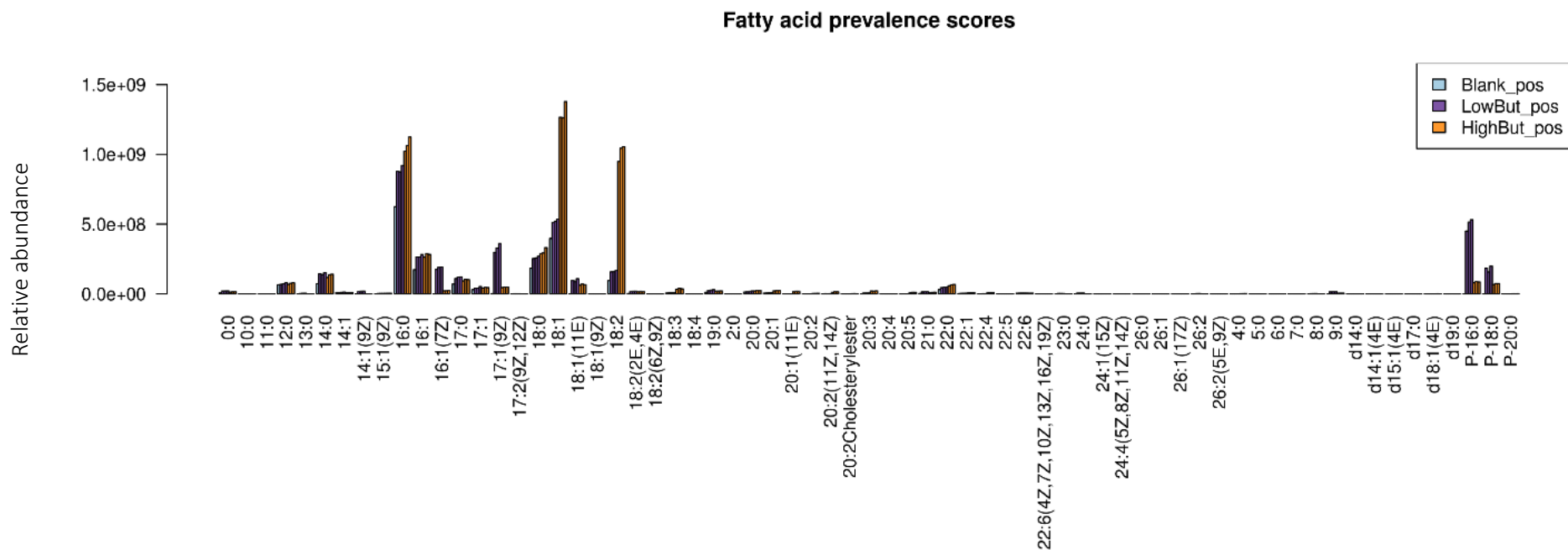
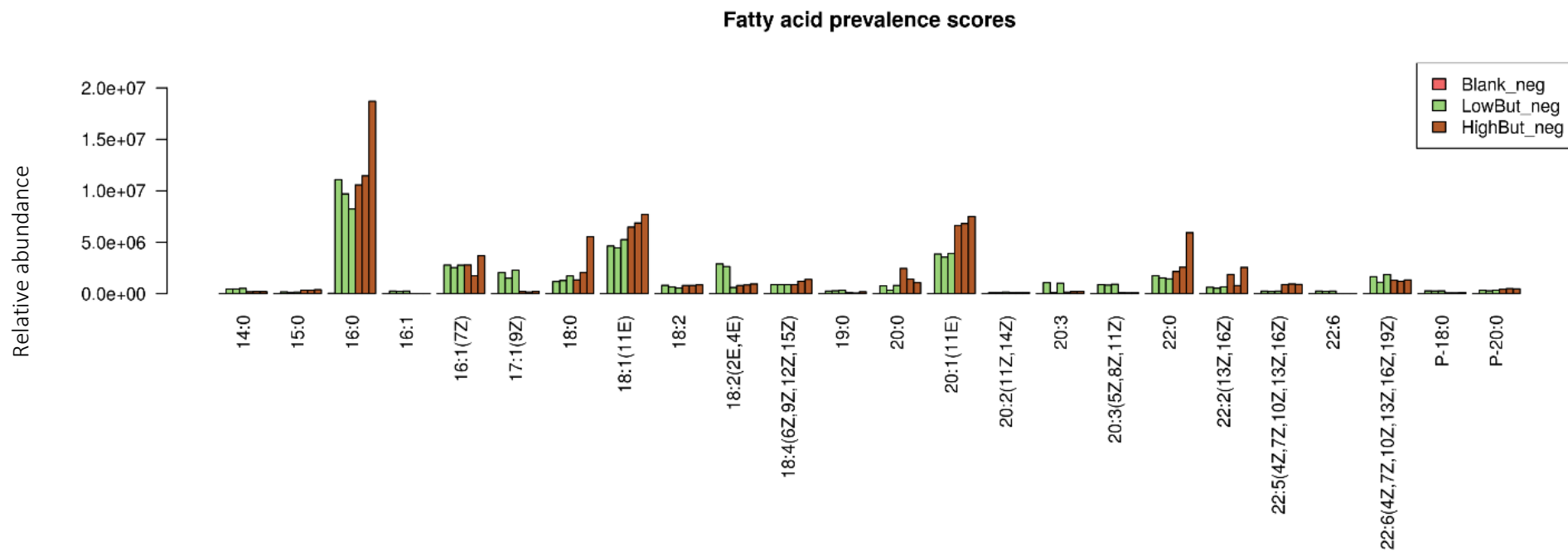


Figure 4.10. Fatty acid prevalence scores of all fatty acids in (A) positive and (B) negative mode found in the LipidBlast database. The different butanol environments are denoted by different coloured bars. Fatty acids were not measured directly and geometrical isomerisms (*Cis/trans*) are often difficult to determine using the databases. Different Y-axis scales have been used

(B)



Following the examination of lipids present in the *C. saccharoperbutylacetonicum* N1-4 biomass time points using thin layer chromatography, the same samples were investigated with HPLC-ESI tandem mass spectrometry. This was done to verify the quantifications of the TLC experiments and to provide a broader overview of the whole lipidome. Due to the lack of standards used in these lipidomic experiments, along with some other issues (discussed later), the interpretation of this data is limited and should be seen as auxiliary to the TLC and earlier lipidomic experiments. Furthermore, the lack of standards means that determining quantifications is difficult, and thus data will be expressed as a relative abundance of annotated features. Samples were run in both positive and negative ionisation mode, and the data was analysed using Progenesis Q1 2.1 (Nonlinear Dynamics) with features annotated using the LipidMaps database. Firstly, the data was filtered by m/z error of < 20 ppm, HPLC peak width of < 2 minutes and whether any possible identifications could be determined using the LIPID MAPS database. Finally, the adducts of these compounds were also refined. Mass charge ratios were assigned an identity based on the mass error (ppm), quality of fragmentation data if present, and likelihood of the suggested lipid's existence in *Clostridia*. From this, 173 compounds were identified for positive ionisation mode and 292 compounds were identified for negative ionisation mode.

Firstly, Figure 4.11. shows the relative abundances (%) of each lipid species, and how these change across the time points of the fermentation for both positive and negative ionisation mode. Based on the negative ionisation mode, the lipidome of these *C. saccharoperbutylacetonicum* N1-4 samples appears to contain mainly ethanolamine species (phosphatidylethanolamine (GPEtn, PE, (PE(O-)) and plasmalyethanolamine (PE(P-)), phosphatidylglycerol (GPGro)), phosphatidic acid (GPA) and Monogalactosyldiacylglycerol (MGDG). The positive ionisation mode also shows large relative amounts of PE, sugar-containing species (monogalactosyldiacylglycerol and digalactosyldiacylglycerol), and diacylglycerol and triacylglycerol. Additionally, a small amount of phosphatidylserine (GPSer) and GPA was detected. Regarding the relative changes in these species' abundances, due the larger error significant changes were difficult to determine. However, these data can be used qualitatively and some

of it corroborates trends seen in previous mass spectrometry and thin layer chromatography data. Relative abundances in the positive ionisation mode appear to remain similar across all time points with perhaps being a small increase in the sugar containing lipids and a small decrease in DG levels. In negative ionisation mode levels of GPA, GPGro and MGDG appear to increase at the later time points in fermentation, whereas ethanolamine containing species appear to decrease across fermentation. This increase on phosphatidylglycerol was seen in the previous lipidomics and TLC experiments and a reduction in PE species was also seen in the previous lipidomics experiments. The total carbon chain length was taken as the sum of carbons in all acyl chains of an annotated species (Figure 4.12). Any discernible change in total carbon chain length (of all acyl chains) is difficult to accurately determine. Longer chain lengths (> 18 carbons per chain in a diacyl species) appear to be slightly skewed towards the later time points, e.g. 36C-42C (sum of both acyl chains) trend towards an increased abundance as fermentation progresses. Smaller total chain lengths appear more evenly distributed across time points, as can be seen in the positive and negative ionisation modes for 30-35C. Species with even larger total carbons (> 50C) are likely to be from TAGs and are thus only seen in positive ionisation mode where TGs are more readily detectable. The mass spectrometry data collectively has shown that the lipids found in *C. saccharoperbutylacetonicum* do change throughout fermentation and that these changes can be quantified. Certain lipids e.g. PG appear to be enriched in high butanol environments and thus may be focal points for membrane-based engineering efforts.

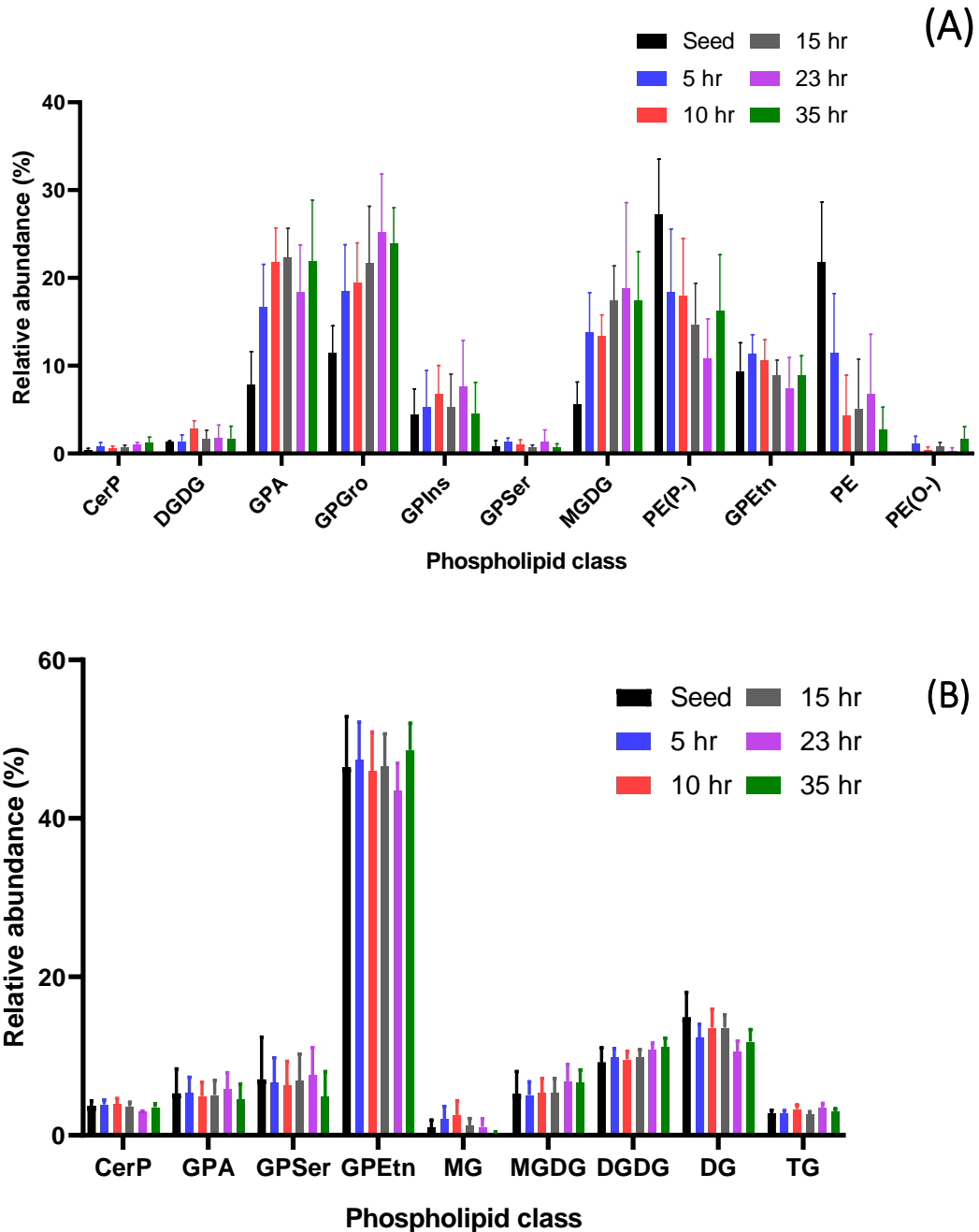


Figure 4.11 Abundance of lipid classes throughout *Clostridium saccharoperbutylacetonicum* N 1-4 (HMT) fermentation. (A) negative ionisation mode (B) positive ionisation mode. The lipid classes are as follows: CerP, ceramides; CL, cardiolipin; DG, diacylglycerides; DGDG, digalactosyldiacylglycerol; GPA, phosphatidic acid; GPEtn / PE, phosphatidylethanolamine; GPGro, phosphatidylglycerol; GPIIns, phosphatidylinositol; GPSer, phosphatidylserine; MGDG, monogalactosyldiacylglycerol; PC, phosphatidylcholine; PE(O-), plasmylethanolamine; PE(P-), plasmylethanolamine; PG, phosphatidylglycerol; PS, phosphatidylserines; SM, sphingomyelins; TG, triacylglycerides. Lipids were extracted from *C. saccharoperbutylacetonicum* N 1-4 (HMT) biomass at certain time points during fermentation. Samples were run on a TOF-MSMS system. The proportions of each lipid class was calculated as a percentage of total abundance of annotated species in the LipidMaps database using Progenesis QI v2.1. (Nonlinear Dynamics).

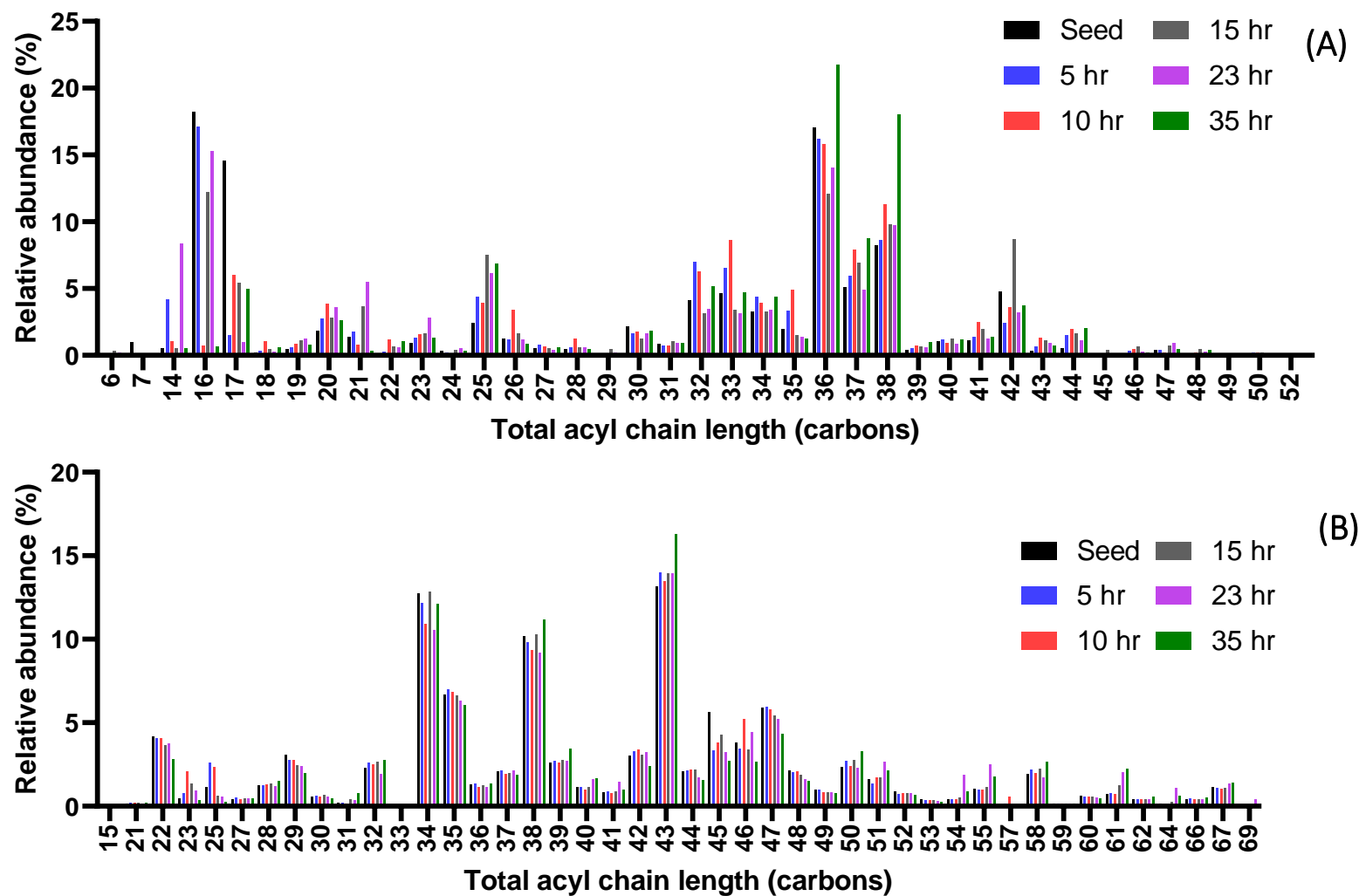


Figure 4.12 Total chain length abundance as a percentage of all annotated acyl chains. (A) negative ionisation mode (B) positive ionisation mode. Lipids were extracted from *C. saccharoperbutylacetonicum* N 1-4 (HMT) biomass at certain time points during fermentation. Samples were run on a TOF-MSMS system. The lipids were extracted run on an ESI-MS/MS in negative and positive ionisation mode. Acyl chain abundance was calculated using the abundance of each chain length as a proportion of the sum of all abundances for a particular time point.

Finally, the unsaturation ratio was calculated and is shown in Figure 4.13 as a relative change (%) from the calculated value in the seed. Unsaturated lipids were taken as any species which contained at least one unsaturated bond. The intensities of these species were then summed and compared to the summed intensities of all species containing no unsaturated bonds. There was found to be no significant change in unsaturation seen throughout the time course. It may be the case that more targeted analysis of the fatty acids using GC-MS is required in order to discern any changes in the unsaturation between samples.

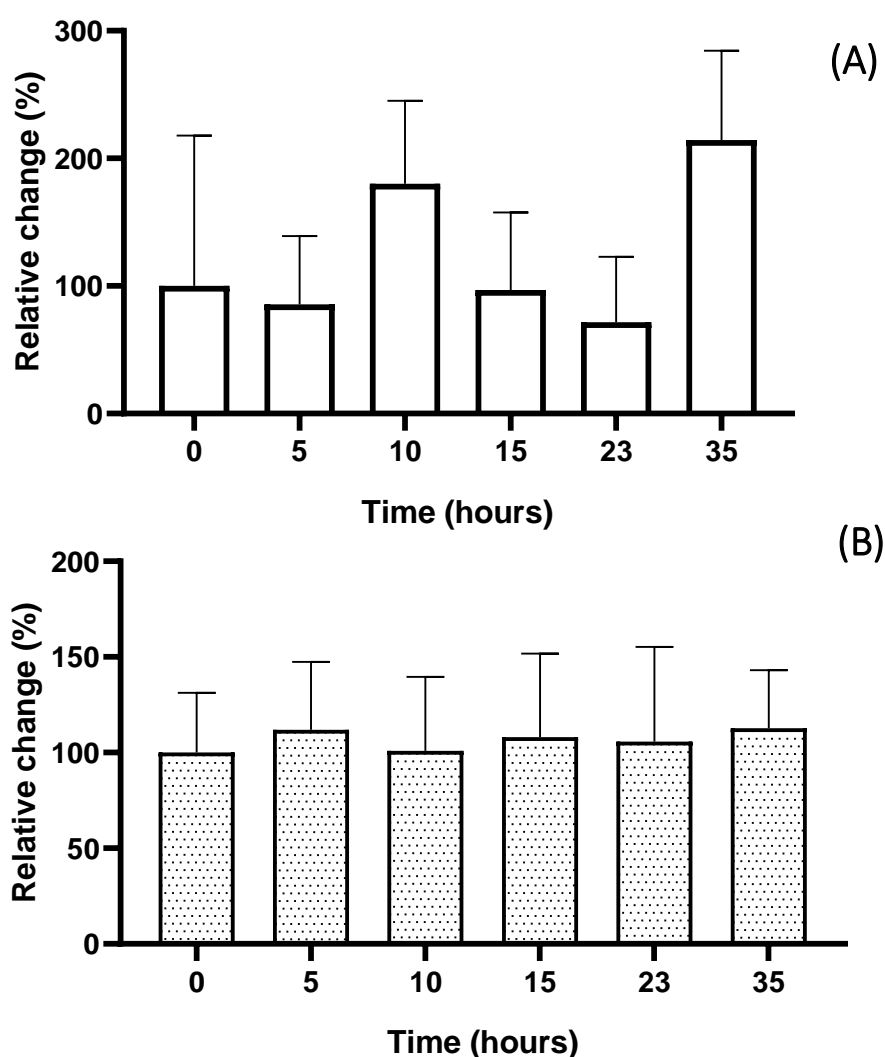


Figure 4.13. The proportion of unsaturated fatty acids over the course of fermentation. (A) negative ionisation mode (B) positive ionisation mode. Lipids were extracted from *Clostridium saccharoperbutylacetonicum* N 1-4 (HMT) biomass at certain time points during fermentation. The lipids were extracted using a modified Bligh-Dyer extraction and were subsequently run on an ESI-MS/MS in negative and positive ionisation mode. The change (%) in unsaturation ratio was calculated as a ratio of lipids containing at least one unsaturated bond with fully saturated lipids. These values were then normalised to the values for the seed time point.

The effect of fermentation on the lipidome of *C. saccharoperbutylacetonicum* N1-4 (HMT) was investigated using thin layer chromatography and lipidomics. Cells were harvested from a low and high butanol environment or alternatively were harvested from several milestones during their lifecycle. This biomass was then extracted and the relative proportion of the lipids at different butanol concentrations were investigated. In summary, some changes were inferred regarding the lipidome. In particular there appears to be an increase in some lipid species (PG, CL, sugar-containing lipids, PA) and a decrease in other, mainly PE lipids containing plasmalogens. All data in this section support the increase of PG suggesting an important role of this species, which has been seen previously in section 3.2.1 Altering headgroup composition. Oleic acid (18:1) is also seen to increase in both TLC and mass spectrometry. Due to the quality of some of the data it is not possible to draw solid conclusions, and this data should be used qualitatively with an aim to inform and support stronger data sets. Interestingly, there was a large number of unknown species detected in both TLC and mass spectrometry. This may suggest that there are lipids made by the cells which are unusual or have unique adducts which are not seen in the LipidMaps database. This may be due to a bias against bacterial lipids in many of the available databases due to the majority of past lipidomics work being carried out in mammalian or other eukaryotes (Appala *et al.*, 2020). Whilst these lipidomics experiments are a useful starting point, they only provide a semi-quantitative overview of the lipid species present. Ultimately this could provide valuable information regarding the lipidomic response of cells to butanol. More targeted work would be of interest.

5. Rational metabolic engineering of *C. saccharoperbutylacetonicum* N 1-4 (HMT) and *E. coli* to increase butanol tolerance and production

5.1 Introduction

The final chapter of this work pertains to efforts made in engineering strains to be more tolerant to butanol or to aim to increase the amount of butanol produced. The strategies used here were based on the results seen in the previous chapters. Namely the importance of lipid composition in butanol mediated membrane toxicity. Efforts were made to engineer strains with a modulated lipid membrane composition. This would provide *in vivo* evidence of the importance of certain lipid species / membrane compositions regarding butanol interaction and may also provide a more robust phenotype. Additionally, the engineering of membrane proteins was investigated. Designing membranes to have an exact, specific composition of lipids is very challenging with current technologies, owing to the dynamicity of the membrane (Bell, 1984). Some advances in membrane engineering are discussed in more depth previously in 1.6.4 Targeted engineering of lipid species. It is likely that only overarching changes to the membrane properties can be made. Whilst this may in fact prove sufficient, specific changes to the membrane can be achieved through modulation of specific proteins within the membrane, or those which lead to an altered lipid composition of the membrane. Both protein and lipid routes have breadth of opportunity can be exploited in engineering to achieve the desired goals. For example with membrane protein engineering involve investigating possible transporters such as TtgB (Basler *et al.*, 2018) or AcrB (Fisher *et al.*, 2014) and other proteins which could be related to butanol toxicity. If successful, these alterations to the various cellular aspects will enable the solventogenic *Clostridia* to tolerate a higher concentration of butanol. This in turn will reduce the cost of post-fermentation product purification and downstream processing per unit of butanol. Based on the reduction in these costs, the entire process of utilising bacterial cell factories to produce butanol via ABE fermentation will become more economically competitive with convention fossil fuel method, thus may be a route to elevating reliance on unsustainable practices.

This chapter represents the culmination and application of the findings in the previous chapters. A deeper understanding of butanol toxicity and the impact on the lipidome *in vivo* has enabled the generation of some target genes for genetic engineering efforts. These alterations were carried out using a CRISPR-Cas based system called CLEAVE™ and in each case, were overexpressed or knocked out. This will give a two-tailed understanding of the effects of these genes and their products on the fermenting cells. The experimental work flow is summaries in Figure 5.1

Initially, the *pssA* knockout construct (PssA-HR) was designed based on the method describes in Methods 2.10 CLEAVE™: Genome editing of *Clostridium saccharoperbutylacetonicum* N1-4 (HMT). This essentially involved the creation of a truncated version of *pssA* flanked either side by 1,000 bp homology regions which were taken from the regions adjacent to *pssA* in the *C. saccharoperbutylacetonicum* N1-4 (HMT) genome. Following this, an appropriate spacer was selected which represents the cleavage site for the CRISPR/ Cas system. This spacer was then subcloned into the targeting vector, S3V9, to test its efficiency again WT *C. saccharoperbutylacetonicum* N1-4 (HMT). The remainder of the work to produce ΔPssA was kindly completed by scientists at Biocleave due to the COVID-19 pandemic and resulting lack

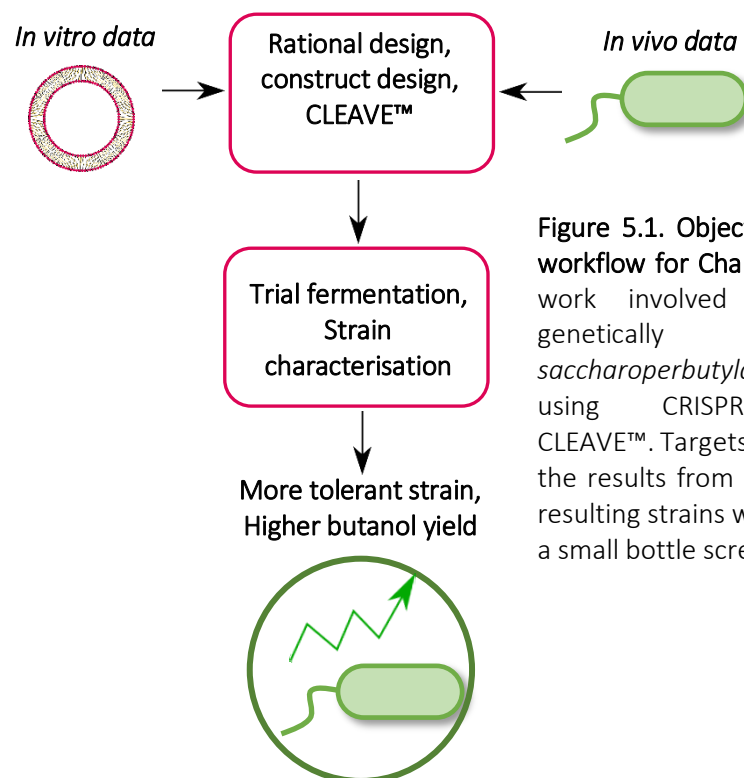


Figure 5.1. Objectives and experimental workflow for Chapter 5. This Chapter of work involved the generation of genetically engineered *C. saccharoperbutylacetonicum* strains using CRISPR-based technology CLEAVE™. Targets were chosen based on the results from Chapters 3 and 4. The resulting strains were characterised with a small bottle screen.

of laboratory access. This involved transforming *C. saccharoperbutylacetonicum* N1-4 (HMT) with PssA-HR and then transforming with S3V9-spacer construct to produce a Δ PssA strain. For overexpression, both *pssA* and *ttgB* were cloned into expression vector pMTL82151 and transformed into *C. saccharoperbutylacetonicum* N1-4 (HMT). The fermentation characteristics of these strains was investigated using a small bottle screening from which OD₆₀₀ and pH were assessed. Further characterisation using HPLC has been delayed due to the COVID-19 pandemic. The *Clostridial glpF* gene was amplified from genomic DNA, cloned into *pET17b* and transformed into *E. coli* (BL21). The effects of GlpF expression on exogenous butanol was then investigated using growth assays with several different stressors.

5.2 Generation of CLEAVE™ constructs and testing their effect on growth in *Clostridium saccharoperbutylacetonicum* N1-4 (HMT)

5.2.1 PssA Knock out (Δ PssA) construct design

Herein, knockouts and overexpression constructs will have the prefixes, ' Δ ' and '+', respectively. The sequence for PssA was obtained from Uniprot (<https://www.uniprot.org/uniprot/M1N653>) and NCBI Reference Sequence: WP_015395195.1. For the generation of the HRs for the homologous recombination of the Δ PssA, the *Clostridium saccharoperbutylacetonicum* N1-4 (HMT), complete genome (CP004121.1) (ENA Browser) was used. The *Clostridial* gene *pssA* is located at 1,970,881 – 1,971,402 and the homology regions chosen were as follows: Homology arm 1: 1,969,881 – 1,970,881, Homology arm 2: 1,971,478 – 1,972,478. This is summarised in Figure 5.2, and the sequences were synthesised by GeneArt synthesis (Thermo Fisher). The proposed spacer sequences are shown within the *PssA* sequence in Figure 5.3. Following synthesis, the spacer sequence was subcloned into the targeting vector (S3V9) (Figure 5.4) using *XhoI* and *ZraI*. The band at 106 bp in lane 2 contains the spacer, direct repeats and restriction sites together.

Homology arm 1: 1969881 - 1970881

Homology arm 2: 1971478 - 1972478

```
tcttcaccatctacagcctctagcacattgtagccttcactttccaataaaaactttaactat
ttctcttatctcgtcattatcatccgcaattaaaatattcctcatagtacttattggccacc
tccatttggttattagtagtatataacgctgtattggttaaatctacattatthaagatgacttaa
gaattcttaagatttagtagtatatgtagattttaagatggttagataaaacttttaattattag
attacaacaagaaggaaaaaattatggatagagcaaaaaactattaataggaaaaatat
tattggcaatattaggtgggatagctattacggttaactattaagatattaccatataattctt
gaaataacaacatcccttgataagtttagggattatataatttctacagggagggttggttc
atTTTTatttatattctttcaaatattacaaccgtgattgcaccaattccaggtgaagtga
ttcaagttgctggtggatcacatatatggagttcctcctgggctaatttataccacattagga
cttatgattgggtgggattatagctttttatttcacaagattaataggagcttcctttataga
aaaactgattaaaaagaaaaaatccaactggcttttgatattatgaatagtaaaaagtta
cagttatattatgtattttttattatacctgggtttccaaaagacttttaatatatgta
gcagggttaactccaataaagccattaaaattccttggaattttacttataagtagatttcc
atggctattagcttccgtaggaataggatctaataattcattatggaaattatattgcaacaa
tagtaatttcacttatagctttaatagcatttgtattagggataatttataaggataagctt
ataagtaagttttccaaggtaatcaagttaatgaacagatgtagttaagtaagtaaaagga
gtcggaggcatgcttgcttatcttatgatagcaaaatttaaagttgaaaaagatttgatctggt
gaataagcaaggcttgaataaatggttatcagccacagaggaggaatttttaatatggaagtaa
aaaaagatgagttttggaaaaatgtaataagaactggtatagaatttatggttatagcttta
ataatttatcttattaaagatttggttaataatctaatatttttacattcttattttcttattt
actatataatttgcaaaaatatatagtaagaaaaacgcgcttgccaagaaccttagtaacga
ttgTTTTatataattattatttttggttaataatattttttgcgtgtaggtatattcctgaa
attataagagaaattcaaatcatatatgaagagctatggaaaataaatgtacctgataattg
gaaaggatataatagatatcttaaggaagcagattgatatacaaaatcttatgatcgcctta
tgaatactttgatagttactggcaaaagcttagtacagggaggtgctaattttatttatttca
ttaatattaagtagctttttatcttagatatagaaagaataaaaaaatttataagcaaatt
taaaacgagtaaaagcatcaagactttacaatcgtcttgagtattttggattaaatttcttaa
attcctttggaaaagtaatacaagctcaatttttaatagcattagtaaattctattctttct
accatagctttatggattatgggattttccacaattaataggcttaggctttatgatattgt
gctaagttttataccgggtgggttgagttataatatctttaataccactttgTTtaatagcat
tcaatgTTggcgggtgtaattaaagtaatatccgttattataatgattgctttattacatggg
ttagaaagttatatattaaatccaaagttaatgtccgataaaacatcattgccagattctt
tatatttataatattagttttgggagacaatttatgggaacatggggattattgTTgggaa
ta
```

Figure 5.2. Generation of the *PssA* knockout ($\Delta PssA$) construct for genome integration. The knockout contained the Met start codon and codons for the last 15 amino acids (including the stop codon). Green coloured sequence is homology arm 1 and pink coloured sequence is homology arm 2. Black and bold sequence is the truncated *PssA* gene which no longer carries the PAM-spacer sequences (see Figure 5.2). Homologous recombination will occur with the genome directed by the homology arms which will result in the replacement of the native *PssA* sequence with the above truncated sequence.

atggttaaaaaatatataccaaatatattaacatttatgaatttatcgtttgaattccttc
aataattgaagtttttaataaaaaatTTtagtagaggagctttatttataattgctgctgct
taatagatagatatgatggcagaattgcaagatattttaaggtatccagtgaaataggaaaa
gaactagattccttagcagatttaatttcctttggagttgcaccggctatattaatattttc
taaataatTTTTTggttttcaggcgtttggcgtgattggaattttcagcacaagcttata
ttatatgtggttgttacagattagcaaaatataatgtttagtgaatttaatggaactttcaca
ggaattccaataactattgcaggtttaattctagcattattttcgttatttgtacctaaaaa
taacgtatttgtaataataactatcagttattttaatgagcggttcttgcttatcttatgatag
caaaatttaagttgaaaaagatttga

Proposed spacers:

ccaaatatattaacatttatgaatttatcgtttgaatt
ccagtgaaataggaaaagaactagattccttagcagatt *
ccggctatattaatatttttctaaatataatTTTTTggttt
ccaataactattgcaggtttaattctagcattattttcg
cctaaaaataacgtatttgttaataataactatcagttatt

Figure 5.3. Generation of the PssA knockout spacer sequences for CLEAVE™. Above is the *pssA* sequence with several proposed spacer sequences within it. The spacer sequence is a ~40 nucleotide long sequences (which are represented as the underlined sequences) flanked upstream by a protospacer adjacent motif (PAM) (shown in red) with a CCN sequence. The final 45 nucleotides (blue) are the same sequence as the truncated *pssA* in the PssA-HR construct. Therefore, the spacers cannot be selected from this area as the CRISPR-Cas system will produce a ds cut at the site of the chosen spacer (which must only be present in the WT and not the knockout). As such it will only produce these ds breaks in WT cells which do not contain the truncated gene. The chosen spacer is denoted by a '*'.

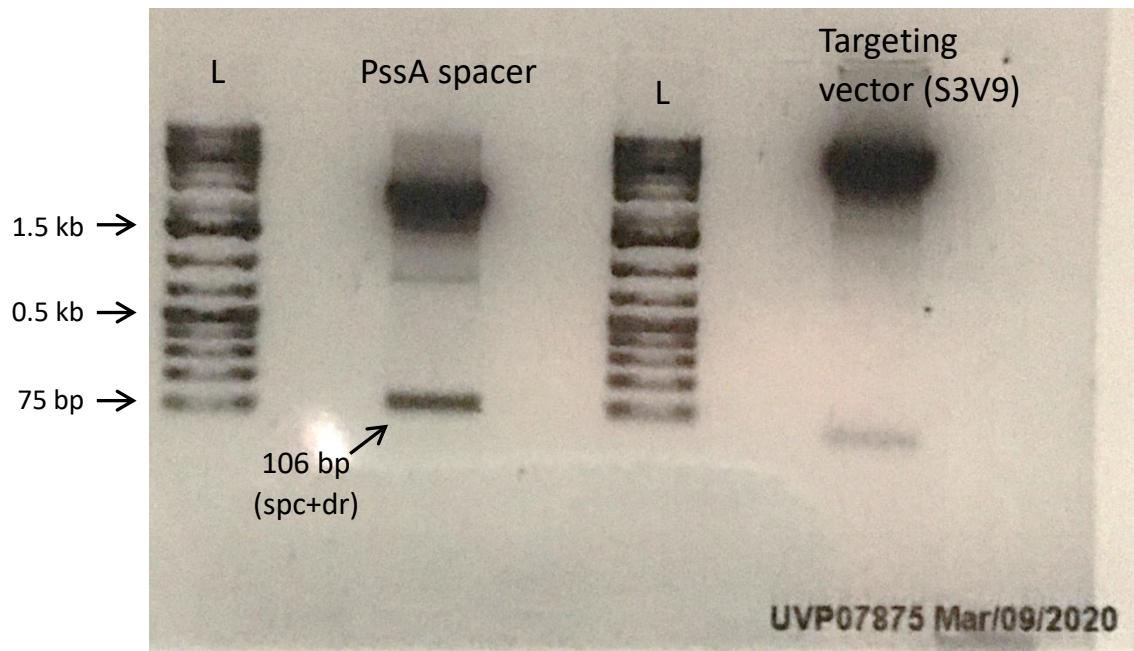


Figure 5.4. Restriction digest of the PssA spacer synthesised by GeneArt, and the targeting vector S3V9. The PssA spacer is in the plasmid pMA-RQ, a standard backbone used by GeneArt. Both were digested with *XhoI* and *ZraI*. The product of 106 bp is the pssa spacer (spc), direct repeats (dr), restriction sites. The ladder (L) used was Generule plus 1 kb (SM1331) (Thermo Fisher Scientific).

5.2.2 CLEAVE™ construct diagnostics and subcloning

Diagnostic colony PCR was carried out on *E. coli* colonies transformed with the spacer containing targeting vector (Figure 5.5). An expected PCR product of ~700 bp was expected for positive colonies. Colonies 1 and 9 were then sent for sequencing. Colony PCR was then done to confirm. The efficiency of the spacer was also tested on WT *Clostridium saccharoperbutylacetonicum* N1-4 (HMT). This was done by transforming N1-4 with the targeting vector with the spacer in it and counting the number of colonies present after 48 h. There was found to be no colonies on the plate transformed with the above PssA spacer sequence suggesting 100 % efficiency. Due to the advent of the COVID-19 pandemic, the progression of these experiments was halted. Biocleave have kindly completed the remainder of the work in making the Δ PssA. This involved subculturing the N1-4 cells transformed with PssA-HR for several days and following this transforming these cells with S3V9-spacer to kill any cells which had not undergone homologous recombination, and thus those which did not contain the deletion. These strains

were then sent to Aston in February 2021 where a small-scale bottle screening was carried out in order to characterise the fermentation of these strains.

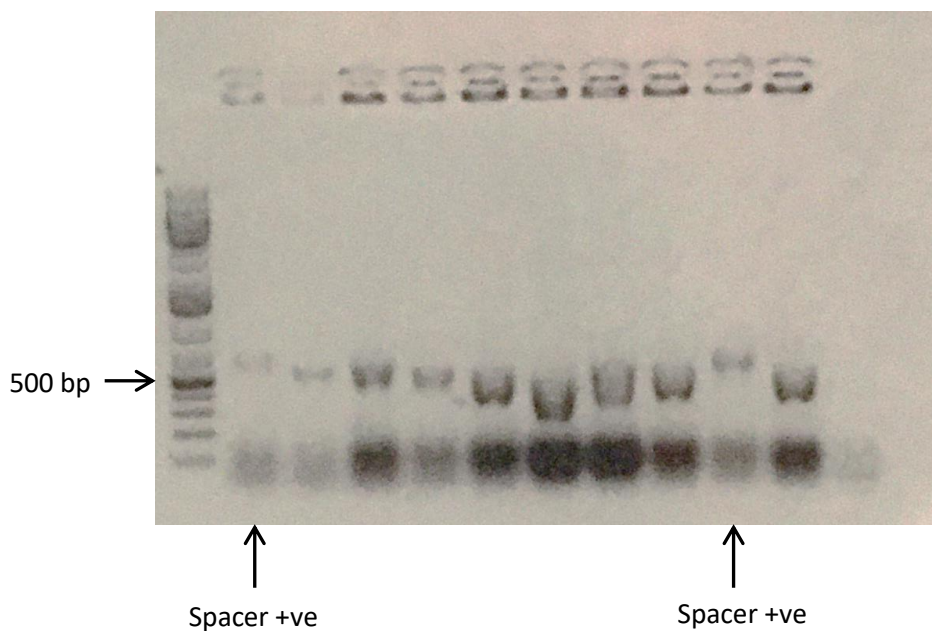


Figure 5.5. Colony PCR of *E. coli* colonies transformed with the targeting vector S3V9 containing the PssA spacer. Positive colonies were expected to produce products at a size of ~700 bp.

5.2.3 TtgB construct cloning

The sequence for *P. putida* TtgB was taken from Uniprot (<https://www.uniprot.org/uniprot/O52248>). Similar protein sequences in *Clostridia* were searched for using protein blast (Figure 5.6) in the organism *Clostridium saccharoperbutylacetonicum* N1-4 (taxid:931276). The top result, with the highest score was chosen (WP_015394794.1) and was synthesised by GeneArt (Thermo Fisher). For quality assurance, the resulting synthesised DNA was investigated using BLAST and had 100 % identity with WP_015394794.1. Both TtgB and PssA were subcloned into the pMTL82151 expression vector, which was then transformed into *C. saccharoperbutylacetonicum* N1-4 at Biocleave. Following electroporation of the constructs, a diagnostic colony PCR (Figure 5.7) was run on several colonies to check successful transformation of pMTL82151 vectors containing either PssA or TtgB sequences for overexpression, or the PssA-HR sequence for genome integration. Positive colonies had a band at 550 bp + insert (bp) which translates to ~3.5 kb for TtgB (Figure 5.7A), ~1 kb for PssA (Figure 5.7B) and ~2.5 kb for PssA-HR (Figure

5.6C). Glycerol stocks were made of positive colonies and were sent along with the above Δ PssA stock to Aston for the small bottle fermentation screen.

Sequences producing significant alignments Download Select columns 100

select all 4 sequences selected [GenPept](#) [Graphics](#) [Distance tree of results](#) [Multiple alignment](#) [New MSA Viewer](#)

Description	Scientific Name	Max Score	Total Score	Query Cover	E value	Per. Ident	Acc. Len	Accession
<input checked="" type="checkbox"/> efflux RND transporter permease subunit [Clostridium saccharoperbutylacetonicum]	Clostridium saccharoperbutylacetonicum	355	355	97%	9e-107	27.41%	1029	WP_015394794.1
<input checked="" type="checkbox"/> efflux RND transporter permease subunit [Clostridium saccharoperbutylacetonicum]	Clostridium saccharoperbutylacetonicum	333	333	98%	6e-99	25.42%	1047	WP_015394064.1
<input checked="" type="checkbox"/> efflux RND transporter permease subunit [Clostridium saccharoperbutylacetonicum]	Clostridium saccharoperbutylacetonicum	223	223	98%	8e-61	22.65%	1030	WP_015393855.1
<input checked="" type="checkbox"/> efflux RND transporter permease subunit [Clostridium saccharoperbutylacetonicum]	Clostridium saccharoperbutylacetonicum	200	200	97%	2e-53	22.65%	1011	WP_015392303.1

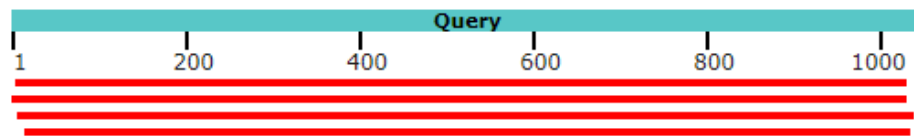


Figure 5.6. TtgB sequence Protein BLAST output. *P. putida* TtgB amino acid (UniProtKB - O52248) sequence was investigated using protein blast (search organism: *Clostridium saccharoperbutylacetonicum* N1-4 (taxid:931276). The top result was chosen as a target for overexpression in fermenting strains.

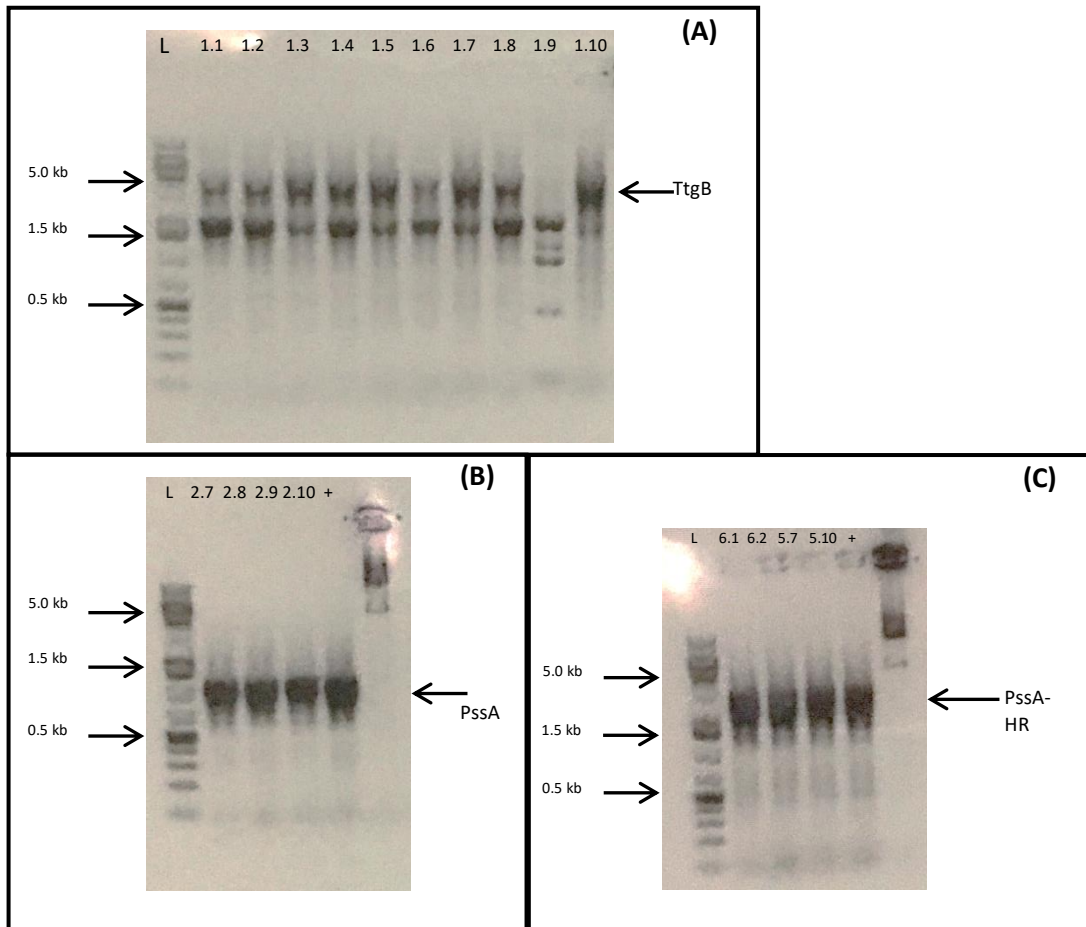


Figure 5.7. Colony PCR of *Clostridium saccharoperbutylacetonicum* N1-4 colonies transformed with the expression vector pMTL82151 containing either (A) TtgB (1.X) at ~3.5 kb in lanes 1.1-1.8 and 1.10. (B) PssA (2.X) at ~1 kb in lanes 2.7-2.10 (colonies 2.1-2.6 were positive, data not shown). (C) PssA-HR (5.X) at ~2.5 kb in lanes 6.1-5.10 (PssA-HR was found in all other colonies, data not shown). Empty pMTL82151 was used as a positive control. Positive colonies were expected to produce products at a size of 550 bp + insert bp. Primers: MH202, MH203 The ladder (L) used was Generuler plus 1 kb (SM1331) (Thermo Fisher Scientific).

5.2.4 Strain characterisation

A small bottle screen was carried out on the above strains (+PssA and Δ PssA and +TtgB). This was done to understand the effects of these modification on the production of and tolerance to butanol in industrially relevant strains. Following overnight incubation and inoculation in fresh media, the OD₆₀₀ and pH of cells was recorded at 0 h, 6 h, 24 h and 48 h. All strains were checked using microscopy and qualitative motility as a crude measurement of viability (to be cross reference later with OD₆₀₀ measurements). Generally, cells appeared healthy and motile, with the Δ PssA perhaps appearing less motile visibly. At 24 h +TtgB appear more motile than +PssA, Δ PssA showed little to no movement. By 48 h there was no movement seen in any of the mutants or WT.

The changes in pH over the course of fermentation is shown in Figure 5.8B. The pH of all fermentations decreases significantly in the first 6 hours of fermentation indicating the production of acids in fermentation. Due to the limits of the timepoints it is unclear at what point the pH is lowest. The pH appears to plateau or slightly increase over the rest of the fermentation. This may indicate a shift to solventogenesis, and the plateau may be due to an overlap of the two growth phases.

The OD₆₀₀ of the different stains is shown in Figure 5.8A. In general, all strains grew until 24 h after which growth plateaued or was much slower. +TtgB strain had a significantly higher OD₆₀₀ at 6 h than the WT. At 24 h, +TtgB also had a higher OD₆₀₀ value than the WT however, this was not significantly different. +PssA showed a very similar growth pattern to the WT strain, with no significant difference in OD₆₀₀ seen at any point during the fermentation. By 6 h Δ PssA had a similar OD₆₀₀ when compared with the other strains, however lagged in growth by 24 h where it completely plateaued. This may be due to a loss of cell viability, which is also reflected in the pH of the Δ PssA culture being lower than the other strains by 24 h and 48 h. The lower pH would indicate there being fewer viable cells capable of utilising the acids as substrate in solventogenesis, hence a more acidic environment would exist. No significant difference was seen in final OD₆₀₀ between the strains WT, +PssA and +TtgB by 48 h, being 11.29, 12.91 and 12.31, respectively. By 48 h, the final OD₆₀₀ of Δ PssA remained significantly lower than all other

strains at 3.70. This data shows that the recombinant strains grow in a similar way to WT, with the exception of Δ PssA which appeared to significantly reduce viability. +TtgB had higher OD₆₀₀ values at all time points after 0 h, however these were not significant. Further fermentation characterisation, in terms of substrate consumption and analyte production needs to be carried out on these strains to further understand their effect.

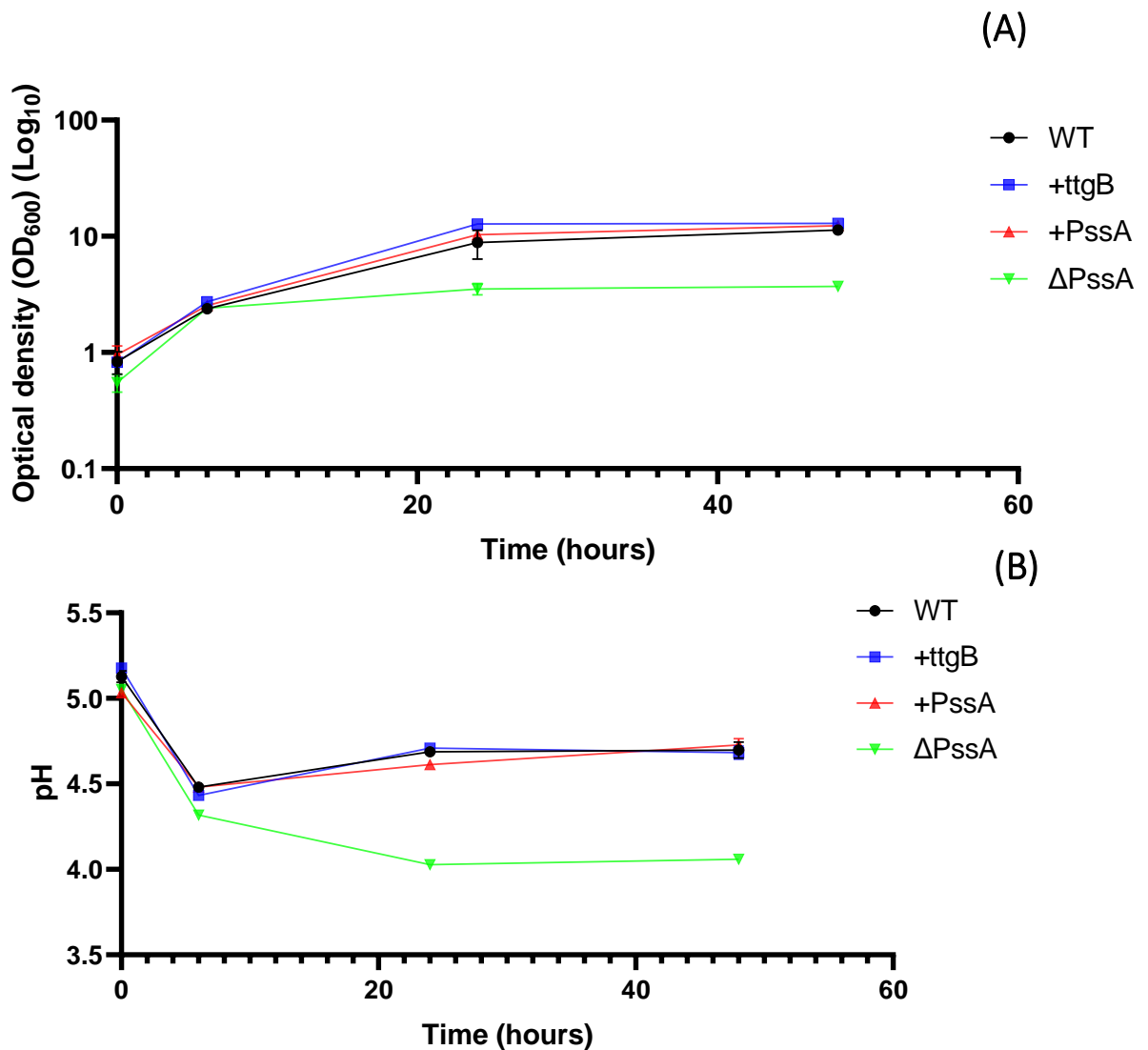
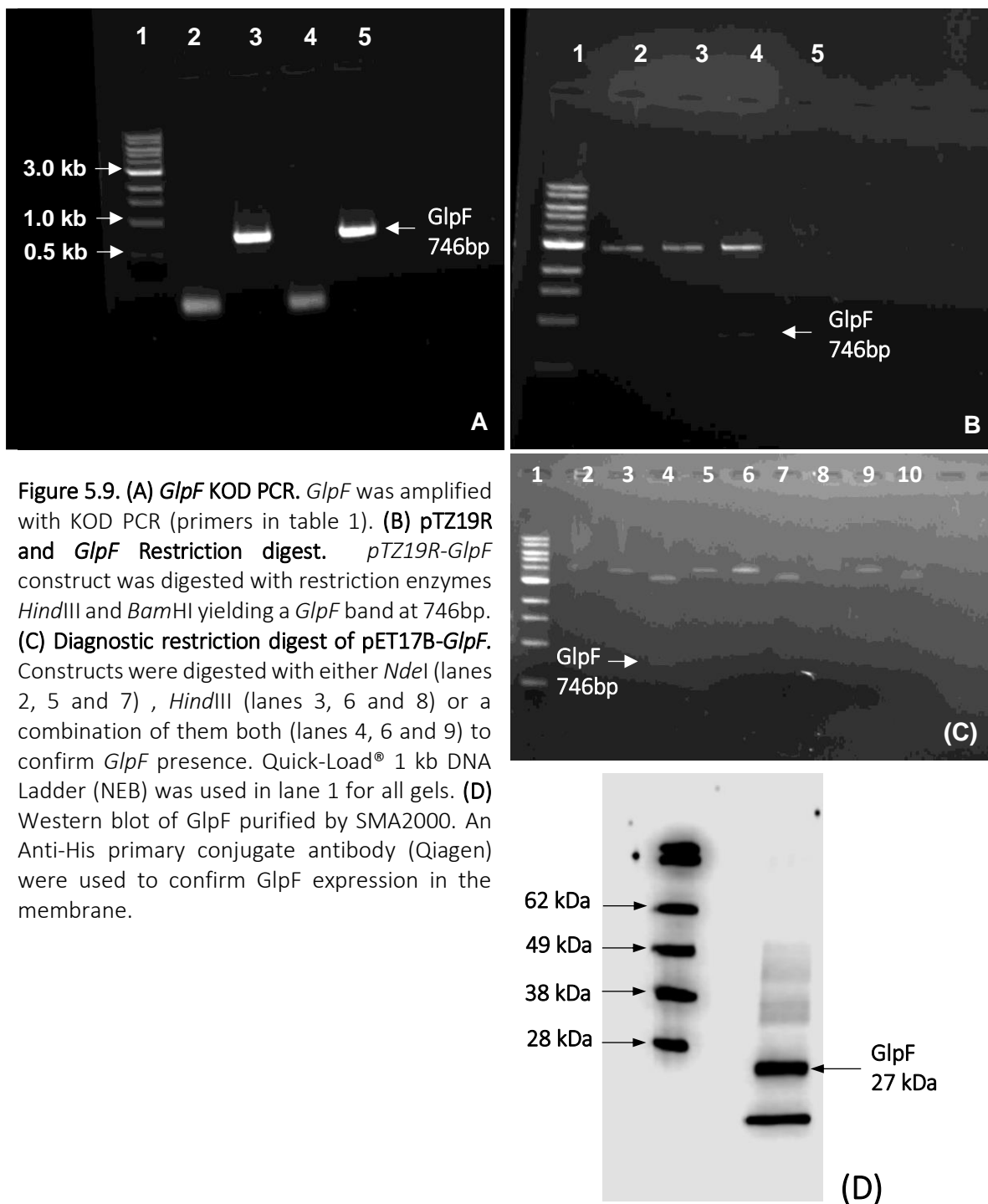


Figure 5.8. Optical density and pH of engineered *Clostridium saccharoperbutylacetonicum* N1-4 (HMT) strains during the small bottle screen. Overexpressing TtgB (+TtgB) and PssA (+PssA) or with PssA knocked out (Δ PssA). These modifications were carried out using CLEAVE™ (Biocleave). Broth samples were taken at 6 h, 24 h and 48 h where the OD₆₀₀ (OD₆₀₀ is on a Log₁₀ scale) external pH and fermentation analytes were measured.

5.2.5 GlpF cloning and expression

Based on previous reports in the literature of GlpF upregulation during ABE fermentation, some preliminary investigations into were undertaken. The *GlpF* gene was amplified by PCR using the primers in Table 1. Figure 5.9 shows the pTZ19R-GlpF construct digested with restriction enzymes *HindIII* and *BamHI*. The cut plasmid can be seen at ~3000 bp and the presence of the *GlpF* insert is confirmed by the drop out band at 746 bp. *GlpF* was then cloned into *pET17B*, the vector used for subsequent expression. The presence of *GlpF* in the *pET17B-GlpF* was confirmed through the use of a diagnostic restriction digest (Figure 5.9). In lanes 2, 5 and 8 constructs were digested with *NdeI* only; in lanes 3, 6 and 9 constructs were digested with *HindIII* only and in lanes 4, 7 and 10 constructs were digested with both *NdeI* and *HindIII*. For plasmid cut with only a single restriction enzyme, there is a band at ~4 kb indicating the presence of linearised pET17B-*GlpF*. Conversely, for the sample cut with both enzymes there is a plasmid band at ~3.3 kb, lower than when cut with either of the restriction enzymes individually. Additionally, *GlpF* can be seen in these lanes at 746 bp. GlpF was overexpressed using 1 mM IPTG, and expression was confirmed with a Western Blot analysis (Figure 5.9). GlpF was extracted from the membrane pellet of the cells using SMA2000 polymer which cut out sections of the membrane ~10 nm in diameter.



The effect of GlpF overexpression on cell growth in exogenous butanol was investigated by measuring the optical density at 600 nm over several hours. Figure 5.10A shows the OD₆₀₀ of GlpF over expressing BL21 *E. coli* cells (+GlpF) compared to the WT control with an empty vector (pET17b). It can be seen that cells overexpressing GlpF had a significantly higher OD₆₀₀ at 2 h and 4 h that the WT for both 0 mg/ml and 5 mg/ml exogenous butanol. Whilst the OD₆₀₀ of +GlpF cells remained higher than WT, there was no significant difference between the time points. Hence there appears to be some benefit to growth when overexpressing GlpF, however it is unclear if this is specific to butanol stress, or whether it has a more general benefit. Other stressors were also tested (Figure 5.10B). Increasing levels of sodium chloride

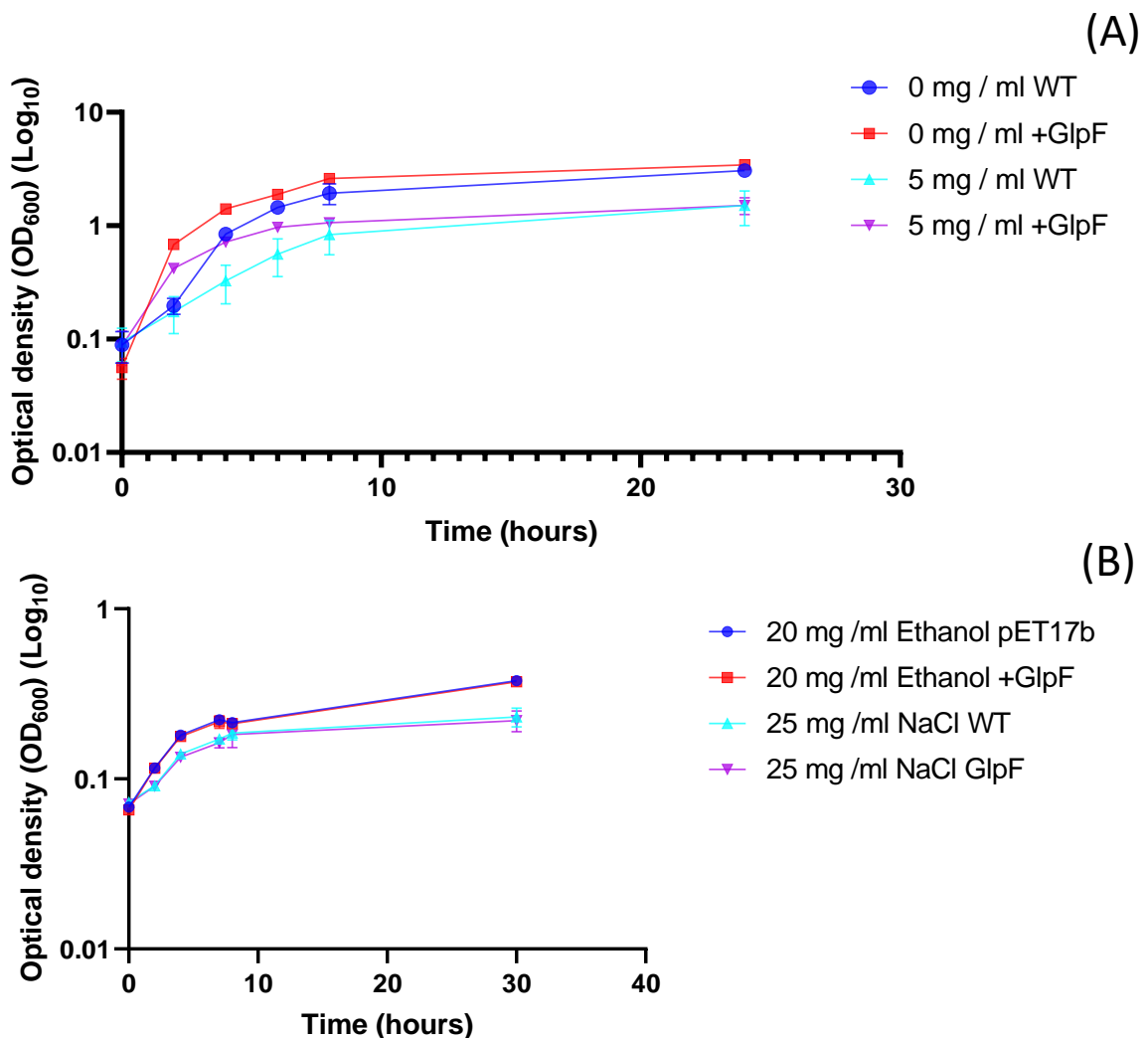


Figure 5.10. Effect of GlpF overexpression in the presence of (A) 5 mg/ml exogenous butanol and (B) Ethanol and NaCl. Overnight cultures were diluted to an OD₆₀₀ of 0.1 after which butanol was spiked in. *E. coli* strains BL21(DE3) and plasmid pET17b were used. Neither WT (pET17b) nor +GlpF were able to grow in 20 mg/ml exogenous butanol (data not shown). OD₆₀₀ is on a Log₁₀ scale. Different Y-axis scales have been used.

were investigated to see whether the effects of GlpF were related to the osmotic stress, as GlpF facilitates water flux. Additionally, the effect of GlpF on ethanol tolerance was carried out to determine whether the GlpF-mediated increase in OD₆₀₀ was a specific to butanol exposure, or whether it could be applied to other alcohols. The expression of GlpF had no significant bearing on the OD₆₀₀ after 30 hours in response to 20 mg /ml ethanol or 25 mg /ml NaCl.

To summarise several targets were chosen for the attempted engineering and modification of ABE fermentations. Firstly, in *Clostridium saccharoperbutylacetonicum* N1-4 (HMT), PssA and TtgB which are proteins involved in lipid biosynthesis and the inner membrane portion of an AcrB-like transporter, respectively. These were either overexpressed or knocked out forming the following mutants: overexpression, +TtgB and +PssA; knockout, Δ PssA. This modification was carried out using CLEAVE™. The overexpression strains showed no significant difference in OD₆₀₀ across fermentation when compared with the WT. The +TtgB strain did have a higher growth rate and a higher optical density at all points in fermentation, however this was not significant. The knockout Δ PssA had a significantly lower OD₆₀₀ later in the fermentation and also had a lower pH at these time points too. The aquaglyceroporin, GlpF was also investigated. GlpF was successfully cloned into an expression vector and overexpressed in *E. coli* BL21. This led to a significant growth advantage early in growth when exposed to exogenous butanol but not to NaCl or ethanol.

6. *Clostridium saccharoperbutylacetonicum* N1-4 (HMT) TtgB homology model

6.1 Introduction

Following work of the previous Chapter, there were plans to investigate the mechanism of the putative transporter TtgB, through the use of proteoliposomes and planar lipid bilayers. Ultimately this was not possible due to the COVID-19 pandemic preventing laboratory access. Hence, the workflow was shifted to the generation of an *in silico* model of TtgB. There currently exists no structure produced for the *Clostridial* protein TtgB and no structure in *P. putida*. Based on a recent paper by Basler and colleagues (2018), it may be the case that TtgB plays an important role in the tolerance of some bacteria to butanol production. The efflux pump, TtgB was found to be the first native efflux system to transport butanol across the cell membrane. Other engineered systems have been developed in the past (see introduction 1.6.5 Efflux systems), but the wild type proteins used in those studies appeared to show no ability to transport butanol across the membrane. Having a 3D structure of TtgB is an important step in determining specific interactions which may drive butanol to be a substrate for the TtgB and not for other similar systems. This could provide information which could be used to produce and engineer proteins which can move butanol across membranes, enabling fermenting cells to reduce intracellular butanol concentrations. The previous bioinformatic data shows us that a homolog of the *P. putida* TtgB exists in *C. saccharoperbutylacetonicum*, and a homology model can be generated to produce a putative 3D structure. The model produced can be used in further molecular dynamic simulations to elucidate whether butanol is a substrate and whether it can enable the translocation of butanol molecules across the membrane.

6.2 TtgB homology model

Two strategies were taken for making the homology model. Initially, the protein sequence for *P. putida* TtgB was taken from UniProt (UniProtKB - O52248). The sequence for this protein in *C. saccharoperbutylacetonicum* N 1-4 was then searched for using BLAST (NIH) and a sequence 98% coverage, a percent identity of 27.41% and an e-value of 2×10^{-53} was found (WP_015394794.1). Following this, the amino acid sequence was aligned to templates from BLAST and HHblits using SWISS-MODEL (Bienert *et al.*, 2017; Waterhouse *et al.*, 2018), and a list of possible models was generated. The models were chosen based on some output criteria, namely the GMQE and QMEAN scores. The GMQE is a global estimate of quality from 0-1 with values closer to 1 being more reliable models with a higher degree of accuracy. The QMEAN score gives an estimate of how comparable the model is to experimental data (Benkert *et al.*, 2011) with scores closer to 0 implying agreement between the model and experimental data of similar sized proteins.

Initially, the top four templates produced from SWISS-MODEL were chosen to make the TtgB model structure from the *Clostridial* amino acid sequence. The first model (shown in Figure 6.2A) was aligned against a crystal structure of the trimeric AcrB in complex with a designed ankyrin-repeat protein (DARPin) inhibitor (Sennhauser *et al.*, 2006). The second model used a aligned against a cryo-EM structure of *A. baumannii* AdeB multidrug efflux pump (SMTL ID : 60ws.1) (Su *et al.*, 2019). The third model used an X-ray diffraction model of AcrB (SMTL ID : 1t9t.1) (Yu *et al.*, 2005). The fourth model used and cryo-EM structure of SMALP-solubilised AcrB and generated a monomeric structure (SMTL ID : 6z12.1) (Johnson *et al.*, 2020), with the previous three models being in a trimeric state. The GMQE scores for each of the four models were: 0.68, 0.66, 0.57 and 0.53, and the QMEAN scores were -2.59, -3.36, -5.67 and -4.00, respectively. Based on these scores obtained from the initial alignments using the amino acid sequence of the *Clostridial* TtgB, the first model appears the best choice. A second approach was taken to try and generate a better model.

The second method started involved generating a homology model of the *P. putida* TtgB (UniProtKB - O52248) using SWISS-MODEL, which was then used to align the *Clostridial* amino acid sequence and generate a model of the *Clostridial* TtgB. This was done to allow for better comparison between TtgB from *P. putida* and TtgB from *Clostridia*. The *P. putida* TtgB model was aligned to two different templates depending on the oligomerisation state. The monomeric form was aligned to a structure of AcrB (SMTL ID : 4dx6.1) (Eicher *et al.*, 2012) with a sequence coverage of 66.09% and a GMQE and QMEAN score of 0.79 and -1.43 respectively. To check for overall structural similarity at this stage, the monomer made from the *P. putida* alignment was then spatially aligned in PyMOL to the initial TtgB monomer model made using the *Clostridial* sequence alignment. There appears to be a high degree of similarity between their structures (Figure 6.1). The trimeric model was aligned to MexB (SMTL ID : 3w9i.1 -2) (Nakashima *et al.*, 2013) with a sequence identity of 78.33% and a GMQE and QMEAN score of 0.77 and -1.54, respectively.

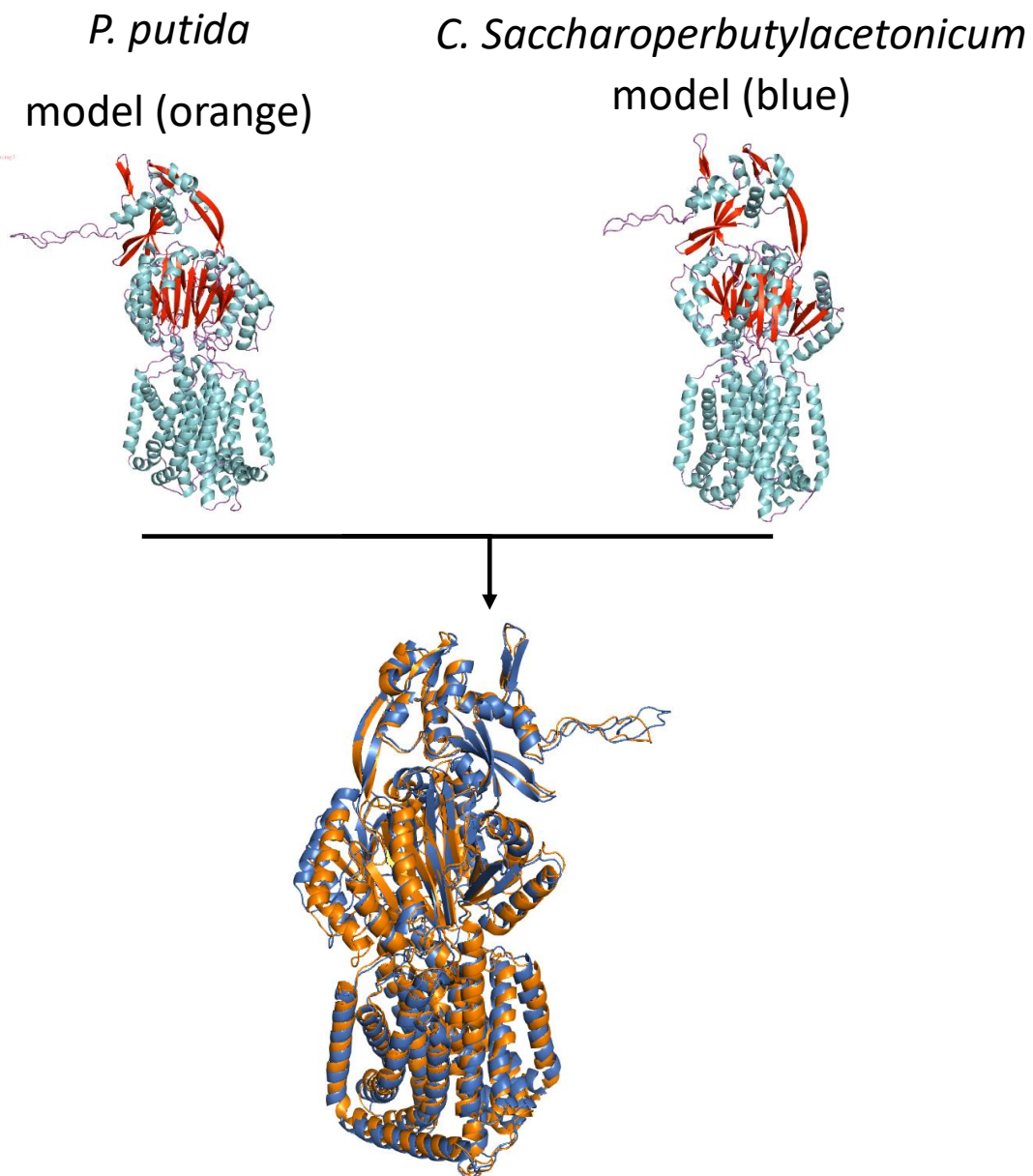
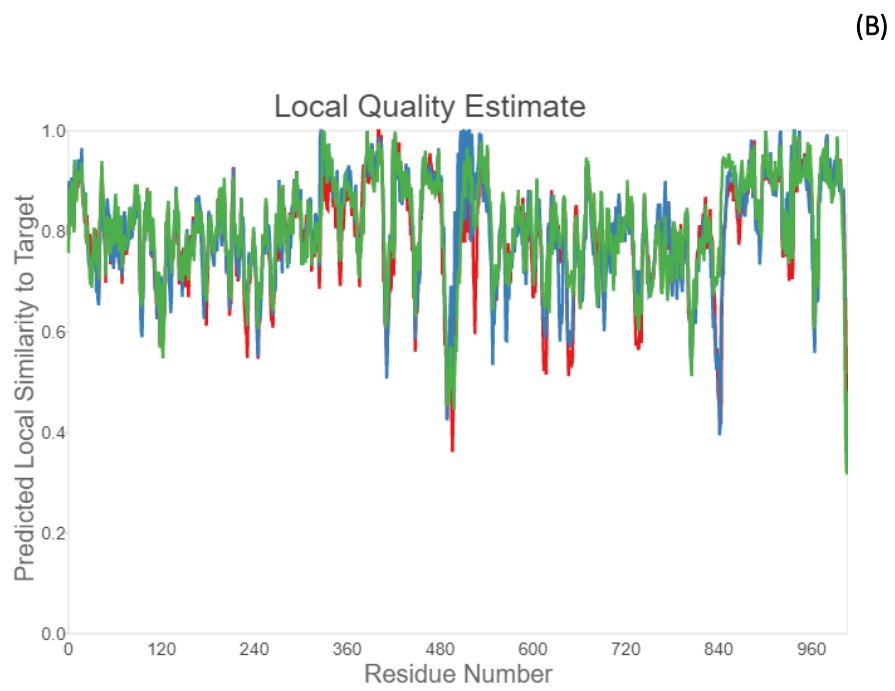
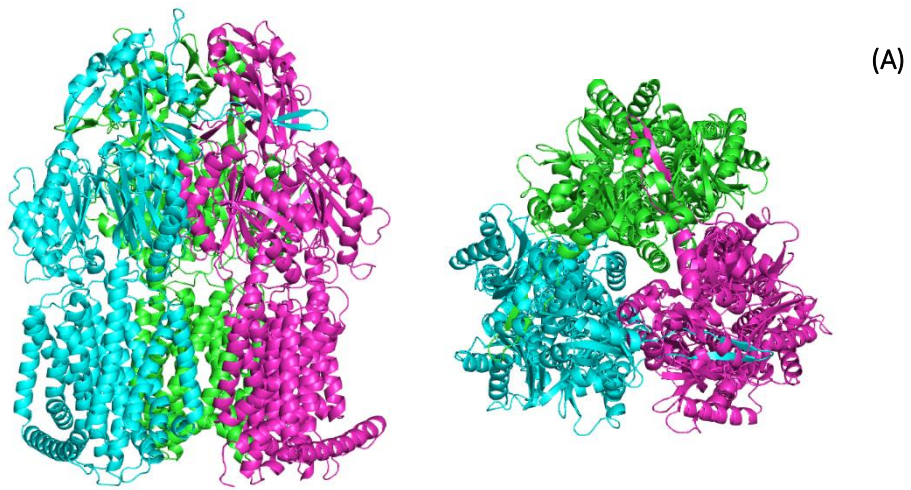


Figure 6.1 Structural alignments of the two TgB homology model monomers, from *P. putida* and *C. saccharoperbutylacetonicum* generated using SWISSPlot. The left model is generated by aligning the *P. putida* amino acid sequence and is represented by the orange cartoon. The right model is the first model generated from aligning the *C. saccharoperbutylacetonicum* amino acid sequence (derived from ntBLAST) and is represented by the dark blue cartoon. The individual monomers are also shown side by side and are coloured according to secondary structure: light blue, α -barrel; red, β -sheets; pink, loops.

Following this, the coordinate file of the monomeric *P. putida* homologue was then used as a template to align the *Clostridial* TtgB amino acid sequence to. This had only a 26.44% sequence identity and generated a TtgB model with a 0.64 GMQE and a -2.66 QMEAN, suggesting that this is an acceptable model to use for alignment, however it was not possible to generate a homotrimeric model. It is unclear as to whether this method provides a more accurate representation of *Clostridial* TtgB when compared to the first model which used a different protein as a template. Using a homologous protein from *P. putida* as a template should provide a better-quality model, however due to the absence of an experimental TtgB structure it was necessary to generate one. This extra step provided a model of *Clostridial* TtgB with better GMQE and QMEAN scores than the first four models suggesting that this may be a more accurate model, however this may be due to the oligomeric state being a monomer. Furthermore, this method could theoretically carry over any error in the modelling of this initial *P. putida* TtgB model to the *Clostridial* TtgB model. The relatively high alignment and accuracy when using the initial *P. putida* model as template does not necessarily mean that the *Clostridial* model generated is accurate. Hence it is important to use experimental structural data whenever possible. Additionally, the functionality of this model will be assayed in molecular dynamic simulations. The initial model was determined to be more suitable for use in the later simulations due to the lower GMQE and QMEAN scores, and it being present as in a tetrameric state which is more similar to the predicted oligomeric state *in vivo*. Other similar systems, such as AcrB are present in the membrane as tetramers (Seeger *et al.*, 2006) and thus it is likely that TtgB also exists as a trimer.

Following this the initial trimeric model underwent analysis by QMEANBrane (Studer *et al.*, 2014), another set of statistical potentials which informs local quality of membrane protein models in their natural oligomeric state (Figure 6.2C). Initially a solvation model is applied to the model to identify transmembrane regions and then statistical potentials are applied to different regions of the protein. This model was also found to be within the range of membrane insertion energies accepted for a membrane protein with the majority of residues scoring > 0.6 for local quality score. The highest quality

regions, i.e. those which mostly agree with the template appear to be the transmembrane helices and the lowest quality regions appear to be the end of the helical regions and some of the loop structures, particularly the loops of the intracellular region (potentially due to a role in substrate recruitment). Regions with low quality estimate values mean that the modelling engine used could not accurately rely on the template when building these regions of the model and thus, may be more unreliable. The QMEANBrane score is calculated based on statistical potential terms pertaining to: all-atom interactions, C β Interaction, solvation and torsion (see Studer *et al.*, 2014). This chosen model showed a 26.71% sequence identity and a 98% coverage with the template, AcrB. There were regions which showed a particularly low alignment with the template, including the loops at the top of the transmembrane helices and areas around the central pore.



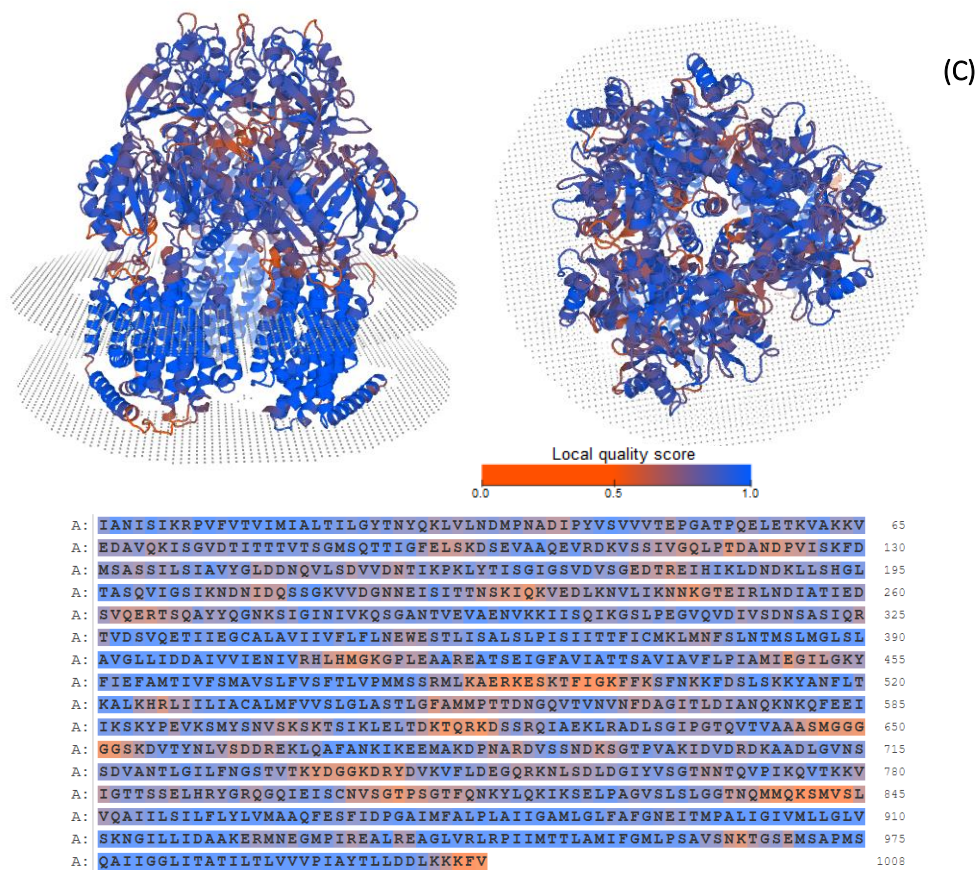


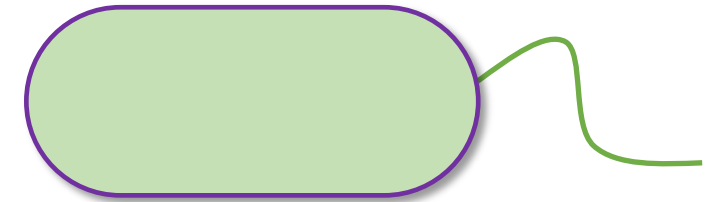
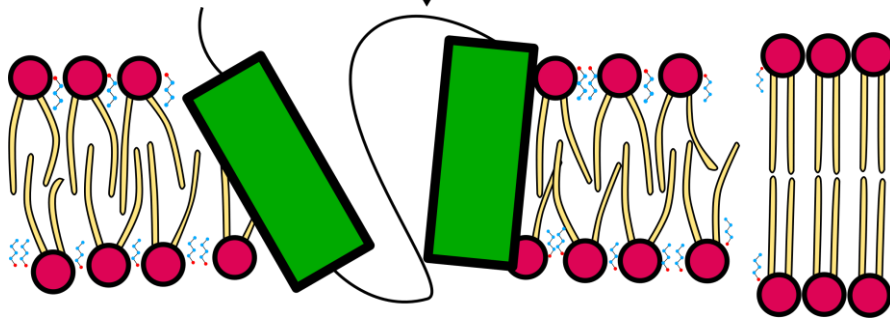
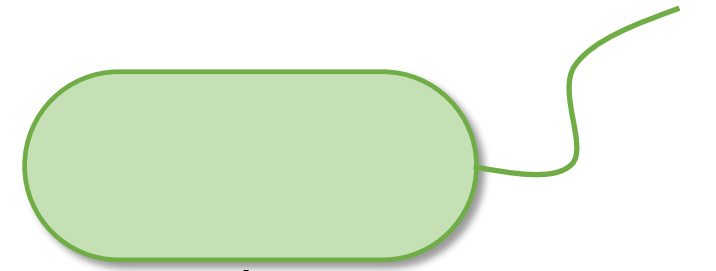
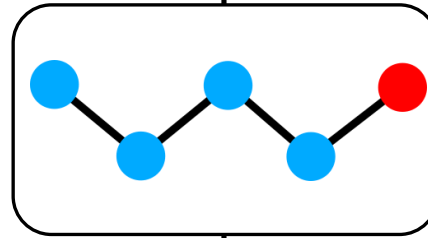
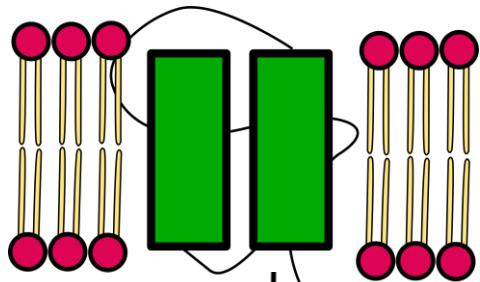
Figure 6.2. *C. saccharoperbutylacetonicum* TtgB homology model and QMEANBrane analysis (A) *C. saccharoperbutylacetonicum* TtgB made using SWISSPlot and aligned against a crystal structure of the trimeric AcrB in complex with a designed ankyrin-repeat protein (DARPin) inhibitor (Sennhauser *et al.*, 2006) visualised in PyMOL. (B) A representative alignment of one of the three monomers and a graph showing the local quality for each residue (Chain A, red line; Chain B, blue line; Chain C, green line). Regions with low quality estimate values mean that the modelling engine used could not accurately rely on the template when building these regions of the model. This results in a drop in local quality for these regions. (C) The QMEANBrane structure showing the protein complex in a membrane (denoted by the grey dots) and coloured to show the local quality score, with blue being values closer to 1 and of higher quality. The highest quality regions, i.e. those which mostly agree with the template appear to be the transmembrane helices and the lowest quality regions appear to be the end of the helical regions and some of the loop structures.

7. General Discussion

Butanol is an important high-value chemical, however the process of its bioproduction is hindered by low yields due to product toxicity, meaning petrochemical routes of production are currently favoured. Enhancing the tolerance of solventogenic *Clostridia* to butanol is paramount if this method is to be competitive with conventional means of obtaining butanol using petroleum-derived products. This body of work aimed to understand more about butanol's interaction with the membrane and how composition affects this; how the lipidome of *Clostridia* respond to butanol; and finally, whether, combining information gained from the first two aims, more tolerant and productive strains can be produced. These ideas are summarised in Figure 7.1.

Membrane perturbation

Effect on lipidome



↑ PG, CL, oleic acid
 ↓ PE-plasmalogen species
 ? PE, fatty acid

- Protein unfolding
- Pore formation (?)
- Fluidisation
- Permeabilisation
- Swelling

Figure 7.1 Overall model of the interactions between butanol and *Clostridia* (A) Membrane perturbation caused by butanol (B) The effects of butanol on the lipidome. Butanol exposure during fermentation interferes with normal membrane function and causes a change in the lipids seen in *Clostridia*. ↑, denotes an increase in these species; ↓, denotes a decrease in these species; ?, denotes further work is needed to determine.

7.1 How does butanol impact membrane properties and functions?

7.1.1 The importance of phospholipid head group and of phosphatidylglycerol

Initial experiments were conducted in order to gain more information around the toxic effects of butanol at the membrane, with the view of designing protective phenotypes. It was found that altering the headgroup composition had impact on the effects of butanol. The reduced fluorescence seen in POPE: POPG liposomes compared to POPC liposomes may be due to an increase in resistance against butanol intercalation. Molecular dynamic simulations comparing POPE: POPG bilayers in a 3:1 molar ratio with POPC bilayers indicate some different physical properties between the bilayers which could account for the increased resistance seen in POPE: POPG (Murzyn *et al.*, 2005). Firstly, the packing of the acyl chains in the upper regions of POPE: POPG is greater compared with POPC. This is indicated by both POPE and POPG lipids having more neighbouring lipids than POPC. It should be noted that the number of neighbouring atoms become comparable between the lipid species beyond carbon 10 in palmitoleic acid and carbon 5 in oleic acid. Hence, this increase in density of POPE: POPG only applies to the upper regions of the acyl chains. However, this may limit the intercalation of butanol into the membrane if lipids are more closely packed together at point of insertion. Secondly, POPE and POPG form more intermolecular water bridges than PC lipids. Water bridges are where a water molecule is concurrently hydrogen bonded to two lipids and may also add to membrane stability (Yamamoto *et al.*, 2015; Pasenkiewicz-Gierula *et al.*, 2016). Additionally, there was found to be 34% more hydrogen bonds formed by PE in a POPE: POPG mixed system than in a pure PE system, resulting in greater stability at the interfacial region (Zhao *et al.*, 2008). POPE and POPG lipids are closer together; due to the larger distance between PC-PC lipids, intramolecular water bridges become more likely than intermolecular water bridges (Murzyn *et al.*, 2005). Cheng and others (2011) found that POPE: POPG bilayers in a 1:1 ratio were more resistant to insertion of several variants of the antimicrobial peptide, aurein than PC/PG bilayers. It was concluded that this was due to the more complementary orientations of POPE and POPG phospholipids in POPE: POPG bilayers. Based on these specific interactions between PE and PG lipids it is possible that their presence in a membrane can convey resistance to solvent damage. Laurdan data

in Figure 3.4 shows POPC membranes to be more fluid than 3 POPE: 1 POPG membranes at the same butanol concentrations, this may signify a relationship between baseline membrane fluidity i.e. fluidity determined by the lipid composition, and the permeability of the liposomes. Greater amounts of POPG were spiked into the liposome models to investigate whether this would have a beneficial impact (Figure 3.3-5). No difference in permeabilisation was seen < 35 mg/ml butanol, however above this the addition of more POPG appeared to reduce permeability. It may be that the addition of more POPG has only a small impact, and thus seemingly does not provide any benefit in the biologically relevant ranges, and only when butanol stress is much greater. The fluidity data showed an interesting effect of spiking in more POPG whereby a 2 POPE: 1 POPG ratio was more rigid than 3 POPE: 1 POPG at higher ends of the biologically relevant butanol concentration range (15-25 mg/ml). This is despite that fact that the phase transition temperature of POPG is lower than that of POPE and therefore increasing the proportion of POPG should theoretically increase the overall fluidity of the system (as in 1 POPE: 1 POPG). Therefore, there is potentially an optimal ratio of POPE: POPG in a membrane that provides the most protection against butanol, in terms of maintaining constant fluidity, with a slight reduction in permeabilisation at higher butanol concentrations. This could be related to the specific interactions of these two lipid species. Altering the amount of PG lipid species in the membrane is therefore a good target for influencing the wider membrane properties and responses to butanol.

It is seen in the lipidomics data that high butanol conditions cause an increase in PG species, and that specifically there is one individual PG species that appears to double in peak area (from 3×10^6 to 6×10^6) (Figure 4.8). This is further supported by the second lipidomics experiments where there is an upward trend of PG lipids across fermentation. A comparison can then be drawn to the molybdenum blue TLC plate where the relative density of POPG also doubles (a 100% increase in density) (Figure 4.9), meaning that the two species are likely the same and that butanol exposure probably elicits and increase in the proportion of POPG in the membrane. The exact identity of the species in the lipidomics data could not be confirmed. It is a safe assumption to make that POPG is likely to play a role in the stress

response of butanol and may make a good target for strain engineering. This is further corroborated with data from the first chapter showing that POPG is protective in the *in vitro* models. Recent transcriptomics analysis of *Clostridium beijerinckii* shocked with butanol show alterations to the expression of lipid synthesis genes (Patakova *et al.*, 2021). Genes related to the synthesis of CL and lyso-PG had higher expression following butanol shock, whereas genes related to LPA, PA, PS and PC had lower levels of expression. This increase in CL and PG species biosynthesis enzymes supports the above changes seen in the TLC and lipidomics analysis. These data bring together several techniques and with different butanol stresses employed, it is clear that PG lipids, as well as specifically POPG are important in the butanol stress response. This also highlights the ability to predict *in vivo* phenomena and interaction using *in vitro* model systems. Following on from this, the enzymes involved in the biosynthesis of the various lipid head groups can be engineered through plasmid-based expression or knocked-out through genome-level deletions using CRISPR-based technology. This will create a strain with a crudely tuneable membrane composition with a focus on PG containing headgroups.

These data (PG results from Chapters 3 and 4) were the basis for the targeting phospholipid biosynthesis as altering composition was predicted to have an impact on butanol tolerance, despite this being a comparatively unexplored area (Sandoval and Papoutsakis, 2016). The enzyme PssA was chosen as a target (see Figure 1.5), and it was hypothesised that knocking out this enzyme would result in an increased PG:PE ratio which in turn would lead to improved growth due to a higher tolerance for butanol. PssA overexpression (+PssA) has previously been shown to convey tolerance to a variety of industrially relevant organic compounds in *E. coli* (Tan *et al.* 2017), however this did not extend to butanol. This trend was seen in this work where +PssA showed very similar characteristics in fermentation to WT (Figure 5.8). The changes seen in the Δ PssA were not as predicted. Data from the Chapter 3 suggested liposome models with more PG were more tolerant to butanol. This was further supported by TLC and lipidomics data from Chapter 4 which showed an increase in PG lipid species throughout fermentation, possibly due to these lipids being involved in tolerance to butanol. Thus, it

was hypothesised that increasing the relative amount of PG in the membrane through knocking out PssA would lead to better growth than WT in fermentation, however this was not the case. By 6 h the Δ PssA strain had a significantly higher OD₆₀₀ than WT perhaps suggesting a growth advantage in the earlier parts of fermentation (Figure 5.8). Interestingly, the growth rate of Δ PssA between 6 – 24 h was significantly lower and there was no growth seen between 24 - 48 h. This drop in growth rate, combined with a generally low motility of the population, and the significantly lower pH (a lower pH would imply that cells are not utilising acids in solventogenesis) suggests lack of cell viability in the population. The viability of these cells after fermentation was not tested. It may simply be that deleting PssA is too drastic a change for the cells to remain viable throughout fermentation. If PssA is the only enzyme responsible for PE synthesis, then deleting it would cause the cells to have no PE in their lipidome. PE is the largest class of lipids found in *Clostridial* (Ogata *et al.*, 1982; Durre, 2005) and thus there may be other important functions mediated by PE lipids which are essential for survival. Because of time limitations due to the COVID-19 pandemic, the exact effect of Δ PssA on the lipidome was not investigated with TLC / lipidomics. This would be an important piece of further work to understand the lack of viability of these mutant seen in mid-late fermentation.

It has been suggested previously that PG can replace PE, but within unknown limits (Nishijima and Raetz, 1979). This was found to be only be partly true in *E. coli* and PG replacing PE lead to a less complex LPS (Rowlett *et al.*, 2017). The loss of PE may have disturbed the balance of charge across the membrane to too great an extent. PE is thought to balance the negative charges of PG and CL, and the introduction of neutral lipids into an anionic membrane (due to lacking PE) has been shown to restore wild type LacY organisation in *E. coli* (Wikström *et al.*, 2009). In Δ PssA *E. coli* mutants LacY had a 5-10 fold lower V_{max} for lactose than WT cells (Bogdanov and Dowhan, 1995). Therefore, lack of PE could potentially affect the topology and structure of membrane protein. The loss of PE in the membrane could also impact the way that PG exerts influence on membrane / protein function due to the propensity for PE to preferentially form interlipid bonds with PG (discussed previously (Murzyn *et al.*,

2005)). The lack of PE also affects membrane protein folding in the inner membranes (Bogdanov *et al.*, 2014) as well as LPS structure and protein assembly in the outer membrane (Rowlett *et al.*, 2017). Deleting PssA, will give rise to a mostly anionic membrane, with no amino-containing lipids. From the above data it is clear that containing some portion of amino-containing lipids (PC, PE, PS) is important for cell viability. Δ PssA mutants have been described as requiring millimolar divalent cations (Bogdanov *et al.*, 2014), the supplementation of this into the TYIR media may be something worth investigating. Based on the above, a more titrated reduction in PE or overexpression of PG may prove more impactful engineering strategy as there may be unforeseen consequences resulting from a large reduction in PE. This could be achieved by creating Δ PgsA and +PgsA mutants which would perhaps be a better method to modulate PG content in the membrane without massively reducing PE, which dilutes the anionic charge. Ultimately, more work needs to be carried out in this field to accurately assess the role of lipid classes in essential membrane linked functions.

7.1.2 Phospholipid tail and fortifying the membrane against butanol with non-phospholipids

The overexpression of +PssA showed similar results to that of Tan and colleagues, (2017) who saw no benefit in exogenous butanol tolerance in *E. coli* when overexpressing PssA. The agreement seen could perhaps mean that the increase in levels of PE in the membrane, whilst not detrimental, will not increase survival / tolerance to butanol. Tan and others (2017) study also noted a concurrent change in fatty acid composition (increased carbon length and percent unsaturation and a decrease in cyclic rings). Due to the untargeted nature of the mass spectrometry in Chapter 4, the changes in fatty acids could not be accurately determined. However, TLC data from Chapter 4 shows a significant increase in oleic acid (18:1) by the end of fermentation. This particular fatty acid was also noted to have increased in abundance in the above study by Tan and colleagues (2017). This would suggest that fatty acids are also subject to change following butanol exposure, and that certain fatty acids may convey advantageous membrane states to protect against butanol. This idea is supported by the *in vitro* experiments seen in Chapter 3 whereby altering the fatty acid components of the membrane led to less permeable liposome models.

Increasing the length of the acyl chains will result in more inter lipid forces and allows for stronger interactions with acyl chains in the adjacent leaflet. Bilayers containing shorter chains are freer to move due to reduced interactions between acyl chain ends of opposite leaflets (Denich et al., 2003). The bond angle of an unsaturated bond in the trans conformation is 6° , compared to 30° in a cis bond, resulting in Trans bonds having a more extended conformation allowing for denser packing and reduced membrane fluidity (Róg et al., 2004). The conversion of cis to Trans is a known response of bacteria to temperature and solvent stress (Okuyama et al., 1991; Heipieper et al., 2007). Trans unsaturated bonds appear to convey resistance to butanol in liposome models and may be related to tolerance *in vivo*. It is possible that the presence of Trans bonds can somewhat counter act the fluidising effect of butanol on the membrane. However, the synthesis of unsaturated bonds in *Clostridia* remains relatively unclear, though is believed that *fabF* plays a role (Zhu et al., 2009; Patakova et al., 2019) making this a potentially

difficult engineering target. Increased chain length is seen in Clostridia with butanol or temperature stress (Baer et al., 1987; Venkataramanan et al., 2014). There appears to be a relationship between increased membrane rigidity and decreased membrane permeabilisation during butanol exposure. This relationship is supported by Chapter 3 where liposomes containing lipids with longer fatty acids were less permeable (Figure 3.5)

Kolek and colleagues (2015), found that the addition of exogenous butanol caused a relative increase in saturation, whilst endogenous butanol (from cells undergoing ABE fermentation) caused a relative decrease in unsaturation. It is unclear why cells would respond in such a way to butanol stress as this would fluidise the membrane further. Alternatively, other changes may be occurring to the membrane to alter its overall properties that do not pertain to the lipid portion of the membrane. If cells are producing more membrane proteins in response to butanol, then this could have an impact on the membrane fluidity. Additionally, unsaturated bonds may be necessary for the proper function of membrane proteins which are upregulated in response to butanol stress. Membrane proteins have been shown to be involved in the maintenance of membrane properties and may regulate the robustness and strength of the cell surface in a tuneable manner (Kaiser *et al.*, 2011). In this scenario despite an increase in unsaturation, the presence of other membrane entities which impact membrane properties e.g. hopanoids, would result in a net reduction in fluidity to counter fluidisation by butanol. This is speculation as quantification of hopanoids was not carried out. It is possible however that the cells would increase the portion of hopanoids in their membrane. It was seen in Chapter 3 that the presence of cholesterol (used as a hopanoid surrogate) resulted in significantly lower permeability at high butanol concentrations (Figure 3.7). Cholesterol is a known regulator of fluidity, acting to disrupt interlipid hydrogen bond to promote fluidity, whilst also interacting with the acyl chains of phospholipids to reduce fluidity (Denich *et al.*, 2003; Sáenz *et al.*, 2015). The presence of hopanoids maintains membrane integrity under stress (Welander *et al.*, 2009; Tushar *et al.*, 2014). The upregulation of hopanoid synthesis genes may aid bacteria in resisting higher butanol concentrations through better

regulation of their membrane's fluidity (Sohlenkamp and Geiger, 2016). In response to ethanol stress, *Zymomonas mobilis* increases the membrane hopanoid content which contribute to the stability and permeability of the membrane, suggesting an adaptive tolerance response (Bringer *et al.*, 1985). The ability for hopanoids to regulate fluidity, an integral part of butanol toxicity, makes them an attractive engineering target (Guo *et al.*, 2019) and manipulating their expression may reduce butanol's interactive damage. Investigating this was beyond the scope of this work but would nonetheless be of interest in the future. This highlights the importance of non-phospholipid elements of the membrane.

The use of exogenous compounds that can intercalate with the lipid bilayer and provide stability to the membrane is an attractive means of improving the ABE process. For example, [previous work by Hinks and colleagues (2015) showed how COE1-5C (a 5 ring oligo-polyphenylene-vinylene conjugated oligoelectrolyte) reduces the toxic effect of butanol on membranes. Using single molecule tracking in a supported bilayer and molecular dynamic simulations, it was revealed that COE1-5C acted as a support for the acyl chains of the lipids reducing fluidity and resulting in an enhanced membrane stability. Another conjugated oligoelectrolyte, S6, was also found to reduce butanol toxicity in *E. coli* (Zhou *et al.*, 2019).

Exogenous membrane-stabilising compounds have the potential to increase butanol productivity, without the need for genetic modification of strains which may lead to unforeseen circumstances due to a lack of knowledge surrounding the nuances of ABE regulation. The 8 supramolecular self-associating amphiphilic (SSA) compounds are membrane active and some have been shown to have antimicrobial properties against MRSA and *E. coli* (Tyuleva *et al.*, 2019; Allen *et al.* 2020). The ability of the non-toxic variants to protect against butanol was investigated. The absence of any observable impact of the compounds on the membrane or on butanol's impact on the membrane may be due to the experimental procedures. The methodology for this series of experiments was the same as previous laurdan based butanol experiments (see Materials and Methods 2.3.1) – this was done to enable comparison between earlier experiments and those utilising the compounds. However, recent work by Allen and colleagues

(2020) on C39 and MRSA and *E. coli* using widefield fluorescence and transmission microscopy may imply that a change in methodology is required to ensure that any active effect of the compounds was not missed. The work shows that C39 self-associating aggregates were present when the compound was first added to the cells. However, these aggregates disappeared following a 24 h incubation and C39 was found to coat *E. coli* and internalise into MRSA. This would suggest that a longer incubation period might be required for liposome assays in order for the compound to adequately form a potentially membrane active structure and fuse to the membrane. Following the initial experiments, further experiments were carried out which included incubating the liposome and the compounds for a longer period of time (Figure 3.11). This seemingly had no impact on the fluidity of the POPC liposomes when exposed to butanol. It is hypothesised that C1 preferentially interacts with both PE and PG headgroups through the formation of hydrogen bonds (White *et al.*, 2020). Thus, it is likely that they will interact with the membrane of fermenting *C. saccharoperbutylacetonicum* N1-4 whose membrane contains PE and PG as major components. Additionally, based on the proposed mechanism (through PE and PG), it may prove useful to alter the liposome constitution used to assay the compounds to a 3 POPE: 1 POPG instead of pure POPC. Despite this, there also appeared to be no effects observed when using a liposome composition containing POPE and POPG (data not shown), however the assay may require further development. It is possible that the compounds interact with the membrane in a different way, possibly through the genesis of more ordered membrane structures, which may have a lesser impact on fluidity. These may still be protective in some regards against butanol (for example through reducing butanol intercalation). To investigate this further, a calcein release assay (similar to the CF release assay) was developed and was to be carried out at the University of Kent as part of the collaboration. However, this was unable to proceed due to the advent of the COVID-19 pandemic. Future work would involve a more comprehensive assessment of the compounds and their effects on the membrane. Whilst the addition of molecules which reduce butanol's detrimental effect on the membrane will undoubtedly lead to reduced purification costs (due to higher yields), it is unclear whether the production and scaling of these membrane stabilising molecules will be economically

viable. If production costs remain high, then it may be that their application does not reduce the net costs of ABE fermentation. As stated previously, the inclusion of these kinds of molecules may incur an additional purification step to remove them from the product which would also impact the molecules cost-effectiveness.

It would still be of interest to investigate synthetic exogenous compounds further as it could shed light on mechanisms to prevent butanol ingress and intercalation into the membranes of *Clostridia*. Additionally, insight into this topic can be obtained through DLS as described in Chapter 3. As butanol is assumed to insert into the membrane and disrupt the interlipid interactions, it might be the case that this increases in overall mass of entities within the membrane causes liposomes and membranes to swell. Alternatively, any increase in diameter could be the result of butanol molecules interacting with the membrane surface and giving the perceived effect of swelling. Thus, understanding more about this mechanism will provide more engineering opportunities to prevent it. The coarse-grained molecular dynamics simulations show butanol to insert into the membrane and exist within the headgroup region of the phospholipids, thus the insertion mechanism is more likely than the aggregation mechanism. This is supported by other molecular dynamics simulations showing butanol interesting into membranes (Hinks *et al.*, 2015; Guo *et al.*, 2020). Furthermore, should butanol merely exist on the outer regions of the lipid there would be little change in fluidity and permeability, which is to the contrary of data in Chapter 3. It is known that membranes undergo swelling when exposed to organic solvents (Sikkema *et al.*, 1995; Murínová and Dercová, 2014) and thus it likely that butanol could cause this response in liposome models. The mechanism of this is based on butanol's amphipathic structure matching that of a phospholipid enabling it to interact with both the apolar acyl chain and the polar phospholipid head group concurrently (Huffer *et al.*, 2011; Kanno *et al.*, 2013). It has been reported that an *E. coli* strain evolved for tolerance to butanol had additional tolerance to polymyxin B, a cationic antimicrobial (Reyes *et al.*, 2013). Polymyxin B's bactericidal effects stem from its ability to form membrane pores as it can insert inbetween phospholipids (Daugelavicius *et al.*, 2000). This dual resistance suggests that the

mechanism of butanol works through insertion in a similar manner to polymyxin B. Additionally, AFM data in (Figure 3.14), also show the presence of pores formed after exposing POPC monolayers to 1% butanol. Due to imperfect lipid deposition during the formation of the monolayers, there were some pores already present before butanol was added. It may have been the case then that butanol was able to enter these already present pores and increase their size. Because of this it remains unclear whether butanol is able to form pores in a fully formed membrane. Following addition of the more concentrated 6% butanol solution to the POPC layer, there was a large amount of detachment of the membrane. This was likely exacerbated by the movement of the cantilever across the surface of the monolayer and would likely not cause the same level of destruction *in vivo*. Alongside the formation or exacerbation of membrane pores a reduction in integrity and force resistance, and vesicle formation of the surface of the bilayer was recorded with AFM. Similar effects on SOPC membrane properties have been seen with butanol using micropipette aspiration, where short chain alcohols were seen to reduce interracial tension and reduce membrane thickness and mechanical moduli (Ly and Longo, 2004). This data along with that of Chapter 3 presents a holistic view of butanol's perturbation of membrane properties. Exposure to butanol leads to fluidisation, permeabilisation, swelling, thinning and weakening and possibly pore formation.

7.2 Butanol has a detergent-like mechanism

A case can be made for butanol having a detergent-like mechanism of membrane perturbation. Like butanol, detergents possess an amphipathic structure and also cause an increase in the size of vesicles without solubilising them (Lichtenberg *et al.*, 2013). The possible formation of pores seen with AFM in would be further evidence for a detergent-like mechanism, as this occurs during detergent solubilisation of vesicles (Lichtenberg *et al.*, 2013). However, it has been suggested that vesicles can only be solubilised by surfactants with a certain hydrophobicity. In such a case where the hydrophobicity is lower than this threshold, only a portion of surfactant molecules enter the vesicles, with the majority remaining in the bulk solution. As the hydrophobicity is increased, more molecules can enter the vesicle which results in

an increase in vesicle size (Lin *et al.*, 2011). It may be the case therefore that butanol has a similar mechanism to detergent / surfactant solubilisation, as seen by the increasing size in DLS and the pore formation seen in AFM. It is unlikely that total solubilisation occurs at biologically relevant concentrations, presumably because the toxic effects of butanol would occur at a far lower concentration. Interestingly, the addition of 1-alcohols, including butanol has been seen to decrease the critical micelle concentration of SDS (Hayase and Hayano, 1978; Rubio *et al.*, 1994). Additionally, butanol may not be hydrophobic enough to result in total solubilisation and may be too insoluble in water to reach a concentration sufficient for this to occur. Ultimately this work has provided a greater understanding of how butanol interacts with the membrane and proposed a possible mechanism for this.

As previously mentioned, there is currently a lack of knowledge of the effect of butanol on membrane proteins, despite them making up a significant portion of the membrane. Previous studies have shown ethanol to influence the function of bilayers and membrane proteins (Huffer *et al.*, 2011; Tóth *et al.*, 2014). For, example, in mammalian systems ethanol has been seen to interact with ion channels by altering intermolecular forces which are required for the kinetic properties of the ion channel (Crews *et al.*, 1996). Therefore, it is possible that butanol may act in a similar way. However, the interaction of ethanol with these types of receptors pertains to several different biochemical processes which alter protein conformation, the contribution weighting of this is unclear (Dopico and Lovinger, 2009). Hence, it may be that membrane protein perturbations are a phenomenon secondary to the interactions with the alcohol and the lipid. The loss of retinal absorbance (an intrinsic chromophore of bR) essentially allows for retinal absorbance to be used as a proxy to measure membrane unfolding. Based on this metric - the exposure to butanol appears to cause a reduction in the retinal absorbance which can be inferred as bR unfolding (Figure 3.15). The similarities in unfolding response when comparing butanol to SDS may suggest that there is a comparable mechanism of action with both leading to bR unfolding. Like detergents, butanol may be able to interact with both lipid and protein. Butanol has previously been

used as a membrane protein extractant for its detergent-like action resulting in solubilisation of membrane proteins. Due to its lipophilicity and limited water solubility, butanol is able to extract membrane proteins into aqueous buffers with low levels of denaturation (Smith, 2017). Based on this, it is possible that any butanol mediated membrane protein damage stems from a perturbation to local membrane stability and inter lipid interactions. It is well known that various membrane characteristics, including lateral pressure are vital for the proper folding and function of membrane proteins (Mitchell, 2012). Therefore, disruption to the membrane will indirectly result in protein unfolding. On the other hand, there have been several successful efforts to engineer tolerance in solventogenic *Clostridia* and *E. coli* to solvents by targeting chaperone systems (Zingaro and Papoutsakis, 2013; Liao *et al.*, 2017), and upregulation of said systems is a part of the butanol stress response (Tomas *et al.*, 2004). This would suggest that cell toxicity is at least somewhat dependent on protein structure and folding and is not entirely based around membrane damage. Therefore, membrane protein stabilisation could also be an important tool for engineering tolerance. There is some evidence to show direct interactions between alcohols and membrane proteins (Dopico and Lovinger, 2009), therefore it is likely a combination of direct interactions and perturbation to bilayer properties that results in membrane protein damage and unfolding.

7.3 How do the cells respond to endogenous butanol?

Elucidating the lipids present in Solventogenic *Clostridia* will prove valuable for developing a deeper understanding of butanol's toxic effects on the cells. Taking the TLC and mass spec data together a general makeup of the lipids found in *Clostridium saccharoperbutylacetonicum* N 1-4 (HMT) can be determined. Whilst there are some limitations in terms of ease and reliability of quantification (discussed later) an approximate, relative proportion can be proposed. The membranes of solventogenic *Clostridia* appear to be mainly comprised of PE and PG containing species, which can be seen in Figures 4.5, 4.6 and 4.10, of which the proportion appears to change following exposure to butanol. This is in line with previous experiments where PE and PG are major and minor membrane

components, respectively (Ogata et al., 1982; Durre, 2005). The exposure to butanol during fermentation elicits a change in the proportions of various lipid classes. Not all changes are discussed in this section, as some are discussed throughout.

The increase in phosphatidic acid (PA) may be an indicator of higher phospholipid production, as PA is a common precursor (see Figure 1.5) (Tang et al., 2018). Under butanol stress the cells will be producing more phospholipids in order to change the composition of the membrane to better deal with butanol's perturbation. Membrane protein binding domains for PA have been reported previously (Putta et al., 2016), and thus an increase in PA could indicate a greater portion of certain membrane proteins in the membrane. This could extend to other lipid classes too. It is possible that specific phospholipid classes are able to influence the properties of the membrane (curvature, fluidity etc,) as well as influence the structure and function of other membrane entities such as proteins through binding or transient interactions. Interestingly these interactions can also be influenced by several factors such as pH, membrane curvature and membrane charge (Tanguy et al., 2018).

There was found to be no significant changes in the abundance of PS species in either of the lipidomic experiments. In the TLC data POPS levels did not significantly change over fermentation however may have appeared to mirror that of the growth rate. When looking at the OD₆₀₀ of the *Clostridia* (Figure 4.1), the exponential growth phase appears to extend from ~5 hours to 15 hours with some slower growth following and stationary phase beginning at 23 hours. The levels of POPS seen in TLC (Figure 4.3) appear to align with this somewhat. The earlier time points have higher levels of POPS than the seed and the last two time points. This may suggest a relationship between growth rates and POPS proportions. In the later time points of 23 h and 35 h population growth had ceased due to a lack of available resources in the growth media which is reflected in the levels of POPS being more similar to that of the seed time point. Also, it may be that POPS levels are lower in the later time points due to the increased butanol in the surrounding environment. Both *E. coli* and *B. subtilis* have been shown to alter their lipid content during normal growth, with some lipid species being over represented in stationary

growth as compared to exponential growth (Giddey *et al.*, 2009). A similar phenomenon has also been seen in *S. cerevisiae* growth during ethanol fermentation (Lairón-Peris *et al.*, 2021). Changes in the membrane composition of *E. coli* may be linked with the proliferation capabilities of the cell (Scherber *et al.*, 2009).

Monogalactosyldiacylglycerol (MGDG) is a glycolipid containing a single galactose residue as its phosphate-headgroup region. Although abundance was not investigated using TLC, a qualitative increase in levels of MGDG was seen in later in fermentation when butanol concentrations were higher (Figure 4.5 and 4.10). However, this was only seen in negative ion mode. The exact role of glycolipids in the membranes of bacteria remains elusive (Sohlenkamp and Geiger, 2016). They may be involved in bilayer stability and membrane protein function, and might be precursors to complex membrane components (Hözl and Dörmann, 2007). Additionally, they have been seen to be overrepresented in phosphate deprivation conditions as phospholipid surrogates (as the sugar is directly bonded to the glycerol) (Hözl and Dörmann, 2007; Martín and Liras, 2021). Damage to phosphate transporters in the cell membrane may reduce the amount of available phosphate eliciting a similar stress which could lead to more glycolipids being produced as they do not require phosphate (Fischer *et al.*, 2006).

Whilst it was hypothesised, based on Chapter 3 results, that an increase in the amount of saturated fatty acids would be seen, there appeared to be no discernible trend for changes in saturation / unsaturation throughout fermentation. (Figure 4.13). However, the increase in abundance of some specific unsaturated chains was seen. Oleic acid (18:1) was seen to increase significantly in the TLC analysis of the time course, as well as the initial mass spectrometry data where higher levels were found in a higher butanol environment. Furthermore, 18:2 was seen to be a higher abundance in the high butanol environment and a decrease in saturation was seen (however this may not be a clear-cut change - some unsaturated fatty acids e.g. *cis*-17:1 were lower in higher butanol environments). This observed increase in abundance for certain unsaturated lipids may initially seem counterproductive. It has been shown that butanol molecules increase membrane fluidity through perturbation of the interlipid forces

which is a major part of the toxic effect of butanol (See Introduction 1.4 Butanol toxicity). Hence, it would be contradictory to increase the amount of unsaturation in the membrane as unsaturated bonds drastically change the properties of the lipid when in a membrane. The double bond will cause a kink in the acyl chain which occupies more space and reduces the strength of the interlipid interactions. It would make sense that the cell would want to increase the rigidity of the membrane by reducing the number of unsaturated bonds in its lipids. This would counteract the fluidising effect of the butanol ingress. It appears from the data that this does not occur and that an increase in unsaturation is seen. Some studies have also seen this phenomenon whereby the unsaturation proportion in *Clostridia* increases in higher butanol levels (Kolek *et al.*, 2015). This is in contrast to many studies which show the more predictable decrease in saturation (Vollherbst Schneck *et al.*, 1984; Venkataramanan *et al.*, 2014). The membrane is complex and different composition may ultimately lead to the same properties. However, in this case, it has been noted that a discrepancy in unsaturation appears to arise due to a difference in methodology. The addition of butanol into the medium of growing cells elicits a stronger more shock-like response where results increased saturation of the lipids (Kolek *et al.*, 2015). Conversely when cells are grown in conditions which allow them to produce endogenous butanol a slower response is seen with increased unsaturation. The large change in environmental stressors (e.g. spiking in 1 % butanol) versus a more long-term change in environment that may be responsible for this difference (Kolek *et al.*, 2015). It remains unclear exactly why the cell increases the degree of unsaturation in the membrane in response to increasing butanol levels throughout fermentation. It is possible that there is a concurrent increase in membrane protein expression during butanol stress occurs. These proteins may require the presence of unsaturated lipids for their optimal structure and function. This would then require the cell to increase the amount of unsaturation in line with the increase membrane protein production. Furthermore, a more fluid membrane allows for easier lateral movement of the protein which may aid a better distribution in the membrane (e.g. a butanol transporter could more easily translocate to a localised site of high butanol concentrations).

The occurrence of a large number of plasmalogen species is telling of *Clostridial* membranes (Patakova *et al.*, 2021). A decrease in plasmalogen containing species was seen in both lipidomics experiments (Figure 4.5 and 4.10). This is interesting as it has been suggested that plasmalogens are important for the response to butanol damage and that they have also been upregulated Kolek *et al.*, (2015). Molecular dynamic simulations have shown the plasmany-PE membrane to be more rigid and thicker, and that the vinyl-ether linkage leads to increased chain order (Rog and Koivuniemi, 2016). It would be sensible to assume that a greater presence of plasmalogens in the membrane would help to counteract the fluidisation of butanol although there appears to only be a small effect when plasmany-PE was spiked into a model membrane (6 POPE: 2 POPG :1 PE-plasm). The membrane fluidity was found to be lower with plasmalogens than the control (3 POPE: 1 POPG) and there was a limited decrease in permeability to CF dye at > 30 mg/ml butanol, suggesting a small protective effect. This butanol concentration was above the biologically relevant range. However, experiments using a greater portion of plasmalogen species, which may have better mimicked the state in the cell, were not trialled. Furthermore, having several models of different plasmalogen content would have been interesting to trial too, however this was limited by the COVID-19 pandemic. It is important to note that increasing membrane rigidity may be an overly simple explanation of the response to butanol. As previously discussed above, some changes to the unsaturation proportion seen would lead to more membrane fluidity, a seemingly counterintuitive response. This would suggest that there are more layers to the response to butanol stress which may go beyond the simple properties of the membrane. Plasmalogens are thought to be protective against reactive oxygen species (Řezanka *et al.*, 2012). They are degraded by ROS and thus may provide protection against any ROS generated in ABE fermentation. Thus, it may be that the reduction seen in their abundance is due to them being degraded following ROS stress in fermentation. Work from Kolek and others (2015) recorded fatty acid content of *C. pasteurianum* (*C. beijerinckii* NRRL B-598) throughout fermentation and noted the higher concentration of plasmalogens coincided with the highest butanol productivity. As speculation it may be that the cells are producing more plasmalogens to protect against the increasing butanol (or precursors / products produced

alongside butanol which may lead to ROS). Interestingly, the amount of plasmalogens decreased in later fermentation, a similar trend to what is seen with the two mass spectrometry experiments in Chapter 4. It is less clear if oxidative damage exists in *Clostridia* due to them being anaerobic. However, it has been suggested that ROS are generated in the solventogenic phase of *C. acetobutylicum* (DSM 1731) (Han *et al.*, 2013), possibly through the oxygen containing products of ABE fermentation. Furthermore the feedstock can contain inhibitors which can contribute to ROS accumulation (Liao *et al.*, 2019). Because the exact function of plasmalogen lipids and their relationship with ROS is unclear, it is difficult to account for differences in the trend of plasmalogen species with butanol concentration when comparing with the literature. Further work is required to elucidate the role of plasmalogens which may help shed light on whether they are structurally protective (increasing rigidity etc.) or whether they soak up ROS which could damage other cellular macromolecules. Ultimately it is clear that they play some role in the butanol stress response and may represent a key molecular target in the future when a deeper understanding is developed.

7.3.1 Limitations of these data sets

When looking at the mass spectrometry and TLC data in Chapter 4, there were some disagreements between the data sets. Levels of PE species decreased in both mass spectrometry experiments, however no significant changes were observed in TLC. This may be due to the fact that POPE was used as the sole representative of PE species in TLC. Whilst palmitoyl and oleoyl are common fatty acids making POPE a common individual lipid species, it is possible that the decreases seen in both mass spectrometry experiments were due to a reduction in abundance of other PE containing species (i.e. not specifically POPE) which may not have been reflected in the TLC quantification. Discrepancies between the relative amounts of specific lipid species seen with TLC and lipidomics may be due to differences in methodologies used in identification. For example, in the TLC experiments the use of specific lipids such as POPG were required as standards to compare migration distance. This, however, only allows for the assumed identification of POPG and not all PG containing lipids - those containing different fatty acids

may interact differently with the TLC plate and may therefore migrate differently. This is in contrast to the lipidomics data which was able to assess the lipid classes as a whole. Hence, mass spectrometry and TLC should be used together (Tuzimski and Sherma, 2016). The lipid specific nature of TLC may therefore also explain the differences seen between the amounts of triglycerides (TG) seen in mass spec and the triacylglycerols (TAG) seen in TLC. The standard used in TLC was TAG which would have contained species with the same fatty acid constituents. Thus, only those TAG species that would interact with the plate in the same way as the standard (those with the same structure as the standard) could be identified in the time course samples, whereas the mass spectrometry identification may have been able to identify triglycerides with different fatty acids. It is possible that the TAGs seen in lipidomics are also present in some capacity on the TLC plates, however they may have migrated differently than the TAG standard used because of the potential difference in fatty acid constituents. Despite this, these two data sets can be used together to make more informed analyses of lipid changes.

7.4 How does butanol transverse the membrane?

It is through a currently unknown mechanism that butanol is able to transverse the membrane of *Clostridia*. The molecular dynamic simulations (Figure 3.13) showed that butanol molecules were unable to diffuse through the hydrophobic core of the membrane. *Pseudomonas putida* TtgB is the only native transporter of butanol (See 1.6.6 Engineering targets in this work, (Basler *et al.* 2018)) known. *Clostridial* *ttgB* was mined from the *C. saccharoperbutylacetonicum* N 1-4 (HMT) genome and was used to create constructs for CLEAVE™ genome editing. The genetically modified strains produced using CLEAVE™ technology were used in a small-scale bottle screen. This was done to investigate the effect of these genetic changes on the cell's growth and metabolite production. As described in the results section (3.2), the +TtgB strain appeared to grow better than the WT and had a significantly higher OD₆₀₀ at 6 h. Whilst +TtgB was still higher at 24 h there was no significant difference seen between the OD₆₀₀ of +TtgB and of the WT. This may suggest an that TtgB provides a benefit to the survival of the cells earlier in fermentation, and that at later time point this difference in survival is lessened. Perhaps it is the case

that TtgB can transport butanol and is most effective when butanol levels are lower, due to protein mediated transport being faster than diffusion at lower concentration. Transporting butanol from the cytoplasm out into the bulk solvent would mean that these butanol molecules could diffuse into the bulk solvent and would not be trapped in the cell where they would always be in close proximity to the cellular membrane. However, later in the fermentation the concentrations of butanol in the bulk solvent may be high enough that butanol molecules will be close to the outer leaflet of the membrane. This would mean that the transport of butanol across the membrane would have a reduced effect as the butanol concentration in the external environment increases. This may be reflected in the OD₆₀₀ difference between +TtgB and WT becoming smaller as the fermentation progresses. To circumvent this, the fermentation of these strains could be combined with *in situ* product recovery. This would essentially enable the maintenance of a butanol concentration gradient away from the cells into the bulk solvent (due to the continuous removal of the butanol from the growth culture), allowing for the transport by +TtgB operate at maximum efficiency. Based on this it is likely that TtgB provided some benefit in terms of an increased tolerance to butanol, or at least an increased growth rate. It remains unclear whether it is the efflux of butanol which accounts for this difference. It may be that the TtgB is involved in the movement of another metabolite and that this is the reason for the improved growth. It would prove useful to carry out transport assays to investigate the ability for TtgB to transport other ABE products as well as butanol, such as those done by Basler and colleagues (2018). Furthermore, producing a Δ TtgB strain would also help to shed light on the function and importance of TtgB.

Developing a model of membrane proteins is important due to the relationship between their structure and function. Synthesising an *in silico* model using homology modelling can be vital when no experimental model exists, as it the case with TtgB. Having a good model can shed light on the roles of these proteins in specific biological phenomenon and can additionally provide an aid to future experimental design. The *Clostridial* TtgB sequence mined from the *C. saccharoperbutylacetonicum* N 1-4 (HMT) genome was used in conjunction with similar membrane protein structures and SWISS-

MODEL to generate a series of homology models. A trimeric TtgB model was generated using AcrB as a template, showing good GMQE and QMEAN scores, of 0.68 and -2.59, respectively, suggesting an acceptable model. This may also suggest a degree of similarity between TtgB and AcrB. Based on this, it may prove useful to investigate the mechanism of AcrB to shed light on TtgB's mechanism of substrate translocation (See Figure 7.2). With AcrB, substrate pathways were initially thought to go through the

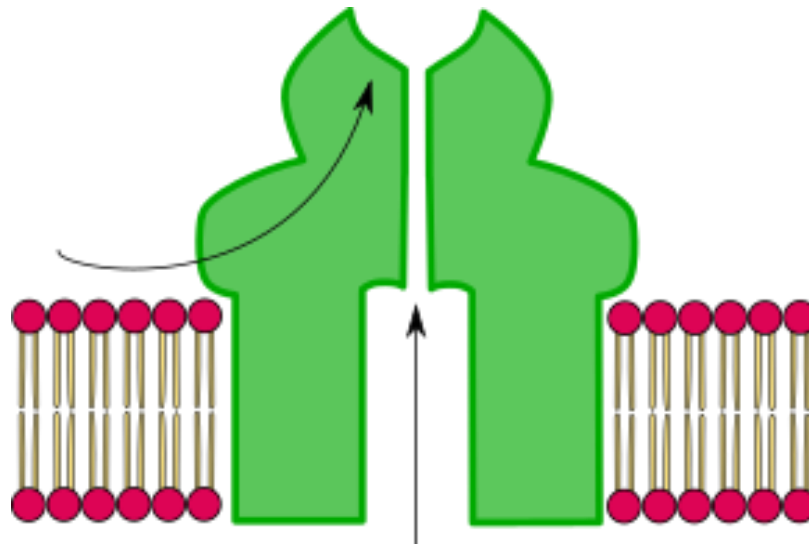


Figure 7.2 Diagram of possible substrate paths through TtgB. The conventional pathway (top left arrow) is taken from the mechanism of AcrB, where substrates in the periplasm bind and are transported through AcrA and TolC into the surrounding medium. *Clostridia* are Gram positive and do not possess a periplasm, therefore, the conventional pathway may not be useful in butanol transport. The second pathway (central pathway) is speculative where substrates move from the cytoplasm through a central pore. This would prove more beneficial as butanol is produced in the cytoplasm.

central pore however, it has been suggested that substrates move through identified channels in each monomer (Sennhauser *et al.*, 2006). This work shows the presence of channels in each monomeric AcrB subunit above the transmembrane helical regions, suggesting substrate recruitment in the periplasmic domain (in Gram-negatives). As *Clostridia* is a Gram-positive bacterium and therefore do not possess a periplasm (due to the presence of a single membrane only), it may be the case that butanol efflux by this route impossible as this would already be in the extracellular region. Perhaps it is possible that because the entrance for these channels is in close proximity to the membrane, they could therefore simply to remove butanol from the bulk solvent-membrane interface which would prevent it from inserting into the membrane in those regions. Furthermore, it is unclear whether there are other

transport mechanism occurring through the central pore of the trimer and also it is unknown how the differences in TtgB's sequence will impact substrate transport. For AcrB it may be the case that the central cavity and vestibule plays a role in the translocation of some substrates (Husain *et al.*, 2011). It has been seen that MexB, an RND transporter similar to AcrB found in *L. lactis* (Gram-positive), was able to export ethidium bromide, suggesting a role of the central pore in substrate movement (Welch *et al.*, 2010). MexB showed promiscuity being able to form a functional complex with AcrA and TolC from *E. coli* and forms the same substrate profile as MexAB-OprM, possibly suggesting a role of MexB in substrate specificity. Additionally, when expressed alone MexB was able to transport ethidium bromide (Welch *et al.*, 2010). It still remains unclear whether the central pore of TtgB (which would create a channel from the cytosol to the extracellular regions of the cell) allows for the translocation of butanol. The further investigation of potential channels in TtgB other than the central pore would be an interesting piece of future work. The model generated could be used in molecular dynamic simulations using all-atom models. This would provide information regarding the binding and potentially the translocation of putative substrates, such as butanol. Additionally, software tools such as CAVER (Jurcik *et al.*, 2018) can be implemented which enables the identification of channels and tunnels in protein structures. This could be useful in developing understanding surrounding possible channels that butanol molecules may be able to pass through. Further, there would be implications for engineering as the certain residues (those involved with substrate binding or translocation) could be mutated in order to further increase butanol flux, with the possibility of ultimately designing bespoke channels. This would make a good complement to an experimental structure of the TtgB-like protein and may also help to elucidate some mechanistic features.

Interestingly, when analysing the original TtgB trimeric model (AcrB as a template) using QMEANBrane the lowest quality regions (those regions where the software is less able to rely on the template) were found to be the end of the helices and some internal loops (Figure 6.2), where orange regions are of lower quality). This low quality may stem from differences between the TtgB sequence and structure of

the AcrB template used to generate the trimeric homology model. This in turn could lead to a difference in substrate specificity, as both the central pore and regions above the transmembrane domains may be involved in substrate movement (Sennhauser *et al.*, 2006). This would also explain why mutated AcrB is able to move butanol across the membrane, but WT AcrB is not (Fisher *et al.*, 2014). It may be that only relatively small changes in the sequence / structure are required to enable movement of butanol as a substrate in AcrB. Interestingly, when Basler and colleagues (2018) applied the same point mutations (M355L, I466, S880P) to *P. putida* TtgB that knocked in butanol activity in AcrB (Fisher *et al.*, 2014), there was found to be a reduction in survival. This could suggest a difference in structure or that the natural specificity of TtgB for butanol is higher than that of the mutated AcrB, and that introducing these mutations cannot lead to anymore gain of function. These residues are all found in the transmembrane helices of AcrB and are thought to impact the conformational changes of the protein. Residue 466 lines the central cavity and thus may be involved with the alcohol interactions. The introduction of a large residue (phenylalanine) at this point may impact the conformational change of the protein. Additionally S880P, may also impact conformational change as proline is known to disrupt helices (Nilsson *et al.*, 1998). The M355L mutation has been suggested to cause a shift in packing and helix arrangement, one that may be large enough to allow substrates to enter into the central pore from the cytoplasm. In combination these mutations did not lead to butanol tolerance, the phenotype of AcrB which did enable butanol movement and therefore, tolerance may already exist in TtgB.

Aside from active transport, it may be that butanol transverses the membrane via a facilitated transport mechanism through GlpF. GlpF was overexpressed in *E. coli* BL21 and the effect of this on growth (measured as OD₆₀₀) in several stressors was recorded. GlpF appeared to have a small benefit to cells when exposed to a low amount of exogenous butanol (5 mg/ml). It is not clear exactly through what mechanism the growth advantage is occurring as this benefit was also seen in culture with no exogenous butanol, suggesting that it is not specific to butanol. To investigate this further, other stressors which may have been mitigate by GlpF expression were also investigated, concentrations of stressors was

based on previous studies (Hosein *et al.*, 2011; Wu *et al.*, 2014; Guo *et al.*, 2017). Firstly, ethanol was tested to see whether the apparent benefit was as a result of general alcohol tolerance. The expression of GlpF appeared to have no benefit on growth in 20 mg/ml ethanol suggesting that it may not have a role in facilitating ethanol flux. This may be because the ethanol was exogenous which would mitigate the benefit of movement through GlpF (although ethanol is able to diffuse through the membrane more readily than butanol and thus may not benefit as much from a transporter / channel). Like butanol, the exact membrane proteins responsible for ethanol transport remain elusive (Kell *et al.*, 2015). Pdr18, a yeast ABC transporter involved in multidrug resistance has been shown to increase ethanol tolerance and production when overexpressed in *S. cerevisiae* (Teixeira *et al.*, 2012). Additionally in yeast, Fps1 an aquaglyceroporin with a similar role to GlpF in bacteria may also be involved (Kell *et al.*, 2015). Secondly, cells were grown in NaCl to elucidate any role that GlpF may have in mitigating osmotic stress. Based on the ability of GlpF to facilitate the flux of water, there was increased potential for this mechanism to be responsible for the increase in growth. Despite this, there was found to be no significant difference in growth between expressing and control strains in 25 mg/ml NaCl. The growth of both strains was inhibited by the addition of NaCl to the media, and the extent of inhibition appeared to be the same for both strains. This would suggest that GlpF overexpression has no benefit to growth in inhibitory concentrations of NaCl. It may have been the case that the benefit pertained to the increased ability to scavenge glycerol, for use as a carbon source or in other metabolic pathways such as phospholipid synthesis. Whilst this explanation may make sense in a more dynamic system, the above experiments in *E. coli* were conducted in LB media which does not contain glycerol. However, there may be other components which can utilise GlpF as a channel other than glycerol. Using molecular dynamics, Hub and De Groot (2008) have shown GlpF to have a lower free energy barrier than POPE and POPC for NH₃, H₂O, glycerol and urea (although this was by a small amount). As exogenous butanol was added and GlpF is a facilitator (passive) it would be unlikely that this passive transport of butanol would be beneficial in this situation. GlpF would only be useful as a butanol facilitator if there was a higher concentration of butanol inside the cell e.g. during fermentation. This again means that the increase

growth seen in *E. coli* was not due to the movement of butanol away from but from another function. Perhaps other toxic metabolites produced during growth can move through GlpF pores and away from the cell, thus reducing their associated toxicities. Ultimately, these experiments should be repeated in *Clostridia* to investigate endogenous butanol in the correct membrane environment. CLEAVE™ constructs were produced, however could not be tested due to COVID-19.

7.5 Alternative strategies

As briefly mentioned previously there are other avenue through which the efficiency of the ABE fermentative process can be improved. which do not necessarily concern the generation of a more robust strain. These include upstream (feedstock selection pretreatment and detoxification) and downstream (product recovery) operations, as well as processes relating to the fermentation set up.

As discussed in the introduction (1.6.1 Non-engineering strategies) there may be increasing competition between fuel crops and food crops, either through the utilisation of food crops as feedstock in fermentation or through competition for limited land. The use of lignocellulose (waste biomass) circumvents this issue but it requires harsh pretreatment before it is suitable for use as a feedstock. Pretreatment can describe a range of enzymatic, chemical and physical methods to obtain the fermentable sugars. It is often the case that several of these different methods are combined, however a small change in operating conditions may have a significant effect on the sugar concentration and composition, and the amount of inhibitory compounds produced. This could then have a negative impact on the subsequent enzymatic hydrolysis and thus the cost of the substrate. These are important considerations and for optimisation, particularly if non-food crop feedstocks become more popular as a consequence of increased commercial interest in ABE fermentation (Birgen *et al.*, 2019). Pretreatment can lead to the production of inhibitory compounds including acids such as methanoic acid which can cause an acid crash in the *Clostridia* (Maddox *et al.*, 2000). Additionally, some of these products may inhibit further enzymatic pretreatment. Methods such as dialysis or solid-phase extraction / activated carbon are used to detoxify these inhibitory compounds. Developing pretreatment protocols which do

not produce these inhibitory compounds (e.g. by conducting at a lower temperature) is desirable (Birgen *et al.*, 2019). Alternatively, some co-culturing methods have been developed (see introduction) whereby a second bacterial species is able to replace an economically costly hydrolysis reaction, conventionally completed chemical / enzymatic means. However, coculturing may increase the risk of contamination. Developing new means of reducing contamination would increase the viability of co-culturing as well as the use of longer-scale fermentations both of which carry a higher risk of contamination than single species batch cultures. Adding a divalent cation chelator could potential reduce phage infection (Yamamoto *et al.*, 1968; Li *et al.*, 2020).

The fermentation itself can also be optimised. This can be through the addition of exogenous additives to mitigate product inhibition or to improve the physiological elements of the fermenting cells. This may include the addition of surfactants to form micelles, trapping butanol molecules inside (Li *et al.*, 2020). Additives may also reduce the toxicity (see section 3.3.4 Addition of exogenous membrane active compounds: SSAs and references therein), however the scalability of these with increasing fermentation volumes may be an issue. Recently, the carotenoids lutein and zeaxanthin have been shown to reduce membrane fluidity and butanol penetration in the membrane of *E. coli* cells by 62% and 38%, respectively (Chia *et al.*, 2021). Furthermore, this group have a suggested using tomato pomace (waste with no commercial value) which would act as both feedstock and a source of carotenoids. This could solve the scalability issue and represents a promising avenue of research. Further studies into compounds with a similar stabilising effect would be interesting to peruse. For example, the membrane-active compounds from the University of Kent shown in the first chapter may require further investigations. However, the addition of exogenous membranes stabilising compounds not produced in a similar way to the carotenoid example above may have a limited application. Whilst they may offer a more tuneable means engineer membrane tolerance compared with genetic approaches, there will be an increasing demand for the compound as the fermentation volumes are scaled up. Depending on the source of the additive, this could incur a great cost to the process and make it less viable. Hence, it is

also important to simultaneously continue with genetic based approaches which will not have this problem.

Several product recovery methodologies exist each, including pervaporation (Azimi *et al.*, 2019), liquid-liquid extraction (LLE), gas stripping and adsorption, each of which having their own advantages and disadvantages (see (Kujawska *et al.*, 2015; Friedl, 2016; Azimi *et al.*, 2019)). Whilst both offering high selectivity, the membranes used in pervaporation and the solid phases used in adsorption can be expensive. LLE also offers high selectivity but may be toxic to the microorganisms and whilst gas stripping is not toxic to the cells it offers low extraction efficiency and specificity. The ideal product recovery system may contain several different methods together. To improve this process, research into a non-toxic liquid extractant, cheaper pervaporation membranes, reusable solid-phases or more complex gas stripping protocols (to increase selectivity) needs to be carried out.

Reducing the generation of inhibitory compounds in feedstock pretreatment and product toxicity will enable a higher cell density to be achieved during fermentation, resulting in more butanol being produced. Whilst this damage can be mitigated with *in situ* product removal, the costs of this may scale with increasing fermentation sizes. Thus, it is paramount to engineer more tolerant strains to reduce somewhat the intensity (and therefore costs) of *in situ* recovery. Improving the above features of ABE fermentation will help to reduce the costs associated with upstream and downstream operations. Combined with the development of robust cell factories the competitiveness of this route of butanol production will increase and will become more viable.

8. Future work and conclusions

8.1 Future work

Whilst this project achieved most of the aims set out in Figures 1.10, 3.1, 4.1 and 5.1, the advent of the COVID-19 pandemic prevented some experiments from being carried out. Therefore, there were a number of future works which would have augmented this study. Firstly, investigating more potentially membrane active compounds that could be used as a fermentative additive to mitigate the damage of butanol, and additionally completing a more thorough investigation into the SSAs from the University of Kent. This will provide a better understanding of how to mitigate butanol membrane perturbations. Developing a more detailed molecular modelling system of the membrane using an all-atom model would be of value. This could be augmented by experimental data concerning the spatial binding / interaction of butanol within the membrane, which could be obtained using FTIR-ATR and particle scattering techniques (such as neutron reflectometry). Method development for assessing the phase transition temperature of various lipid model following butanol exposure was in progress before COVID-19 and would be interesting to finish. Redoing the steric trapping experiments but placing the bR in a SMALP (styrene-maleic acid lipid particle) as opposed to a bicelles may enable a more specific understanding of butanol's interaction with membrane proteins. SMALPs have been used previously as scaffold for investigating membrane protein structure and function (Postis *et al.*, 2015). It may be that the SMALP provides a more stability to the lipid portion of the membrane (due to the imposed lateral pressure of the SMA's overall structure) reducing the possible indirect effect of membrane fluidisation on the folding of the bR. Styrene maleic acid (SMA) is a co-polymers which can insert into the membrane and forms disc-like structures containing phospholipids and membrane proteins within it. The SMA polymer surrounds this portion of membrane forming a stable nanoparticle (Pollock *et al.*, 2018).

It would be interesting to investigate further the importance of PG lipids and related cardiolipin. Previously cardiolipin (CL) has been reported to be a major component of the *C. saccharoperbutylacetonicum* membranes (Durre, 2005). Whilst standards were not included in the TLC

analysis, lipidomic analysis shows levels of CL were higher in the high butanol environment than in the low butanol environment suggesting a potential involvement of this lipid too. This is likely based on the similarities between the structures of PG and CL (CL is formed by the condensation of two PG molecules and contains four acyl chains with one glycerol headgroup). It is unclear whether PG and CL comigrate in the solvent system used. It would be interesting to trial different solvent systems using a CL standard to investigate this further. Future TLC could be done using a CL standard PG and CL are both negatively charged lipids and likely have a similar effect on membrane properties because of this. Therefore, it could be assumed that they act in a similar way and are both protective against butanol.

The role of CL in other stressors has been examined. It has been suggested that CL can stabilise the membrane in response to compounds that induce fluidisation and acyl chain disorder such as toluene (Murínová and Dercová, 2014). Toluene increases the acyl chain area to which the cell can respond by increasing the amount of CL in its membrane at the expense of PE. This effectively increases the headgroup volume as CL has a larger headgroup volume than PE and can therefore compensate for the increase in acyl chain volume. A reduction in CL content in *P. putida* was found to lead to a decrease in survival after toluene exposure (Bernal *et al.*, 2007). Osmotic stress in *E. coli* also leads to increased CL, constant PG, and reduced PE. The bacteria's survival may be linked to an increase in the ratio of anionic to zwitterionic lipids in the membrane (Romantsov *et al.*, 2009). CL clearly plays some role in the stress response of membrane in bacteria; therefore, it is interesting that no CL was detected in the second round of mass spectrometry experiment. This is likely due to the mass range being 250-1250 Da for these experiments when CL is generally larger than this (as it contains four acyl chains, instead of the normal two acyl chains). As alluded to earlier, further experiments could use a more targeted method in order to quantify CL changes in different butanol environments. The ingress of butanol into the membrane may reduce charge density by increasing the area per lipid. The increased amount of anionic headgroups can counter this. Guo and colleagues (2020) report that a lower outer membrane charge density is more likely to allow for more butanol assimilation, suggesting a link between greater charge density

and reduced butanol integration. Additionally, PE is a non-bilayer forming lipids (based on the shape of PE). A reduction in the portion of these types of lipids in favour of bilayer forming lipids e.g. PC and PG (Dowhan *et al.*, 2016), would improve bilayer stability with increasing solvent concentrations. PG lipids would likely be the choice as PC lipids are absent or in very low concentrations in *Clostridial* membranes. CL also likely plays a role in membrane curvature, localising at highly curved regions of the membrane (Beltrán-Heredia *et al.*, 2019), however the importance of this for butanol toxicity is unclear. Perhaps CL may be important in this regard if butanol impact the membrane curvature. Thus, based on the above data, having more PG lipids in the membrane yields a more resistant state of the membrane. This change is also seen *in vivo* where cells increase the amount of PG and CL.

A more targeted lipidomic approach to investigate the changes in the fatty acids of the phospholipids would be of interest. Particularly those which have proved difficult to detect accurately, for example cyclopropanation and accurate identification of acyl fatty acids. Cyclopropanation is a methylation modification made to unsaturated bonds via cyclopropane fatty acid synthase (CFA) encoded by the CFA gene (*cfa*). This results in a cyclic alkane moiety comprised of two carbons from the original acyl chain and the additional carbon from the methylation reaction (Grogan and Cronan, 1997). Cyclopropanation of double bonds may also mediate protection against butanol stress as they are thought to reduce membrane fluidity (To *et al.*, 2011) and relative proportions of CFA in the membrane has increased upon exposure to butanol (Vollherbst Schneck *et al.*, 1984). A *cfaB* knockout in *P. putida* DOE-T1E resulted in greater solvent sensitivity compared to wild type (Pini *et al.*, 2009). Zhao and colleagues (2003) overexpressed the cyclopropane fatty acid (CFA) synthase gene in *C. acetobutylicum* and yielded resistance to butanol, however solvent production was impaired, suggesting a relationship between CFA and solventogenesis which may be responsible for the perceived increase in resistance. The replacement of unsaturated bond with CFA may make membranes more stable through promoting higher membrane order by limiting the rotations around the cyclopropane functional group (Poger and Mark, 2015). Patakova and others (2019) found *C. beijerinckii* *cfa* expression to be upregulated during

fermentation when butanol was clearly detectable, potentially suggesting a regulatory relationship between butanol and CFA synthase expression. Later work by the same group also showed *cfa* to be upregulated 30 minutes after the addition of butanol (Patakova *et al.*, 2021). It has been indicated that the role of cyclopropanation is dual actioned – there is an increase in order of the acyl chains (cyclopropane FAs are more ordered than their unsaturated counterparts) whilst an overall increase in membrane fluidity is seen (due to interference with lipid packing) (Poger and Mark, 2015). Due to the lack of appropriate standards and sufficient fragmentation data the prevalence of cyclopropanation could not be determined. Again, this may require a more targeted methodology in order to accurately gauge. The molecular weight of cyclopropane moiety would be the same as an unmodified acyl chain with an additional carbon. For example pentene has the formula C₅H₁₀ (CH₃CH=CHCH₂CH₃), which would be the same as a butane chain with a cyclopropane addition (CH₃CH(CH₂)CHCH₃). This could potentially lead to difficulty in differentiation between CFA and unsaturated acyl chains when using untargeted mass spectrometry and may also have caused some cyclopropanated acyl chains to be misidentified as unsaturated bonds. It would be interesting to trial techniques such as transesterified gas chromatography coupled to a mass spectrometer. This would remove the fatty acids from the rest of the lipids forming fatty acid methyl esters (FAME), enabling a more specific analysis of the fatty acid composition.

Finally, the further characterisation of the currently CLEAVE™ strains and their fermentations is of interest. In addition to this, the production of more strains such as Δ GlpF and +GlpF, Δ PgsA and +PgsA and Δ TtgB mutants in *C. saccharoperbutylacetonicum* N 1-4 (HMT) would be of interest in understanding the response to butanol more, and to developing more protective phenotypes.

8.2 Conclusions

In conclusion, butanol is a high-value chemical with promising applications as a biofuel as well as broad-use industrially relevant platform chemical. The upscaling of butanol production via the more sustainable cell factory route is plagued by the associated product toxicity from ABE fermentation, with

butanol constituting to the majority of this toxicity. Due to this the generation of butanol using this method is economically costly and, despite growing international interest in this technology, remains to realise its full potential. There are many parts to the fermentation process which can be improved, such as feedstock optimisation and downstream processing and product recovery. The most important, however, is the generation of a highly robust and tolerant strain to be used in fermentation as this still remains a major bottleneck. In order for this to come to fruition, a deeper understanding of butanol's interaction with the membrane, and how the cells react to rising butanol levels is needed. There have been several previous studies which have investigated the stress response of many types of bacteria to exogenous and endogenous butanol, both in terms of transcriptomics and metabolomics. Additionally, there are many studies which have aimed to engineer more productive and tolerant strains with this knowledge. This work aimed to increase the understanding surrounding butanol's interaction with the membrane, pertaining to the phospholipids and the membrane proteins therein.

Firstly, using liposomes as *in vitro* model membranes, the effects of butanol on the membrane were investigated using a range of spectroscopic techniques. It was found that exposure to butanol led to membrane fluidisation, swelling and an increase in permeabilisation, along with a reduction in integrity and force resistance. Compositional variations in the phospholipids of the membrane were investigated to try and obtain lipid phenotype that would provide more protection. It was seen that increasing the portion of some species that reduce membrane fluidity made liposomes less permeable. This included increasing the fatty acid chain length and altering the proportion of different geometric isomers of unsaturated bonds. Increasing the portion of POPG, an anionic lipid seemed to reduce liposome permeability too. It should be noted that some species which increased the rigidity of the membrane appeared to have no impact on the associated toxicity of butanol. Furthermore, butanol was found to cause membrane protein unfolding in bicelles. The aims for this Chapter set out in Figure 1.7 and 3.1 were largely met. A deeper and more holistic understanding of how butanol perturbs membrane properties and functions has been generated.

A combination of thin layer chromatography and lipidomics were employed to investigate the changes that *Clostridium saccharoperbutylacetonicum* N 1-4 (HMT) undergo throughout fermentation. Total lipids were extracted from cell mass using a modified Bligh Dyer extraction method. Levels of oleic acid and POPG were significantly higher in later time points of fermentation. Lipidomics revealed a reduction in PE lipids and an increase in PG lipids, consistent with TLC. There were some discrepancies between TLC and lipidomics, possibly due to different methodologies. It is clear that the cells undergo a shift in membrane composition following increasing butanol concentrations in fermentation. The aims for Chapter 4 set out in Figure 1.7 and 4.1 were mostly met through and have shed light on how the lipidome of solventogenic *Clostridia* changes throughout fermentation. However, more targeted lipidomic analysis is needed for a complete understanding. This would represent the first analysis of the whole lipidome of *C. saccharoperbutylacetonicum* N 1-4 (HMT) throughout fermentation. These data provide understanding as to how the cells respond to rising butanol levels and will be of use in future engineering endeavours.

Chapter 6 of this thesis pertained to the culmination of previous experiments to generate a more tolerant and highly producing strain. This involved selecting some protein targets for genetic engineering and these include an enzyme, PssA involved in lipid biosynthesis, and two membrane proteins: a transporter, TtgB and a channel, GlpF. GlpF showed a non-butanol specific increase to *E. coli* growth rate, potentially suggesting an unrelated mechanism of action. The transporter TtgB was overexpressed and showed a significant increase in growth rate in early portions of the fermentation. PssA was overexpressed and knocked out using CLEAVE™. There was no discernible impact of overexpression and knocking out PssA appeared to significantly reduce the viability of the cells in the later stages of fermentation. It would be interesting to see the changes in the lipid composition between the Δ PssA, +PssA and WT and see if there is any correlation with the response to butanol. Also, how these changes impact the structure and function of membrane proteins found to be important in the butanol stress response. Creating a Δ TtgB would help to solidify the role of this transporter in enabling

a higher growth rate in a butanol-specific mechanism. Ultimately the aims of Chapter 6 set out in Figures 1.7 and 5.1 were not met entirely. Some genetically engineered strains were produced, however due to the COVID-19 pandemic, their characterisation was limited in its scope. At time of writing, no other work has attempted to modify the lipidome of *C. saccharoperbutylacetonicum* N 1-4 (HMT) in order to improve tolerance to butanol. Additionally, there have been no butanol transporters / channels native to *C. saccharoperbutylacetonicum* N 1-4 (HMT) identified.

Collectively, the work in this thesis has enabled a more detailed understanding as to how butanol negatively impacts the cellular membrane and its constituents. Further the response of the cell in terms of its lipidomic changes has also been elucidated to a certain degree. Finally, industrially relevant strains have been genetically engineered with the aim of obtaining a highly producing strain. There are still more questions to be answered regarding the ideas explored in the above work. However, this work provides insights into product toxicity and rationale metabolomic engineering strategies which will be valuable in the development of the ABE process as a whole. When combined with improved feedstock utilisation (e.g. lignocellulose and non-food crops) and processing (*in situ* recovery), the economic feasibility of this process can be greatly improved such that it can rival conventional means and reduce the dependence on non-renewable fossil fuel based methods.

References

- Abd-Alla, M.H. and Elsadek El-Enany, A.W. (2012) Production of acetone-butanol-ethanol from spoilage date palm (*Phoenix dactylifera* L.) fruits by mixed culture of *Clostridium acetobutylicum* and *Bacillus subtilis* *Biomass and Bioenergy*, 42 172–178.
- Abdelaal, A.S., Ageez, A.M., Abd El-Hadi, A.E.H.A., and Abdallah, N.A. (2015) Genetic improvement of n-butanol tolerance in *Escherichia coli* by heterologous overexpression of *groESL* operon from *Clostridium acetobutylicum* *3 Biotech*, 5(4) 401–410.
- Agu, C.V., Lai, S.M., Ujor, V., Biswas, P.K., Jones, A., Gopalan, V., and Ezeji, T.C. (2018) Development of a high-throughput assay for rapid screening of butanologenic strains *Scientific Reports*, 8(1) 3379.
- Allen, N., White, L.J., Boles, J.E., Williams, G.T., Chu, D.F., Ellaby, R.J., Shepherd, H.J., Ng, K.K.L., Blackholly, L.R., Wilson, B., Mulvihill, D.P., and Hiscock, J.R. (2020) Towards the Prediction of Antimicrobial Efficacy for Hydrogen Bonded, Self-Associating Amphiphiles *ChemMedChem*, 15(22) 2193–2205.
- Alsaker, K. V., Paredes, C., and Papoutsakis, E.T. (2010) Metabolite stress and tolerance in the production of biofuels and chemicals: Gene-expression-based systems analysis of butanol, butyrate, and acetate stresses in the anaerobe *Clostridium acetobutylicum* *Biotechnology and Bioengineering*, 105(6) 1131–1147.
- Antizar-Ladislao, B. and Turrion-Gomez, J.L. (2008) Second-generation biofuels and local bioenergy systems *Biofuels, Bioproducts and Biorefining*.
- Appala, K., Bimpeh, K., Freeman, C., and Hines, K.M. (2020) Recent applications of mass spectrometry in bacterial lipidomics *Analytical and Bioanalytical Chemistry*, 412(24) 5935–5943.
- Atmadjaja, A.N., Holby, V., Harding, A.J., Krabben, P., Smith, H.K., and Jenkinson, E.R. (2019) CRISPR-Cas, a highly effective tool for genome editing in *Clostridium saccharoperbutylacetonicum* N1-4(HMT) *FEMS Microbiology Letters*, 366(6) 59.
- Atsumi, S., Wu, T.Y., MacHado, I.M.P., Huang, W.C., Chen, P.Y., Pellegrini, M., and Liao, J.C. (2010) Evolution, genomic analysis, and reconstruction of isobutanol tolerance in *Escherichia coli* *Molecular Systems*

Biology, 6 449.

- Azimi, H., Thibault, J., and Tezel, F.H. (2019) Separation of Butanol Using Pervaporation: A Review of Mass Transfer Models *Journal of Fluid Flow, Heat and Mass Transfer*.
- Baer, S.H., Blaschek, H.P., and Smith, T.L. (1987) Effect of Butanol Challenge and Temperature on Lipid Composition and Membrane Fluidity of Butanol-Tolerant *Clostridium acetobutylicum*. *Applied and environmental microbiology*, 53(12) 2854–61.
- Ballongue, J., Amine, J., Masion, E., Petitdemange, H., and Gay, R. (1985) Induction of acetoacetate decarboxylase in *Clostridium acetobutylicum* *FEMS Microbiology Letters*, 29(3) 273–277.
- Basler, G., Thompson, M., Tullman-Ercek, D., and Keasling, J. (2018) A *Pseudomonas putida* efflux pump acts on short-chain alcohols. *Biotechnology for Biofuels*, 11 136.
- Baumgarten, T. and Heipieper, H.J. (2016) Outer Membrane Vesicle Secretion: From Envelope Stress to Biofilm Formation *In: Stress and Environmental Regulation of Gene Expression and Adaptation in Bacteria*. Hoboken, NJ, USA: Wiley Blackwell, 1322–1327.
- Baumgarten, T., Sperling, S., Seifert, J., von Bergen, M., Steiniger, F., Wick, L.Y., and Heipieper, H.J. (2012) Membrane vesicle formation as a multiple-stress response mechanism enhances *pseudomonas putida* DOT-T1E cell surface hydrophobicity and biofilm formation *Applied and Environmental Microbiology*, 78(17) 6217–6224.
- Belin, B.J., Busset, N., Giraud, E., Molinaro, A., Silipo, A., and Newman, D.K. (2018) Hopanoid lipids: From membranes to plant-bacteria interactions *Nature Reviews Microbiology*.
- Bell, F.P. (1984) The Dynamic State of Membrane Lipids: The Significance of Lipid Exchange and Transfer Reactions to Biomembrane Composition, Structure, Function, and Cellular Lipid Metabolism *In: Membrane Fluidity*. Springer US, 543–562.
- Beltrán-Heredia, E., Tsai, F.C., Salinas-Almaguer, S., Cao, F.J., Bassereau, P., and Monroy, F. (2019) Membrane curvature induces cardiolipin sorting *Communications Biology*, 2(1) 1–7.
- Benkert, P., Biasini, M., and Schwede, T. (2011) Toward the estimation of the absolute quality of individual protein structure models *Bioinformatics*, 27(3) 343–350.

- Berezina, O. V., Brandt, A., Yarotsky, S., Schwarz, W.H., and Zverlov, V. V (2009) Isolation of a new butanol-producing Clostridium strain: High level of hemicellulosic activity and structure of solventogenesis genes of a new Clostridium saccharobutylicum isolate *Systematic and Applied Microbiology*, 32(7) 449–459.
- Bernal, P., Muñoz-Rojas, J., Hurtado, A., Ramos, J.L., and Segura, A. (2007) A Pseudomonas putida cardiolipin synthesis mutant exhibits increased sensitivity to drugs related to transport functionality *Environmental Microbiology*, 9(5) 1135–1145.
- Besada-Lombana, P.B., Fernandez-Moya, R., Fenster, J., and Da Silva, N.A. (2017) Engineering Saccharomyces cerevisiae fatty acid composition for increased tolerance to octanoic acid *Biotechnology and Bioengineering*, 114(7) 1531–1538.
- Bienert, S., Waterhouse, A., De Beer, T.A.P., Tauriello, G., Studer, G., Bordoli, L., and Schwede, T. (2017) The SWISS-MODEL Repository-new features and functionality *Nucleic Acids Research*, 45(D1) D313–D319.
- Bio-butanol Market Size | Industry Analysis Report, 2022 [online] (2020. Available from: <https://www.grandviewresearch.com/industry-analysis/bio-butanol-industry> [Accessed 27 Apr 2020].
- Birgen, C., Dürre, P., Preisig, H.A., and Wentzel, A. (2019) Butanol production from lignocellulosic biomass: Revisiting fermentation performance indicators with exploratory data analysis *Biotechnology for Biofuels*.
- Bligh, E.G. and Dyer, W.J. (1959) A RAPID METHOD OF TOTAL LIPID EXTRACTION AND PURIFICATION *Canadian Journal of Biochemistry and Physiology*, 37(8) 911–917.
- Bogdanov, M. and Dowhan, W. (1995) Phosphatidylethanolamine is required for in vivo function of the membrane-associated lactose permease of escherichia coli *Journal of Biological Chemistry*, 270(2) 732–739.
- Bogdanov, M., Dowhan, W., and Vitrac, H. (2014) Lipids and topological rules governing membrane protein assembly *Biochimica et Biophysica Acta - Molecular Cell Research*.
- Bothun, G.D., Boltz, L., Kurniawan, Y., and Scholz, C. (2016) Cooperative effects of fatty acids and n-butanol on lipid membrane phase behavior *Colloids and Surfaces B: Biointerfaces*, 139 62–67.

- Bowles, L. and Ellefson, W. (1985) Effects of Butanol on *Clostridium-Acetobutylicum* *Applied and Environmental Microbiology*, 50(5) 1165–1170.
- Bowring, S.N. and Morris, J.G. (1985) Mutagenesis of *Clostridium acetobutylicum* *Journal of Applied Bacteriology*, 58(6) 577–584.
- Braverman, N.E. and Moser, A.B. (2012) Functions of plasmalogen lipids in health and disease *Biochimica et Biophysica Acta - Molecular Basis of Disease*.
- Brenac, L., Baidoo, E.E.K., Keasling, J.D., and Budin, I. (2019) Distinct functional roles for hopanoid composition in the chemical tolerance of *Zymomonas mobilis* *Molecular Microbiology*, 112(5) 1564–1575.
- Bringer, S., Härtner, T., Poralla, K., and Sahm, H. (1985) Influence of ethanol on the hopanoid content and the fatty acid pattern in batch and continuous cultures of *Zymomonas mobilis* *Archives of Microbiology*, 140(4) 312–316.
- Brynildsen, M.P. and Liao, J.C. (2009) An integrated network approach identifies the isobutanol response network of *Escherichia coli* *Molecular Systems Biology*, 5 277.
- Canetta, E., Adya, A.K., and Walker, G.M. (2006) Atomic force microscopic study of the effects of ethanol on yeast cell surface morphology *FEMS Microbiology Letters*, 255(2) 308–315.
- Chakrabarti, N., Tajkhorshid, E., Roux, B., and Pomes, R. (2004) Molecular basis of proton blockage in aquaporins *Structure*, 12(1) 65–74.
- Chang, Y.-C. and Bowie, J.U. (2014) Measuring membrane protein stability under native conditions *Proceedings of the National Academy of Sciences*, 111(1) 219–224.
- Charpentier, E. (2015) CRISPR-Cas9: how research on a bacterial RNA-guided mechanism opened new perspectives in biotechnology and biomedicine *EMBO Molecular Medicine*, 7(4) 363–365.
- Cheng, J.T.J., Hale, J.D., Elliott, M., Hancock, R.E.W., and Straus, S.K. (2011) The importance of bacterial membrane composition in the structure and function of aurein 2.2 and selected variants *Biochimica et Biophysica Acta (BBA) - Biomembranes*, 1808(3) 622–633.
- Chia, G.W.N., Seviour, T., Kjelleberg, S., and Hinks, J. (2021) Carotenoids improve bacterial tolerance towards biobutanol through membrane stabilization *Environmental Science: Nano*, 8(1) 328–341.

- Chin, W.C., Lin, K.H., Liu, C.C., Tsuge, K., and Huang, C.C. (2017) Improved n-butanol production via co-expression of membrane-targeted tilapia metallothionein and the *Clostridial* metabolic pathway in *Escherichia coli* *BMC Biotechnology*, 17(1) 36.
- Cho, C., Hong, S., Moon, H.G., Jang, Y.S., Kim, D., and Lee, S.Y. (2019) Engineering *Clostridial* aldehyde/alcohol dehydrogenase for selective butanol production *mBio*, 10(1).
- Cho, C. and Lee, S.Y. (2017) Efficient gene knockdown in *Clostridium acetobutylicum* by synthetic small regulatory RNAs *Biotechnology and Bioengineering*, 114(2) 374–383.
- Choi, Y.J., Lee, J., Jang, Y.-S., and Lee, S.Y. (2014) Metabolic engineering of microorganisms for the production of higher alcohols. *mBio*, 5(5) e01524-14.
- Clifton, L.A., Skoda, M.W.A., Le Brun, A.P., Ciesielski, F., Kuzmenko, I., Holt, S.A., and Lakey, J.H. (2015) Effect of divalent cation removal on the structure of Gram-negative bacterial outer membrane models *Langmuir*, 31(1) 404–412.
- Corin, K. and Bowie, J.U. (2020) How bilayer properties influence membrane protein folding *Protein Science*, 29(12) 2348–2362.
- Crews, F.T., Morrow, A.L., Criswell, H., and Breese, G. (1996) Effects of ethanol on ion channels *International Review of Neurobiology*, 39(39) 283–367.
- Croux, C., Nguyen, N.P.T., Lee, J., Raynaud, C., Saint-Prix, F., Gonzalez-Pajuelo, M., Meynial-Salles, I., and Soucaille, P. (2016) Construction of a restriction-less, marker-less mutant useful for functional genomic and metabolic engineering of the biofuel producer *Clostridium acetobutylicum* *Biotechnology for Biofuels*, 9(1) 23.
- Daugelavicius, R., Bakiene, E., and Bamford, D.H. (2000) Stages of polymyxin B interaction with the *Escherichia coli* cell envelope. *Antimicrobial Agents and Chemotherapy*, 44(11) 2969–78.
- Dawaliby, R., Trubbia, C., Delporte, C., Masureel, M., Van Antwerpen, P., Kobilka, B.K., and Govaerts, C. (2016) Allosteric regulation of G protein-coupled receptor activity by phospholipids *Nature Chemical Biology*, 12(1) 35–39.
- Dehoux, P., Marvaud, J.C., Abouelleil, A., Earl, A.M., Lambert, T., and Dauga, C. (2016) Comparative genomics

- of *Clostridium bolteae* and *Clostridium clostridioforme* reveals species-specific genomic properties and numerous putative antibiotic resistance determinants *BMC Genomics*, 17(1).
- Denich, T., Beaudette, L., Lee, H., and Trevors, J.. (2003) Effect of selected environmental and physico-chemical factors on bacterial cytoplasmic membranes *Journal of Microbiological Methods*, 52(2) 149–182.
- Dong, H., Zhao, C., Zhang, T., Lin, Z., Li, Y., and Zhang, Y. (2016) Engineering *Escherichia coli* cell factories for n-butanol production *In: Advances in Biochemical Engineering/Biotechnology*. Springer, Berlin, Heidelberg, 141–163.
- Dong, H., Zhao, C., Zhang, T., Zhu, H., Lin, Z., Tao, W., Zhang, Y., and Li, Y. (2017) A systematically chromosomally engineered *Escherichia coli* efficiently produces butanol *Metabolic Engineering*, 44 284–292.
- Dopico, A.M. and Lovinger, D.M. (2009) Acute alcohol action and desensitization of ligand-gated ion channels. *Pharmacological reviews*, 61(1) 98–114.
- Dörr, J.M., Scheidelaar, S., Koorengevel, M.C., Dominguez, J.J., Schäfer, M., van Walree, C.A., and Killian, J.A. (2016) The styrene–maleic acid copolymer: a versatile tool in membrane research *European Biophysics Journal*.
- Dowhan, W., Bogdanov, M., and Mileykovskaya, E. (2016) Functional Roles of Lipids in Membranes *In: Biochemistry of Lipids, Lipoproteins and Membranes: Sixth Edition*. Elsevier Inc., 1–40.
- Dunlop, M.J., Dossani, Z.Y., Szmids, H.L., Chu, H.C., Lee, T.S., Keasling, J.D., Hadi, M.Z., and Mukhopadhyay, A. (2011) Engineering microbial biofuel tolerance and export using efflux pumps. *Molecular systems biology*, 7 487.
- Dürr, U.H.N., Soong, R., and Ramamoorthy, A. (2013) When detergent meets bilayer: Birth and coming of age of lipid bicelles *Progress in Nuclear Magnetic Resonance Spectroscopy*.
- Durre, P. (2005) *Handbook of Clostridia*.
- Dürre, P. (2007) Biobutanol: An attractive biofuel *Biotechnology Journal*.
- Eberlein, C., Baumgarten, T., Starke, S., and Heipieper, H.J. (2018) Immediate response mechanisms of Gram-

- negative solvent-tolerant bacteria to cope with environmental stress: *cis-trans* isomerization of unsaturated fatty acids and outer membrane vesicle secretion *Applied Microbiology and Biotechnology*.
- Eckert, C.A. and Trinh, C. (2016) *Biotechnology for Biofuel Production and Optimization* Biotechnology for Biofuel Production and Optimization.
- Eicher, T., Cha, H.J., Seeger, M.A., Brandstätter, L., El-Delik, J., Bohnert, J.A., Kern, W. V., Verrey, F., Grütter, M.G., Diederichs, K., and Pos, K.M. (2012) Transport of drugs by the multidrug transporter AcrB involves an access and a deep binding pocket that are separated by a switch-loop *Proceedings of the National Academy of Sciences of the United States of America*, 109(15) 5687–5692.
- ENA Browser [online] (2021. Available from: <https://www.ebi.ac.uk/ena/browser/view/CP004121.1> [Accessed 22 Mar 2021]).
- Epand, R.M. and Epand, R.F. (2009) Lipid domains in bacterial membranes and the action of antimicrobial agents *Biochimica et Biophysica Acta - Biomembranes*.
- Evans, A., Ribble, W., Schexnaydre, E., and Waldrop, G.L. (2017) Acetyl-CoA carboxylase from *Escherichia coli* exhibits a pronounced hysteresis when inhibited by palmitoyl-acyl carrier protein *Archives of Biochemistry and Biophysics*, 636 100–109.
- Fadeel, B. and Xue, D. (2009) The ins and outs of phospholipid asymmetry in the plasma membrane: roles in health and disease. *Critical Reviews in Biochemistry and Molecular Biology*, 44 (5) 264-277.
- Fischer, C.R., Klein-Marcuschamer, D., and Stephanopoulos, G. (2008) Selection and optimization of microbial hosts for biofuels production *Metabolic Engineering*, 10(6) 295–304.
- Fischer, R.J., Oehmcke, S., Meyer, U., Mix, M., Schwarz, K., Fiedler, T., and Bahl, H. (2006) Transcription of the *pst* operon of *Clostridium acetobutylicum* is dependent on phosphate concentration and pH *Journal of Bacteriology*, 188(15) 5469–5478.
- Fisher, M.A., Boyarskiy, S., Yamada, M.R., Kong, N., Bauer, S., and Tullman-Ercek, D. (2014) Enhancing tolerance to short-chain alcohols by engineering the *Escherichia coli* AcrB efflux pump to secrete the non-native substrate n-butanol *ACS Synthetic Biology*, 3(1) 30–40.

- Fletcher, E., Pilizota, T., Davies, P.R., McVey, A., and French, C.E. (2016) Characterization of the effects of n-butanol on the cell envelope of *E. coli* *Applied Microbiology and Biotechnology*, 100(22) 9653–9659.
- Foo, J.L. and Leong, S.S.J. (2013) Directed evolution of an *E. coli* inner membrane transporter for improved efflux of biofuel molecules *Biotechnology for Biofuels*, 6(1) 81.
- Formanek, J., Mackie, R., and Blaschek, H.P. (1997) *Enhanced Butanol Production by Clostridium beijerinckii BA101 Grown in Semidefined P2 Medium Containing 6 Percent Maltodextrin or Glucose* APPLIED AND ENVIRONMENTAL MICROBIOLOGY.
- Friedl, A. (2016) Downstream process options for the ABE fermentation *FEMS Microbiology Letters*, 363(9) fnw073.
- Fuchs, B., Süß, R., Teuber, K., Eibisch, M., and Schiller, J. (2011) Lipid analysis by thin-layer chromatography-A review of the current state *Journal of Chromatography A*.
- Gallego-García, A., Monera-Girona, A.J., Pajares-Martínez, E., Bastida-Martínez, E., Pérez-Castaño, R., Iniesta, A.A., Fontes, M., Padmanabhan, S., and Elías-Arnanz, M. (2019) A bacterial light response reveals an orphan desaturase for human plasmalogen synthesis *Science*, 366(6461) 128–132.
- García, J.J., Martínez-Ballarín, E., Millán-Plano, S., Allué, J.L., Albendea, C., Fuentes, L., and Escanero, J.F. (2005) Effects of trace elements on membrane fluidity *In: Journal of Trace Elements in Medicine and Biology*. Urban & Fischer, 19–22.
- García, V., Pääkkilä, J., Ojamo, H., Muurinen, E., and Keiski, R.L. (2011) Challenges in biobutanol production: How to improve the efficiency? *Renewable and Sustainable Energy Reviews*, 15(2) 964–980.
- Geiger, O., Sohlenkamp, C., and López-lara, I.M. (2019) Biogenesis of Fatty Acids, Lipids and Membranes *Biogenesis of Fatty Acids, Lipids and Membranes*, 87–107.
- Gheshlaghi, R., Scharer, J.M., Moo-Young, M., and Chou, C.P. (2009) Metabolic pathways of *Clostridia* for producing butanol *Biotechnology Advances*.
- Gidden, J., Denson, J., Liyanage, R., Ivey, D.M., and Lay, J.O. (2009) Lipid compositions in *Escherichia coli* and *Bacillus subtilis* during growth as determined by MALDI-TOF and TOF/TOF mass spectrometry *International Journal of Mass Spectrometry*, 283(1–3) 178–184.

- Glick, B.R. (1995) Metabolic load and heterologous gene expression *Biotechnology Advances*.
- Goksu, E.I., Vanegas, J.M., Blanchette, C.D., Lin, W.C., and Longo, M.L. (2009) AFM for structure and dynamics of biomembranes *Biochimica et Biophysica Acta - Biomembranes*.
- Gottumukkala, L.D., Parameswaran, B., Valappil, S.K., Mathiyazhakan, K., Pandey, A., and Sukumaran, R.K. (2013) Biobutanol production from rice straw by a non acetone producing *Clostridium sporogenes* BE01 *Bioresource Technology*, 145 182–187.
- Grogan, D.W. and Cronan, J.E. (1997) Cyclopropane ring formation in membrane lipids of bacteria. *Microbiology and molecular biology reviews : MMBR*, 61(4) 429–441.
- Guo, J., Chia, G.W.N., Berezhnoy, N. V., Cazenave-Gassiot, A., Kjelleberg, S., Hinks, J., Mu, Y., and Seviour, T. (2020) Bacterial lipopolysaccharide core structures mediate effects of butanol ingress *Biochimica et Biophysica Acta - Biomembranes*, 1862(2) 183150.
- Guo, J., Ho, J.C.S., Chin, H., Mark, A.E., Zhou, C., Kjelleberg, S., Liedberg, B., Parikh, A.N., Cho, N.-J., Hinks, J., Mu, Y., and Seviour, T. (2019) Response of microbial membranes to butanol: Interdigitation vs. Disorder *Physical Chemistry Chemical Physics*, 21(22) 11903–11915.
- Guo, Y., Winkler, J., and Kao, K.C. (2017) Insights on Osmotic Tolerance Mechanisms in *Escherichia coli* Gained from an *rpoC* Mutation. *Bioengineering (Basel, Switzerland)*, 4(3).
- Han, B., Ujor, V., Lai, L.B., Gopalan, V., and Ezeji, T.C. (2013) Use of proteomic analysis to elucidate the role of calcium in acetone-butanol-ethanol fermentation by *Clostridium beijerinckii* NCIMB 8052 *Applied and Environmental Microbiology*, 79(1) 282–293.
- Hayase, K. and Hayano, S. (1978) Effect of alcohols on the critical micelle concentration decrease in the aqueous sodium dodecyl sulfate solution *Journal of Colloid And Interface Science*, 63(3) 446–451.
- Heipieper, H.J., Neumann, G., Cornelissen, S., and Meinhardt, F. (2007) Solvent-tolerant bacteria for biotransformations in two-phase fermentation systems *Applied Microbiology and Biotechnology*, 74(5) 961–973.
- Henderson, C.M. and Block, D.E. (2014) Examining the role of membrane lipid composition in determining the ethanol tolerance of *Saccharomyces cerevisiae* *Applied and Environmental Microbiology*, 80(10) 2966–

2972.

- Hénin, J., Tajkhorshid, E., Schulten, K., and Chipot, C. (2008) Diffusion of glycerol through Escherichia coli aquaglyceroporin GlpF *Biophysical Journal*, 94(3) 832–839.
- Hinks, J., Wang, Y., Matysik, A., Kraut, R., Kjelleberg, S., Mu, Y., Bazan, G.C., Wuertz, S., and Seviour, T. (2015) Increased Microbial Butanol Tolerance by Exogenous Membrane Insertion Molecules *ChemSusChem*, 8(21) 3718–3726.
- Holtwick, R., Meinhardt, F., and Keweloh, H. (1997) *cis-Trans Isomerization of Unsaturated Fatty Acids: Cloning and Sequencing of the cti Gene from Pseudomonas putida P8* Downloaded from APPLIED AND ENVIRONMENTAL MICROBIOLOGY.
- Hözl, G. and Dörmann, P. (2007) Structure and function of glyco-glycerolipids in plants and bacteria *Progress in Lipid Research*.
- Hosein, A.M., Breidt, F., and Smith, C.E. (2011) Modeling the Effects of Sodium Chloride, Acetic Acid, and Intracellular pH on Survival of Escherichia coli O157:H7 † *Applied and Environmental Microbiology*, 77(3) 889–895.
- Huang, L., Gibbins, L.N., and Forsberg, C.W. (1985) Transmembrane pH gradient and membrane potential in Clostridium acetobutylicum during growth under acetogenic and solventogenic conditions *Applied and Environmental Microbiology*, 50(4) 1043–1047.
- Hub, J.S. and De Groot, B.L. (2008) Mechanism of selectivity in aquaporins and aquaglyceroporins *Proceedings of the National Academy of Sciences of the United States of America*, 105(4) 1198–1203.
- Huffer, S., Clark, M.E., Ning, J.C., Blanch, H.W., and Clark, D.S. (2011) Role of alcohols in growth, lipid composition, and membrane fluidity of yeasts, bacteria, and archaea. *Applied and Environmental Microbiology*, 77(18) 6400–8.
- Husain, F., Bikhchandani, M., and Nikaido, H. (2011) Vestibules are part of the substrate path in the multidrug efflux transporter AcrB of Escherichia coli *Journal of Bacteriology*.
- Isar, J. and Rangaswamy, V. (2012) Improved n-butanol production by solvent tolerant Clostridium beijerinckii *Biomass and Bioenergy*, 37 9–15.

- Ivanova, P.T., Milne, S.B., Myers, D.S., and Brown, H.A. (2009) Lipidomics: a mass spectrometry based systems level analysis of cellular lipids *Current Opinion in Chemical Biology*.
- Jang, Y.S., Malaviya, A., and Lee, S.Y. (2013) Acetone-butanol-ethanol production with high productivity using *Clostridium acetobutylicum* BKM19 *Biotechnology and Bioengineering*, 110(6) 1646–1653.
- Jarboe, L.R., Klauda, J.B., Chen, Y., Davis, K.M., and Santoscoy, M.C. (2018) Engineering the microbial cell membrane to improve bioproduction *ACS Symposium Series*, 1310 25–39.
- Jensen, M., Tajkhorshid, E., and Schulten, K. (2001) The mechanism of glycerol conduction in aquaglyceroporins *Structure*, 9(11) 1083–1093.
- Jensen, M.O., Park, S., Tajkhorshid, E., and Schulten, K. (2002) Energetics of glycerol conduction through aquaglyceroporin GlpF *Proceedings of the National Academy of Sciences*, 99(10) 6731–6736.
- Jia, H., Fan, Y., Feng, X., and Li, C. (2014) Enhancing Stress-Resistance for Efficient Microbial Biotransformations by Synthetic Biology *Frontiers in Bioengineering and Biotechnology*, 2 44.
- Jiang, Y., Guo, D., Lu, J., Dürre, P., Dong, W., Yan, W., Zhang, W., Ma, J., Jiang, M., and Xin, F. (2018) Consolidated bioprocessing of butanol production from xylan by a thermophilic and butanogenic *Thermoanaerobacterium* sp. M5 *Biotechnology for Biofuels*, 11(1) 89.
- Jiang, Y., Liu, J., Jiang, W., Yang, Y., and Yang, S. (2015) Current status and prospects of industrial bio-production of n-butanol in China *Biotechnology Advances*.
- Jiang, Y., Xu, C., Dong, F., Yang, Y., Jiang, W., and Yang, S. (2009) Disruption of the acetoacetate decarboxylase gene in solvent-producing *Clostridium acetobutylicum* increases the butanol ratio *Metabolic Engineering*, 11(4–5) 284–291.
- Johnson, R.M., Fais, C., Parmar, M., Cheruvara, H., Marshall, R.L., Hesketh, S.J., Feasey, M.C., Ruggerone, P., Vargiu, A. V., Postis, V.L.G., Muench, S.P., and Bavro, V.N. (2020) Cryo-EM Structure and Molecular Dynamics Analysis of the Fluoroquinolone Resistant Mutant of the AcrB Transporter from *Salmonella* *Microorganisms*, 8(6) 943.
- Jones, D.P. (2008) Radical-free biology of oxidative stress *AJP: Cell Physiology*, 295(4) C849–C868.
- Jones, D.T. and Woods, D.R. (1986) Acetone-butanol fermentation revisited. *Microbiological Reviews*, 50(4)

484–524.

- Jones, S.W., Tracy, B.P., Gaida, S.M., and Papoutsakis, E.T. (2011) Inactivation of σ^F in *Clostridium acetobutylicum* ATCC 824 blocks sporulation prior to asymmetric division and abolishes σ^E and σ^G protein expression but does not block solvent formation *Journal of Bacteriology*, 193(10) 2429–2440.
- Jurcik, A., Bednar, D., Byska, J., Marques, S.M., Furmanova, K., Daniel, L., Kokkonen, P., Brezovsky, J., Strnad, O., Stourac, J., Pavelka, A., Manak, M., Damborsky, J., and Kozlikova, B. (2018) CAVER Analyst 2.0: Analysis and visualization of channels and tunnels in protein structures and molecular dynamics trajectories *Bioinformatics*, 34(20) 3586–3588.
- Kaiser, H.J., Surma, M.A., Mayer, F., Levental, I., Grzybek, M., Klemm, R.W., Da Cruz, S., Meisinger, C., Müller, V., Simons, K., and Lingwood, D. (2011) Molecular convergence of bacterial and eukaryotic surface order *Journal of Biological Chemistry*, 286(47) 40631–40637.
- Kannenbergh, E. and Poralla, K. (1982) The influence of hopanoids on growth of *Mycoplasma mycoides* *Archives of Microbiology*, 133(2) 100–102.
- Kanno, M., Katayama, T., Tamaki, H., Mitani, Y., Meng, X.-Y., Hori, T., Narihiro, T., Morita, N., Hoshino, T., Yumoto, I., Kimura, N., Hanada, S., and Kamagata, Y. (2013) Isolation of butanol- and isobutanol-tolerant bacteria and physiological characterization of their butanol tolerance. *Applied and Environmental Microbiology*, 79(22) 6998–7005.
- Keis *et al.* (2001) Emended descriptions of *Clostridium acetobutylicum* and *Clostridium beijerinckii*, and descriptions of *Clostridium saccharoperbutylacetonicum* sp. nov. and *Clostridium saccharobutylicum* sp. nov. *International Journal of Systematic and Evolutionary Microbiology*, 51, 2095–2103.
- Kell, D.B., Swainston, N., Pir, P.P., and Oliver, S.G. (2015) Membrane transporter engineering in industrial biotechnology and whole cell biocatalysis *Trends in Biotechnology*, 33(4) 237–246.
- Klein, N., Neumann, J., O’Neil, J.D., and Schneider, D. (2015) Folding and stability of the aquaglyceroporin GlpF: Implications for human aqua(glycero)porin diseases *Biochimica et Biophysica Acta - Biomembranes*.
- Koebnik, R., Locher, K.P., and Van Gelder, P. (2000) Structure and function of bacterial outer membrane proteins: barrels in a nutshell *Molecular Microbiology*, 37(2) 239–253.

- Kolek, J., Patáková, P., Melzoch, K., Sigler, K., and Řezanka, T. (2015) Changes in membrane plasmalogens of *Clostridium pasteurianum* during butanol fermentation as determined by lipidomic analysis *PLoS ONE*, 10(3).
- Koynova, R. and Tenchov, B. (2013) Encyclopedia of Biophysics *Encyclopedia of Biophysics*, (January).
- Kranenburg, M., Vlaar, M., and Smit, B. (2004) Simulating induced interdigitation in membranes *Biophysical Journal*, 87(3) 1596–1605.
- Kujawska, A., Kujawski, J., Bryjak, M., and Kujawski, W. (2015) ABE fermentation products recovery methods - A review *Renewable and Sustainable Energy Reviews*.
- Kurniawan, Y., Scholz, C., and Bothun, G.D. (2013) N-butanol partitioning into phase-separated heterogeneous lipid monolayers *Langmuir*, 29(34) 10817–10823.
- Kurniawan, Y., Venkataramanan, K.P., Scholz, C., and Bothun, G.D. (2012) N-butanol partitioning and phase behavior in DPPC/DOPC membranes *Journal of Physical Chemistry B*, 116(20) 5919–5924.
- Lairón-Peris, M., Routledge, S.J., Linney, J.A., Alonso-del-Real, J., Spickett, C.M., Pitt, A.R., Guillamon, J.M., Barrio, E., Goddard, A.D., and Querol, A. (2021) Analysis of lipid composition reveals mechanisms of ethanol tolerance in the model yeast *Saccharomyces cerevisiae* *Applied and Environmental Microbiology*.
- Lee, S.-H.Y.H.Y.H., Jang, Y.-S.S., Lee, J.J.Y.J.J., Lee, J.J.Y.J.J., Park, J.H., Im, J.A., Eom, M.-H.H., Lee, J.J.Y.J.J., Lee, S.-H.Y.H.Y.H., Song, H., Cho, J.-H.H., Seung, D.Y., Lee, S.-H.Y.H.Y.H., Jang, Y.-S.S., Lee, J.J.Y.J.J., Lee, J.J.Y.J.J., Park, J.H., Im, J.A., Eom, M.-H.H., Lee, J.J.Y.J.J., Lee, S.-H.Y.H.Y.H., Song, H., Cho, J.-H.H., and Seung, D.Y. (2012) Enhanced butanol production obtained by reinforcing the direct butanol-forming route in *Clostridium acetobutylicum*. *mBio*, 3(5) e00314-12.
- Lee, S.K., Chou, H., Ham, T.S., Lee, T.S., and Keasling, J.D. (2008) Metabolic engineering of microorganisms for biofuels production: from bugs to synthetic biology to fuels *Current Opinion in Biotechnology*.
- Lee, S.Y., Jang, Y.S., Lee, J.Y., Lee, J., Park, J.H., Im, J.A., Eom, M.H., Lee, J., Lee, S.H., Song, H., Cho, J.H., and Seung, D.Y. (2012) Enhanced butanol production obtained by reinforcing the direct butanol-forming route in *Clostridium acetobutylicum* *mBio*, 3(5).

- Lee, S.Y., Park, J.H., Jang, S.H., Nielsen, L.K., Kim, J., and Jung, K.S. (2008) Fermentative butanol production by *Clostridia Biotechnology and Bioengineering*, 101(2) 209–228.
- Lehmann, D., Hönicke, D., Ehrenreich, A., Schmidt, M., Weuster-Botz, D., Bahl, H., and Lütke-Eversloh, T. (2012) Modifying the product pattern of *Clostridium acetobutylicum*: Physiological effects of disrupting the acetate and acetone formation pathways *Applied Microbiology and Biotechnology*, 94(3) 743–754.
- Lepage, C., Fayolle, F., Hermann, M., and Vandecasteele, J.-P. (1987) Changes in Membrane Lipid Composition of *Clostridium acetobutylicum* during Acetone–Butanol Fermentation: Effects of Solvents, Growth Temperature and pH *Microbiology*, 133(1987) 103–110.
- Li, H., Ma, M.L., Luo, S., Zhang, R.M., Han, P., and Hu, W. (2012) Metabolic responses to ethanol in *Saccharomyces cerevisiae* using a gas chromatography tandem mass spectrometry-based metabolomics approach *International Journal of Biochemistry and Cell Biology*, 44(7) 1087–1096.
- Li, Q., Chen, J., Minton, N.P., Zhang, Y., Wen, Z., Liu, J., Yang, H., Zeng, Z., Ren, X., Yang, J., Gu, Y., Jiang, W., Jiang, Y., and Yang, S. (2016) CRISPR-based genome editing and expression control systems in *Clostridium acetobutylicum* and *Clostridium beijerinckii* *Biotechnology Journal*, 11(7) 961–972.
- Li, S., Huang, L., Ke, C., Pang, Z., and Liu, L. (2020) Pathway dissection, regulation, engineering and application: Lessons learned from biobutanol production by solventogenic *Clostridia Biotechnology for Biofuels*.
- Li, S.B., Qian, Y., Liang, Z.W., Guo, Y., Zhao, M.M., and Pang, Z.W. (2016) Enhanced butanol production from cassava with *Clostridium acetobutylicum* by genome shuffling *World Journal of Microbiology and Biotechnology*, 32(4) 1–10.
- Liao, Z., Guo, X., Hu, J., Suo, Y., Fu, H., and Wang, J. (2019) The significance of proline on lignocellulose-derived inhibitors tolerance in *Clostridium acetobutylicum* ATCC 824 *Bioresource Technology*, 272 561–569.
- Liao, Z., Zhang, Y., Luo, S., Suo, Y., Zhang, S., and Wang, J. (2017) Improving cellular robustness and butanol titers of *Clostridium acetobutylicum* ATCC824 by introducing heat shock proteins from an extremophilic bacterium *Journal of Biotechnology*, 252 1–10.
- Lichtenberg, D., Ahyayauch, H., Goñi, F.M., Lix, F., and Goñi, M. (2013) *The Mechanism of Detergent*

Solubilization of Lipid Bilayers. Biophysical Society.

- Lin, C.M., Chang, G.P., Tsao, H.K., and Sheng, Y.J. (2011) Solubilization mechanism of vesicles by surfactants: Effect of hydrophobicity *Journal of Chemical Physics*, 135(4) 045102.
- Liu, P., Chernyshov, A., Najdi, T., Fu, Y., Dickerson, J., Sandmeyer, S., and Jarboe, L. (2013) Membrane stress caused by octanoic acid in *Saccharomyces cerevisiae* *Applied Microbiology and Biotechnology*, 97(7) 3239–3251.
- Liu, X.B., Gu, Q.Y., and Yu, X. Bin (2013) Repetitive domestication to enhance butanol tolerance and production in *Clostridium acetobutylicum* through artificial simulation of bio-evolution *Bioresource Technology*, 130 638–643.
- Liu, Z., Ying, Y., Li, F., Ma, C., and Xu, P. (2010) Butanol production by *Clostridium beijerinckii* ATCC 55025 from wheat bran *Journal of Industrial Microbiology and Biotechnology*, 37(5) 495–501.
- Lucena, D., Mauri, M., Schmidt, F., Eckhardt, B., and Graumann, P.L. (2018) Microdomain formation is a general property of bacterial membrane proteins and induces heterogeneity of diffusion patterns *BMC Biology*, 16(1) 97.
- Luo, L.H., Seo, P.-S., Seo, J.-W., Heo, S.-Y., Kim, D.-H., and Kim, C.H. (2009) Improved ethanol tolerance in *Escherichia coli* by changing the cellular fatty acids composition through genetic manipulation *Biotechnology Letters*, 31(12) 1867–1871.
- Lütke-Eversloh, T. and Bahl, H. (2011) Metabolic engineering of *Clostridium acetobutylicum*: Recent advances to improve butanol production *Current Opinion in Biotechnology*.
- Ly, H. V and Longo, M.L. (2004) The influence of short-chain alcohols on interfacial tension, mechanical properties, area/molecule, and permeability of fluid lipid bilayers *Biophysical Journal*, 87(2) 1013–1033.
- Maddox, I.S., Steiner, E., Hirsch, S., Wessner, S., Gutierrez, N.A., Gapes, J.R., and Schuster, K.C. (2000) The cause of ‘acid-crash’ and ‘acidogenic fermentations’ during the batch acetone-butanol-ethanol (ABE-) fermentation process. *Journal of molecular microbiology and biotechnology*, 2(1) 95–100.
- Malanovic, N. and Lohner, K. (2016) Antimicrobial peptides targeting Gram-positive bacteria *Pharmaceuticals*.

- Mangiarotti, A., Genovese, D.M., Naumann, C.A., Monti, M.R., and Wilke, N. (2019) Hopanoids, like sterols, modulate dynamics, compaction, phase segregation and permeability of membranes *Biochimica et Biophysica Acta - Biomembranes*, 1861(12).
- Mao, S., Luo, Y., Bao, G., Zhang, Y., Li, Y., and Ma, Y. (2011) Comparative analysis on the membrane proteome of *Clostridium acetobutylicum* wild type strain and its butanol-tolerant mutant *Molecular BioSystems*, 7(5) 1660–1677.
- Mao, S., Luo, Y., Zhang, T., Li, J., Bao, G., Zhu, Y., Chen, Z., Zhang, Y., Li, Y., and Ma, Y. (2010) Proteome reference map and comparative proteomic analysis between a wild type *Clostridium acetobutylicum* DSM 1731 and its mutant with enhanced butanol tolerance and butanol yield *Journal of Proteome Research*, 9(6) 3046–3061.
- Marchal, R., Ropars, M., Pourquié, J., Fayolle, F., and Vandecasteele, J.P. (1992) Large-scale enzymatic hydrolysis of agricultural lignocellulosic biomass. Part 2: Conversion into acetone-butanol *Bioresource Technology*, 42(3) 205–217.
- Marquardt, D., Geier, B., and Pabst, G. (2015) Asymmetric lipid membranes: Towards more realistic model systems *Membranes*.
- Martín, J.F. and Liras, P. (2021) Molecular mechanisms of phosphate sensing, transport and signalling in streptomycetes and related actinobacteria *International Journal of Molecular Sciences*, 22(3) 1–20.
- Mascal, M. (2012) Chemicals from biobutanol: Technologies and markets *Biofuels, Bioproducts and Biorefining*.
- Maurya, S.R., Chaturvedi, D., and Mahalakshmi, R. (2013) Modulating lipid dynamics and membrane fluidity to drive rapid folding of a transmembrane barrel *Scientific Reports*, 3(1) 1–6.
- May, K.L. and Silhavy, T.J. (2017) Making a membrane on the other side of the wall *Biochimica et Biophysica Acta - Molecular and Cell Biology of Lipids*.
- van Meer, G. (2011) Dynamic transbilayer lipid asymmetry *Cold Spring Harbor Perspectives in Biology*, 3(5) 1–11.
- Meroueh, S.O., Bencze, K.Z., Heseck, D., Lee, M., Fisher, J.F., Stemmler, T.L., and Mobashery, S. (2006) Three-dimensional structure of the bacterial cell wall peptidoglycan *Proceedings of the National Academy of Sciences*, 103(12) 5000–5005.

- Sciences of the United States of America*, 103(12) 4404–4409.
- Mileykovskaya, E. and Dowhan, W. (2000) Visualization of phospholipid domains in *Escherichia coli* by using the cardiolipin-specific fluorescent dye 10-N-nonyl acridine orange *Journal of Bacteriology*, 182(4) 1172–1175.
- Miloshevsky, G. V. and Jordan, P.C. (2004) Water and ion permeation in bAQP1 and GlpF channels: A kinetic Monte Carlo study *Biophysical Journal*, 87(6) 3690–3702.
- Mitchell, D.C. (2012) Progress in understanding the role of lipids in membrane protein folding *Biochimica et Biophysica Acta (BBA) - Biomembranes*, 1818(4) 951–956.
- Mordor Intelligence (2018) Bio-Butanol Market | Size | Share | Industry Analysis | Outlook [online] 2018. Available from: <https://www.mordorintelligence.com/industry-reports/bio-butanol-market> [Accessed 22 Apr 2018].
- Mukhopadhyay, A. (2015) Tolerance engineering in bacteria for the production of advanced biofuels and chemicals *Trends in Microbiology*.
- Murínová, S. and Dercová, K. (2014) Response mechanisms of bacterial degraders to environmental contaminants on the level of cell walls and cytoplasmic membrane *International Journal of Microbiology*.
- Murzyn, K., Róg, T., and Pasenkiewicz-Gierula, M. (2005) Phosphatidylethanolamine-phosphatidylglycerol bilayer as a model of the inner bacterial membrane, 88(2).
- Nakashima, R., Sakurai, K., Yamasaki, S., Hayashi, K., Nagata, C., Hoshino, K., Onodera, Y., Nishino, K., and Yamaguchi, A. (2013) Structural basis for the inhibition of bacterial multidrug exporters *Nature*, 500(7460) 102–106.
- Nanda, S., Golemi-Kotra, D., McDermott, J.C., Dalai, A.K., Gökalp, I., and Kozinski, J.A. (2017) Fermentative production of butanol: Perspectives on synthetic biology *New Biotechnology*.
- Ndaba, B., Chiyanzu, I., and Marx, S. (2015) N-Butanol derived from biochemical and chemical routes: A review *Biotechnology Reports*.
- Nilsson, I.M., Sääf, A., Whitley, P., Gafvelin, G., Waller, C., and Von Heijne, G. (1998) Proline-induced disruption

- of a transmembrane α -helix in its natural environment *Journal of Molecular Biology*, 284(4) 1165–1175.
- Nishijima, M. and Raetz, C.R.H. (1979) *Membrane Lipid Biogenesis in Escherichia coli: Identification of Genetic Loci for Phosphatidylglycerophosphate Synthetase and Construction of Mutants Lacking Phosphatidylglycerol***Journal of Biological Chemistry*.
- Ogata, S., Yoshino, S., and Okuma, Y. (1982) *CHEMICAL COMPOSITION OF AUTOPLAST MEMBRANE OF CLOSTRIDIUM SACCHAROPERBUTYLACETONICUM*. *Gen. Appl. Microbiol.*
- Okuyama, H., Okajima, N., Sasaki, S., Higashi, S., and Murata, N. (1991) The *cis/trans* isomerization of the double bond of a fatty acid as a strategy for adaptation to changes in ambient temperature in the psychrophilic bacterium, *Vibrio* sp. strain ABE-1 *Biochimica et Biophysica Acta (BBA) - Lipids and Lipid Metabolism*, 1084(1) 13–20.
- Paredes, C.J., Alsaker, K. V., and Papoutsakis, E.T. (2005) A comparative genomic view of *Clostridial* sporulation and physiology *Nature Reviews Microbiology*.
- Parsons, J.B. and Rock, C.O. (2011) Is bacterial fatty acid synthesis a valid target for antibacterial drug discovery? *Current Opinion in Microbiology*, 14(5) 544–549.
- Parsons, J.B. and Rock, C.O. (2013) Bacterial lipids: Metabolism and membrane homeostasis *Progress in Lipid Research*.
- Pasenkiewicz-Gierula, M., Baczynski, K., Markiewicz, M., and Murzyn, K. (2016) Computer modelling studies of the bilayer/water interface *Biochimica et Biophysica Acta (BBA) - Biomembranes*, 1858(10) 2305–2321.
- Patakova, P., Branska, B., Sedlar, K., Vasylykivska, M., Jureckova, K., Kolek, J., Koscova, P., and Provaznik, I. (2019) Acidogenesis, solventogenesis, metabolic stress response and life cycle changes in *Clostridium beijerinckii* NRRL B-598 at the transcriptomic level *Scientific Reports*, 9(1) 1–21.
- Patakova, P., Kolek, J., Jureckova, K., Branska, B., Sedlar, K., Vasylykivska, M., and Provaznik, I. (2021) Deeper below the surface — transcriptional changes in selected genes of *Clostridium beijerinckii* in response to butanol shock *MicrobiologyOpen*, 10 1–14.

- Patakova, P., Kolek, J., Sedlar, K., Koscova, P., Branska, B., Kupkova, K., Paulova, L., and Provaznik, I. (2017) Comparative analysis of high butanol tolerance and production in *Clostridia* *Biotechnology Advances*, 15 Dec.
- Peralta-Yahya, P.P. and Keasling, J.D. (2010) Advanced biofuel production in microbes *Biotechnology Journal*.
- Phillips, R., Ursell, T., Wiggins, P., and Sens, P. (2009) Emerging roles for lipids in shaping membrane-protein function *Nature*.
- Pini, C.V., Bernal, P., Godoy, P., Ramos, J.L., and Segura, A. (2009) Cyclopropane fatty acids are involved in organic solvent tolerance but not in acid stress resistance in *Pseudomonas putida* DOT-T1E *Microbial Biotechnology*, 2(2 SPEC. ISS.) 253–261.
- Poger, D. and Mark, A.E. (2013) The relative effect of sterols and hopanoids on lipid bilayers: When comparable is not identical *Journal of Physical Chemistry B*, 117(50) 16129–16140.
- Poger, D. and Mark, A.E. (2015) A ring to rule them all: The effect of cyclopropane fatty acids on the fluidity of lipid bilayers *Journal of Physical Chemistry B*, 119(17) 5487–5495.
- Pollock, N.L., Lee, S.C., Patel, J.H., Gulamhussein, A.A., and Rothnie, A.J. (2018) Structure and function of membrane proteins encapsulated in a polymer-bound lipid bilayer *Biochimica et Biophysica Acta (BBA) - Biomembranes*, 1860(4) 809–817.
- Postis, V., Rawson, S., Mitchell, J.K., Lee, S.C., Parslow, R.A., Dafforn, T.R., Baldwin, S.A., and Muench, S.P. (2015) The use of SMALPs as a novel membrane protein scaffold for structure study by negative stain electron microscopy *Biochimica et Biophysica Acta - Biomembranes*, 1848(2) 496–501.
- Putta, P., Rankenberg, J., Korver, R.A., van Wijk, R., Munnik, T., Testerink, C., and Kooijman, E.E. (2016) Phosphatidic acid binding proteins display differential binding as a function of membrane curvature stress and chemical properties *Biochimica et Biophysica Acta - Biomembranes*, 1858(11) 2709–2716.
- Rabari, D. and Banerjee, T. (2013) Biobutanol and n-propanol recovery using a low density phosphonium based ionic liquid at T=298.15K and p=1atm *Fluid Phase Equilibria*, 355 26–33.
- Ramos, J.L., Duque, E., Gallegos, M.-T., Godoy, P., Ramos-González, M.I., Rojas, A., Terán, W., and Segura, A. (2002) Mechanisms of Solvent Tolerance in Gram-Negative Bacteria *Annual Review of Microbiology*,

56(1) 743–768.

- Ravagnani, A., Jennert, K.C.B., Steiner, E., Grünberg, R., Jefferies, J.R., Wilkinson, S.R., Young, D.I., Tidswell, E.C., Brown, D.P., Youngman, P., Gareth Morris, J., and Young, M. (2000) Spo0A directly controls the switch from acid to solvent production in solvent-forming *Clostridia* *Molecular Microbiology*, 37(5) 1172–1185.
- Reyes, L.H., Abdelaal, A.S., and Kao, K.C. (2013) Genetic determinants for n-butanol tolerance in evolved *Escherichia coli* mutants: Cross adaptation and antagonistic pleiotropy between n-butanol and other stressors *Applied and Environmental Microbiology*, 79(17) 5313–5320.
- Reyes, L.H., Almario, M.P., and Kao, K.C. (2011) Genomic library screens for genes involved in n-butanol tolerance in *Escherichia coli* *PLoS ONE*, 6(3) e17678.
- Řezanka, T., Křesinová, Z., Kolouchová, I., and Sigler, K. (2012) Lipidomic analysis of bacterial plasmalogens *Folia Microbiologica*, 57(5) 463–472.
- Roach, C., Feller, S.E., Ward, J.A., Shaikh, S.R., Zerouga, M., and Stillwell, W. (2004) Comparison of *cis* and *trans* fatty acid containing phosphatidylcholines on membrane properties *Biochemistry*, 43(20) 6344–6351.
- Rog, T. and Koivuniemi, A. (2016) The biophysical properties of ethanolamine plasmalogens revealed by atomistic molecular dynamics simulations. *Biochimica et biophysica acta*, 1858(1) 97–103.
- Róg, T., Murzyn, K., Gurbiel, R., Takaoka, Y., Kusumi, A., and Pasenkiewicz-Gierula, M. (2004) Effects of phospholipid unsaturation on the bilayer nonpolar region: a molecular simulation study. *Journal of lipid research*, 45(2) 326–36.
- Romantsov, T., Guan, Z., and Wood, J.M. (2009) Cardiolipin and the osmotic stress responses of bacteria *Biochimica et Biophysica Acta - Biomembranes*.
- Routledge, S.J., Linney, J.A., and Goddard, A.D. (2019) Liposomes as models for membrane integrity *Biochemical Society Transactions*, 47(3).
- Rowlett, V.W., Mallampalli, V.K.P.S., Karlstaedt, A., Dowhan, W., Taegtmeier, H., Margolin, W., and Vitrac, H. (2017) Impact of membrane phospholipid alterations in *Escherichia coli* on cellular function and bacterial stress adaptation *Journal of Bacteriology*, 199(13).

- Rubio, D.A.R., Zanette, D., Nome, F., and Bunton, C.A. (1994) Effect of 1-Butanol on Micellization of Sodium Dodecyl Sulfate and on Fluorescence Quenching by Bromide Ion *Langmuir*, 10(4) 1151–1154.
- Rutherford, B.J., Dahl, R.H., Price, R.E., Szmids, H.L., Benke, P.I., Mukhopadhyay, A., and Keasling, J.D. (2010) Functional genomic study of exogenous n-butanol stress in *Escherichia coli* *Applied and Environmental Microbiology*, 76(6) 1935–1945.
- Sáenz, J.P., Grosser, D., Bradley, A.S., Lagny, T.J., Lavrynenko, O., Broda, M., and Simons, K. (2015) Hopanoids as functional analogues of cholesterol in bacterial membranes *Proceedings of the National Academy of Sciences of the United States of America*, 112(38) 11971–11976.
- Sandoval, N.R. and Papoutsakis, E.T. (2016) Engineering membrane and cell-wall programs for tolerance to toxic chemicals: Beyond solo genes *Current Opinion in Microbiology*.
- Sandoval, N.R., Venkataramanan, K.P., Groth, T.S., and Papoutsakis, E.T. (2015) Whole-genome sequence of an evolved *Clostridium pasteurianum* strain reveals Spo0A deficiency responsible for increased butanol production and superior growth *Biotechnology for Biofuels*, 8(1) 227.
- Scheffers, D.-J. and Pinho, M.G. (2005) Bacterial Cell Wall Synthesis: New Insights from Localization Studies *Microbiology and Molecular Biology Reviews*, 69(4) 585–607.
- Scherber, C.M., Schottel, J.L., and Aksan, A. (2009) Membrane phase behavior of *Escherichia coli* during desiccation, rehydration, and growth recovery *Biochimica et Biophysica Acta - Biomembranes*, 1788(11) 2427–2435.
- Schlebach, J.P., Cao, Z., Bowie, J.U., and Park, C. (2012) Revisiting the folding kinetics of bacteriorhodopsin *Protein Science*, 21(1) 97–106.
- Seeger, M.A., Schiefner, A., Eicher, T., Verrey, F., Diederichs, K., and Pos, K.M. (2006) Structural asymmetry of AcrB trimer suggests a peristaltic pump mechanism *Science*, 313(5791) 1295–1298.
- Sennhauser, G., Amstutz, P., Briand, C., Storchenegger, O., and Grütter, M.G. (2006) Drug Export Pathway of Multidrug Exporter AcrB Revealed by DARPIn Inhibitors *PLoS Biology*, 5(1) e7.
- Shen, C.R., Lan, E.I., Dekishima, Y., Baez, A., Cho, K.M., and Liao, J.C. (2011) Driving forces enable high-titer anaerobic 1-butanol synthesis in *Escherichia coli* *Applied and Environmental Microbiology*, 77(9) 2905–

2915.

- Shinoda, W. (2016) Permeability across lipid membranes *Biochimica et Biophysica Acta - Biomembranes*, 1858(10) 2254–2265.
- Sigler, K., Chaloupka, J., Brozmanová, J., Stadler, N., and Höfer, M. (1999) Oxidative stress in microorganisms I. Microbial vs. higher cells - Damage and defenses in relation to cell aging and death. *Folia microbiologica*, 44(6) 587–624.
- Sikkema, J., de Bont, J.A., and Poolman, B. (1995) Mechanisms of membrane toxicity of hydrocarbons *Microbiol Rev*, 59(2) 201–222.
- Simons, K. and Ikonen, E. (1997) Functional rafts in cell membranes *Nature*.
- Smith, S.M. (2017) Strategies for the Purification of Membrane Proteins *In: Methods in molecular biology (Clifton, N.J.)*. 389–400.
- Sohlenkamp, C. and Geiger, O. (2016) Bacterial membrane lipids: diversity in structures and pathways *FEMS Microbiology Reviews*, (1) 133–159.
- Steen, E.J., Chan, R., Prasad, N., Myers, S., Petzold, C.J., Redding, A., Ouellet, M., and Keasling, J.D. (2008) Metabolic engineering of *Saccharomyces cerevisiae* for the production of n-butanol *Microbial Cell Factories*, 7(1) 36.
- Stewart, J.C.M. (1980) Colorimetric determination of phospholipids with ammonium ferrothiocyanate *Analytical Biochemistry*, 104(1) 10–14.
- Strahl, H. and Errington, J. (2017) Bacterial Membranes: Structure, Domains, and Function *Annual Review of Microbiology*, 71(1) 519–538.
- Stroud, R.M., Miercke, L.J., O'Connell, J., Khademi, S., Lee, J.K., Remis, J., Harries, W., Robles, Y., and Akhavan, D. (2003) Glycerol facilitator GlpF and the associated aquaporin family of channels *Current Opinion in Structural Biology*.
- Studer, G., Biasini, M., and Schwede, T. (2014) Assessing the local structural quality of transmembrane protein models using statistical potentials (QMEANBrane) *In: Bioinformatics*. Oxford University Press, i505.
- Su, C.C., Morgan, C.E., Kambakam, S., Rajavel, M., Scott, H., Huang, W., Emerson, C.C., Taylor, D.J., Stewart,

- P.L., Bonomo, R.A., and Yu, E.W. (2019) Cryo-electron microscopy structure of an acinetobacter baumannii multidrug efflux pump *mBio*, 10(4).
- Sun, C., Zhang, S., Xin, F., Shanmugam, S., and Wu, Y.R. (2018) Genomic comparison of Clostridium species with the potential of utilizing red algal biomass for biobutanol production *Biotechnology for Biofuels*, 11(1) 42.
- Surisetty, V.R., Dalai, A.K., and Kozinski, J. (2011) Alcohols as alternative fuels: An overview *Applied Catalysis A: General*.
- Szulczyk, K.R. (2010) Which is a better transportation fuel—butanol or ethanol? *Int J Energy Environ*, 1(3) 501–512.
- Tan, Z., Khakbaz, P., Chen, Y., Lombardo, J., Yoon, J.M., Shanks, J. V., Klauda, J.B., and Jarboe, L.R. (2017) Engineering Escherichia coli membrane phospholipid head distribution improves tolerance and production of biorenewables *Metabolic Engineering*, 44 1–12.
- Tan, Z., Yoon, J.M., Nielsen, D.R., Shanks, J. V., and Jarboe, L.R. (2016) Membrane engineering via *trans* unsaturated fatty acids production improves Escherichia coli robustness and production of biorenewables *Metabolic Engineering*, 35 105–113.
- Tang, Y., Xia, H., and Li, D. (2018) Membrane phospholipid biosynthesis in bacteria *In: Advances in Membrane Proteins: Part I: Mass Processing and Transportation*. Springer Singapore, 77–119.
- Tanguy, E., Kassas, N., and Vitale, N. (2018) Protein–phospholipid interaction motifs: A focus on phosphatidic acid *Biomolecules*.
- Tashiro, Y., Takeda, K., Kobayashi, G., Sonomoto, K., Ishizaki, A., and Yoshino, S. (2004) High butanol production by Clostridium saccharoperbutylacetonicum N1-4 in fed-batch culture with pH-Stat continuous butyric acid and glucose feeding method *Journal of Bioscience and Bioengineering*, 98(4) 263–268.
- Teixeira, M.C., Godinho, C.P., Cabrito, T.R., Mira, N.P., and Sá-Correia, I. (2012) Increased expression of the yeast multidrug resistance ABC transporter Pdr18 leads to increased ethanol tolerance and ethanol production in high gravity alcoholic fermentation. *Microbial cell factories*, 11 98.

- Tian, B., Guan, Z., and Goldfine, H. (2013) An ethanolamine-phosphate modified glycolipid in *Clostridium acetobutylicum* that responds to membrane stress *Biochimica et Biophysica Acta - Molecular and Cell Biology of Lipids*, 1831(6) 1185–1190.
- Tippkötter, N., Duwe, A.M., Wiesen, S., Sieker, T., and Ulber, R. (2014) Enzymatic hydrolysis of beech wood lignocellulose at high solid contents and its utilization as substrate for the production of biobutanol and dicarboxylic acids *Bioresource Technology*, 167 447–455.
- To, T.M.H., Grandvalet, C., and Tourdot-Maréchal, R. (2011) Cyclopropanation of membrane unsaturated fatty acids is not essential to the acid stress response of *Lactococcus lactis* subsp. *cremoris* *Applied and Environmental Microbiology*, 77(10) 3327–3334.
- Tomas, C.A., Beamish, J., and Papoutsakis, E.T. (2004) Transcriptional Analysis of Butanol Stress and Tolerance in *Clostridium acetobutylicum* *Journal of Bacteriology*, 186(7) 2006–2018.
- Tóth, M.E., Víg, L., and Sántha, M. (2014) Alcohol stress, membranes, and chaperones *Cell Stress and Chaperones*.
- Tummala, S.B., Junne, S.G., and Papoutsakis, E.T. (2003) Antisense RNA downregulation of coenzyme A transferase combined with alcohol-aldehyde dehydrogenase overexpression leads to predominantly alcohologenic *Clostridium acetobutylicum* fermentations *Journal of Bacteriology*, 185(12) 3644–3653.
- Tushar, L., Sasikala, C., and Ramana, C. V. (2014) Draft Genome Sequence of *Rhodomicrobium udaipurensis* JA643T with Special Reference to Hopanoid Biosynthesis *DNA Research*, 21(6) 639–647.
- Tuzimski, T. and Sherma, J. (2016) Thin-Layer Chromatography and Mass Spectrometry for the Analysis of Lipids *In: Encyclopedia of Lipidomics*. Springer Netherlands, 1–20.
- Tyuleva, S.N., Allen, N., White, L.J., Pépés, A., Shepherd, H.J., Saines, P.J., Ellaby, R.J., Mulvihill, D.P., and Hiscock, J.R. (2019) A symbiotic supramolecular approach to the design of novel amphiphiles with antibacterial properties against MSRA *Chemical Communications*, 55(1) 95–98.
- U.S. Energy Administration Information (2018) *Table 10.3 Fuel Ethanol Overview Feed- stock a Losses and Co-products b*.
- van Uitert, I., Le Gac, S., and van den Berg, A. (2010) The influence of different membrane components on the

- electrical stability of bilayer lipid membranes *Biochimica et Biophysica Acta - Biomembranes*, 1798(1) 21–31.
- Venkataramanan, K.P., Kurniawan, Y., Boatman, J.J., Haynes, C.H., Taconi, K.A., Martin, L., Bothun, G.D., and Scholz, C. (2014) Homeoviscous response of *Clostridium pasteurianum* to butanol toxicity during glycerol fermentation *Journal of Biotechnology*, 179 8–14.
- Vollherbst Schneck, K., Sands, J.A., and Montenecourt, B.S. (1984) Effect of butanol on lipid composition and fluidity of *Clostridium acetobutylicum* ATCC 824 *Applied and Environmental Microbiology*, 47(1) 193–194.
- Wang, F., Kashket, S., and Kashket, E.R. (2005) Maintenance of Δ pH by a butanol-tolerant mutant of *Clostridium beijerinckii* *Microbiology*, 151(2) 607–613.
- Wang, Q., Venkataramanan, K.P., Huang, H., Papoutsakis, E.T., and Wu, C.H. (2013) Transcription factors and genetic circuits orchestrating the complex, multilayered response of *Clostridium acetobutylicum* to butanol and butyrate stress *BMC Systems Biology*, 7.
- Wang, S., Dong, S., Wang, P., Tao, Y., and Wang, Y. (2017a) Genome editing in *Clostridium saccharoperbutylacetonicum* N1-4 with the CRISPR-Cas9 system *Applied and Environmental Microbiology*, 83(10).
- Wang, S., Zhang, Y., Dong, H., Mao, S., Zhu, Y., Wang, R., Luan, G., and Li, Y. (2011) Formic acid triggers the ‘acid crash’ of acetone-butanol-ethanol fermentation by *Clostridium acetobutylicum* *Applied and Environmental Microbiology*, 77(5) 1674–1680.
- Wang, Y., Zhang, Z.T., Seo, S.O., Choi, K., Lu, T., Jin, Y.S., and Blaschek, H.P. (2015) Markerless chromosomal gene deletion in *Clostridium beijerinckii* using CRISPR/Cas9 system *Journal of Biotechnology*, 200 1–5.
- Wang, Y.F., Tian, J., Ji, Z.H., Song, M.Y., and Li, H. (2016) Intracellular metabolic changes of *Clostridium acetobutylicum* and promotion to butanol tolerance during biobutanol fermentation *International Journal of Biochemistry and Cell Biology*, 78 297–306.
- Wang, Z., Gerstein, M., and Snyder, M. (2009) RNA-Seq: a revolutionary tool for transcriptomics. *Bioinformatics: A Practical Guide to the Analysis of Genes and Proteins*, 10(1) 57–63.

- Wassenaar, T.A., Ingólfsson, H.I., Böckmann, R.A., Tieleman, D.P., and Marrink, S.J. (2015) Computational lipidomics with insane: A versatile tool for generating custom membranes for molecular simulations *Journal of Chemical Theory and Computation*, 11(5) 2144–2155.
- Waterhouse, A., Bertoni, M., Bienert, S., Studer, G., Tauriello, G., Gumienny, R., Heer, F.T., De Beer, T.A.P., Rempfer, C., Bordoli, L., Lepore, R., and Schwede, T. (2018) SWISS-MODEL: Homology modelling of protein structures and complexes *Nucleic Acids Research*, 46(W1) W296–W303.
- Welander, P. V, Hunter, R.C., Zhang, L., Sessions, A.L., Summons, R.E., and Newman, D.K. (2009) Hopanoids play a role in membrane integrity and pH homeostasis in *Rhodospseudomonas palustris* TIE-1. *Journal of bacteriology*, 191(19) 6145–56.
- Welch, A., Awah, C.U., Jing, S., Van Veen, H.W., and Venter, H. (2010) Promiscuous partnering and independent activity of MexB, the multidrug transporter protein from *Pseudomonas aeruginosa* *Biochemical Journal*, 430(2) 355–364.
- White, L.J., Boles, J.E., Allen, N., Alesbrook, L.S., Sutton, J.M., Hind, C.K., Hilton, K.L.F., Blackholly, L.R., Ellaby, R.J., Williams, G.T., Mulvihill, D.P., and Hiscock, J.R. (2020) Controllable hydrogen bonded self-association for the formation of multifunctional antimicrobial materials *Journal of Materials Chemistry B*, 8(21) 4694–4700.
- White, L.J., Wells, N.J., Blackholly, L.R., Shepherd, H.J., Wilson, B., Bustone, G.P., Runacres, T.J., and Hiscock, J.R. (2017) Towards quantifying the role of hydrogen bonding within amphiphile self-association and resultant aggregate formation *Chemical Science*, 8(11) 7620–7630.
- Wikström, M., Kelly, A.A., Georgiev, A., Eriksson, H.M., Klement, M.R., Bogdanov, M., Dowhan, W., and Wieslander, Å. (2009) Lipid-engineered *Escherichia coli* membranes reveal critical lipid headgroup size for protein function *Journal of Biological Chemistry*, 284(2) 954–965.
- Wu, X., Altman, R., Eiteman, M.A., and Altman, E. (2014) Adaptation of *Escherichia coli* to elevated sodium concentrations increases cation tolerance and enables greater lactic acid production. *Applied and Environmental Microbiology*, 80(9) 2880–8.
- Xu, M., Zhao, J., Yu, L., Tang, I.C., Xue, C., and Yang, S.T. (2014) Engineering *Clostridium acetobutylicum* with a

- histidine kinase knockout for enhanced n-butanol tolerance and production *Applied Microbiology and Biotechnology*, 99(2) 1011–1022.
- Xu, M., Zhao, J., Yu, L., and Yang, S.T. (2017) Comparative genomic analysis of *Clostridium acetobutylicum* for understanding the mutations contributing to enhanced butanol tolerance and production *Journal of Biotechnology*, 263 36–44.
- Xue, C., Zhao, X.Q., Liu, C.G., Chen, L.J., and Bai, F.W. (2013) Prospective and development of butanol as an advanced biofuel *Biotechnology Advances*.
- Yamamoto, E., Akimoto, T., Yasui, M., and Yasuoka, K. (2015) Origin of subdiffusion of water molecules on cell membrane surfaces *Scientific Reports*, 4(1) 4720.
- Yamamoto, N., Fraser, D., and Mahler, H.R. (1968) Chelating Agent Shock of Bacteriophage T5 *Journal of Virology*, 2(9) 944–950.
- Yang, Y., Lang, N., Yang, G., Yang, S., Jiang, W., and Gu, Y. (2016) Improving the performance of solventogenic *Clostridia* by reinforcing the biotin synthetic pathway *Metabolic Engineering*, 35 121–128.
- Yao, J. and Rock, C.O. (2017) Exogenous fatty acid metabolism in bacteria *Biochimie*, 141 30–39.
- Yazawa, H., Kamisaka, Y., Kimura, K., Yamaoka, M., and Uemura, H. (2011) Efficient accumulation of oleic acid in *Saccharomyces cerevisiae* caused by expression of rat elongase 2 gene (rELO2) and its contribution to tolerance to alcohols *Applied Microbiology and Biotechnology*, 91(6) 1593–1600.
- Yu, E.W., Aires, J.R., McDermott, G., and Nikaido, H. (2005) A periplasmic drug-binding site of the AcrB multidrug efflux pump: A crystallographic and site-directed mutagenesis study *Journal of Bacteriology*, 187(19) 6804–6815.
- Zhang, F., Wen, Y., and Guo, X. (2014) CRISPR/Cas9 for genome editing: progress, implications and challenges *Human Molecular Genetics*, 23(R1) R40–R46.
- Zhang, Y.M. and Rock, C.O. (2008) Membrane lipid homeostasis in bacteria *Nature Reviews Microbiology*.
- Zhang, Z., Lohr, L., Escalante, C., and Wetzstein, M. (2010) Food versus fuel: What do prices tell us? *Energy Policy*, 38(1) 445–451.
- Zhao, Y., Hindorff, L.A., Chuang, A., Monroe-Augustus, M., Lyrystis, M., Harrison, M.L., Rudolph, F.B., and

- Bennett, G.N. (2003) Expression of a cloned cyclopropane fatty acid synthase gene reduces solvent formation in *Clostridium acetobutylicum* ATCC 824 *Applied and Environmental Microbiology*, 69(5) 2831–2841.
- Zheng, Y.N., Li, L.Z., Xian, M., Ma, Y.J., Yang, J.M., Xu, X., and He, D.Z. (2009) Problems with the microbial production of butanol *Journal of Industrial Microbiology and Biotechnology*.
- Zhou, C., Chia, G.W.N., Ho, J.C.S., Moreland, A.S., Seviour, T., Liedberg, B., Parikh, A.N., Kjelleberg, S., Hinks, J., and Bazan, G.C. (2019) A Chain-Elongated Oligophenylenevinylene Electrolyte Increases Microbial Membrane Stability *Advanced Materials*, 31(18) 1–6.
- Zhu, L., Cheng, J., Luo, B., Feng, S., Lin, J., Wang, S., Cronan, J.E., and Wang, H. (2009) Functions of the *Clostridium acetobutylicum* FabF and FabZ proteins in unsaturated fatty acid biosynthesis *BMC Microbiology*, 9(1) 119.
- Zingaro, K.A. and Papoutsakis, E.T. (2012) Toward a semisynthetic stress response system to engineer microbial solvent tolerance *mBio*, 3(5) e00308-12.
- Zingaro, K.A. and Terry Papoutsakis, E. (2013) GroESL overexpression imparts *Escherichia coli* tolerance to i-, n-, and 2-butanol, 1,2,4-butanetriol and ethanol with complex and unpredictable patterns *Metabolic Engineering*, 15(1) 196–205.